


Article

# Functional Characterization of Clinically-Relevant Rare Variants in *ABCG2* Identified in a Gout and Hyperuricemia Cohort

Yu Toyoda <sup>1</sup> , Andrea Mančíková <sup>2</sup>, Vladimír Krylov <sup>2</sup>, Keito Morimoto <sup>1</sup>, Kateřina Pavelcová <sup>3</sup>, Jana Bohatá <sup>3</sup>, Karel Pavelka <sup>3</sup>, Markéta Pavlíková <sup>4</sup>, Hiroshi Suzuki <sup>1</sup>, Hirotaka Matsuo <sup>5</sup>, Tappei Takada <sup>1</sup> and Blanka Stiburkova <sup>3,6,\*</sup>

<sup>1</sup> Department of Pharmacy, The University of Tokyo Hospital, Tokyo 113-8655, Japan; ytoyoda-tky@umin.ac.jp (Y.T.); kmorimoto-tky@umin.ac.jp (K.M.); suzukihi-tky@umin.ac.jp (H.S.); tappei-tky@umin.ac.jp (T.T.)

<sup>2</sup> Department of Cell Biology, Faculty of Science, Charles University, 128 00 Prague 2, Czech Republic; andrea.mancikova@email.cz (A.M.); vladimir.krylov@natur.cuni.cz (V.K.)

<sup>3</sup> Institute of Rheumatology, 128 50 Prague 2, Czech Republic; pavelcova@revma.cz (K.P.); bohata@revma.cz (J.B.); pavelka@revma.cz (K.P.)

<sup>4</sup> Department of Probability and Mathematical Statistics, Faculty of Mathematics and Physics, Charles University, 121 16 Prague 2, Czech Republic; pavlikova@karlin.mff.cuni.cz

<sup>5</sup> Department of Integrative Physiology and Bio-Nano Medicine, National Defense Medical College, Saitama 359-8513, Japan; hmatsuo@ndmc.ac.jp

<sup>6</sup> Department of Pediatrics and Adolescent Medicine, First Faculty of Medicine, Charles University and General University Hospital, 121 08 Prague 2, Czech Republic

\* Correspondence: stiburkova@revma.cz; Tel.: +420-234-075-319

Received: 20 March 2019; Accepted: 15 April 2019; Published: 18 April 2019



**Abstract:** ATP-binding cassette subfamily G member 2 (*ABCG2*) is a physiologically important urate transporter. Accumulating evidence demonstrates that congenital dysfunction of *ABCG2* is an important genetic risk factor in gout and hyperuricemia; recent studies suggest the clinical significance of both common and rare variants of *ABCG2*. However, the effects of rare variants of *ABCG2* on the risk of such diseases are not fully understood. Here, using a cohort of 250 Czech individuals of European descent (68 primary hyperuricemia patients and 182 primary gout patients), we examined exonic non-synonymous variants of *ABCG2*. Based on the results of direct sequencing and database information, we experimentally characterized nine rare variants of *ABCG2*: R147W (rs372192400), T153M (rs753759474), F373C (rs752626614), T421A (rs199854112), T434M (rs769734146), S476P (not annotated), S572R (rs200894058), D620N (rs34783571), and a three-base deletion K360del (rs750972998). Functional analyses of these rare variants revealed a deficiency in the plasma membrane localization of R147W and S572R, lower levels of cellular proteins of T153M and F373C, and null urate uptake function of T434M and S476P. Accordingly, we newly identified six rare variants of *ABCG2* that showed lower or null function. Our findings contribute to deepening the understanding of *ABCG2*-related gout/hyperuricemia risk and the biochemical characteristics of the *ABCG2* protein.

**Keywords:** *ABCG2*/BCRP; common disease; European cohort; exon sequence; functional study; gout susceptibility; heritability of serum uric acid; multiple rare variant; urate transporter; WGA

## 1. Introduction

Gout—a common disease with increasing global occurrence, typically causing severe pain and physical disability—results from hyperuricemia characterized by elevated serum uric acid (SUA)

concentrations [1]. Indeed, uric acid accumulation in the body causes hyperuricemia and subsequently increases the risk of gout. Although not all individuals with hyperuricemia develop symptomatic gout, the risk of gout increases in proportion to the elevation of urate in circulation. Humans do not have a functional uricase (urate-degrading enzyme) [2], so uric acid is the final metabolite in the purine catabolic pathway in humans. Hence, urate excretion from the body is necessary for the maintenance of uric acid homeostasis. Moreover, accumulating evidence suggests that the net amount of excreted uric acid is regulated mainly by urate transporters, such as urate transporter 1 (URAT1, a renal urate re-absorber) [3], solute carrier family 2 member 9 (SLC2A9, also known as glucose transporter member 9) [4–6], and ATP-binding cassette subfamily G member 2 (ABCG2, a high capacity urate exporter expressed in the kidney and intestine) [7–9]. Importantly, we recently reported that decreased extra-renal urate excretion caused by ABCG2 dysfunction is a common mechanism of hyperuricemia [7,10,11].

As a 655-amino acid *N*-linked glycoprotein expressed on the renal and intestinal brush border membranes, ABCG2 transports its substrates, such as urate, from the cytosol to the extracellular space in an ATP-dependent manner [12]. The human *ABCG2* gene consists of 16 exons and 15 introns and is located on chromosome 4q21–q22 [13], a region that showed one of the most significant associations with gout susceptibility in a series of Genome-wide association studies (GWASs) [8,14–19]. Hitherto, 45 allelic variants have been found in the *ABCG2* gene with most of the variants having been reported to have wide ethnic differences in allele frequency. In contrast, two single nucleotide polymorphisms have been reported in *ABCG2*: c.34G>A (V12M) and c.421C>A (Q141K) are recognized as common variants in a relatively large number of ethnic groups [20]. Biochemical characterizations revealed that the V12M variant has no effects on the expression and urate transport activity of ABCG2, whereas the Q141K variant decreases the cellular function of ABCG2 through reduction of its protein levels [12]. In addition to Q141K, ABCG2 Q126X (c.376C>T), which is common in the Japanese population but rare in other populations, has additionally been identified as a hyperuricemia- and gout-risk allele [9–11,21]. Given that these two variants are associated with a significantly increased risk of gout (odds ratio > 3) [9,21], the effects of common variants of *ABCG2* on gout susceptibility are likely to be genetically strong. However, although some information is available [22–24], the effects of rare variants are not fully understood.

In our previous study employing genetic analyses for gout patients in Japan and functional analyses of some non-synonymous rare variants of *ABCG2*, we found that multiple rare and common variants of *ABCG2* are independently associated with gout risk [22]. Nevertheless, this “Common Disease, Multiple Common and Rare variant” model for the association between *ABCG2* and gout needs to be further validated, especially in other populations. To this point, we recently identified ten non-synonymous variants of *ABCG2*, including two common variants and eight rare variants, using a cohort of 145 patients with gout in the Czech Republic [23,24]. Among the rare variants, only an intron splicing variant c.689+1G>A that causes a frameshift-dependent premature stop codon was identified as an *ABCG2* null variant via functional assays [24]. However, regarding the other rare variants, whether each one is associated with gout risk in the Czech population remains to be elucidated. Moreover, owing to lack of molecular analyses, the previous study could not determine the effects of each rare variant on the urate transport activity of ABCG2 [23]. Importantly, except for a rare variant K360del (c.1079\_1081delAGA), the rare variants identified in the Czech population [23] were not found in the Japanese population [22]. Therefore, further studies on clinical risk prediction for gout in terms of rare *ABCG2* variants as well as the functional validation of such variants are required.

In the present study, we employed an enlarged cohort of 250 patients with hyperuricemia or gout to determine non-synonymous allelic variants of *ABCG2* related to the risk of such diseases. Based on the results of the sequence analysis of *ABCG2* and database information, nine rare exonic variants of *ABCG2* (R147W, T153M, K360del, F373C, T421A, T434M, S476P, S572R, D620N) were subjected to functional analyses. Here, we demonstrate the novel effects of these rare exonic variants on the expression, cellular localization, and function of ABCG2 protein as a urate transporter via molecular analyses. Our

findings might support a “Common Disease, Multiple Common and Rare variant” hypothesis for the association between *ABCG2* and gout susceptibility in a European population. Additionally, these findings about population-specific genetic variants could deepen our understanding of the heritability of SUA levels and gout, which were previously estimated to be 27–41% and approximately 30%, respectively, in Europeans [14].

## 2. Materials and Methods

### 2.1. Clinical Subjects

The analyzed set consists of two groups: a hyperuricemic group consisting of 68 subjects and a gout group consisting of 182 subjects, which was an enlarged cohort compared to that containing 145 gout subjects described previously [23]. The main cohort of 58 primary hyperuricemia subjects and 177 subjects with gout was selected from patients of the Institute of Rheumatology, Prague, the Czech Republic. The 10 pediatric subjects with hyperuricemia and five with gout was selected from patients of the Department of Pediatrics and Adolescent Medicine, Charles University, Prague as previously described [25].

In terms of SUA, the definition of hyperuricemia was as follows: (1) men > 420  $\mu\text{mol/L}$  on two repeated measurements taken at least 4 weeks apart and (2) women and children under 15 years > 360  $\mu\text{mol/L}$  on two repeated measurements taken at least 4 weeks apart. Gouty arthritis was diagnosed according to the American College of Rheumatology criteria: (1) the presence of sodium urate crystals seen in the synovial fluid using a polarized microscope or (2) at least six of 12 clinical criteria being met [26]. Patients suffering from secondary gout and other purine metabolic disorders associated with pathological concentrations of SUA were excluded. The control group consisted of 132 normouricemic subjects, which was an enlarged control population compared to that containing 115 subjects described previously [23], was selected from among the personnel of the Institute of Rheumatology. All tests were performed in accordance with standards set by the institutional ethics committees, which approved the project in Prague (no.6181/2015).

### 2.2. PCR Amplification of *ABCG2* and Sequence Analysis

*ABCG2* coding regions were analyzed from genomic DNA, as described previously [23]. The reference sequence was defined as version ENST00000237612.7 (location: Chromosome 4: 88,090,269–88,158,912 reverse strand) ([www.ensembl.org](http://www.ensembl.org)). The reference protein sequence was defined as Q9UNQ0 (<http://www.uniprot.org/uniprot>).

### 2.3. Materials

ATP, AMP, creatine phosphate disodium salt tetrahydrate, and creatine phosphokinase type I from rabbit muscle were purchased from Sigma-Aldrich (St. Louis, MO, USA) and [8-<sup>14</sup>C]-uric acid (53 mCi/mmol) were purchased from American Radiolabeled Chemicals (St. Louis, MO, USA). All other chemicals used were commercially available and of analytical grade.

### 2.4. Preparation of *ABCG2* Mutants' Expression Vectors

To express human *ABCG2* (NM\_004827.3) fused with the EGFP-tag at its N-terminus (EGFP-*ABCG2*) and EGFP (control), we used an *ABCG2*/pEGFP-C1 plasmid that was generated in our previous study [27]. Using a site-directed mutagenesis technique, vectors expressing different *ABCG2* variants were generated from an *ABCG2* wild-type (WT)/pEGFP-C1 plasmid. To confirm the introduction of mutations, each variant cDNA of *ABCG2* fused with EGFP generated in the plasmid was subjected to full sequencing using the BigDye Terminator v3.1 (Applied Biosystems Inc., Foster City, CA, USA) and an Applied Biosystems 3130 Genetic Analyzer (Applied Biosystems Inc.) according to the methods described in our previous study [27].

## 2.5. Cell Culture

Human embryonic kidney 293 cell-derived 293A cells were purchased from Life Technologies (Carlsbad, CA, USA) and cultured in Dulbecco's Modified Eagle's Medium (DMEM; Nacalai Tesque, Kyoto, Japan) supplemented with 10% fetal bovine serum (Biowest, Nuaille, France), 1% penicillin/streptomycin, 2 mM L-glutamine (Nacalai Tesque), and 1 × Non-Essential Amino Acid (Life Technologies) at 37 °C in an atmosphere of 5% CO<sub>2</sub> as described previously [27]. All experiments were carried out with 293A cells at passages 10–16.

Each vector plasmid for ABCG2 WT or its mutants was transfected into 293A cells by using polyethyleneimine MAX (PEI-MAX; 1 mg/mL in milliQ water, pH 7.0; Polysciences Inc., Warrington, PA, USA) as described previously [27] with some modifications. The amount of plasmid DNA used for transfection was adjusted to be the same for ABCG2 WT and its mutants. In brief, each plasmid was mixed with PEI-MAX (1 µg of plasmid/5 µL of PEI-MAX for 5 × 10<sup>5</sup> 293A cells) in Opti-MEM™ (Thermo Fisher Scientific K.K., Kanagawa, Japan) and incubated for 20 min at room temperature. 293A cells were collected after treatment with a 2.5 g/L-Trypsin and 1 mmol/L-EDTA solution (Nacalai Tesque), followed by centrifugation at 1000× g for 5 min. The cell pellet was re-suspended in fresh DMEM, and the resulting suspension was mixed with plasmid/PEI-MAX mixture (50:50, v/v). Then, the cells were re-seeded at a concentration of 1.4 × 10<sup>5</sup> cells/cm<sup>2</sup> onto a collagen-coated glass bottom dish (cover size 22 × 22 mm and 0.16–0.19 mm thick; Matsunami Glass Inc., Tokyo, Japan) for confocal microscopy or cell culture plates for whole cell lysate preparation. The medium was replaced with a fresh medium after the first 24 h of incubation.

## 2.6. Preparation of Whole Cell Lysates

At indicated periods after the plasmid transfection, whole cell lysates were prepared in an ice-cold lysis buffer A containing 50 mM Tris/HCl (pH 7.4), 1 mM dithiothreitol, 1% (w/v) Triton X-100, and a protease inhibitor cocktail for general use (Nacalai Tesque) as described previously [28]. Protein concentration of the whole cell lysate was quantified using a BCA Protein Assay Kit (Pierce, Rockford, IL, USA) with bovine serum albumin (BSA) as a standard according to the manufacturer's protocol. For glycosidase treatment, the whole cell lysate samples were incubated with PNGase F (New England Biolabs Japan Inc., Tokyo, Japan) (1.25 U/µg of protein) at 37 °C for 10 min as described previously [29,30], and then subjected to immunoblotting.

## 2.7. Preparation of ABCG2-Expressing Plasma Membrane Vesicles

The membrane vesicles were prepared from ABCG2-expressing 293A cells as described previously [24] with minor modifications. In brief, 293A cells seeded on 145-mm tissue culture dishes (CELLSTAR, 145 × 20 mm; Greiner Japan, Tokyo, Japan; 10 dishes/variant) at approximately 80% confluency were transiently transfected with each plasmid using PEI-MAX (24 µg of plasmid/120 µL of PEI-MAX/145-mm dish). Forty-eight hours after the transfection, the cells were collected and subjected to plasma membrane isolation. The 293A cells were suspended in a hypotonic buffer (1 mM Tris/HCl, 0.1 mM EDTA, pH 7.4, and the protease inhibitor cocktail for general use) and gently stirred for 1 h on ice. Then, the solution was ultra-centrifuged at 100,000× g for 30 min at 4 °C, and the pellet was diluted with an ice-cold isotonic buffer (10 mM Tris/HCl, 250 mM sucrose, pH 7.4), then homogenized with a dounce tissue homogenizer (Cat#: 2-4527-03; ASONE, Osaka, Japan) on ice. The crude membrane fraction was carefully layered over a 38% sucrose solution (5 mM Tris/HEPES, pH 7.4). After ultra-centrifugation at 280,000× g for 45 min at 4 °C, the turbid layer at the interface was collected, suspended in the isotonic buffer, and ultra-centrifuged at 100,000× g for 30 min at 4 °C. The membrane fraction was collected and re-suspended in an isotonic buffer and then passed through a 25-gauge needle. The resulting plasma membrane vesicles were rapidly frozen in liquid N<sub>2</sub> and kept at −80 °C until used. The protein concentration was measured using the BCA Protein Assay Kit.

## 2.8. Immunoblotting

Expression of ABCG2 protein in whole cell lysate and plasma membrane vesicles was examined by immunoblotting according to the methods reported in our previous study [31]. In brief, the prepared samples were mixed with a sodium dodecyl sulfate polyacrylamide gel electrophoresis (SDS-PAGE) sample buffer solution containing 10% 2-mercaptoethanol, separated by electrophoresis on poly-acrylamide gels, and then transferred to Polyvinylidene Difluoride membranes (Immobilon; Millipore Corporation, Billerica, MA, USA) by electroblotting at 15 V for 60 min.

For blocking, the membrane was incubated in Tris-buffered saline containing 0.05% Tween 20 and 3% BSA (Nacalai Tesque) (TBST-3% BSA) for 1 h at room temperature. Blots were probed with a rabbit anti-EGFP polyclonal antibody (A11122; Life Technologies; diluted 1000 fold in TBST 0.1% BSA), a rabbit anti- $\alpha$ -tubulin antibody (ab15246; Abcam Inc., Cambridge, MA, USA; diluted 1000 fold), or a rabbit anti- $\text{Na}^+/\text{K}^+$ -ATPase  $\alpha$  antibody (sc-28800; Santa Cruz Biotechnology Inc., Santa Cruz, CA, USA; diluted 1000 fold) followed by incubation with a donkey anti-rabbit immunoglobulin G (IgG)-horseradish peroxidase (HRP)-conjugated antibody (NA934V; diluted 3000 fold). HRP-dependent luminescence was developed using the ECL<sup>TM</sup> Prime Western Blotting Detection Reagent (GE Healthcare UK Ltd., Buckinghamshire, UK) and detected using a multi-imaging Analyzer Fusion Solo 4<sup>TM</sup> system (Vilber Lourmat, Eberhardzell, Germany). The band density was quantified using the Fusion software (Vilber Lourmat) to assess protein expression levels.

## 2.9. Confocal Laser Scanning Microscopic Observation

For confocal laser scanning microscopy, 48 h after the transfection, 293A cells were fixed with ice-cold methanol for 10 min and then washed three times with PBS (-). Then, the cells were incubated with TO-PRO-3 Iodide (Molecular Probes, Eugene, OR, USA) diluted 250 fold in PBS (-) for 10 min at room temperature. After the visualization of nuclei, the cells were washed with PBS (-) twice and then mounted in VECTASHIELD Mounting Medium (Vector Laboratories, Burlingame, CA, USA). To analyze the localization of EGFP-fused ABCG2 protein, fluorescence was detected using a FV10i Confocal Laser Scanning Microscope (Olympus, Tokyo, Japan).

To visualize plasma membranes, we used a fluorescent wheat germ agglutinin (WGA) conjugate (WGA, Alexa Fluor<sup>®</sup> 594 conjugate; Thermo Fisher Scientific K.K.) according to the manufacturer's protocol, with minor modifications. Specifically, the cells were fixed with 4% paraformaldehyde for 15 min at room temperature and then washed three times with PBS (-). Then, the cells were treated with WGA (10  $\mu\text{g}/\text{mL}$ ) in PBS (-) for 10 min at room temperature. After washing with PBS (-), the cells were treated with PBS (-) containing 0.02% (w/v) Triton X-100 and then subjected to TO-PRO-3 Iodide staining as described above.

## 2.10. Urate Transport Assay

The urate transport assay with ABCG2-expressing plasma membrane vesicles was conducted using a rapid filtration technique [31–33]. As described in our previous report [31], we used 20  $\mu\text{M}$  of radiolabeled urate in reaction mixtures (10 mM Tris/HCl, 250 mM sucrose, 10 mM  $\text{MgCl}_2$ , 10 mM creatine phosphate, 1 mg/mL creatine phosphokinase, 0.25 mg/mL each plasma membrane vesicle, pH 7.4, and 50 mM ATP or AMP as the absence of ATP) which were incubated for 10 min at 37°C for the evaluation of ABCG2 function as an ATP-dependent urate transporter. The urate transport activity was calculated as an incorporated clearance defined as the incorporated level of urate [DPM/mg protein/min]/urate level in the incubation mixture [DPM/ $\mu\text{L}$ ]. ATP-dependent urate transport was calculated by subtracting the urate transport activity in the absence of ATP from that in the presence of ATP. Furthermore, ATP-dependent urate transport activities of each ABCG2 variant were described as the percent of the activity of ABCG2 WT.

In addition, because urate uptake assays for the identified ABCG2 variants were conducted using a *Xenopus laevis* oocyte expression system, the relevant information is shown in the Supplemental Data [34].

### 2.11. Schematic Illustration of ABCG2 Protein

According to the structure of human ABCG2, which was determined by cryo-electron microscopy [35], 2D topology of ABCG2 protein was constructed, and the obtained-topology data were plotted and modified using the T(E)Xtopo package [36]. Information of highly conserved peptide motifs among ABC transporters, such as Walker A, Walker B, and signature C, in ABCG2 protein were obtained from a previous report [37].

### 2.12. Statistical Analysis

Clinical data were summarized as absolute and relative frequencies for categorical variables and as medians with interquartile range (IQR) and data range for continuous variables. Hyperuricemic and gout sub-cohorts were compared using either Fisher's exact test for categorical variables or Wilcoxon sum-rank test for continuous variables. Kruskal-Wallis test (one-way non-parametric ANOVA) and pairwise Wilcoxon tests with Bonferroni correction (for post-hoc comparisons) were used to compare ages of gout/hyperuricemia onset among groups with zero, one, and two allelic variants of interest. Fisher's exact test was used to compare the family gout history and the presence of alleles of interest. For individual allelic variants, minor allele frequency (MAF) data were excreted from the public databases NCBI and ExomAc and compared to cohort MAF in this study using a binomial test. Statistical language and environment R (version 3.5.0) (R Foundation for Statistical Computing, Vienna, Austria) was used for clinical data analyses.

Regarding experimental results, all statistical analyses were performed by using EXCEL 2013 (Microsoft Corp., Redmond, WA, USA) with Statcel3 add-in software (OMS publishing Inc., Saitama, Japan) according to our previous study [38]. The specific statistical tests that were used for individual experiments are described in the figure legends. Statistical significance was defined in terms of *P* values less than 0.05 or 0.01.

## 3. Results and Discussion

### 3.1. Subjects

The main demographic and biochemical characteristics of the subjects are summarized in Table 1. Our cohort (a total of 250 patients recruited from the Czech Republic) consisted of 182 individuals with primary gout (166 male/16 female) among which 66 patients (36% of the cohort) had a positive family history of gout. In a sub-cohort of 68 hyperuricemia patients (48 male/20 female), 31 patients (46% of the sub-cohort) had a positive family history. With respect to medications, 58 patients (23%) did not take any urate-lowering therapy medication, 175 patients (70%) took allopurinol, and 17 patients (7%) took febuxostat (the details are summarized in Supplemental Table S1). Considering that ABCG2 is one of the most influential genetic risk factors for gout and hyperuricemia, we next examined a relationship between non-synonymous mutations in ABCG2 and the risk of such diseases in our gout/hyperuricemia cohort.

**Table 1.** Demographic, biochemical, and genetic characteristics of gout and hyperuricemia cohorts.

Characteristic	All Patients (N = 250)		Gout Patients (N = 182)		Hyperuricemia Patients (N = 68)		P-Value #	
	N	%	N	%	N	%		
Gender	Male	214	85.6	166	91.2	48	70.6	0.0002
	Female	36	14.4	16	16.8	20	29.4	
Familial occurrence		97	38.8 (40.2 *)	66	36.3 (36.5 *)	31	45.6 (51.7 *)	0.0480

Table 1. Cont.

Characteristic	N	Median (IQR)	Range	N	Median (IQR)	Range	N	Median (IQR)	Range	P-Value †
Age at examination [years]	250	51.5 (25.0)	3–90	182	54.0 (21.0)	11–90	68	36.0 (42.0)	3–78	<0.0001
BMI at examination	209	28.4 (5.8)	16–50	151	28.4 (5.4)	19.5–50	58	28.1 (6.4)	16–41	0.0822
Gout/hyperuricemia onset † [years]	236	40.0 (28.0)	1.2–84	181	40.0 (24.0)	8–84	55	27.0 (40.5)	1.2–76	0.0070
SUA at examination, with medication [ $\mu\text{mol/L}$ ]	201	375.0 (134.0)	163–808	159	372.0 (128.0)	163–808	42	424.0 (140.0)	240–628	0.0515
FEUA at examination, with medication	194	3.4 (2.0)	0.9–14	158	3.4 (1.9)	0.9–14	36	3.8 (2.1)	1.3–8	0.5862

# Fisher's exact test for categorical and † Wilcoxon two-sample sum rank test were used to compare the gout sub-group with the hyperuricemia sub-group; \* relative frequencies when missing information about familial occurrence was excluded; † onset (gout) and age of ascertainment (hyperuricemia). IQR, interquartile range; SUA, serum uric acid; FEUA, fractional excretion of uric acid.

### 3.2. Identification of ABCG2 Variants in a Gout/Hyperuricemia Cohort

To determine non-synonymous allelic variants in *ABCG2* relating to the risk of gout or hyperuricemia, we performed targeted exon sequencing of *ABCG2* in our cohort. The results—all identified variants and their allele frequencies—are summarized in Table 2. We identified 11 exonic non-synonymous variants including two common variants: p.V12M (rs2231137) and p.Q141K (rs2231142), which are well-characterized, nine rare variants: p.R147W (rs372192400), p.T153M (rs753759474), p.F373C (rs752626614), p.T421A (rs199854112), p.T434M (rs769734146), p.S476P (not annotated), p.S572R (rs200894058), p.D620N (rs34783571), and a three-base deletion p.K360del (rs750972998). The *ABCG2* genotype frequency of our gout/hyperuricemia cohort was compared to MAF data from the Exome Aggregation Consortium (<http://exac.broadinstitute.org/>) and 1000 Genomes (<http://www.internationalgenome.org/>), which addressed a European-origin population (Table 2). The frequency of Q141K (a common variant linked to the risk of gout/hyperuricemia [9–11,21]) in our cohort (0.238)—0.247 in the gout sub-cohort (87 heterozygotes and 16 homozygotes) and 0.213 in the hyperuricemia sub-cohort (19 heterozygotes and 5 homozygotes)—was significantly higher than that was reported in the European-origin population (0.094). Several rare variants were present at higher allele frequencies in our cohort compared with the control population as shown in Table 2. However, as a limitation in this study, we note that our cohort population was not sufficiently large for a detailed analysis of the individual effect of each rare variant, owing to very low MAF on the disease risk. To overcome this limitation, analysis of a larger data set will be needed in the future.

Next, we focused on the combination of the common and rare variants of *ABCG2*. In total, 115 gout/hyperuricemia patients (46.0% of case) harbored at least one of the identified 11 non-synonymous variants (Supplemental Table S1). Among the patients, 23 individuals harbored two non-synonymous variants: 16 patients were homozygous for Q141K while seven patients had Q141K and one of the other variants. No patients harbored three or more of the non-synonymous variants, and no participants were found to be homozygous for rare variants. Interestingly, we found an association between the number of non-synonymous variants in *ABCG2* and the age of onset of gout/hyperuricemia in our cohort (Supplemental Figure S2). The median age of onset among patients with zero, one, or two variants were 42, 40, and 22 years, respectively ( $P < 0.0002$ , Kruskal-Wallis test). Post-hoc analysis revealed that the group with two variants significantly differs from the other groups, suggesting that an increased number of non-synonymous alleles might cause an earlier age of onset.

Regarding family history, patients with non-synonymous variants had familial gout in 54 of 111 cases (48.6%), whereas patients who did not have non-synonymous variants had familial gout in 43 of 130 (33%) cases (Figure 1). This association was statistically significant (odds ratio = 1.91, 95% CI: 1.10, 3.34;  $P = 0.0176$ , Fisher's exact test). Considering that a previous study with a small cohort had found only borderline significance ( $P = 0.053$ ) for this association [23], our result can be considered to be a strength of this study. As previously described, these findings suggest the epidemiological

importance of *ABCG2* common and rare variants for gout/hyperuricemia risk in the Czech population, supporting a “Common Disease, Multiple Common and Rare variant” hypothesis for the association between *ABCG2* and gout, which was proposed in our previous study on Japanese gout patients [22].

**Table 2.** Identified *ABCG2* variants and their mutant allele frequency.

ABCG2 Variants (rs Number)	Gout (N = 182)		Hyperuricemia (N = 68)		All Patients (N = 250)			Normouricemia (N = 132)		Population MAF	P-Value #
	N	MAF	N	MAF	N	MAF	95% CI *	N	MAF		
<b>Common</b>											
V12M (rs2231137)	8	0.0220	1	0.0074	9	0.0180	0.0083, 0.0339	5	0.0189	0.0610	<0.0001
Q141K (rs2231142)	90	0.2473	29	0.2132	119	0.2380	0.2013, 0.2778	22	0.0833	0.0940	<0.0001
<b>Rare</b>											
		N		N		N	MAF		N		Population MAF
R147W (rs372192400)	1		0		1		0.0020		1		0.0001
T153M (rs753759474)	1		0		1		0.0020		0		0.0001
F373C (rs752626614)	1		0		1		0.0020		0		0.0000
T421A (rs199854112)	0		1		1		0.0020		0		0.0001
T434M (rs769734146)	1		1		2		0.0040		1		0.0000
S476P (Not annotated)	1		0		1		0.0020		0		No data
S572R (rs200894058)	1		0		1		0.0020		0		0.0002
D620N (rs34783571)	2		0		2		0.0040		0		0.0040
K360del (rs750972998)	1		0		1		0.0020		0		0.0001

For common variants: \* A 95% confidence interval (CI) for minor allele frequency (MAF) was estimated; # Binomial test was used (all patients vs population control). Comparative information on the obtained MAFs for the cases in this study versus those for the 132 normouricemic subjects in the control group from the Institute of Rheumatology (Prague, Czech Republic) is shown. For rare variants: due to very small counts of each rare variant, MAF for the whole sample of 250 patients was given as well as population MAF (if available).

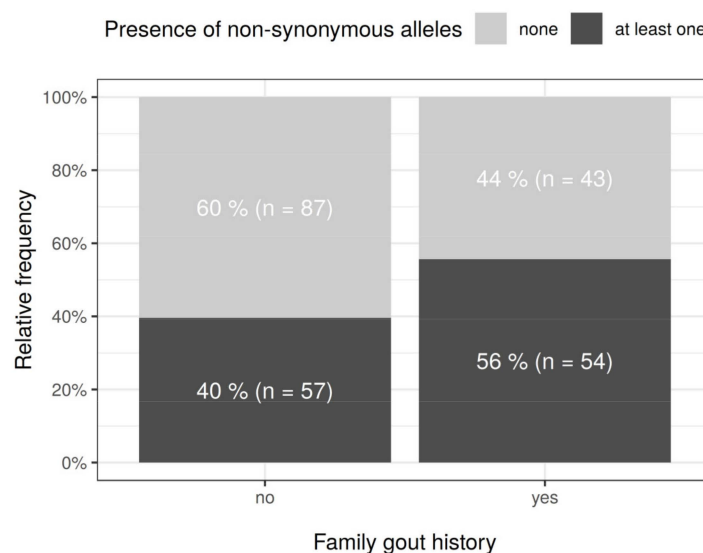


**Figure 1.** Family history of gout and the numbers of allelic variants in *ABCG2*. Depending on the presence or absence of family gout history, proportion of gout patients with or without any of the 11 non-synonymous alleles identified in *ABCG2* is summarized. The presence of *ABCG2* allelic variants was associated with the gout family history (odds ratio = 1.91, 95% CI: 1.10, 3.34;  $P = 0.0176$ , Fisher’s exact test).



Importantly, regarding the identified rare variants of ABCG2, T421A was a novel variant and the effects of the other variants on the protein function of ABCG2 as a urate transporter have not yet been characterized. Thus, we conducted a series of functional analyses to assess the rare variants that we identified (Table 2); the positions of each mutant are described in Figure 2.

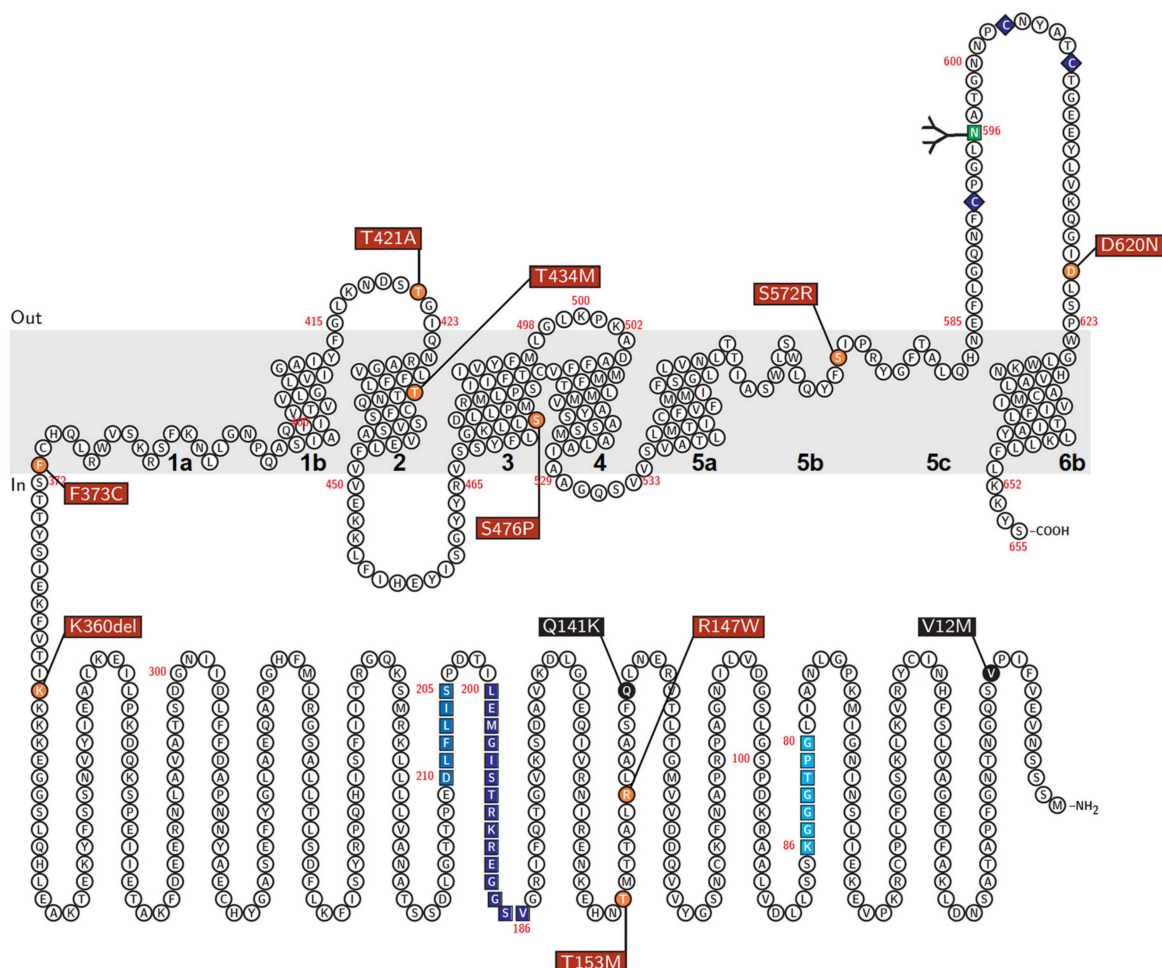


**Figure 2.** Schematic illustration of a putative topological model of human ABCG2 protein. Red box, rare variants analyzed in the present study; Black box, common variants. Helices in the transmembrane domain are numbered (1a to 6b) according to a previous study [34]. Asn596 is an N-linked glycosylation site. Unique motifs common to ABC proteins: Walker A (amino acids 80–86), Walker B (amino acids 205–210), and signature C (amino acids 186–200) in ABCG2 protein are indicated by colors.

### 3.3. Effect of Each Mutation on the Glycosylation Status of ABCG2 Protein

To investigate the effect of each non-synonymous mutation in the *ABCG2* gene on the intracellular processing and function of ABCG2 protein, we transiently expressed ABCG2 WT and its nine variants (R147W, T153M, K360del, F373C, T421A, T434M, S476P, S572R, and D620N) in 293A cells. Each expression vector was prepared using a site-directed mutagenesis technique from an ABCG2 WT/pEGFP-C1 plasmid and confirmed by DNA sequence. To address the former topic, we first performed immunoblot analyses using the anti-EGFP antibody for the detection of EGFP-tagged ABCG2. The results revealed that the R147W and S572R variants did not produce a matured glycoprotein (Figure 3A). Moreover, using N-glycosylase (PNGase F)-treated whole cell lysates, we compared the levels of ABCG2 protein in the cells among the variants and WT (Figure 3B). Since the Q141K variant reportedly reduces ABCG2 protein level [39–41], we employed this variant as a control in this study. The reducing effect of Q141K on the ABCG2 protein level detected in the present study

(Figure 3) was almost comparable to that in a previous study [41] which, like us, also used a similar transient expression strategy to validate *ABCG2* mutations in vitro. This consistency supports the reliability of the following results. Semi-quantitative evaluation of immunoblot signals showed that each variant decreased the levels of ABCG2 protein; the R147W and S572R variants showed significant effects (<25% of WT), the T153M and F373C variants had profound effects on reducing ABCG2 protein level (<50% of WT), and the other variants only mildly affected the protein expression of ABCG2.

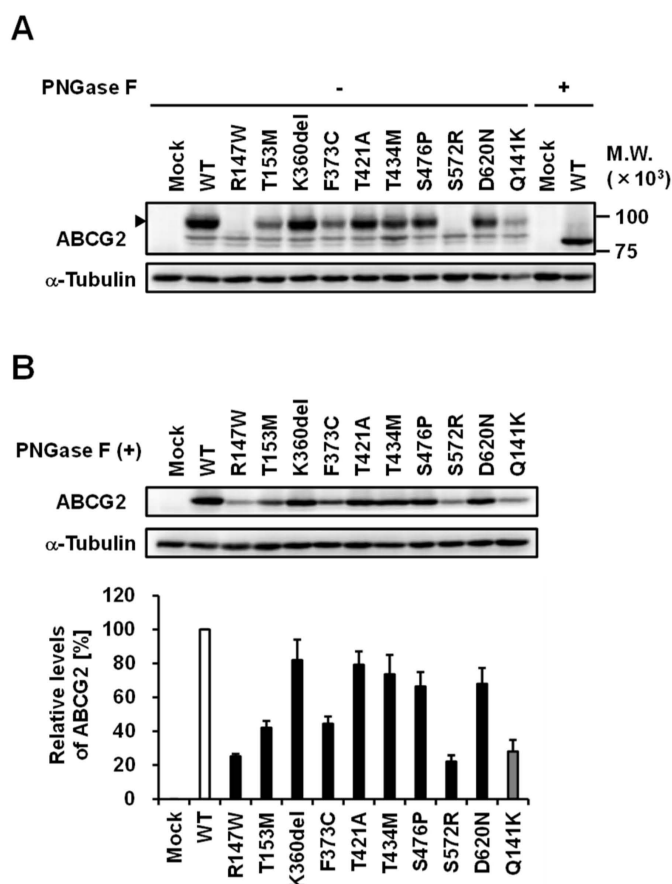


**Figure 3.** Effects of each mutation on the maturation status and protein levels of ABCG2 in transiently transfected 293A cells. **(A)** Immunoblot detection of ABCG2 wild-type (WT) and its variants in the whole cell lysate samples that were prepared 48 h after the transfection. Arrowhead, matured ABCG2 as a glycoprotein;  $\alpha$ -Tubulin, a loading control. **(B)** Relative protein levels of ABCG2 WT and its variants. The signal intensity ratio (ABCG2/ $\alpha$ -tubulin) of the immunoreactive bands was determined and normalized to that in ABCG2 WT-expressing cells. Data are expressed as the mean  $\pm$  SD.  $n = 3$ .

### 3.4. Effect of Each Mutation on the Intracellular Localization of ABCG2 Protein

We next investigated the effect of each mutation on the intracellular localization of the ABCG2 protein. Confocal microscopic observation demonstrated that ABCG2 WT and most of the variants localized on the plasma membrane of the cells (Figure 4A). In contrast, the R147W and S572R variants that hardly experienced protein maturation processing in the cells were not localized on the plasma membrane. This result was supported by high magnification image observation under a fluorescent WGA (a plasma membrane probe)-treated condition (Figure 4B). Thus, we concluded that the R147W and S572R variants have little function as a urate transporter on the plasma membrane and we performed further analyses for the other seven variants, as described below.

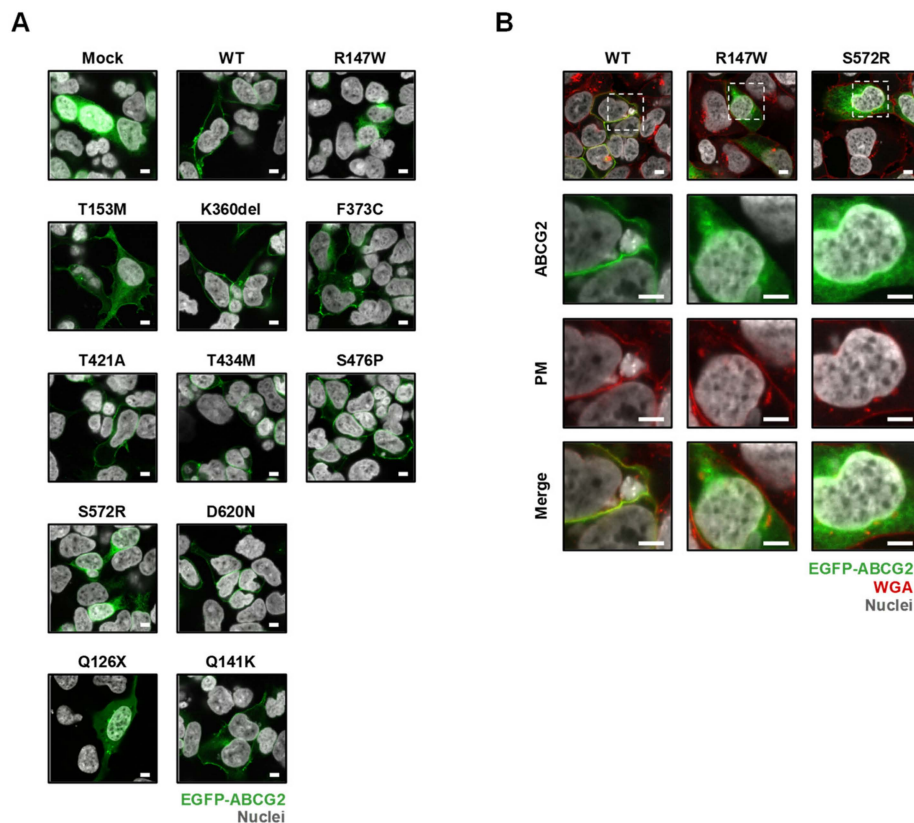


**Figure 4.** Effects of each mutation on the cellular localization of ABCG2 protein in transiently transfected 293A cells. **(A)** Intracellular localization of ABCG2 variants. Q126X (a stop gain variant that is deficient in the plasma membrane localization [22]) and Q141K are controls. **(B)** High magnification images of cells transfected with R147W and S572R variants indicate that these mutations impaired localization to the plasma membrane of the cells. Framed areas in the panels of top lane were observed under a higher magnification. Confocal microscopic images were obtained 48 h after the transfection. Nuclei were stained with TO-PRO-3 iodide (gray). Plasma membrane (PM) was labeled with Alexa Fluor® 594-conjugated wheat germ agglutinin (WGA) (red). Bars indicate 5  $\mu$ m.

### 3.5. Effect of Each Mutation on the Urate Transport Activity of ABCG2 Protein

To investigate the seven ABCG2 variants that localized on the plasma membrane, we performed functional assays using ABCG2-expressing plasma membrane vesicles. Prior to the assay, the expression of each ABCG2 variant on the plasma membrane vesicles was confirmed by immunoblot analysis (Figure 5A), which supported the results obtained through confocal microscopy (Figure 4A). Then, the ABCG2 function was evaluated as an ATP-dependent urate transport into the vesicles (Figure 5B). The results show that the T434M and S476P variants diminished the function of the ABCG2 protein. Although the T153M and F373C variants-expressing plasma membrane vesicles exhibited reduced activity of urate transport as compared with ABCG2 WT (Figure 5B), this difference in the ABCG2 function between WT and these two variants was rescued by the normalization of urate transport activity by ABCG2 protein expression on plasma membrane vesicles (Supplemental Figure S3). These results suggest that the T153M and F373C variants do not affect ABCG2 function qualitatively (via alteration of its intrinsic transporter activity), but rather do so quantitatively (via decreasing its cellular protein level). The other ABCG2 variants (K360del, T421A, and D620N) had little effect on ABCG2 function. Additionally, supportive results were obtained from the *Xenopus oocyte* expression system.

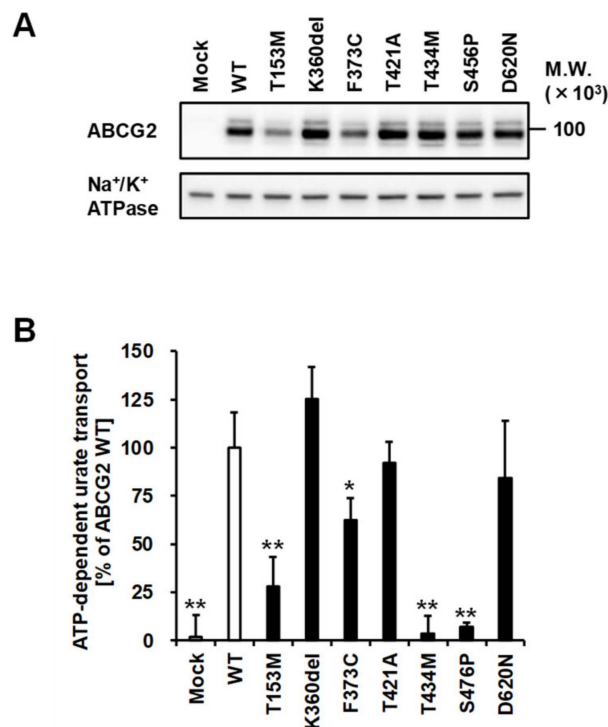


**Figure 5.** Functional validation of each ABCG2 variant as ATP-dependent urate transporters. (A) Immunoblot detection of ABCG2 WT and its variants expressed in plasma membrane vesicles prepared from 293A cells. Na<sup>+</sup>/K<sup>+</sup> ATPase, a loading control. (B) ATP-dependent transport of urate by ABCG2 WT and its variants. The data are shown as % of WT; data are expressed as the mean ± SD. *n* = 3. Statistical analyses for significant differences were performed using Bartlett's test, followed by a Dunnett's test (\*, *P* < 0.05; \*\*, *P* < 0.01 vs WT).

### 3.6. Integration of the Obtained Data

Finally, we integrated the results of functional analyses (Figures 3–5) and classified the nine ABCG2 variants according to their effects on the intracellular processing and protein function of ABCG2 (Supplemental Figure S4). As summarized in Table 3, five of the eight rare variants of ABCG2 found in our gout/hyperuricemia cohort were less functional or null. Although the available information was limited, the allele frequencies of such less functional or null variants in the cohort tended to be higher than those in the European-origin population (Table 2). To this point, there was little inconsistency between the results of functional analyses and genetic analyses. However, a more comprehensive understanding requires further studies with a larger data set.

**Table 3.** Summary of the effects of each mutation on ABCG2 protein and its function.

rs Number	Nucleotide Change	AA Change	PM Localization	Protein Level on PM	Urate Transport	Effect on the Cellular ABCG2 Function
rs372192400	439C>T	R147W	–	N.D.	N.D.	Null
rs753759474	458C>T	T153M	+	+	+	Decrease to about a quarter
rs750972998	1079_1081delAGA	K360del	+	++	++	N.S.
rs752626614	1118T>G	F373C	+	+	++	Decrease to about half
rs199854112	1261A>G	T421A	+	++	++	N.S.
rs769734146	1301C>T	T434M	+	++	–	Almost null
Not annotated	1426T>C	S476P	+	++	–	Almost null
rs200894058	1714A>C	S572R	–	N.D.	N.D.	Null
rs34783571	1858G>A	D620N	+	++	++	N.S.

The effects in each column are relatively indicated by: ++, comparable to WT; +, positive in localization or less than ++; –, negative (disruption). AA, amino acid; PM, plasma membrane; N.D., not determined; N.S. not significantly different.

Regarding three rare variants—K360del, T421A, and D620N—that were functionally comparable to WT, their allele frequencies in our cohort were not significantly different from those in the European-origin population (Table 2). Thus, at least in their individual cases, these rare variants might have smaller effects on gout/hyperuricemia risk compared with the other identified rare variants. To further elucidate whether the presence of such functional rare variants could affect disease risk, future studies will be required to assess enlarged cohorts in terms of haplotype. With respect to biochemistry, our results indicated that K360, T421, and D620 are not essential for the function of the ABCG2 protein. With respect to D620N, a previous study, using an insect cell expression system, reported that this amino acid substitution had little effect on the ABCG2-mediated transport of porphyrin, which is an endogenous substrate of ABCG2 [37]; a similar result was obtained in this study, supporting the adequacy of functional validation we carried out. Considering that these three amino acid positions (K360, T421, and D620) are not predicted to be located in the transmembrane domains of ABCG2 (Figure 2), these positions could have a flexibility in the kind of amino acids and little effect on the appropriate structures of the ABCG2 transporter during its molecular function on the plasma membrane.

Additionally, our findings provide insights into the amino acid positions that are important for ABCG2 function. Interestingly, in null or approximately null variants of ABCG2, the original amino acids (R147, T434, S476, and S572) are conserved with several major mammalian species (Figure 6). Among them, R147 is close to Q141, while the others are in transmembrane domains (Figure 2). Given that the Q141K and R147W variants decreased the protein levels of ABCG2 (Figure 3), peptides around these two amino acids might be important for the stabilization of ABCG2 protein. Since the S572R variant likewise diminished ABCG2 protein levels (Figure 3), the S572 residue, which is located in the boundary region between helices 5b and 5c (Figure 2), may be important. Interestingly, a previous study reported that an artificial mutation I573A (a neighbor position of S572) disrupted maturation and reduced plasma membrane localization of ABCG2 protein [42], which could support the biochemical importance of the boundary region in the intracellular stability of the ABCG2 protein. Regarding T434 and S476, there is a possibility that these amino acids might be involved in the formation of a penetrating pathway for ABCG2 substrates or may be critical for the dynamics of the function of the ABCG2 transporter.

Before closing, we would like to discuss the necessity for the analyses of rare *ABCG2* variants. Based on the recent findings of GWASs of clinically defined gout [16,43], common variants of *ABCG2* are extremely important in gout pathogenesis. However, because the *ABCG2* gene is reportedly to be highly-polymorphic with population specificity [44], there will be population-specific rare variants of *ABCG2* that could be a genetic risk factor of gout. Indeed, such rare variants that were found in the present study with the Czech Republic population were distinct from those found in our previous study with a Japanese population [22]. Considering the theoretical limitations in GWAS analyses, which focus on only single nucleotide polymorphisms (SNPs), the clinical and experimental approaches that we employed in this study could be a reasonable way to identify pathophysiologically important rare variants. Given that many SNPs in *ABCG2* have been studied [20], identification and validation of population-specific rare variants will be important for achieving more effective and accurate prediction of ABCG2-related gout/hyperuricemia risk.

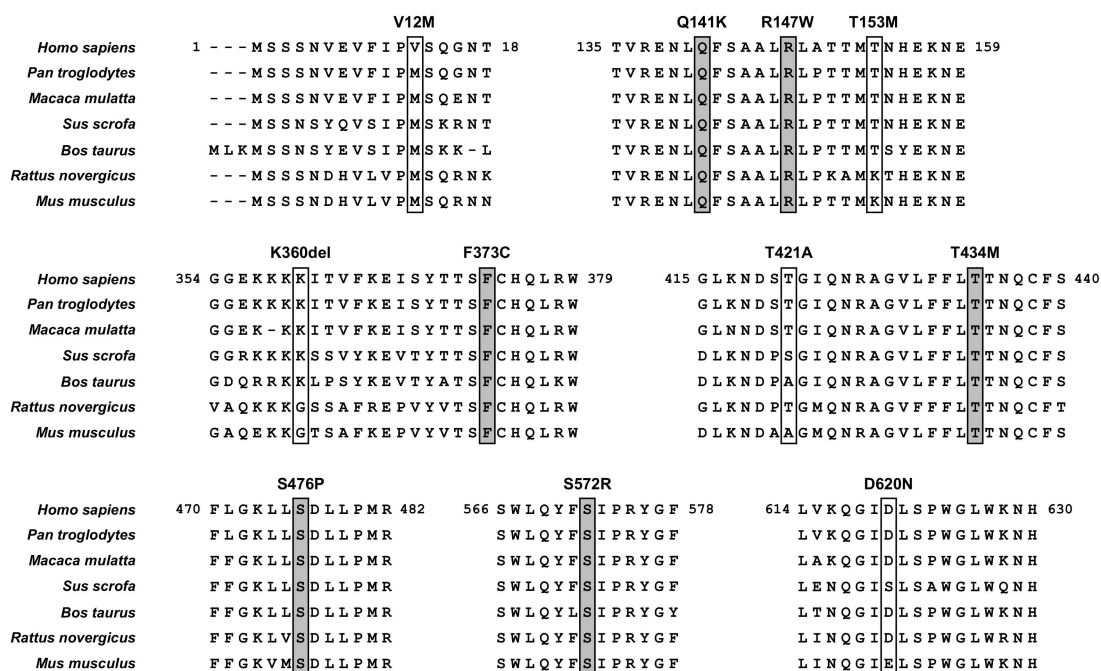


**Figure 6.** ABCG2 amino acids evolutionary conserved among seven mammalian species. The positions of non-synonymous substitutions conserved among seven species examined in the present study are grey labelled. Regarding Abcg2 protein in each species, NCBI Reference Sequence ID and amino acid sequence identity (*vs* human ABCG2, NM\_004827.3) are summarized as below: *Pan troglodytes* (Chimpanzee, GABE01009237.1), 99%; *Macaca mulatta* (Rhesus macaque, NM\_001032919.1, 96%; *Sus scrofa* (Pig, NM\_214010.1), 84%; *Bos taurus* (Bovine, NM\_001037478.3), 84%; *Rattus norvegicus* (Rat, NM\_181381.2), 81%; *Mus musculus* (Mouse, NM\_011920.3), 81%. Multiple sequence alignments and homology calculations were carried out using the GENETYX software (GENETYX Co., Tokyo, Japan) with the ClustalW2.1 Windows program according to our previous study [27].

#### 4. Conclusions

In the present study, we explored the exonic non-synonymous variants of *ABCG2* using a cohort of 250 individuals (68 primary hyperuricemia patients and 182 primary gout patients) recruited from a European descent population in the Czech Republic. Patients with non-synonymous variants showed an earlier onset of gout (Supplemental Figure S2), which is consistent with the results of previous studies [21,23]. The enlarged cohort enabled us to reveal that the numbers of non-synonymous variants of *ABCG2* could affect the frequency of familial gout (Figure 1), which was inconclusive in our previous study because of the small sample size [23]. Moreover, as summarized in Table 3, we successfully characterized the nine rare variants of *ABCG2* (Figures 3–5). Additionally, given that *ABCG2* is recognized to be an important determinant of the pharmacokinetic characteristics of its substrate drugs [45,46], this information will be significant for the field of pharmacogenomics.

In summary, our findings will deepen our understanding of *ABCG2*-related gout/hyperuricemia risk as well as the biochemical characteristics of the *ABCG2* protein. To achieve a more accurate evaluation of an individual’s risk for gout, addressing rare *ABCG2* variants is of importance. Furthermore, for effective genotyping in clinical situations, uncovering the population-specificities of such rare variants will be important.

**Supplementary Materials:** The following are available online at <http://www.mdpi.com/2073-4409/8/4/363/s1>, Supplemental Figure S1: Urate accumulation in *Xenopus* oocytes expressing URAT1 WT and *ABCG2* variants after a 30 min incubation in ND-96 solution containing 600 μM radiolabeled uric acid. Supplemental Figure S2: Onset of gout/age of ascertainment of hyperuricemia and the numbers of allelic variants in *ABCG2*, Supplemental Figure S3: Urate transport activities relative to *ABCG2* protein levels, Supplemental Figure S4: Schematic illustration of

the effects of each rare mutation we studied on the intracellular processing and function of ABCG2 protein, Supplemental Table S1: Medication and number of allelic variants in the gout and hyperuricemia cohorts.

**Author Contributions:** Conceptualization, Y.T., T.T., and B.S.; validation, Y.T., K.M., and K.P. (Kateřina Pavelcová); formal analysis, Y.T., and A.M.; investigation, Y.T., V.K., K.P. (Karel Pavelka), J.B., K.P. (Karel Pavelka), M.P., and T.T.; i.e., Y.T. and T.T. were responsible for experimental design using mammalian cells; Y.T. performed the experimental work using mammalian cells and analyzed the data; A.M. and V.K. worked on experiments using *Xenopus* oocytes, and analyzed the data; K.P. (Kateřina Pavelcová) and J.B. conducted sequencing analyses for clinical samples; K.P. (Karel Pavelka) was responsible for clinical observations; M.P. performed statistical analyses; data curation, Y.T., T.T., and B.S.; writing—original draft preparation, Y.T. and B.S.; writing—review and editing, Y.Y., T.T. and B.S.; supervision, H.S., H.M., and B.S.; project administration, B.S.; funding acquisition, Y.T., T.T. and B.S.; A.M. was a co-first author.

**Funding:** The present study was supported by the JSPS KAKENHI Grant Numbers 15H05610 (to Y.T.); 16H1808 and 18KK0247 (to T.T.) as well as a grant from the Czech Republic Ministry of Health AZV 15-26693 A to B.S. T.T. has received research grants from Gout Research Foundation, The Uehara Memorial Foundation, Mochida Memorial Foundation for Medical and Pharmaceutical Research, The Takeda Medical Foundation, and MSD Life Science Foundation, Public Interest Incorporated Foundation.

**Acknowledgments:** All authors are grateful to all the patients who kindly took part in this study as well as our colleagues at the Institute of Rheumatology (Prague, Czech Republic) for their help in recruiting patients for the study. We would like to thank Editage ([www.editage.jp](http://www.editage.jp)) for English language editing.

**Conflicts of Interest:** The authors declare no conflict of interest.

## Abbreviations

ABCG2	ATP-binding cassette subfamily G member 2
BCRP	Brest cancer resistance protein
CI	Confidence interval
GWAS	Genome-wide association study
IQR	Interquartile range
MAF	Minor allele frequency
PM	Plasma membrane
SNP	Single nucleotide polymorphism
SUA	Serum uric acid
TBST	Tris-buffered saline containing 0.05% Tween 20
WT	Wild-type

## References

1. Dalbeth, N.; Merriman, T.R.; Stamp, L.K. Gout. *Lancet* **2016**, *388*, 2039–2052. [[CrossRef](#)]
2. Yeldandi, A.V.; Wang, X.D.; Alvares, K.; Kumar, S.; Rao, M.S.; Reddy, J.K. Human urate oxidase gene: Cloning and partial sequence analysis reveal a stop codon within the fifth exon. *Biochem. Biophys. Res. Commun.* **1990**, *171*, 641–646. [[CrossRef](#)]
3. Enomoto, A.; Kimura, H.; Chairoungdua, A.; Shigeta, Y.; Jutabha, P.; Cha, S.H.; Hosoyamada, M.; Takeda, M.; Sekine, T.; Igarashi, T.; et al. Molecular identification of a renal urate anion exchanger that regulates blood urate levels. *Nature* **2002**, *417*, 447–452. [[CrossRef](#)] [[PubMed](#)]
4. Vitart, V.; Rudan, I.; Hayward, C.; Gray, N.K.; Floyd, J.; Palmer, C.N.; Knott, S.A.; Kolcic, I.; Polasek, O.; Graessler, J.; et al. SLC2A9 is a newly identified urate transporter influencing serum urate concentration, urate excretion and gout. *Nat. Genet.* **2008**, *40*, 437–442. [[CrossRef](#)] [[PubMed](#)]
5. Matsuo, H.; Chiba, T.; Nagamori, S.; Nakayama, A.; Domoto, H.; Phetdee, K.; Wiriyasermkul, P.; Kikuchi, Y.; Oda, T.; Nishiyama, J.; et al. Mutations in glucose transporter 9 gene SLC2A9 cause renal hypouricemia. *Am. J. Hum. Genet.* **2008**, *83*, 744–751.
6. Caulfield, M.J.; Munroe, P.B.; O'Neill, D.; Witkowska, K.; Charchar, F.J.; Doblado, M.; Evans, S.; Eyheramendy, S.; Onipinla, A.; Howard, P.; et al. SLC2A9 is a high-capacity urate transporter in humans. *PLoS Med.* **2008**, *5*, e197. [[CrossRef](#)]
7. Ichida, K.; Matsuo, H.; Takada, T.; Nakayama, A.; Murakami, K.; Shimizu, T.; Yamanashi, Y.; Kasuga, H.; Nakashima, H.; Nakamura, T.; et al. Decreased extra-renal urate excretion is a common cause of hyperuricemia. *Nat. Commun.* **2012**, *3*, 764. [[CrossRef](#)] [[PubMed](#)]

8. Woodward, O.M.; Kottgen, A.; Coresh, J.; Boerwinkle, E.; Guggino, W.B.; Kottgen, M. Identification of a urate transporter, ABCG2, with a common functional polymorphism causing gout. *Proc. Natl. Acad. Sci. USA* **2009**, *106*, 10338–10342. [[CrossRef](#)]
9. Matsuo, H.; Takada, T.; Ichida, K.; Nakamura, T.; Nakayama, A.; Ikebuchi, Y.; Ito, K.; Kusanagi, Y.; Chiba, T.; Tadokoro, S.; et al. Common defects of ABCG2, a high-capacity urate exporter, cause gout: A function-based genetic analysis in a Japanese population. *Sci. Transl. Med.* **2009**, *1*, 5ra11. [[CrossRef](#)]
10. Nakayama, A.; Matsuo, H.; Nakaoka, H.; Nakamura, T.; Nakashima, H.; Takada, Y.; Oikawa, Y.; Takada, T.; Sakiyama, M.; Shimizu, S.; et al. Common dysfunctional variants of ABCG2 have stronger impact on hyperuricemia progression than typical environmental risk factors. *Sci. Rep.* **2014**, *4*, 5227. [[CrossRef](#)] [[PubMed](#)]
11. Matsuo, H.; Nakayama, A.; Sakiyama, M.; Chiba, T.; Shimizu, S.; Kawamura, Y.; Nakashima, H.; Nakamura, T.; Takada, Y.; Oikawa, Y.; et al. ABCG2 dysfunction causes hyperuricemia due to both renal urate underexcretion and renal urate overload. *Sci. Rep.* **2014**, *4*, 3755. [[CrossRef](#)] [[PubMed](#)]
12. Robey, R.W.; To, K.K.; Polgar, O.; Dohse, M.; Fetsch, P.; Dean, M.; Bates, S.E. ABCG2: A perspective. *Adv. Drug Deliv. Rev.* **2009**, *61*, 3–13. [[CrossRef](#)]
13. Knutsen, T.; Rao, V.K.; Ried, T.; Mickley, L.; Schneider, E.; Miyake, K.; Ghadimi, B.M.; Padilla-Nash, H.; Pack, S.; Greenberger, L.; et al. Amplification of 4q21-q22 and the MXR gene in independently derived mitoxantrone-resistant cell lines. *Genes Chromosomes Cancer* **2000**, *27*, 110–116. [[CrossRef](#)]
14. Major, T.J.; Dalbeth, N.; Stahl, E.A.; Merriman, T.R. An update on the genetics of hyperuricaemia and gout. *Nat. Rev. Rheumatol.* **2018**, *14*, 341–353. [[CrossRef](#)]
15. Nakayama, A.; Nakaoka, H.; Yamamoto, K.; Sakiyama, M.; Shaikat, A.; Toyoda, Y.; Okada, Y.; Kamatani, Y.; Nakamura, T.; Takada, T.; et al. GWAS of clinically defined gout and subtypes identifies multiple susceptibility loci that include urate transporter genes. *Ann. Rheum. Dis.* **2017**, *76*, 869–877. [[CrossRef](#)] [[PubMed](#)]
16. Matsuo, H.; Yamamoto, K.; Nakaoka, H.; Nakayama, A.; Sakiyama, M.; Chiba, T.; Takahashi, A.; Nakamura, T.; Nakashima, H.; Takada, Y.; et al. Genome-wide association study of clinically defined gout identifies multiple risk loci and its association with clinical subtypes. *Ann. Rheum. Dis.* **2016**, *75*, 652–659. [[CrossRef](#)] [[PubMed](#)]
17. Kottgen, A.; Albrecht, E.; Teumer, A.; Vitart, V.; Krumsiek, J.; Hundertmark, C.; Pistis, G.; Ruggiero, D.; O’Seaghdha, C.M.; Haller, T.; et al. Genome-wide association analyses identify 18 new loci associated with serum urate concentrations. *Nat. Genet.* **2013**, *45*, 145–154. [[CrossRef](#)]
18. Kolz, M.; Johnson, T.; Sanna, S.; Teumer, A.; Vitart, V.; Perola, M.; Mangino, M.; Albrecht, E.; Wallace, C.; Farrall, M.; et al. Meta-analysis of 28,141 individuals identifies common variants within five new loci that influence uric acid concentrations. *PLoS Genet.* **2009**, *5*, e1000504. [[CrossRef](#)] [[PubMed](#)]
19. Dehghan, A.; Kottgen, A.; Yang, Q.; Hwang, S.J.; Kao, W.L.; Rivadeneira, F.; Boerwinkle, E.; Levy, D.; Hofman, A.; Astor, B.C.; et al. Association of three genetic loci with uric acid concentration and risk of gout: A genome-wide association study. *Lancet* **2008**, *372*, 1953–1961. [[CrossRef](#)]
20. Heyes, N.; Kapoor, P.; Kerr, I.D. Polymorphisms of the Multidrug Pump ABCG2: A Systematic Review of Their Effect on Protein Expression, Function, and Drug Pharmacokinetics. *Drug Metab. Dispos.* **2018**, *46*, 1886–1899. [[CrossRef](#)]
21. Matsuo, H.; Ichida, K.; Takada, T.; Nakayama, A.; Nakashima, H.; Nakamura, T.; Kawamura, Y.; Takada, Y.; Yamamoto, K.; Inoue, H.; et al. Common dysfunctional variants in ABCG2 are a major cause of early-onset gout. *Sci. Rep.* **2013**, *3*, 2014. [[CrossRef](#)] [[PubMed](#)]
22. Higashino, T.; Takada, T.; Nakaoka, H.; Toyoda, Y.; Stiburkova, B.; Miyata, H.; Ikebuchi, Y.; Nakashima, H.; Shimizu, S.; Kawaguchi, M.; et al. Multiple common and rare variants of ABCG2 cause gout. *RMD Open* **2017**, *3*, e000464. [[CrossRef](#)]
23. Stiburkova, B.; Pavelcova, K.; Zavada, J.; Petru, L.; Simek, P.; Cepek, P.; Pavlikova, M.; Matsuo, H.; Merriman, T.R.; Pavelka, K. Functional non-synonymous variants of ABCG2 and gout risk. *Rheumatology (Oxford)* **2017**, *56*, 1982–1992. [[CrossRef](#)] [[PubMed](#)]
24. Stiburkova, B.; Miyata, H.; Zavada, J.; Tomcik, M.; Pavelka, K.; Storkanova, G.; Toyoda, Y.; Takada, T.; Suzuki, H. Novel dysfunctional variant in ABCG2 as a cause of severe tophaceous gout: Biochemical, molecular genetics and functional analysis. *Rheumatology (Oxford)* **2016**, *55*, 191–194. [[CrossRef](#)] [[PubMed](#)]
25. Stiburkova, B.; Pavelcova, K.; Pavlikova, M.; Jesina, P.; Pavelka, K. The impact of dysfunctional variants of ABCG2 on hyperuricemia and gout in pediatric-onset patients. *Arthritis Res. Ther.* **2019**, *21*, 77. [[CrossRef](#)] [[PubMed](#)]



26. Wallace, S.L.; Robinson, H.; Masi, A.T.; Decker, J.L.; McCarty, D.J.; Yu, T.F. Preliminary criteria for the classification of the acute arthritis of primary gout. *Arthritis Rheum.* **1977**, *20*, 895–900. [[CrossRef](#)] [[PubMed](#)]
27. Toyoda, Y.; Takada, T.; Miyata, H.; Ishikawa, T.; Suzuki, H. Regulation of the Axillary Osmidrosis-Associated ABCC11 Protein Stability by N-Linked Glycosylation: Effect of Glucose Condition. *PLoS ONE* **2016**, *11*, e0157172. [[CrossRef](#)]
28. Toyoda, Y.; Sakurai, A.; Mitani, Y.; Nakashima, M.; Yoshiura, K.; Nakagawa, H.; Sakai, Y.; Ota, I.; Lezhava, A.; Hayashizaki, Y.; et al. Earwax, osmidrosis, and breast cancer: Why does one SNP (538G>A) in the human ABC transporter ABCC11 gene determine earwax type? *FASEB J.* **2009**, *23*, 2001–2013. [[CrossRef](#)]
29. Toyoda, Y.; Takada, T.; Gomi, T.; Nakagawa, H.; Ishikawa, T.; Suzuki, H. Clinical and Molecular Evidence of ABCC11 Protein Expression in Axillary Apocrine Glands of Patients with Axillary Osmidrosis. *Int. J. Mol. Sci.* **2017**, *18*, 417. [[CrossRef](#)]
30. Nakagawa, H.; Wakabayashi-Nakao, K.; Tamura, A.; Toyoda, Y.; Koshihara, S.; Ishikawa, T. Disruption of N-linked glycosylation enhances ubiquitin-mediated proteasomal degradation of the human ATP-binding cassette transporter ABCG2. *FEBS J.* **2009**, *276*, 7237–7252. [[CrossRef](#)]
31. Miyata, H.; Takada, T.; Toyoda, Y.; Matsuo, H.; Ichida, K.; Suzuki, H. Identification of Febuxostat as a New Strong ABCG2 Inhibitor: Potential Applications and Risks in Clinical Situations. *Front. Pharmacol.* **2016**, *7*, 518. [[CrossRef](#)] [[PubMed](#)]
32. Toyoda, Y.; Takada, T.; Suzuki, H. Halogenated hydrocarbon solvent-related cholangiocarcinoma risk: Biliary excretion of glutathione conjugates of 1,2-dichloropropane evidenced by untargeted metabolomics analysis. *Sci. Rep.* **2016**, *6*, 24586. [[CrossRef](#)] [[PubMed](#)]
33. Takada, T.; Yamamoto, T.; Matsuo, H.; Tan, J.K.; Ooyama, K.; Sakiyama, M.; Miyata, H.; Yamanashi, Y.; Toyoda, Y.; Higashino, T.; et al. Identification of ABCG2 as an Exporter of Uremic Toxin Indoxyl Sulfate in Mice and as a Crucial Factor Influencing CKD Progression. *Sci. Rep.* **2018**, *8*, 11147. [[CrossRef](#)] [[PubMed](#)]
34. Hurba, O.; Mancikova, A.; Krylov, V.; Pavlikova, M.; Pavelka, K.; Stiburkova, B. Complex analysis of urate transporters SLC2A9, SLC22A12 and functional characterization of non-synonymous allelic variants of GLUT9 in the Czech population: No evidence of effect on hyperuricemia and gout. *PLoS ONE* **2014**, *30*, e107902. [[CrossRef](#)]
35. Taylor, N.M.I.; Manolaridis, I.; Jackson, S.M.; Kowal, J.; Stahlberg, H.; Locher, K.P. Structure of the human multidrug transporter ABCG2. *Nature* **2017**, *546*, 504–509. [[CrossRef](#)]
36. Beitz, E. T(E)Xtopo: Shaded membrane protein topology plots in LAT(E)X2epsilon. *Bioinformatics* **2000**, *16*, 1050–1051. [[CrossRef](#)]
37. Tamura, A.; Watanabe, M.; Saito, H.; Nakagawa, H.; Kamachi, T.; Okura, I.; Ishikawa, T. Functional validation of the genetic polymorphisms of human ATP-binding cassette (ABC) transporter ABCG2: Identification of alleles that are defective in porphyrin transport. *Mol. Pharmacol.* **2006**, *70*, 287–296.
38. Toyoda, Y.; Takada, T.; Umezawa, M.; Tomura, F.; Yamanashi, Y.; Takeda, K.; Suzuki, H. Identification of hepatic NPC1L1 as an NAFLD risk factor evidenced by ezetimibe-mediated steatosis prevention and recovery. *FASEB BioAdv.* **2019**, in press. [[CrossRef](#)]
39. Kondo, C.; Suzuki, H.; Itoda, M.; Ozawa, S.; Sawada, J.; Kobayashi, D.; Ieiri, I.; Mine, K.; Ohtsubo, K.; Sugiyama, Y. Functional analysis of SNPs variants of BCRP/ABCG2. *Pharm. Res.* **2004**, *21*, 1895–1903. [[CrossRef](#)]
40. Nakagawa, H.; Toyoda, Y.; Wakabayashi-Nakao, K.; Tamaki, H.; Osumi, M.; Ishikawa, T. Ubiquitin-mediated proteasomal degradation of ABC transporters: A new aspect of genetic polymorphisms and clinical impacts. *J. Pharm. Sci.* **2011**, *100*, 3602–3619. [[CrossRef](#)]
41. Zambo, B.; Bartos, Z.; Mozner, O.; Szabo, E.; Varady, G.; Poor, G.; Palinkas, M.; Andrikovics, H.; Hegedus, T.; Homolya, L.; et al. Clinically relevant mutations in the ABCG2 transporter uncovered by genetic analysis linked to erythrocyte membrane protein expression. *Sci. Rep.* **2018**, *8*, 7487. [[CrossRef](#)] [[PubMed](#)]
42. Haider, A.J.; Cox, M.H.; Jones, N.; Goode, A.J.; Bridge, K.S.; Wong, K.; Briggs, D.; Kerr, I.D. Identification of residues in ABCG2 affecting protein trafficking and drug transport, using co-evolutionary analysis of ABCG2 sequences. *Biosci. Rep.* **2015**, *35*, e00241. [[CrossRef](#)] [[PubMed](#)]
43. Li, C.; Li, Z.; Liu, S.; Wang, C.; Han, L.; Cui, L.; Zhou, J.; Zou, H.; Liu, Z.; Chen, J.; et al. Genome-wide association analysis identifies three new risk loci for gout arthritis in Han Chinese. *Nat. Commun.* **2015**, *6*, 7041. [[CrossRef](#)] [[PubMed](#)]

44. Sakiyama, M.; Matsuo, H.; Takada, Y.; Nakamura, T.; Nakayama, A.; Takada, T.; Kitajiri, S.; Wakai, K.; Suzuki, H.; Shinomiya, N. Ethnic differences in ATP-binding cassette transporter, sub-family G, member 2 (ABCG2/BCRP): Genotype combinations and estimated functions. *Drug Metab. Pharmacokinet.* **2014**, *29*, 490–492. [[CrossRef](#)] [[PubMed](#)]
45. Giacomini, K.M.; Huang, S.M.; Tweedie, D.J.; Benet, L.Z.; Brouwer, K.L.; Chu, X.; Dahlin, A.; Evers, R.; Fischer, V.; Hillgren, K.M.; et al. Membrane transporters in drug development. *Nat. Rev. Drug Discov.* **2010**, *9*, 215–236. [[PubMed](#)]
46. Toyoda, Y.; Takada, T.; Suzuki, H. Inhibitors of human ABCG2: From technical background to recent updates with clinical implications. *Front. Pharmacol.* **2019**, *10*, 208. [[CrossRef](#)]



© 2019 by the authors. Licensee MDPI, Basel, Switzerland. This article is an open access article distributed under the terms and conditions of the Creative Commons Attribution (CC BY) license (<http://creativecommons.org/licenses/by/4.0/>).

## Supplementary Materials:

# Functional Characterization of Clinically-Relevant Rare Variants in *ABCG2* Identified in a Gout and Hyperuricemia Cohort

Yu Toyoda <sup>1</sup>, Andrea Mančíková <sup>2</sup>, Vladimír Krylov <sup>2</sup>, Keito Morimoto <sup>1</sup>, Kateřina Pavelcová <sup>3</sup>, Jana Bohatá <sup>3</sup>, Karel Pavelka <sup>3</sup>, Markéta Pavlíková <sup>5</sup>, Hiroshi Suzuki <sup>1</sup>, Hirotaka Matsuo <sup>4</sup>, Tappei Takada <sup>1</sup> and Blanka Stiburkova <sup>3,6,\*</sup>

<sup>1</sup> Department of Pharmacy, The University of Tokyo Hospital, Tokyo 113-8655, Japan; ytoyoda-tky@umin.ac.jp (Y.T.), kmorimoto-tky@umin.ac.jp (K.M.), suzukihi-tky@umin.ac.jp (H.S.), tappei-tky@umin.ac.jp (T.T.)

<sup>2</sup> Department of Cell Biology, Faculty of Science, Charles University, 128 00 Prague 2, Czech Republic; andrea.mancikova@email.cz (A.M.), vladimir.krylov@natur.cuni.cz (V.K.)

<sup>3</sup> Institute of Rheumatology, 128 50 Prague 2, Czech Republic; pavelcova@revma.cz (Kat.P.), bohata@revma.cz (J.B.), pavelka@revma.cz (Kar.P.), stiburkova@revma.cz (B.S.)

<sup>4</sup> Department of Integrative Physiology and Bio-Nano Medicine, National Defense Medical College, Saitama 359-8513, Japan; hmatsuo@ndmc.ac.jp (H.M.)

<sup>5</sup> Department of Probability and Mathematical Statistics, Faculty of Mathematics and Physics, Charles University, 121 16 Prague 2, Czech Republic; pavlikova@karlin.mff.cuni.cz (M.P.)

<sup>6</sup> Department of Pediatrics and Adolescent Medicine, First Faculty of Medicine, Charles University and General University Hospital, 121 08 Prague 2, Czech Republic

\* Correspondence: stiburkova@revma.cz; Tel.: +420-234-075- 319 (B.S.)

Received: 20 March 2019; Accepted: 15 April 2019; Published: date

## 1. Supplemental Methods

### 1.1. Sub-cloning and *in vitro* Transcription

Using the GeneArt™ Site-Directed Mutagenesis System and AccuPrime™ Pfx DNA Polymerase (Invitrogen, Carlsbad, CA, USA), vectors for *in vitro* transcription of different *ABCG2* variants were generated from the full-length *ABCG2* wild-type (WT) open reading frame (ORF) inserted in the pCMV6-AC vector (ORIGENE, Rockville, MD, USA). Appropriate cRNAs were prepared using an Invitrogen™ Ambion™ mMACHINE™ T7 Transcription Kit (Invitrogen) and stored at  $-80\text{ }^{\circ}\text{C}$  until used. In a similar manner, the cRNA of URAT1 (NM\_144585.3) was obtained from the full-length URAT1 WT ORF inserted in the pcDNA 3 vector (Thermo Fisher, Vilnius, Lithuania). Before *in vitro* transcription, template plasmids were linearized using *Not* I.

### 1.2. Preparation of URAT1 and *ABCG2* Expressing Oocytes

Female *Xenopus laevis* was anesthetized in a 0.1% ethyl 3-aminobenzoate methanesulfonate solution (Sigma-Aldrich, Steinheim, Germany) and then transferred on ice. After surgical incision, part of the ovary was cut from the abdominal cavity. To obtain defolliculated oocytes, extracted oocytes were treated with 2 mg/mL Collagenase A (Sigma-Aldrich) in a  $\text{Ca}^{2+}$ -free OR2 solution (82.5 mM, 2.5 mM KCl, 2.5 mM  $\text{CaCl}_2$ , 1 mM  $\text{MgCl}_2$ , 5 mM HEPES, and pH 7.4) for 90 min at  $18\text{ }^{\circ}\text{C}$  with gentle shaking, and then washed in fresh OR2 solution. Under stereomicroscopic observation, only oocytes with a diameter  $> 1\text{ mm}$  (at stages V–VI) were transferred to ND-96 solution (96 mM NaCl, 2mM KCl, 1.8 mM  $\text{CaCl}_2$ , 1 mM  $\text{MgCl}_2$ , 5 mM HEPES, and pH 7.5) for subsequent microinjection. Using a pneumatic microinjector (Narishige, Tokyo, Japan), 50 ng of cRNA was injected into each oocyte and the oocytes were subjected to further incubation at  $18\text{ }^{\circ}\text{C}$ .

### 1.3. Urate Transport Assay in *Xenopus* Oocytes

Urate transport assay in *Xenopus leavis* oocytes was carried out according to the methods describe in a previous study [S1]. In brief, two days after cRNA injection, intact oocytes were transferred into an ND-96 solution (a standard incubation buffer for oocyte uptake assay) containing 600  $\mu$ M radiolabeled uric acid ([8- $^{14}$ C]-uric acid; American Radiolabeled Chemicals, St. Louis, MO, USA). After incubation for 30 min at 18 °C, oocytes were washed in cold ND-96 solution three times, and then lysed using 1N NaOH and neutralized using 2N HCl in scintillation tubes. In an Ultima Gold™ scintillation cocktail (SigmaAldrich), radioactivities of oocytes that had incorporated radiolabeled urate were measured using a Hewlett Packard Liquid Scintillator (TRI-CARB 2900TR, PerkinElmer, Downers Grove, IL, USA). Uptake of uric acid was analyzed for 30 oocytes in total for each allelic variant.

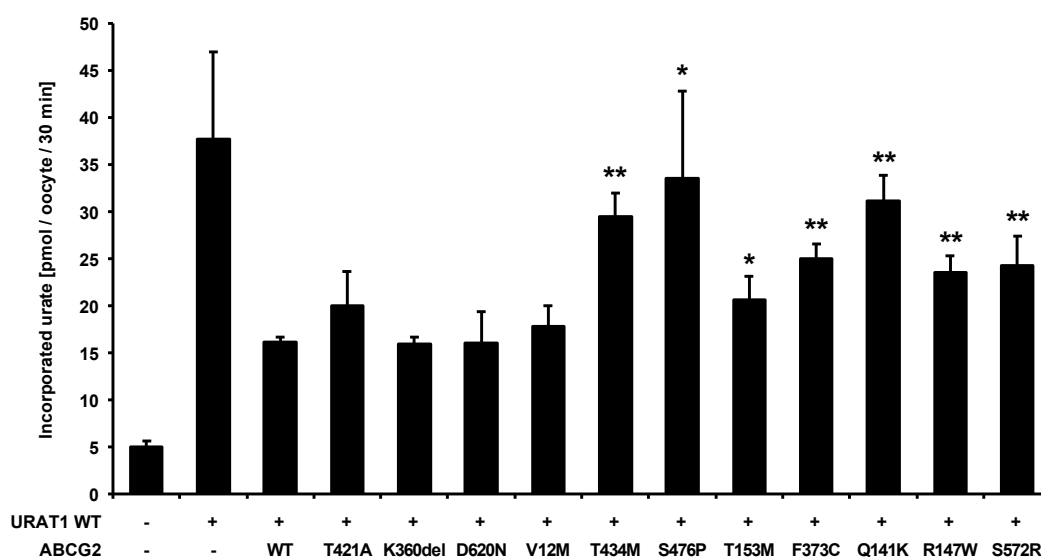
### 1.4. Statistical Analysis

Data from the oocyte uptake assay were analyzed by one-way analysis of variance (ANOVA) and differences between groups (ABCG2 WT *vs* each allelic variant) were examined through a two-sample *t*-test. Statistical significance was defined in terms of *P* values less than 0.05 or 0.01.

## 2. Supplemental Results

### 2.1. Urate Uptake in *Xenopus* Oocytes Expressing URAT1 and ABCG2

In this assay, each ABCG2 variant was co-expressed with URAT1 WT that was used for the enhancement of urate uptake into oocytes. To estimate the urate efflux ability of each ABCG2 variant, the net accumulation of radiolabeled urate into the URAT1 WT/ABCG2 double-expressing oocytes was examined for 30 min in ND-96 solution. As expected, among the tested groups, only URAT1 WT-expressing oocytes had the maximum capacity for urate accumulation and URAT1 WT/ABCG2 WT-expressing oocytes showed the lowest capacity for urate accumulation (**Supplemental Figure S1**). The results suggest that oocytes expressing seven ABCG2 variants (T434M, S474P, T153M, F373C, Q141K, R147W, and S572R) could have lower capacity for urate efflux compared with oocytes expressing ABCG2 WT.



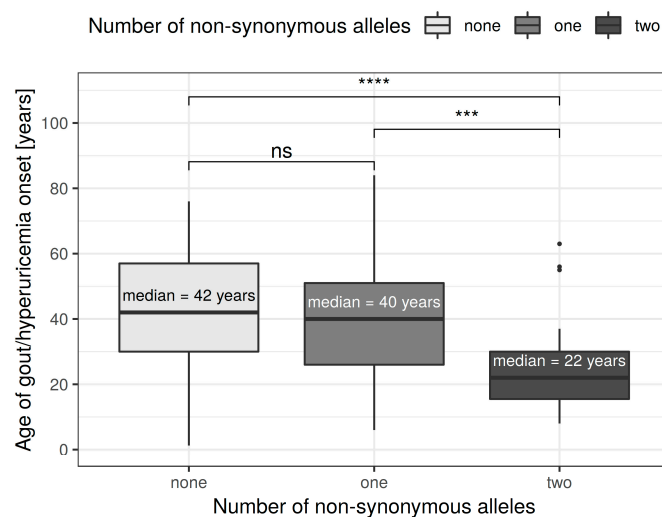
**Supplemental Figure S1.** Urate accumulation in *Xenopus* oocytes expressing URAT1 WT and ABCG2 variants after a 30 min incubation in ND-96 solution containing 600  $\mu$ M radiolabeled uric acid. In the oocytes expressing seven variants, higher urate accumulation was detected compared with ABCG2 WT. \*, *P* < 0.05; \*\*, *P* < 0.01.

### Supplemental Table S1

**Supplemental Table S1.** Medication and number of allelic variants in the gout and hyperuricemia cohorts.

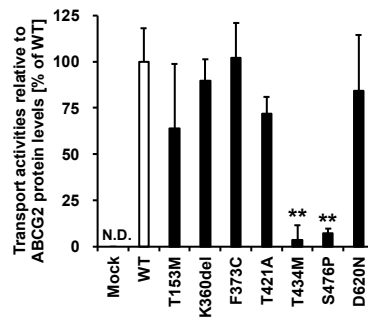
Characteristic	All patients (N = 250)		Gout (N = 182)		Hyperuricemia (N = 68)		P-value <sup>#</sup>
	N	%	N	%	N	%	
<b>Medication</b>							
Nothing	58	23.2	28	15.4	30	44.1	0.0000
Allopurinol	175	70.0	137	75.3	38	55.9	
Febuxostat	17	6.8	17	9.3	0	0.0	
<b>Number of Q141K</b>							
0	147	58.8	103	56.6	44	64.7	0.3682
1	87	34.8	68	37.4	19	27.9	
2	16	6.4	11	6.0	5	7.4	
<b>Number of V12M</b>							
0	241	96.4	174	95.6	67	98.5	0.4511
1	9	3.6	8	4.4	1	1.5	
<b>At least one variant</b>							
0	135	54.0	92	50.5	43	63.2	0.0873
1 or 2	115	46.0	90	49.5	25	36.8	
<b>Number of variants</b>							
0	135	54.0	92	50.5	43	63.2	0.1121
1	92	36.8	74	40.7	18	26.5	
2	23	9.2	16	8.8	7	10.3	

<sup>#</sup> Fisher's exact test was used to compare the gout cohort with the hyperuricemic cohort in terms of the use of medication, Q141K and V12M genotype distribution, and the number/presence of 11 studied allelic variants. There was no patient with three or more non-synonymous variants in *ABCG2*.

**Supplemental Figure S2**

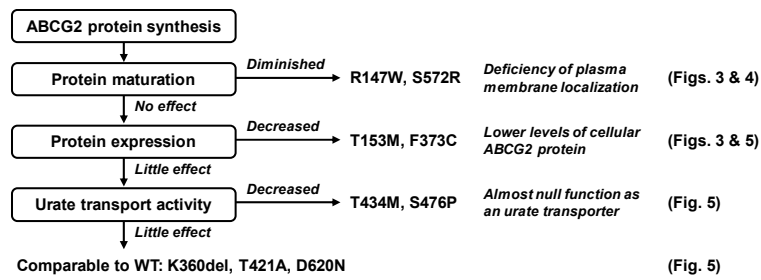
**Supplemental Figure S2.** Onset of gout/ age of ascertainment of hyperuricemia and the numbers of allelic variants in *ABCG2*. According to the number of the 11 non-synonymous alleles identified in *ABCG2*, information on onset age was summarized as a box-and-whiskers plot. Based on the Kruskal-Wallis test, there were significant differences among groups ( $P < 0.0002$ ); post-hoc comparisons (pairwise Wilcoxon tests with Bonferroni correction) showed significant differences between the two-allele group and both none- and one-allele groups. \*\*\*,  $P < 0.001$ ; \*\*\*\*,  $P < 0.0001$ ; ns, not significantly different between groups.

Supplemental Figure S3



**Supplemental Figure S3.** Urate transport activities relative to ABCG2 protein levels. ABCG2 protein levels were determined semi-quantitatively by immunoblotting. For this purpose, the signal intensity ratio (ABCG2/Na<sup>+</sup>/K<sup>+</sup> ATPase) of the immunoreactive bands shown in Figure 5A was determined and normalized to that in ABCG2 WT-expressing cells. The data are shown as % of WT; data are expressed as the mean ± SD. *n* = 3. Statistical analyses for significant differences were performed using Bartlett’s test, followed by a Dunnett’s test (\*, *P* < 0.05; \*\*, *P* < 0.01 vs WT). N.D., not determined.

Supplemental Figure S4



**Supplemental Figure S4.** Schematic illustration of the effects of each rare mutation we studied on the intracellular processing and function of ABCG2 protein.



## Article

# Identification of Two Dysfunctional Variants in the ABCG2 Urate Transporter Associated with Pediatric-Onset of Familial Hyperuricemia and Early-Onset Gout

Yu Toyoda <sup>1</sup>, Kateřina Pavelcová <sup>2,3</sup>, Jana Bohatá <sup>2,3</sup>, Pavel Ješina <sup>4</sup>, Yu Kubota <sup>1</sup>, Hiroshi Suzuki <sup>1</sup>,  
Tappei Takada <sup>1</sup> and Blanka Stiburkova <sup>2,4,\*</sup>

<sup>1</sup> Department of Pharmacy, The University of Tokyo Hospital, Tokyo 113-8655, Japan; ytoyoda-ty@umin.ac.jp (Y.T.); yukubota-ty@umin.ac.jp (Y.K.); suzukihi-ty@umin.ac.jp (H.S.); tappei-ty@umin.ac.jp (T.T.)

<sup>2</sup> Institute of Rheumatology, 128 00 Prague, Czech Republic; pavelcova@revma.cz (K.P.); bohata@revma.cz (J.B.)

<sup>3</sup> Department of Rheumatology, First Faculty of Medicine, Charles University, 121 08 Prague, Czech Republic

<sup>4</sup> Department of Pediatrics and Inherited Metabolic Disorders, First Faculty of Medicine, Charles University and General University Hospital, 121 00 Prague, Czech Republic; pavel.jesina@vfn.cz

\* Correspondence: stiburkova@revma.cz; Tel.: +420-234-075-319

**Abstract:** The *ABCG2* gene is a well-established hyperuricemia/gout risk locus encoding a urate transporter that plays a crucial role in renal and intestinal urate excretion. Hitherto, p.Q141K—a common variant of *ABCG2* exhibiting approximately one half the cellular function compared to the wild-type—has been reportedly associated with early-onset gout in some populations. However, compared with adult-onset gout, little clinical information is available regarding the association of other uricemia-associated genetic variations with early-onset gout; the latent involvement of *ABCG2* in the development of this disease requires further evidence. We describe a representative case of familial pediatric-onset hyperuricemia and early-onset gout associated with a dysfunctional *ABCG2*, i.e., a clinical history of three generations of one Czech family with biochemical and molecular genetic findings. Hyperuricemia was defined as serum uric acid (SUA) concentrations 420  $\mu\text{mol/L}$  for men or 360  $\mu\text{mol/L}$  for women and children under 15 years on two measurements, performed at least four weeks apart. The proband was a 12-year-old girl of Roma ethnicity, whose SUA concentrations were 397–405  $\mu\text{mol/L}$ . Sequencing analyses focusing on the coding region of *ABCG2* identified two rare mutations—c.393G>T (p.M131I) and c.706C>T (p.R236X). Segregation analysis revealed a plausible link between these mutations and hyperuricemia and the gout phenotype in family relatives. Functional studies revealed that p.M131I and p.R236X were functionally deficient and null, respectively. Our findings illustrate why genetic factors affecting *ABCG2* function should be routinely considered in clinical practice as part of a hyperuricemia/gout diagnosis, especially in pediatric-onset patients with a strong family history.

**Keywords:** *ABCG2* genotype; clinico-genetic analysis; ethnic specificity; genetic variations; precision medicine; rare variant; Roma; serum uric acid; SUA-lowering therapy; urate transporter



**Citation:** Toyoda, Y.; Pavelcová, K.; Bohatá, J.; Ješina, P.; Kubota, Y.; Suzuki, H.; Takada, T.; Stiburkova, B. Identification of Two Dysfunctional Variants in the ABCG2 Urate Transporter Associated with Pediatric-Onset of Familial Hyperuricemia and Early-Onset Gout. *Int. J. Mol. Sci.* **2021**, *22*, 1935. <https://doi.org/10.3390/ijms22041935>

Academic Editor: Thomas Falguières  
Received: 30 November 2020  
Accepted: 10 February 2021  
Published: 16 February 2021

**Publisher's Note:** MDPI stays neutral with regard to jurisdictional claims in published maps and institutional affiliations.



**Copyright:** © 2021 by the authors. Licensee MDPI, Basel, Switzerland. This article is an open access article distributed under the terms and conditions of the Creative Commons Attribution (CC BY) license (<https://creativecommons.org/licenses/by/4.0/>).

## 1. Introduction

Serum urate concentration is a complex phenotype influenced by both genetic and environmental factors, as well as interactions between them. Hyperuricemia results from an imbalance between endogenous production and excretion of urate. This disorder is a central feature in the pathogenesis of gout [1], which progresses through several degrees, i.e., asymptomatic hyperuricemia, acute gouty arthritis, intercritical gout, and chronic tophaceous gout. While not all individuals with hyperuricemia develop symptomatic gout, the risk of gout increases in proportion to the elevation of urate in circulation. In addition to hyperuricemia, the risk is also associated with gender, weight, age, environmental,

and genetic factors [2,3], and interactions between them all. Recent data suggest that the number of gout patients under the age of 40 years (early-onset) is increasing [4]. These early-onset patients may have different clinical signs and co-morbidities from those who present with gout at a later age [5,6]. Given the development of earlier metabolic disorders in the early-onset gout patients compared with common gout patients [5], together with the need for continuous management of health from their younger age, understanding the risks of early-onset gout is clinically important.

More and more evidence suggests that the net amount of excreted uric acid is mainly regulated by physiologically important urate transporters, such as urate transporter 1 (URAT1, known as SLC22A12, a renal urate re-absorber) [7], glucose transporter member 9 (GLUT9, also known as SLC2A9) [8,9], and ATP-binding cassette transporter G2 (ABCG2, a high capacity urate exporter expressed in the kidneys and intestines) [10–13]. Dysfunction of URAT1 and GLUT9 reportedly cause inherited hypouricemia type 1 and type 2, respectively, while dysfunction of ABCG2 is a risk factor for hyperuricemia and gout [1,14]. Additionally, the ABCG2 population-attributable percent risk for hyperuricemia has been reported to be 29.2%, which is much higher than for those with more typical environmental risks such as BMI  $\geq$  25.0 (18.7%), heavy drinking (15.4%), and age  $\geq$  60 years old (5.74%) [15]. Hence, dysfunctional variants of ABCG2 may affect clinical outcomes by influencing the accumulation of uric acid in the body.

The ABCG2 protein, which is an N-linked glycoprotein composed of 655-amino acid, is a homodimer membrane transporter found in a variety of tissues [16–18]. ABCG2 is expressed on the brush border membranes of renal and intestinal epithelial cells, where ABCG2 is involved in the ATP-dependent excretion of numerous substrates from the cytosol into the extracellular space. ABCG2 was historically first described as a drug transporter linked to breast cancer resistance [19–21], which led to many studies that focused on its critical role in drug pharmacokinetics. To date, not only xenobiotics but also endogenous substances, including uremic toxin [22] and urate [11,12], have been identified as ABCG2 substrates.

In the context of hyperuricemia/gout, there are about 50 allelic variants, including a number of rare variants with minor allele frequencies (MAF)  $<$  0.01%, which have been found in the ABCG2 gene. Wide ethnic differences have been found relative to the frequencies of these alleles. There are two well-studied, common ABCG2 allelic variants—p.V12M (c.34G>A, rs2231137) and p.Q141K (c.421C>A, rs2231142) that have highly variable frequencies depending on ethnicity. Both are commonly found in Asians (in a relatively large number of ethnic groups) but are rarely found in Europeans [23]. A minor allele of p.V12M appears to be protective regarding susceptibility to gout [24]; however, this apparent effect is due to linkage disequilibrium between p.V12M and other dysfunctional ABCG2 variants [25]. In other words, the V12M mutation has little impact on the function of ABCG2. On the other hand, the p.Q141K variant decreases ABCG2 levels, which reduces the cellular function of ABCG2, as a urate exporter, by 50% [12]. In addition to p.Q141K, p.Q126X (c.376C>T, rs72552713), which is common in the Japanese population (MAF, 2.8%) [26] but rare in other populations, has been identified as hyperuricemia- and gout-risk allele [12]. Given that p.Q141K and p.Q126X variants are both associated with a significantly increased risk of gout, the effects of dysfunctional variants of ABCG2, relative to gout susceptibility, are genetically strong [27].

In a recent study focusing on 10 single nucleotide polymorphisms in 10 genes (ABCG2, GLUT9/SLC2A9, SLC17A1, SLC16A9, GCKR, SLC22A11, INHBC, RREB1, PDZK1, and NRXN2) that are strongly associated with serum uric acid (SUA) concentrations, only ABCG2 p.Q141K was associated with early-onset gout ( $<$  40 years of age) in European and Polynesian subjects [28]. Additionally, in a previous study, we found that the MAF of p.Q141K in a cohort of hyperuricemia and gout with pediatric-onset was 38.7%, which was significantly higher than adult-onset (21.2%) as well as normouricemic controls (8.5%) [29]. This information suggests that ABCG2 dysfunction could be strongly associated with pediatric-onset hyperuricemia and early-onset gout; however, compared with adult-onset



gout, little clinical information is available, except for the ABCG2 p.Q141K, regarding early-onset gout linked to other SUA-associated mutations. Furthermore, the latent involvement of ABCG2 in the development of this disease requires further evidence.

In this study, we investigated the genetic cause of pediatric-onset hyperuricemia and early-onset gout over three generations of a single family. Based on a positive family history of hyperuricemia or gout, we identified two rare mutations, c.393G>T (p.M131I) and c.706C>T (p.R236X), in the ABCG2 gene. A series of biochemical assays revealed that ABCG2 p.M131I and p.R236X were functionally deficient and null, respectively. Our results also contributed to a more in-depth understanding of the effects of rare ABCG2 variants, which is a highly polymorphic gene, on its function as a physiologically important transporter.

## 2. Results

### 2.1. Subjects

The clinical and biochemical data from this study are summarized in Table 1. Repeated biochemical analysis of the proband (a 12-year-old girl with chronic asymptomatic hyperuricemia) showed elevated serum urate (397–405  $\mu\text{mol/L}$ ; 6.67–6.81 mg/dL) with a decreased fractional excretion of uric acid (FE-UA) (2.2–3.5%). No clinical or laboratory symptoms of renal disease were present in the patient. The girl's mother (38-years-old) had previously presented with asymptomatic hyperuricemia (420–439  $\mu\text{mol/L}$ ; 7.06–7.38 mg/dL of serum urate); both the maternal grandfather (66-years-old) and the maternal uncle (40-years-old) had presented with hyperuricemia (500–537  $\mu\text{mol/L}$ ; 8.41–9.03 mg/dL) and early-onset gout, with the first gout attack occurring in the uncle when he was 35-years-old. The girl's father (38-years-old) presented with asymptomatic hyperuricemia (487  $\mu\text{mol/L}$ ; 8.19 mg/dL of serum urate), which seemed to be associated with metabolic syndrome (i.e., hypertriglyceridemia, hypertension, and central obesity). Metabolic investigation for purine metabolism (i.e., hypoxanthine and xanthine levels in the urine) found normal urinary excretion, suggesting that hyperuricemia in our patients and family relatives was not caused by an excess production of uric acid. Thus, we focused on the physiologically important urate transporters, especially ABCG2, which regulate urate handling in the body as described below.

**Table 1.** Clinical and biochemical data of a family with early-onset hyperuricemia and gout.

	Proband	Mother	Maternal uncle	Maternal grandfather	Father
<b>Age of onset (HA/gout)</b>	12 years (HA)	35 years (HA)	35 years (gout)	43 years (gout)	30–35 (HA)
<b>Main symptoms</b>	Asymptomatic Astigmatism;	Asymptomatic	Gout	Gout	Asymptomatic
<b>Other symptoms or diseases</b>	Bilateral cataracts; Myopia; Bronchial asthma; Obesity	Thyropathy; Vertebrogenic Algic syndrome	T2D; Hypertension; Obesity; Thyropathy	T2D; Hypertension	Bronchial asthma; Hypertriglyceridemia; Hypertension; Central obesity
<b>SUA before treatment [<math>\mu\text{mol/L}</math> (mg/dL)]</b>	397–405 (6.67–6.81)	420–439 (7.06–7.38)	>500 (>8.41)	537 (9.03)	487 (8.19)
<b>UUA [mmol/mol creatinine]</b>	3.34	1.47	2.10	n.d.	2.45
<b>FE-UA [%]</b>	2.2	4.6	2.9	n.d.	3.9
<b>Therapy</b>	No	No	Allopurinol (100 mg per day)	Colchicine; Allopurinol (300 mg per day)	No
<b>SUA during treatment [<math>\mu\text{mol/L}</math> (mg/dL)]</b>	n.d.	n.d.	446 (7.50) (non-compliance)	422 (7.09) (non-compliance)	n.d.

HA, hyperuricemia; SUA, serum uric acid; UUA, urine uric acid; FE-UA, fractional excretion of uric acid; T2D, type 2 diabetes mellitus; n.d., not determined. Reference ranges are as follows. SUA: 120–360  $\mu\text{mol/L}$  (2.02–6.05 mg/dL) (< 15 years and female), 120–420  $\mu\text{mol/L}$  (2.02–7.06 mg/dL) (male); UUA: 0.1–1.0 mmol/mol creatinine (< 15 years), 0.1–0.8 mmol/mol creatinine ( $\geq$  15 years); FE-UA: 5–20% (<13 years), 5–12% (male), 5–15% (female).

## 2.2. Genetic Analysis

Targeted exon sequencing analyses of *ABCG2* revealed that the proband had two rare heterozygous non-synonymous mutations, i.e., (1) c.393G>T (p.M131I, rs759726272) and (2) c.706C>T (p.R236X, rs140207606). No other exonic mutations were found, including previously characterized common genetic risk factors for hyperuricemia/gout, such as *ABCG2* c.376C>T (p.Q126X) and c.421C>A (p.Q141K). Moreover, a segregation analysis of the family confirmed the two mutations as probably being disease-associated mutations. Heterozygous c.393G>T and c.706C>T were identified through the maternal line in the mother, uncle, and grandfather of the proband. The pedigree is shown in Figure 1 along with representative electropherograms of partial *ABCG2* sequences showing a heterozygous missense mutation (c.393G>T) in exon 5 and a nonsense mutation (c.706C>T) in exon 7. Moreover, sequencing analyses, including analyses of previously known SUA-associated loci, found no disease-associated non-synonymous mutations in *GLUT9* and *URAT1*. Although two mutations, c.73G>A (p.G25R, rs2276961) and c.844G>A (p.V282I, rs16890979), were found in *GLUT9*; however, previous studies have shown that they would not cause hyperuricemia/gout [30,31].

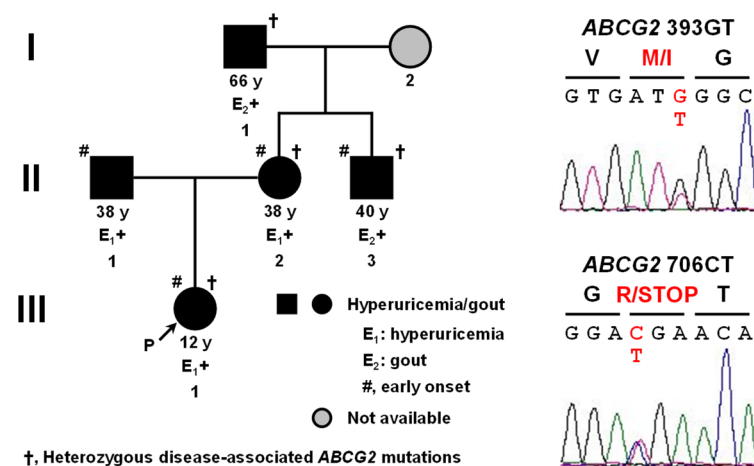


**Figure 1.** Identification of novel disease-associated mutations c.393G>T (p.M131I) and c.706C>T (p.R236X) in *ABCG2*. Left, the pedigree of a Czech family with early-onset hyperuricemia and gout; Right, representative electropherograms of partial sequences of *ABCG2* showing the heterozygous point mutations (red) discovered in our present study. I–III, generation of the family; P, proband; y, years old.

Further sequencing analyses revealed that neither of these *ABCG2* mutations was detected in a previously enrolled cohort of 360 patients with hyperuricemia/gout and a cohort of 132 normouricemia control subjects of European descent [32]. However, in another control group of 60 subjects of Roma ethnicity [33], although serum urate and FE-UA values were not available, we found one copy of c.393G>T (p.M131I), but without c.706C>T (p.R236X), in a male hemodialysis patient with severe chronic kidney disease. This finding suggested that c.393G>T (p.M131I) and c.706C>T (p.R236X) can occur independently, which led us to examine the effect of each non-synonymous mutation on the *ABCG2* protein.

Additionally, the independent genetic origin of these two *ABCG2* mutations was also strongly supported by supplementary analyses of MAF data that is openly available from the Exome Aggregation Consortium (<http://exac.broadinstitute.org/> (accessed on 30 November 2020)). With regard to c.393G>T (p.M131I), only six heterozygotes of the minor allele (393T) were found in a cohort of 64,397 European subjects (MAF, 0.0047%); with even fewer carriers in other populations (total worldwide MAF frequency = 0.0021%). With regard to c.706C>T (p.R236X), 48 heterozygotes of the minor allele (706T) were found in a cohort of 645,050 European subjects (MAF = 0.0372%, which is almost 8 times greater

than the MAF of c.393G>T); in other populations, frequencies ranging from 0.0000% in European Finnish to 0.1254% (the highest) in Ashkenazi Jewish were found.

### 2.3. Functional Analysis

To investigate the effect of the two identified non-synonymous mutations (p.M131I and p.R236X) on the intracellular processing and function of the ABCG2 protein, we conducted several biochemical analyses using transiently ABCG2-expressing mammalian cells (Figure 2). First, immunoblotting for *N*-glycosidase (PNGase F)-treated whole cell lysates (Figure 2A) demonstrated that p.M131I had a minimal effect on protein levels and *N*-linked glycosylation status, while the p.R236X variant was detected as truncated forms of the protein with weaker band intensities compared to ABCG2 wild-type (WT), as would be expected based on its amino acid sequence. Confocal microscopy (Figure 2B) showed that, like ABCG2 WT, the p.M131I variant was mainly located on the plasma membrane, while the p.R236X variant exhibited little plasma membrane localization. Expression of the p.M131I variant as a glycoprotein on plasma membrane-derived vesicles was confirmed using immunoblotting (Figure 2C). Next, using a vesicle transport assay [34] with an optimized experimental procedure for determining the initial rate of urate transport by ABCG2 based on our previous studies [12,35], ABCG2 function was evaluated as having ATP-dependent urate transport activity into plasma membrane vesicles (Figure 2D). The functional assay revealed that contrary to the WT, p.M131I had limited ATP-dependent urate transport activity, with the ABCG2-mediated urate transport activity of this variant calculated to be  $14 \pm 2\%$  of the WT controls. The p.R236X variant was functionally null (Figure 2D), which was consistent with the results of our biochemical analyses (Figure 2A–C).

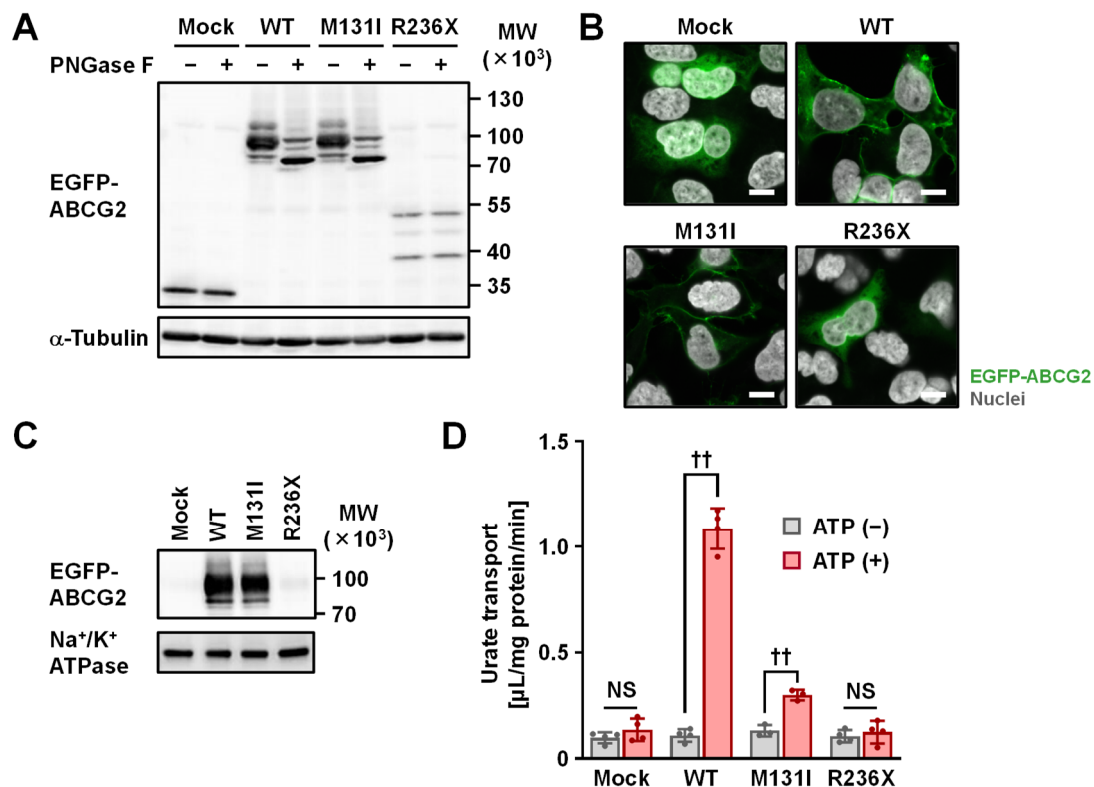


**Figure 2.** Functional characterization of disease-associated ABCG2 mutations. (A) Immunoblot of whole cell lysate samples.  $\alpha$ -Tubulin used as the loading control. WT, wild-type. (B) Confocal microscopy of intracellular localization. Nuclei were stained with TO-PRO-3 iodide (gray). Bars, 10  $\mu$ m. (C) Immunoblot of plasma membrane vesicles.  $\text{Na}^+/\text{K}^+$  ATPase as the loading control. (D) Urate transport activity. The incubation condition was 37  $^{\circ}\text{C}$  for 10 min in the presence of 20  $\mu\text{M}$  radiolabeled urate. Data are expressed as the mean  $\pm$  SD.  $n = 3$ –4.  $\dagger\dagger$ ,  $P < 0.01$ ; NS, not significantly different between groups (two-sided *t*-test).

### 3. Discussion

In this study, we found and analyzed a representative case of pediatric-onset hyperuricemia and early-onset gout in a Czech family associated with two newly identified, one functionally deficient and the other a null mutation, in *ABCG2*. A positive family history of hyperuricemia/gout in the context of *ABCG2* dysfunction was observed in the maternal line (the mother, maternal uncle, and maternal grandfather) of the proband (a young girl, of Roma ethnicity, with chronic asymptomatic hyperuricemia); her father exhibited elevated serum urate that seemed to be associated with metabolic syndrome. Although a decrease in net renal urate excretion was observed in all cases of hyperuricemia in this family, which was characterized by FE-UA < 5%, our findings suggest that the hyperuricemia was linked to heterogeneity. Moreover, the familial hyperuricemia/gout observed in this study was not associated with a common variant, such as p.Q141K, but with a rare *ABCG2* variant; this supports the recently proposed genetic concept, i.e., the “Common Disease, Multiple Common and Rare Variant” model [25,36], for the association between hyperuricemia/gout and the *ABCG2* gene.

Our findings of *ABCG2* variants will provide deeper insights into amino acid positions that are critical for normal *ABCG2* function. Based on cryo-electron microscopy (cryo-EM) of *ABCG2* [37], both the M131 and R236 residues are in the cytoplasmic region of the N-terminus of the *ABCG2* protein. Regarding p.M131I, the original amino acid (M131) sequence is conserved in several major mammalian species (Figure 3). Unlike the p.Q141K variant, which affects intracellular processing of the *ABCG2* protein [38], the p.M131I variant disrupts *ABCG2*'s function as a urate transporter, with little effect on the *ABCG2* protein or its cellular localization. A plausible explanation for the molecular mechanism of the p.M131I effect is that this amino acid substitution could affect *ABCG2* substrate specificity and/or affect its ATPase activity, including the binding affinity of ATP, which is the driving force for ABC transporters. The latter possibility is supported by a structural feature that the M131 residue is located near the conserved glutamine (Q126) within a Q-loop in the nucleotide-binding domain of *ABCG2*, a key element for the catalytic cycle of ATP binding and hydrolysis [37,39]. Further studies are needed to address this biochemical issue, which may deepen the mechanistic insight of *ABCG2* protein. With regard to p.R236X, the acquired stop codon results in the production of a shortened *ABCG2* variant (only about one-third the amino acid length of the native *ABCG2* protein) that lacks all the transmembrane domains essential for normal protein function as a membrane transporter. This is consistent with our results demonstrating that the p.R236X variant is functionally null. Thus, the c.[393G>T; c.706C>T] (p.[M131I; R236X]) variant does not function as a urate transporter.

		<b>M131I</b>																				
<i>Homo sapiens</i>	126	Q	D	D	V	V	M	G	T	L	T	V	R	E	N	L	Q	F	S	A	A	145
<i>Pan troglodytes</i>		Q	D	D	V	V	M	G	T	L	T	V	R	E	N	L	Q	F	S	A	A	
<i>Macaca mulatta</i>		Q	D	D	V	V	M	G	T	L	T	V	R	E	N	L	Q	F	S	A	A	
<i>Sus scrofa</i>		Q	D	D	V	V	M	G	T	L	T	V	R	E	N	L	Q	F	S	A	A	
<i>Bos taurus</i>		Q	D	D	V	V	M	G	T	L	T	V	R	E	N	L	Q	F	S	A	A	
<i>Rattus norvegicus</i>		Q	D	D	V	V	M	G	T	L	T	V	R	E	N	L	Q	F	S	A	A	
<i>Mus musculus</i>		Q	D	D	V	V	M	G	T	L	T	V	R	E	N	L	Q	F	S	A	A	

**Figure 3.** *ABCG2* M131 is shown to be evolutionary conserved among seven mammalian species. Regarding the *Abcg2* protein in each species, the NCBI Reference Sequence IDs are summarized as *Pan troglodytes* (Chimpanzee), GABE01009237.1; *Macaca mulatta* (Rhesus macaque), NM\_001032919.1; *Sus scrofa* (Pig), NM\_214010.1; *Bos taurus* (Bovine), NM\_001037478.3; *Rattus norvegicus* (Rat), NM\_181381.2; *Mus musculus* (Mouse), NM\_011920.3. Multiple sequence alignments and homology calculations were carried out using GENETYX software (GENETYX, Tokyo, Japan) and the ClustalW2.1 Windows program, per the protocol used in our previous study [40].

To discuss the expected independence in the genetic origin of two *ABCG2* mutations identified in this study, we will focus on the genetic specificity of each population. The Czech family studied in this study is of Roma ethnicity. The Roma composes a transnational ethnic population of 8–10 million, with the original homeland being India; currently, they are the largest and the most widespread ethnic minority in Europe. The founder effect and subsequent genetic isolation of the Roma have led to a population specificity regarding the genetic background of specific human diseases. In other words, mutations associated with rare diseases found in the Roma population tend to be at extremely low frequencies in other European populations, and vice versa. Indeed, several genetic variants causing rare diseases are unique to the Roma, and many of these mutations have only recently been discovered, e.g., Charcot Marie Tooth disease type 4D and 4G (OMIM 601455 and 605285), Congenital cataract facial dysmorphism neuropathy (OMIM 604166), Gitelman syndrome (OMIM 263800), and Galactokinase deficiency (OMIM 230200) [41,42]. In light of the genetic specificity found in the Roma, we investigated the frequency of two identified *ABCG2* mutants (c.393G>T and c.706C>T) in our control cohort of 60 subjects of Roma origin (see Section 2.2 in Results). MAFs of c.393G>T in the Roma cohort and European population were 0.833% (1 allele/120 subjects) and 0.002% (6 alleles/64,397 subjects), respectively. Although the sample size of our control cohort was very modest, it could be large enough to imply that the origin of c.393G>T might be the Roma population. On the other hand, the prevalence of c.706C>T was higher in Europeans than in the Roma, suggesting that these two *ABCG2* mutations could have different genetic origins.

For clinical practice, our findings suggest a need for further discussion about the potential benefits of urate-lowering therapy after a diagnosis of hyperuricemia in pediatric-onset patients with *ABCG2* dysfunction. Interestingly, harboring p.Q141K is reportedly associated with inadequate response to allopurinol (characterized by a smaller reduction in serum urate concentrations compared with WT) [29,43–45]; allopurinol, which inhibits uric acid production, is a well-known and widely used drug for lowering SUA. Although the mechanisms of action for the inadequate response are still unclear, other SUA-lowering drugs may be somewhat better in terms of efficacy for patients with a dysfunctional *ABCG2* allele, which puts them at higher risk of developing hyperuricemia/gout. On the other hand, among the clinically-used inhibitors for the production of uric acid (i.e., allopurinol, febuxostat, and topiroxostat), only febuxostat, to the best of our knowledge, strongly and clinically inhibits *ABCG2* function as a urate transporter [35]. This is also supported by a recent clinical study that showed orally-administered febuxostat inhibits intestinal *ABCG2* in humans [46]. In this context, the efficacy of febuxostat as an SUA-lowering drug can be partially blocked by *ABCG2* inhibition, except in cases of completely null *ABCG2* function. Considering this complexity, as well as risks of adverse effects [47], the best SUA-lowering drugs, including uricosuric agents and uric acid production inhibitors, should be carefully determined for each patient.

Additionally, we can emphasize the clinical importance of the documentation regarding the family we addressed in this study, given the infrequency of detailed studies on SUA levels in children. Indeed, pediatric-onset of hyperuricemia is relatively rare in clinical practice; it is often associated with rare conditions (e.g., purine metabolic disorders; kidney disorders including uromodulin-associated disorders; metabolic genetic disorders including glycogen storage disease, hereditary fructose intolerance, and mitochondrial disorders). As we showed previously [48], the levels of SUA and FE-UA are quite dynamic in the first year of life. In brief, the SUA levels are low in infancy (131–149  $\mu\text{mol/L}$ ; 2.2–2.5 mg/dL at 2–3 months of age) due to the high FE-UA levels (>10%); the FE-UA levels decrease to approximately 8% at age 1 and then stay through childhood, which is associated with mean SUA levels (208–268  $\mu\text{mol/L}$ ; 3.5–4.5 mg/dL) of children. At adolescence (after age 12), the FE-UA levels significantly decrease in boys but not in girls, resulting in a further significant increase in SUA levels in young men but not in young women. These pieces of information support the rarity of our case of which proband is a 12-year-old girl

with chronic asymptomatic hyperuricemia characterized by elevated serum urate (397–405  $\mu\text{mol/L}$ ; 6.67–6.81 mg/dL) and the decreased FE-UA (2.2–3.5%).

Some limitations warrant mention. It is unclear whether there could have been other genetic factors also affecting the early-onset phenotypes in the family we studied, although harboring dysfunctional *ABCG2* mutations is the most plausible explanation, as the study showed. A previous study showed that in the context of extra-renal underexcretion hyperuricemia, a genetic dysfunction of *ABCG2* increased SUA levels and apparent urinary urate excretion, which was coupled with decreased intestinal urate excretion. Thus, we can assume the presence of latent mechanisms causing the decreased (<5%) FE-UA levels observed in our patients. Although there is little information available regarding this, a possible factor could be increased renal urate reabsorption, which can be mediated by up-regulation of renal urate re-absorbers, including *URAT1/SLC22A12*, *GLUT9/SLC2A9*, and *organic anion transporter 10* (known as *SLC22A13*) [49]. In this context, genetic variations affecting the expression of such genes will be the targets of future studies.

In conclusion, we found a representative case of pediatric hyperuricemia with familial gout that harbored two dysfunctional *ABCG2* mutations. Genetic variations in *ABCG2* should be kept in mind during diagnostic procedures for pediatric-onset hyperuricemia. Considering *ABCG2* genotypes will be beneficial for patients with early-onset and/or familial hyperuricemia and gout. This type of genetic information will also allow a personalized approach regarding the best urate-lowering treatment (i.e., uric acid production inhibitors or uricosuric agents) for patients with dysfunctional *ABCG2* variants, as well as the best time to initiate pharmacotherapy for hyperuricemia.

## 4. Materials and Methods

### 4.1. Clinical Subjects

The studied proband and her family members were Czechs of Roma ethnicity diagnosed with familial (early-onset) hyperuricemia/gout. Written informed consent was obtained from each subject before enrollment in the study. All tests were performed in accordance with standards set by the institutional ethics committees, which approved 30 June 2015 the project no. 6181/2015. All the procedures were performed in accordance with the Declaration of Helsinki.

Hyperuricemia was defined as serum urate levels greater than 420  $\mu\text{mol/L}$  (7.06 mg/dL) for men or 360  $\mu\text{mol/L}$  (6.05 mg/dL) for women and children under 15 years on two measurements, performed at least four weeks apart. Gouty arthritis was diagnosed according to the American College of Rheumatology criteria, as follows: (1) the presence of sodium urate crystals seen in synovial fluid (using a polarized microscope, Nikon Eclipse E200, Tokyo, Japan) or (2) at least six of 12 clinical criteria being met [50].

The proband was a 12-year-old girl with a complicated perinatal anamnesis. She was born at 31 weeks of gestation with an Apgar score of 4-7-8, a birth weight of 1690 g, and a birth length of 40 cm; additionally, she developed early asphyxia syndrome. She also experienced repeated respiratory infections and was later diagnosed with bronchial asthma. She is also under the care of an ophthalmologist for myopia and astigmatism; she was also investigated for sudden onset mild bilateral cortical cataracts. She was obese (BMI = 27); her psychomotor development corresponded to her age.

### 4.2. Clinical Investigations and Sequence Analyses

Urate and creatinine levels were measured as described previously [51] using a specific enzymatic method and the Jaffé reaction, which was adapted for an auto-analyzer (Hitachi Automatic Analyzer 902; Roche, Basel, Switzerland). Metabolic investigations of purine metabolism (hypoxanthine and xanthine levels in urine) were also conducted using a method established in a previous study [51]. The proband was screened for metabolic (e.g., glycogen storage disease, hereditary fructose intolerance, and mitochondrial disorders) and kidney disease associated with hyperuricemia (e.g., uromodulin-associated disorders), using our previously published diagnostic algorithm [29].

All coding regions and exon-intron boundaries in *ABCG2* and *GLUT9/SLC2A9*, and exons 7 and 9 in *URAT1/SLC22A12* were analyzed from genomic DNA, as described previously [29,33,52]. The reference sequence for *ABCG2* was defined as version ENST00000237612.7 (location: Chromosome 4: 88,090,269–88,158,912 reverse strand) ([www.ensembl.org](http://www.ensembl.org) (accessed on 30 November 2020)). For *GLUT9/SLC2A9* (NM\_020041.2; NP\_064425.2; SNP source dbSNP 132) and *URAT1/SLC22A12* (NM\_144585.3), the reference genomic sequence was defined as version NC\_000004.12 (Chromosome 4: 9,771,153–10,054,936) and NC\_000011.8 (Chromosome 11: 64,114,688–64,126,396), respectively.

It is worth special mention that the world's highest frequency of the main dysfunctional variants of URAT1, p.T467M (MAF, 5.6%) and p.L415\_G417del (MAF, 1.9%), was recently identified in a Roma population (1,016 individuals) from specific regions of the Czech Republic, Slovakia, and Spain [33,53]. According to MAF data from the Exome Aggregation Consortium, p.T467M (rs200104135) showed only one heterozygous allele in a cohort of 15,296 in a South Asian population (MAF, 0.003%) and no occurrence in other ethnic populations; no occurrence of the p.L415\_G417del allele was seen in the whole population, which supports the Roma-specific prevalence of these two URAT1 variants. For this reason, we looked for both URAT1 variants and confirmed that neither variant was present in our studied family.

#### 4.3. Materials

ATP, AMP, creatine phosphate disodium salt tetrahydrate, and creatine phosphokinase type I from rabbit muscle were purchased from Sigma-Aldrich (St. Louis, MO, USA), and [8-<sup>14</sup>C]-uric acid (55 mCi/mmol) was purchased from American Radiolabeled Chemicals (St. Louis, MO, USA). All other chemicals were commercially available and of analytical grade.

#### 4.4. Preparation of ABCG2 Variants Expression Vector

To express human ABCG2 (NM\_004827.3) fused with EGFP at its N-terminus (EGFP-ABCG2) and EGFP (control), we used an ABCG2/pEGFP-C1 plasmid (open reading frame of ABCG2 was inserted into the *Hind*III and the *Apa* I sites of a pEGFP-C1 vector plasmid) that was from our previous study [32]. Of note, the functionality and expression of such construct were confirmed by previous studies we and other groups conducted [32,36,54–56]. Using a site-directed mutagenesis technique, the ABCG2 p.M131I (c.393G>T)/pEGFP-C1 plasmid and the ABCG2 R236X (c.706C>T)/pEGFP-C1 plasmid were generated from an ABCG2 WT/pEGFP-C1 plasmid, respectively. The introduction of each mutation was confirmed by full sequencing using BigDye Terminator v3.1 (Applied Biosystems, Foster City, CA, USA) and an Applied Biosystems 3130 Genetic Analyzer (Applied Biosystems), as described previously [40].

#### 4.5. Cell Culture and Transfection

Human embryonic kidney 293 cell-derived 293A cells were purchased from Life Technologies (Carlsbad, CA, USA) and cultured in Dulbecco's Modified Eagle's Medium (DMEM; Nacalai Tesque, Kyoto, Japan) supplemented with 10% fetal bovine serum (Life Technologies), 1% penicillin/streptomycin, 2 mM L-glutamine (Nacalai Tesque), and 1 × Non-Essential Amino Acid (Life Technologies) at 37 °C in an atmosphere of 5% CO<sub>2</sub>. Each vector plasmid for ABCG2 WT, p.M131I, or p.R236X was transfected into 293A cells by using polyethyleneimine MAX (PEI-MAX; 1 mg/mL in milli-Q water, pH 7.0; Polysciences, Warrington, PA, USA) as described previously [57]. The amount of plasmid DNA used for transfection was adjusted per sample group.

#### 4.6. Preparation of Whole-Cell Lysates

Forty-eight hours after transfection, whole-cell lysates were prepared in ice-cold lysis buffer A containing 50 mM Tris/HCl (pH 7.4), 1 mM dithiothreitol, 1% (w/v) Triton X-100, and a protease inhibitor cocktail for general use (Nacalai Tesque) as described

previously [58]. The protein concentration of the whole cell lysate was quantified using a BCA Protein Assay Kit (Pierce, Rockford, IL, USA) with bovine serum albumin (BSA) as a standard according to the manufacturer's protocol. Before glycosidase treatment, the whole cell lysate samples were incubated with PNGase F (New England Biolabs Japan, Tokyo, Japan) (1.25 U/ $\mu$ g of protein) at 37 °C for 10 min as described previously [59], and then subjected to immunoblotting.

#### 4.7. Preparation of ABCG2-Expressing Plasma Membrane Vesicles

Plasma membrane vesicles were prepared from ABCG2-expressing 293A cells, as described previously [36]. The resulting plasma membrane vesicles were rapidly frozen in liquid N<sub>2</sub> and kept at −80 °C until used. The protein concentration of the plasma membrane vesicles was measured using a BCA Protein Assay Kit, as described above.

#### 4.8. Immunoblotting

Expression of ABCG2 protein in whole-cell lysates and plasma membrane vesicles was assessed using immunoblotting as described previously [36], with minor modifications. In brief, the prepared samples were mixed with a sodium dodecyl sulfate-polyacrylamide gel electrophoresis sample buffer solution containing 10% 2-mercaptoethanol, separated by electrophoresis on polyacrylamide gels, and then transferred to Polyvinylidene Difluoride membranes (Immobilon; Millipore, Billerica, MA, USA) by electroblotting at 15 V for 60 min. For blocking, the membrane was incubated in Tris-buffered saline containing 0.05% Tween 20 and 3% BSA (Nacalai Tesque) (TBST-3% BSA). After overnight incubation at room temperature, blots were probed with rabbit anti-EGFP polyclonal antibodies (A11122; Life Technologies; diluted 1,500 fold in TBST-0.1% BSA), a rabbit anti- $\alpha$ -tubulin antibodies (ab15246; Abcam, Cambridge, MA, USA; diluted 1,000 fold), or a rabbit anti-Na<sup>+</sup>/K<sup>+</sup>-ATPase  $\alpha$  antibodies (sc-28800; Santa Cruz Biotechnology, Santa Cruz, CA, USA; diluted 1,000 fold) followed by incubation with a donkey anti-rabbit immunoglobulin G (IgG)-horseradish peroxidase (HRP)-conjugated antibody (NA934V; diluted 4,000 fold for EGFP-ABCG2 or 3,000 fold for  $\alpha$ -tubulin and Na<sup>+</sup>/K<sup>+</sup>-ATPase). HRP-dependent luminescence was developed using ECL<sup>TM</sup> Prime Western Blotting Detection Reagent (GE Healthcare UK, Buckinghamshire, UK) and detected using a multi-imaging Fusion Solo 4<sup>TM</sup> analyzer system (Vilber Lourmat, Eberhardzell, Germany).

#### 4.9. Confocal Laser Scanning Microscopic Observation

For confocal laser scanning microscopy, 48 h after transfection, 293A cells were fixed with ice-cold methanol for 10 min, and then the nuclei were visualized with TO-PRO-3 Iodide (Molecular Probes, Eugene, OR, USA) as described previously [36]. To analyze the localization of EGFP-fused ABCG2 protein, fluorescence was detected using an FV10i Confocal Laser Scanning Microscope (Olympus, Tokyo, Japan).

#### 4.10. Urate Transport Assay

The urate transport assay, with ABCG2-expressing plasma membrane vesicles, was conducted using a rapid filtration technique described in our previous studies [27,36], with some minor modifications. In brief, each plasma membrane vesicle (0.5 mg/mL) was incubated with 20  $\mu$ M of radiolabeled urate in a reaction mixture (total 20  $\mu$ L: 10 mM Tris/HCl, 250 mM sucrose, 10 mM MgCl<sub>2</sub>, 10 mM creatine phosphate, 1 mg/ml creatine phosphokinase, pH 7.4, and 50 mM ATP, or AMP as an ATP substitute) for 10 min at 37 °C. After incubation, the reaction mixture was mixed with 980  $\mu$ L of ice-cold stop buffer (2 mM EDTA, 0.25 M sucrose, 0.1 M NaCl, 10 mM Tris-HCl, at a of pH 7.4); the resulting solution was rapidly filtered through an MF-Millipore Membrane (HAWP02500; 0.45  $\mu$ m pore size and 25 mm diameter; Millipore). After washing with 5 ml of ice-cold stop buffer five times, the plasma membrane vesicles on the filter were dissolved in Clear-sol II (Nacalai Tesque). Then, the radioactivity in the plasma membrane vesicles was measured using a liquid scintillator (Tri-Carb 3110TR; PerkinElmer, Waltham, MA, USA).



The urate transport activity was calculated as the incorporated clearance ( $\mu\text{L}/\text{mg}$  protein/min) defined as the incorporated level of urate [disintegrations per minute (DPM)/mg protein/min]/urate level in the incubation mixture [DPM/ $\mu\text{L}$ ]. ATP-dependent urate transport was calculated by subtracting the urate transport activity in the absence of ATP from that in the presence of ATP; ABCG2-mediated urate transport activity was calculated by subtracting ATP-dependent urate transport activity of control plasma membrane vesicles from that of ABCG2-expressing plasma membrane vesicles.

#### 4.11. Statistical Analysis

All statistical analyses were performed by using EXCEL 2019 (Microsoft, Redmond, WA, USA) with Statcel4 add-in software (OMS publishing, Saitama, Japan). The number of biological replicates ( $n$ ) is described in the figure legends. In single pairs of quantitative data, after comparing the variances of a data set (using the  $F$ -test), an unpaired Student's  $t$ -test was performed. Statistical significance was defined in terms of  $P$  values less than 0.05 or 0.01.

**Author Contributions:** Conceptualization, Y.T., T.T., and B.S.; validation, Y.T., Y.K., and B.S.; formal analysis, Y.T.; investigation, Y.T., K.P., J.B., P.J., and Y.K. (i.e., Y.T. performed the experimental work using mammalian cells and analyzed the data; Y.K. supported the experimental work; K.P. and J.B. conducted sequencing analyses for clinical samples; P.J. was responsible for clinical observations; Y.T. performed statistical analyses); data curation, Y.T., T.T., and B.S.; writing—original draft preparation, Y.T., and B.S.; writing—review and editing, Y.T., T.T., and B.S.; supervision, H.S. and B.S.; project administration, B.S.; funding acquisition, Y.T., T.T., and B.S. All authors have read and agreed to the published version of the manuscript.

**Funding:** The study was supported by the JSPS KAKENHI Grant, numbers 19K16441 (to Y.T.); 16H01808, 18KK0247, and 20H00568 (to T.T.). The study was also supported by grants from the Czech Republic Ministry of Health RVO 00023728 (Institute of Rheumatology), RVO VFN64165, and BBMRI-CZ LM2018125 (to B.S.); T.T. received research grants from “Gout and uric acid foundation of Japan”; “Takeda Science Foundation”; “Suzuken Memorial Foundation”; “Mochida Memorial Foundation for Medical and Pharmaceutical Research”; “The Pharmacological Research Foundation, Tokyo.”

**Institutional Review Board Statement:** The studied proband and her family members were Czechs of Roma ethnicity diagnosed with familial (early-onset) hyperuricemia/gout. Written informed consent was obtained from each subject before enrollment in the study. All tests were performed in accordance with standards set by the institutional ethics committees, which approved the project (no. 6181/2015). All the procedures were performed in accordance with the Declaration of Helsinki.

**Informed Consent Statement:** Informed consent was obtained from all subjects involved in the study.

**Data Availability Statement:** Data supporting the findings of this study are included in this published article or are available from the corresponding author on reasonable request.

**Acknowledgments:** We would like to express our appreciation to all who took part in this study.

**Conflicts of Interest:** The authors declare no conflict of interest.

#### Abbreviations

ABCG2	ATP-binding cassette transporter G2
ATP	Adenosine triphosphate
FE-UA	Fractional excretion of uric acid
GLUT9	Glucose transporter 9
MAF	Minor allele frequency
SUA	Serum uric acid
URAT1	Urate transporter 1
WT	Wild-type

## References

1. Dalbeth, N.; Choi, H.K.; Joosten, L.A.B.; Khanna, P.P.; Matsuo, H.; Perez-Ruiz, F.; Stamp, L.K. Gout. *Nat. Rev. Dis. Primers* **2019**, *5*, 69. [[CrossRef](#)]
2. Kawamura, Y.; Nakaoka, H.; Nakayama, A.; Okada, Y.; Yamamoto, K.; Higashino, T.; Sakiyama, M.; Shimizu, T.; Ooyama, H.; Ooyama, K.; et al. Genome-wide association study revealed novel loci which aggravate asymptomatic hyperuricaemia into gout. *Ann. Rheum. Dis.* **2019**, *78*, 1430–1437. [[CrossRef](#)]
3. Dehlin, M.; Jacobsson, L.; Roddy, E. Global epidemiology of gout: Prevalence, incidence, treatment patterns and risk factors. *Nat. Rev. Rheumatol.* **2020**, *16*, 380–390. [[CrossRef](#)] [[PubMed](#)]
4. Kuo, C.F.; Grainge, M.J.; See, L.C.; Yu, K.H.; Luo, S.F.; Zhang, W.; Doherty, M. Epidemiology and management of gout in Taiwan: A nationwide population study. *Arthritis Res. Ther.* **2015**, *17*, 13. [[CrossRef](#)]
5. Pascart, T.; Norberciak, L.; Ea, H.K.; Guggenbuhl, P.; Liote, F. Patients with early-onset gout and development of earlier severe joint involvement and metabolic comorbid conditions: Results from a cross-sectional epidemiologic survey. *Arthritis Care Res.* **2019**, *71*, 986–992. [[CrossRef](#)] [[PubMed](#)]
6. Zhang, B.; Fang, W.; Zeng, X.; Zhang, Y.; Ma, Y.; Sheng, F.; Zhang, X. Clinical characteristics of early- and late-onset gout: A cross-sectional observational study from a Chinese gout clinic. *Medicine* **2016**, *95*, e5425. [[CrossRef](#)] [[PubMed](#)]
7. Enomoto, A.; Kimura, H.; Chairoungdua, A.; Shigeta, Y.; Jutabha, P.; Cha, S.H.; Hosoyamada, M.; Takeda, M.; Sekine, T.; Igarashi, T.; et al. Molecular identification of a renal urate anion exchanger that regulates blood urate levels. *Nature* **2002**, *417*, 447–452. [[CrossRef](#)]
8. Matsuo, H.; Chiba, T.; Nagamori, S.; Nakayama, A.; Domoto, H.; Phetdee, K.; Wiriyasermkul, P.; Kikuchi, Y.; Oda, T.; Nishiyama, J.; et al. Mutations in glucose transporter 9 gene SLC2A9 cause renal hypouricemia. *Am. J. Hum. Genet.* **2008**, *83*, 744–751. [[CrossRef](#)]
9. Vitart, V.; Rudan, I.; Hayward, C.; Gray, N.K.; Floyd, J.; Palmer, C.N.; Knott, S.A.; Kolcic, I.; Polasek, O.; Graessler, J.; et al. SLC2A9 is a newly identified urate transporter influencing serum urate concentration, urate excretion and gout. *Nat. Genet.* **2008**, *40*, 437–442. [[CrossRef](#)] [[PubMed](#)]
10. Ichida, K.; Matsuo, H.; Takada, T.; Nakayama, A.; Murakami, K.; Shimizu, T.; Yamanashi, Y.; Kasuga, H.; Nakashima, H.; Nakamura, T.; et al. Decreased extra-renal urate excretion is a common cause of hyperuricemia. *Nat. Commun.* **2012**, *3*, 764. [[CrossRef](#)]
11. Woodward, O.M.; Kottgen, A.; Coresh, J.; Boerwinkle, E.; Guggino, W.B.; Kottgen, M. Identification of a urate transporter, ABCG2, with a common functional polymorphism causing gout. *Proc. Natl. Acad. Sci. USA* **2009**, *106*, 10338–10342. [[CrossRef](#)] [[PubMed](#)]
12. Matsuo, H.; Takada, T.; Ichida, K.; Nakamura, T.; Nakayama, A.; Ikebuchi, Y.; Ito, K.; Kusanagi, Y.; Chiba, T.; Tadokoro, S.; et al. Common defects of ABCG2, a high-capacity urate exporter, cause gout: A function-based genetic analysis in a Japanese population. *Sci. Transl. Med.* **2009**, *1*, 5ra11. [[CrossRef](#)]
13. Hoque, K.M.; Dixon, E.E.; Lewis, R.M.; Allan, J.; Gamble, G.D.; Phipps-Green, A.J.; Halperin Kuhns, V.L.; Horne, A.M.; Stamp, L.K.; Merriman, T.R.; et al. The ABCG2 Q141K hyperuricemia and gout associated variant illuminates the physiology of human urate excretion. *Nat. Commun.* **2020**, *11*, 2767. [[CrossRef](#)]
14. Major, T.J.; Dalbeth, N.; Stahl, E.A.; Merriman, T.R. An update on the genetics of hyperuricaemia and gout. *Nat. Rev. Rheumatol.* **2018**, *14*, 341–353. [[CrossRef](#)]
15. Nakayama, A.; Matsuo, H.; Nakaoka, H.; Nakamura, T.; Nakashima, H.; Takada, Y.; Oikawa, Y.; Takada, T.; Sakiyama, M.; Shimizu, S.; et al. Common dysfunctional variants of ABCG2 have stronger impact on hyperuricemia progression than typical environmental risk factors. *Sci. Rep.* **2014**, *4*, 5227. [[CrossRef](#)] [[PubMed](#)]
16. Vlaming, M.L.; Lagas, J.S.; Schinkel, A.H. Physiological and pharmacological roles of ABCG2 (BCRP): Recent findings in Abcg2 knockout mice. *Adv. Drug Deliv. Rev.* **2009**, *61*, 14–25. [[CrossRef](#)] [[PubMed](#)]
17. Robey, R.W.; To, K.K.; Polgar, O.; Dohse, M.; Fetsch, P.; Dean, M.; Bates, S.E. ABCG2: A perspective. *Adv. Drug Deliv. Rev.* **2009**, *61*, 3–13. [[CrossRef](#)]
18. Sarkadi, B.; Homolya, L.; Hegedus, T. The ABCG2/BCRP transporter and its variants—From structure to pathology. *FEBS Lett.* **2020**, *594*, 4012–4034. [[CrossRef](#)]
19. Allikmets, R.; Schriml, L.M.; Hutchinson, A.; Romano-Spica, V.; Dean, M. A human placenta-specific ATP-binding cassette gene (ABCP) on chromosome 4q22 that is involved in multidrug resistance. *Cancer Res.* **1998**, *58*, 5337–5339.
20. Doyle, L.A.; Yang, W.; Abruzzo, L.V.; Krogmann, T.; Gao, Y.; Rishi, A.K.; Ross, D.D. A multidrug resistance transporter from human MCF-7 breast cancer cells. *Proc. Natl. Acad. Sci. USA* **1998**, *95*, 15665–15670. [[CrossRef](#)]
21. Miyake, K.; Mickley, L.; Litman, T.; Zhan, Z.; Robey, R.; Cristensen, B.; Brangi, M.; Greenberger, L.; Dean, M.; Fojo, T.; et al. Molecular cloning of cDNAs which are highly overexpressed in mitoxantrone-resistant cells: Demonstration of homology to ABC transport genes. *Cancer Res.* **1999**, *59*, 8–13. [[PubMed](#)]
22. Takada, T.; Yamamoto, T.; Matsuo, H.; Tan, J.K.; Ooyama, K.; Sakiyama, M.; Miyata, H.; Yamanashi, Y.; Toyoda, Y.; Higashino, T.; et al. Identification of ABCG2 as an exporter of uremic toxin indoxyl sulfate in mice and as a crucial factor influencing CKD progression. *Sci. Rep.* **2018**, *8*, 11147. [[CrossRef](#)]
23. Heyes, N.; Kapoor, P.; Kerr, I.D. Polymorphisms of the multidrug pump ABCG2: A systematic review of their effect on protein expression, function, and drug pharmacokinetics. *Drug Metab. Dispos. Biol. Fate Chem.* **2018**, *46*, 1886–1899. [[CrossRef](#)] [[PubMed](#)]

24. Stiburkova, B.; Pavelcova, K.; Zavada, J.; Petru, L.; Simek, P.; Cepek, P.; Pavlikova, M.; Matsuo, H.; Merriman, T.R.; Pavelka, K. Functional non-synonymous variants of ABCG2 and gout risk. *Rheumatology* **2017**, *56*, 1982–1992. [[CrossRef](#)] [[PubMed](#)]
25. Higashino, T.; Takada, T.; Nakaoka, H.; Toyoda, Y.; Stiburkova, B.; Miyata, H.; Ikebuchi, Y.; Nakashima, H.; Shimizu, S.; Kawaguchi, M.; et al. Multiple common and rare variants of ABCG2 cause gout. *RMD Open* **2017**, *3*, e000464. [[CrossRef](#)]
26. Maekawa, K.; Itoda, M.; Sai, K.; Saito, Y.; Kaniwa, N.; Shirao, K.; Hamaguchi, T.; Kunitoh, H.; Yamamoto, N.; Tamura, T.; et al. Genetic variation and haplotype structure of the ABC transporter gene ABCG2 in a Japanese population. *Drug Metab. Pharmacokinet.* **2006**, *21*, 109–121. [[CrossRef](#)]
27. Matsuo, H.; Ichida, K.; Takada, T.; Nakayama, A.; Nakashima, H.; Nakamura, T.; Kawamura, Y.; Takada, Y.; Yamamoto, K.; Inoue, H.; et al. Common dysfunctional variants in ABCG2 are a major cause of early-onset gout. *Sci. Rep.* **2013**, *3*, 2014. [[CrossRef](#)] [[PubMed](#)]
28. Zaidi, F.; Narang, R.K.; Phipps-Green, A.; Gamble, G.G.; Tausche, A.K.; So, A.; Riches, P.; Andres, M.; Perez-Ruiz, F.; Doherty, M.; et al. Systematic genetic analysis of early-onset gout: ABCG2 is the only associated locus. *Rheumatology* **2020**, *59*, 2544–2549. [[CrossRef](#)]
29. Stiburkova, B.; Pavelcova, K.; Pavlikova, M.; Jesina, P.; Pavelka, K. The impact of dysfunctional variants of ABCG2 on hyperuricemia and gout in pediatric-onset patients. *Arthritis Res. Ther.* **2019**, *21*, 77. [[CrossRef](#)]
30. Hurba, O.; Mancikova, A.; Krylov, V.; Pavlikova, M.; Pavelka, K.; Stiburkova, B. Complex analysis of urate transporters SLC2A9, SLC22A12 and functional characterization of non-synonymous allelic variants of GLUT9 in the Czech population: No evidence of effect on hyperuricemia and gout. *PLoS ONE* **2014**, *9*, e107902. [[CrossRef](#)]
31. Pavelcova, K.; Bohata, J.; Pavlikova, M.; Bubenikova, E.; Pavelka, K.; Stiburkova, B. Evaluation of the influence of genetic variants of SLC2A9 (GLUT9) and SLC22A12 (URAT1) on the development of hyperuricemia and gout. *J. Clin. Med.* **2020**, *9*, 2510. [[CrossRef](#)]
32. Toyoda, Y.; Pavelcova, K.; Klein, M.; Suzuki, H.; Takada, T.; Stiburkova, B. Familial early-onset hyperuricemia and gout associated with a newly identified dysfunctional variant in urate transporter ABCG2. *Arthritis Res. Ther.* **2019**, *21*, 219. [[CrossRef](#)] [[PubMed](#)]
33. Stiburkova, B.; Sebesta, I.; Ichida, K.; Nakamura, M.; Hulkova, H.; Krylov, V.; Kryspinova, L.; Jahnova, H. Novel allelic variants and evidence for a prevalent mutation in URAT1 causing renal hypouricemia: Biochemical, genetics and functional analysis. *Eur. J. Hum. Genet.* **2013**, *21*, 1067–1073. [[CrossRef](#)] [[PubMed](#)]
34. Toyoda, Y.; Takada, T.; Suzuki, H. Inhibitors of human ABCG2: From technical background to recent updates with clinical implications. *Front. Pharmacol.* **2019**, *10*, 208. [[CrossRef](#)]
35. Miyata, H.; Takada, T.; Toyoda, Y.; Matsuo, H.; Ichida, K.; Suzuki, H. Identification of febuxostat as a new strong ABCG2 inhibitor: Potential applications and risks in clinical situations. *Front. Pharmacol.* **2016**, *7*, 518. [[CrossRef](#)]
36. Toyoda, Y.; Mancikova, A.; Krylov, V.; Morimoto, K.; Pavelcova, K.; Bohata, J.; Pavelka, K.; Pavlikova, M.; Suzuki, H.; Matsuo, H.; et al. Functional characterization of clinically-relevant rare variants in ABCG2 identified in a gout and hyperuricemia cohort. *Cells* **2019**, *8*, 363. [[CrossRef](#)]
37. Manolaridis, I.; Jackson, S.M.; Taylor, N.M.I.; Kowal, J.; Stahlberg, H.; Locher, K.P. Cryo-EM structures of a human ABCG2 mutant trapped in ATP-bound and substrate-bound states. *Nature* **2018**, *563*, 426–430. [[CrossRef](#)]
38. Nakagawa, H.; Toyoda, Y.; Wakabayashi-Nakao, K.; Tamaki, H.; Osumi, M.; Ishikawa, T. Ubiquitin-mediated proteasomal degradation of ABC transporters: A new aspect of genetic polymorphisms and clinical impacts. *J. Pharm. Sci.* **2011**, *100*, 3602–3619. [[CrossRef](#)]
39. Eckenstaler, R.; Benndorf, R.A. 3D structure of the transporter ABCG2—What's new? *Br. J. Pharmacol.* **2020**, *177*, 1485–1496. [[CrossRef](#)] [[PubMed](#)]
40. Toyoda, Y.; Takada, T.; Miyata, H.; Ishikawa, T.; Suzuki, H. Regulation of the axillary osmidrosis-associated ABCC11 protein stability by N-linked glycosylation: Effect of glucose condition. *PLoS ONE* **2016**, *11*, e0157172. [[CrossRef](#)] [[PubMed](#)]
41. Morar, B.; Gresham, D.; Angelicheva, D.; Tournev, I.; Gooding, R.; Guerguelcheva, V.; Schmidt, C.; Abicht, A.; Lochmuller, H.; Tordai, A.; et al. Mutation history of the Roma/Gypsies. *Am. J. Hum. Genet.* **2004**, *75*, 596–609. [[CrossRef](#)] [[PubMed](#)]
42. Kalaydjieva, L.; Morar, B.; Chaix, R.; Tang, H. A newly discovered founder population: The Roma/Gypsies. *Bioessays* **2005**, *27*, 1084–1094. [[CrossRef](#)]
43. Roberts, R.L.; Wallace, M.C.; Phipps-Green, A.J.; Topless, R.; Drake, J.M.; Tan, P.; Dalbeth, N.; Merriman, T.R.; Stamp, L.K. ABCG2 loss-of-function polymorphism predicts poor response to allopurinol in patients with gout. *Pharm. J.* **2017**, *17*, 201–203. [[CrossRef](#)]
44. Wen, C.C.; Yee, S.W.; Liang, X.; Hoffmann, T.J.; Kvale, M.N.; Banda, Y.; Jorgenson, E.; Schaefer, C.; Risch, N.; Giacomini, K.M. Genome-wide association study identifies ABCG2 (BCRP) as an allopurinol transporter and a determinant of drug response. *Clin. Pharmacol. Ther.* **2015**, *97*, 518–525. [[CrossRef](#)]
45. Horvathova, V.; Bohata, J.; Pavlikova, M.; Pavelcova, K.; Pavelka, K.; Senolt, L.; Stiburkova, B. Interaction of the p.Q141K variant of the ABCG2 gene with clinical data and cytokine levels in primary hyperuricemia and gout. *J. Clin. Med.* **2019**, *8*, 1965. [[CrossRef](#)]
46. Lehtisalo, M.; Keskitalo, J.E.; Tornio, A.; Lapatto-Reiniluoto, O.; Deng, F.; Jaatinen, T.; Viinamaki, J.; Neuvonen, M.; Backman, J.T.; Niemi, M. Febuxostat, but not allopurinol, markedly raises the plasma concentrations of the breast cancer resistance protein substrate rosuvastatin. *Clin. Transl. Sci.* **2020**, *13*, 1236–1243. [[CrossRef](#)] [[PubMed](#)]

47. Mackenzie, I.S.; Ford, I.; Nuki, G.; Hallas, J.; Hawkey, C.J.; Webster, J.; Ralston, S.H.; Walters, M.; Robertson, M.; De Caterina, R.; et al. Long-term cardiovascular safety of febuxostat compared with allopurinol in patients with gout (FAST): A multicentre, prospective, randomised, open-label, non-inferiority trial. *Lancet* **2020**, *396*, 1745–1757. [[CrossRef](#)]
48. Stiburkova, B.; Bleyer, A.J. Changes in serum urate and urate excretion with age. *Adv. Chronic Kidney Dis.* **2012**, *19*, 372–376. [[CrossRef](#)]
49. Higashino, T.; Morimoto, K.; Nakaoka, H.; Toyoda, Y.; Kawamura, Y.; Shimizu, S.; Nakamura, T.; Hosomichi, K.; Nakayama, A.; Ooyama, K.; et al. Dysfunctional missense variant of OAT10/SLC22A13 decreases gout risk and serum uric acid levels. *Ann. Rheum. Dis.* **2020**, *79*, 164–166. [[CrossRef](#)]
50. Wallace, S.L.; Robinson, H.; Masi, A.T.; Decker, J.L.; McCarty, D.J.; Yu, T.F. Preliminary criteria for the classification of the acute arthritis of primary gout. *Arthritis Rheum.* **1977**, *20*, 895–900. [[CrossRef](#)] [[PubMed](#)]
51. Mraz, M.; Hurba, O.; Bartl, J.; Dolezel, Z.; Marinaki, A.; Fairbanks, L.; Stiburkova, B. Modern diagnostic approach to hereditary xanthinuria. *Urolithiasis* **2015**, *43*, 61–67. [[CrossRef](#)] [[PubMed](#)]
52. Stiburkova, B.; Ichida, K.; Sebesta, I. Novel homozygous insertion in SLC2A9 gene caused renal hypouricemia. *Mol. Genet. Metab.* **2011**, *102*, 430–435. [[CrossRef](#)]
53. Stiburkova, B.; Gabrikova, D.; Cepek, P.; Simek, P.; Kristian, P.; Cordoba-Lanus, E.; Claverie-Martin, F. Prevalence of URAT1 allelic variants in the Roma population. *Nucleosides Nucleotides Nucleic Acids* **2016**, *35*, 529–535. [[CrossRef](#)] [[PubMed](#)]
54. Khunweeraphong, N.; Szollosi, D.; Stockner, T.; Kuchler, K. The ABCG2 multidrug transporter is a pump gated by a valve and an extracellular lid. *Nat. Commun.* **2019**, *10*, 5433. [[CrossRef](#)] [[PubMed](#)]
55. Orban, T.I.; Seres, L.; Ozvegy-Laczka, C.; Elkind, N.B.; Sarkadi, B.; Homolya, L. Combined localization and real-time functional studies using a GFP-tagged ABCG2 multidrug transporter. *Biochem. Biophys. Res. Commun.* **2008**, *367*, 667–673. [[CrossRef](#)]
56. Takada, T.; Suzuki, H.; Sugiyama, Y. Characterization of polarized expression of point- or deletion-mutated human BCRP/ABCG2 in LLC-PK1 cells. *Pharm. Res.* **2005**, *22*, 458–464. [[CrossRef](#)]
57. Stiburkova, B.; Miyata, H.; Zavada, J.; Tomcik, M.; Pavelka, K.; Storkanova, G.; Toyoda, Y.; Takada, T.; Suzuki, H. Novel dysfunctional variant in ABCG2 as a cause of severe tophaceous gout: Biochemical, molecular genetics and functional analysis. *Rheumatology* **2016**, *55*, 191–194. [[CrossRef](#)]
58. Toyoda, Y.; Sakurai, A.; Mitani, Y.; Nakashima, M.; Yoshiura, K.; Nakagawa, H.; Sakai, Y.; Ota, I.; Lezhava, A.; Hayashizaki, Y.; et al. Earwax, osmidrosis, and breast cancer: Why does one SNP (538G>A) in the human ABC transporter ABCC11 gene determine earwax type? *FASEB J.* **2009**, *23*, 2001–2013. [[CrossRef](#)]
59. Nakagawa, H.; Wakabayashi-Nakao, K.; Tamura, A.; Toyoda, Y.; Koshihara, S.; Ishikawa, T. Disruption of N-linked glycosylation enhances ubiquitin-mediated proteasomal degradation of the human ATP-binding cassette transporter ABCG2. *FEBS J.* **2009**, *276*, 7237–7252. [[CrossRef](#)] [[PubMed](#)]

Article

# Interaction of the p.Q141K Variant of the *ABCG2* Gene with Clinical Data and Cytokine Levels in Primary Hyperuricemia and Gout

Veronika Horváthová<sup>1,2,†</sup>, Jana Bohatá<sup>1,3,†</sup> , Markéta Pavlíková<sup>4</sup>, Kateřina Pavelcová<sup>1,3</sup>, Karel Pavelka<sup>1,3</sup>, Ladislav Šenolt<sup>1,3</sup> and Blanka Stibůrková<sup>1,3,5,\*</sup>

<sup>1</sup> Institute of Rheumatology, 128 50 Prague, Czech Republic; veronika@horvath.cz (V.H.); bohata@revma.cz (J.B.); pavelcova@revma.cz (K.P.); pavelka@revma.cz (K.P.); senolt@revma.cz (L.Š.)

<sup>2</sup> Faculty of Science, Charles University, 128 00 Prague, Czech Republic

<sup>3</sup> Department of Rheumatology, First Faculty of Medicine, Charles University, 128 50 Prague, Czech Republic

<sup>4</sup> Department of Probability and Mathematical Statistics, Faculty of Mathematics and Physics, Charles University, 186 75 Prague, Czech Republic; marketa@ucw.cz

<sup>5</sup> Department of Pediatrics and Adolescent Medicine, First Faculty of Medicine, Charles University, General University Hospital in Prague, 120 00 Prague, Czech Republic

\* Correspondence: stiburkova@revma.cz; Tel.: +420-234-075-319; Fax: +420-224-914-451

† They declare the equal contribution.

Received: 7 October 2019; Accepted: 11 November 2019; Published: 14 November 2019



**Abstract:** Gout is an inflammatory arthritis influenced by environmental risk factors and genetic variants. The common dysfunctional p.Q141K allele of the *ABCG2* gene affects gout development. We sought after the possible association between the p.Q141K variant and gout risk factors, biochemical, and clinical determinants in hyperuricemic, gouty, and acute gouty arthritis cohorts. Further, we studied the correlation of p.Q141K allele and levels of pro-/anti-inflammatory cytokines. Coding regions of the *ABCG2* gene were analyzed in 70 primary hyperuricemic, 182 gout patients, and 132 normouricemic individuals. Their genotypes were compared with demographic and clinical parameters. Plasma levels of 27 cytokines were determined using a human multiplex cytokine assay. The p.Q141K variant was observed in younger hyperuricemic/gout individuals ( $p = 0.0003$ ), which was associated with earlier disease onset ( $p = 0.004$ ), trend toward lower BMI ( $p = 0.056$ ), and C-reactive protein (CRP,  $p = 0.007$ ) but a higher glomerular filtration rate (GFR,  $p = 0.035$ ). Levels of 19 cytokines were higher, mainly in patients with acute gouty arthritis ( $p < 0.001$ ), irrespective of the presence of the p.Q141K variant. The p.Q141K variant influences the age of onset of primary hyperuricemia or gout and other disease-linked risk factors and symptoms. There was no association with cytokine levels in the circulation.

**Keywords:** p.Q141K; *ABCG2*; cytokines; gout; hyperuricemia; acute gouty arthritis

## 1. Introduction

Gout is the most common type of inflammatory arthritis in adults that develops as a consequence of elevated urate levels. Gout has four phases: asymptomatic hyperuricemia, acute gouty arthritis, intercritical gout, and chronic tophaceous gout [1]. The attacks are caused by an inflammatory response to monosodium urate (MSU) crystals that deposit in joints, tendons, and surrounding tissues. Before the development of gout, patients show asymptomatic hyperuricemia (elevated levels of serum uric acid  $>420 \mu\text{mol/L}$  for men and  $>360 \mu\text{mol/L}$  for women). Not all individuals with hyperuricemia develop symptomatic gout, but the risk increases in proportion to the elevation of urate in circulation.

Heritability of serum urate levels and gout in Europeans has been estimated to be approximately 30% [2].

The mechanism of gouty inflammation is coupled with the formation and activation of the NOD-like receptor P3 (NLRP3) inflammasome with subsequent production of pro-inflammatory cytokines. MSU crystals by themselves are not responsible for the induction of expression and assembly of inflammasome components. The first signal involves priming monocyte-derived macrophages, which then start binding ligands (S100A8 and S100A9 proteins, long-chain free fatty acids) to Toll-like receptors (TLR) [3]. The second signal, triggered by MSU crystals, leads to activation of multiprotein intracellular NLRP3 inflammasomes, which contain pro-caspase 1 [4]. Next, active caspase 1 cleaves precursors of interleukins 1 beta and 18 (pro-IL-1 $\beta$  and pro-IL-18) to generate the active forms (IL-1 $\beta$  and IL-18) [5,6]. Secretion of IL-1 $\beta$  leads to recruitment of neutrophils to the site of inflammation, production of additional pro-inflammatory cytokines, and bone/cartilage degradation [3,7]. IL-1 $\beta$  and IL-18 induced other pro-inflammatory cytokines IL-6, IL-8, IL-17, and tumor necrosis factor alpha (TNF $\alpha$ ), which synergistically potentiate gouty inflammation [8–10].

Risk of gout development is conditioned not only by hyperuricemia but also by gender, weight, age, environmental and genetic factors, and their interactions. The main cause of hyperuricemia is a defect in renal excretion of urate. Today 10 genes for the main urate transporters are known, including ATP-binding cassette subfamily G member 2 (*ABCG2*), which has the greatest influence on urate excretion. The *ABCG2* protein is a homodimeric membrane transporter with functions in a variety of tissues, including xenobiotic transport. Many population-specific variants of the *ABCG2* gene have been found e.g., the common non-synonymous variants p.Q126X (rs72552713), p.V12M (rs2231137), and p.Q141K (rs2231142) [11,12]. The p.Q126X variant is specific to East Asian populations and has a well-known genetic impact on gout induction. It decreases *ABCG2* urate transport by 96%. A second common variant in Caucasians is p.V12M, which showed a protective role in gout development and has no influence on urate transport in human embryonic kidney derived cells [13,14]. The missense p.Q141K variant (minor frequency allele (MAF), present in the Central European Caucasian population at around 9.4%) is localized in the nucleotide-binding domain and leads to decreased binding of adenosine triphosphate (ATP) and reduces transport function by almost 50% [14–16]. Carriers of p.Q141K tend to have a higher chance of developing an earlier gout onset and have an increased risk of a poor response to allopurinol [12,17–20]. Moreover, p.Q141K may also influence progression from asymptomatic hyperuricemia to gout by promoting the immune response to MSU crystals. This suggests a hypothetical molecular pathway that connects non-functional variants of urate transporters and the innate immune response [1]. In previous studies, pro-inflammatory cytokines affected *ABCG2* gene expression. Its expression could be upregulated or downregulated by IL-1 $\beta$  and TNF $\alpha$  treatment, either alone or in combination with other biologically active molecules such as estrogen [21–23].

In our previous studies using an *ABCG2* analysis of Czech patients with hyperuricemic/gout, we found that both the rare and common p.Q141K variants are independently associated with hyperuricemia and gout [12,13]. Moreover, we found a significantly higher frequency of the minor allele p.Q141K variant in pediatric-onset patients when compared to adult-onset patients [24]. Our latest published study demonstrated the effects of rare variants on the expression, cellular localization, and function of *ABCG2* [25].

The aim of this study was to analyze (1) the association of the p.Q141K variant with known risk factors of gout (e.g., age, BMI, etc.), (2) the possible link between the risk of the p.Q141K allele and levels of biochemical parameters connected with gout (CRP, estimated glomerular filtration rate calculated using the Modification of Diet in Renal Disease (eGFR-MDRD)), and finally (3) the relationship between the p.Q141K allele and pro-/anti-inflammatory cytokines using human multiplex cytokine assay in patients with primary hyperuricemia, gout, acute gouty arthritis, and normouricemic individuals. Relationships between the p.Q141K variant and cytokine plasma levels were addressed for the first time.

## 2. Experimental Section

### 2.1. Cohort and Subcohorts

The study cohort comprised 182 patients with primary gout (166 males, 16 females; median age = 54 years), including 17 patients (23 samples) having a gout attack, and 70 patients with asymptomatic hyperuricemia (50 males, 20 females; median age = 38 years) from the biobank of the Institute of Rheumatology, Prague, the Czech Republic. Gout patients met the 1977 American Rheumatism Association preliminary classification criteria [26]. Primary hyperuricemic patients were classified as serum uric acid (SUA)  $>420 \mu\text{mol/L}$  for men and  $\text{SUA} > 360 \mu\text{mol/L}$  for women on two measurements. Two repetitive measurements of purine metabolites (xanthine, hypoxanthine, and oxypurinol), serum uric acid (SUA), and biochemical parameters were performed to exclude the impact of purine metabolic disorders in all patients. The first xanthine, hypoxanthine, and oxypurinol metabolites, SUA, and biochemical determination were performed during allopurinol/febuxostat treatment. The second measurement was done before the start of treatment or 72 h after a temporary interruption of SUA lowering therapy. Patients were compared to 132 normouricemic individuals from the general population, with no history of primary hyperuricemia, gout, or autoimmune disease (54 males, 78 females; median age = 41 years). All patients and normouricemic subjects were examined for the functional p.Q141K variant of the *ABCG2* gene, as published previously [13]. All demographic (age of disease onset and age of examination/sampling, sex, body mass index (BMI)), biochemical (SUA with/off treatment, fractional excretion of uric acid (FE-UA), estimated glomerular filtration rate calculated using the Modification of Diet in Renal Disease formula (eGFR-MDRD), serum creatinine, and maximal C-reactive protein (CRP)), genetic (familial occurrence, presence of the wild-type p.Q141K variant (GG), heterozygotic (GT), and homozygotic (TT) form and its MAF) and presence and type of medical treatment characteristics of patients and normouricemic individuals are stated in Table 1. This study was approved by the local ethics committee, and all patients and normouricemic individuals signed informed consent.

**Table 1.** Main demographic, biochemical, and genetic characteristics of the normouricemic (*n* = 132), hyperuricemic (*n* = 70), and gout-suffering subjects (*n* = 182).

	Normouricemic Subjects (N = 132)		Hyperuricemic Patients (N = 69)		Gout Patients (N = 177)		Fisher Test <i>p</i> -Value
	<i>n</i>	%	<i>n</i>	%	<i>n</i>	%	
Sex M/F	54/78	40.9/59.1	50/20	71.4/28.6	166/16	91.2/8.8	<0.0001
Familial occurrence	Not collected		31	50.0	66	63.5	0.0717
No treatment	132	100.0	31	44.3	28	15.4	<0.0001
Allopurinol treatment	Not applicable		39	55.7	137	75.3	
Febuxostat treatment			0	0.0	17	9.3	
p.Q141K, GG	103	86.6/78.0	44	64.7/62.9	100	57.5/56.5	<0.0001
GT	15	12.6/11.4	19	27.9/27.1	66	37.9/37.3	
TT	1	0.8/0.8	5	7.4/7.1	8	4.6/4.5	
no data	13	9.8	2	2.9	2	1.7	
p.Q141K, MAF	17	7.1	29	21.3	90	25	<0.0001
Data on interleukins subjects/measurements	132/132		44/53		132/149/23 during attack		
	Median (IQR)	Range	Median (IQR)	Range	Median (IQR)	Range	KW Test <i>p</i> -Value
Age of onset, years	Not applicable		28.5 (39.2)	1.2–76	42.0 (24.0)	11–84	0.0035
Age now, years	41.0 (25.0)	18–76	38.0 (42.0)	3–78	54.0 (21.0)	11–90	<0.0001
BMI (N = 127/59/146) #	25.5 (4.9)	17.9–38.5	28.1 (6.5)	16–41	28.4 (5.4)	19.5–50	<0.0001
SUA off treatment, μmol/L (N = 132/46/112) #	337 (118.2)	140–617	448 (116.8)	253–608	462 (124.5)	181–683	<0.0001
SUA on treatment, μmol/L (N = 0/42/155) #	Not applicable		424 (140)	240–628	372 (126.0)	163–725	0.0352
FE-UA *	Not collected		3.7 (2.0)	1.6–20	3.6 (1.6)	0.8–14.3	0.6959
eGFR-MDRD, mL/min/1.73 m <sup>2</sup> *	Not collected		88.0 (36.0)	27.6–426	86.0 (26.0)	24–154	0.2965
Serum creatinine, μmol/L *	75.5 (22.2)	49–121	79.0 (20.5)	26–132	82.0 (20.5)	47–226	0.0016
Max CRP ** (N = 132/54/146) #	1.3 (1.9)	0.1–17.9	1.9 (4.6)	0.2–153.1	4.0 (6.4)	0.2–222.4	<0.0001

\* Mean of measurements taken during subject follow-ups. \*\* Maximum of measurements taken during subject follow-ups. #Some parameters had missing data; in case missing data amounted for 5% or more, real N is mentioned in parentheses. Reference levels: SUA 120–416 μmol/L for men, 120–360 μmol/L for women; FE-UA 7.3 ± 1.3 for men, 10.3 ± 4.2 for women; eGFR-MDRD > 90 mL/min/1.73 m<sup>2</sup> for healthy subjects (levels decline with age); serum creatinine 64–104 μmol/L for men, 49–90 μmol/L for women; CRP 0–5 mg/L. GG—variant; GT—heterozygotic; TT—homozygotic; MAF—minor frequency allele; IQR—interquartile range; BMI—body mass index; SUA—serum uric acid; FE-UA—fractional excretion of uric acid; eGFR-MDRD—estimated glomerular filtration rate calculated using the Modification of Diet in Renal Disease; CRP—C-reactive protein; KW test—Kruskal–Wallis test.



## 2.2. Cytokine Detection

In total, 27 cytokines (IL-1 $\beta$ , IL-1ra, IL-2, IL-4, IL-5, IL-6, IL-7, IL-8, IL-9, IL-10, IL-12, IL-13, IL-15, IL-17, IP-10, MCP-1, FGF-basic, eotaxin, G-CSF, GM-CSF, IFN- $\gamma$ , MIP-1 $\alpha$ , MIP-1 $\beta$ , PDGF, RANTES, TNF- $\alpha$ , and VEGF) were determined in 149 selected plasma samples from 132 (out of 182) gout patients, in 23 samples from 17 gout patients during an inflammatory attack, in 44 (out of 70) hyperuricemic patients, and in 132 normouricemic subjects. Samples were tested using commercial Bio-Plex Pro™ Human Cytokine 27-plex Assay kits (Bio-Rad, California, USA) and a Bio-Plex 200 system (Bio-Rad, California, USA). Plasma samples were prepared using a standard protocol and aliquoted to storage at  $-80^{\circ}\text{C}$  until analyzed.

## 2.3. Statistical Analysis

Data were summarized as means with standard deviations (SD) and/or medians with interquartile ranges (IQR) where appropriate. Continuous subject characteristics between groups were compared using the Kruskal–Wallis ANOVA, and categorical characteristics were compared using the Fisher exact test. Associations between characteristics of the diagnostic group (i.e., with the normouricemic, hyperuricemic, or gouty status) and the p.Q141K allele dose were modeled using linear regression with interactions; creatinine and CRP values were log-transformed for a better fit. Associations between cytokine measurements and diagnostic groups and the p.Q141K allele dose were modeled using linear mixed models with group and allele dose as fixed effects and subject ID as the random factor since some individuals were measured multiple times. All cytokine measurements, except for eotaxin, were log-transformed for a better fit. The Benjamini–Hochberg multiple comparisons correction was used where appropriate. All analyses were performed using statistical language and environment R, version 3.4.4.

## 3. Results

### 3.1. Analysis of the p.Q141K Variant in Normouricemic and Patient Cohort

First, we analyzed the presence of the p.Q141K allele in the *ABCG2* gene in our study cohort. From 132 normouricemic subjects with an MAF = 7.1%, 15 were heterozygote, and one was homozygote for p.Q141K variant. In the hyperuricemic cohort with an MAF = 21.3%, 19 were heterozygous, and five were homozygous for the p.Q141K allele. Finally, in gout patients with an MAF = 25%, 68 patients were GT heterozygotes and 11 were TT homozygotes. Gout and hyperuricemic patients had significantly more heterozygous and homozygous variants and hence, a significantly higher p.Q141K frequency than normouricemic subjects ( $p < 0.0001$ ) (Table 1).

### 3.2. Analysis of the p.Q141K Variant and Its Relationship with Risk Factors for Gout

Age, BMI, CRP, and GFR are known risk factors for gout. For each of these, we found expected differences between the diagnostic groups but their association with a diagnostic status varied depending on the p.Q141K allele dose.

Risk of gout and hyperuricemia increases proportionally with age. In our cohort, patients with hyperuricemia or gout were older than normouricemic individuals ( $p < 0.0001$ , Figure 1A) during the time of the study. However, hyperuricemic and gout patients homozygous for p.Q141K were significantly younger than wild-types and heterozygotes ( $p = 0.0003$ ). Furthermore, hyperuricemia and gout manifested earlier in p.Q141K homozygotes ( $p = 0.004$ , Figure 1B).

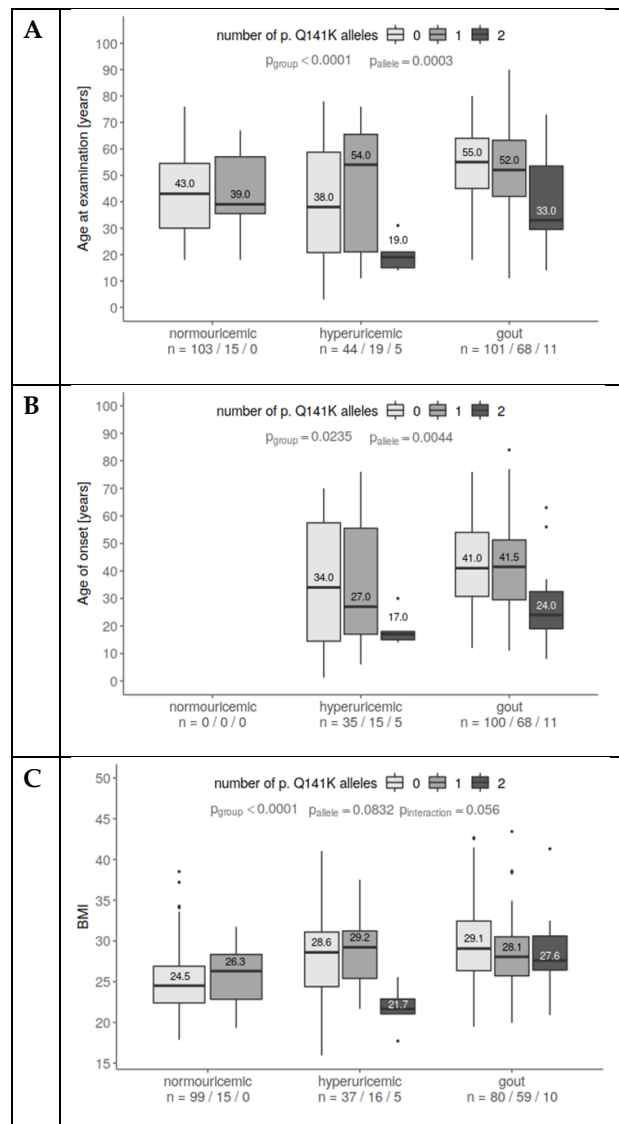


**Figure 1.** The association of p.Q141K alleles with age at examination, age of onset, and BMI. (A) Gout patients were older than hyperuricemic and normouricemic subjects. Homozygotes for p.Q141K were younger than wild type/heterozygotes. Interactions suggest different associations for normouricemic subjects. (B) There are no substantial differences in the age of onset between hyperuricemia and gout individuals. p.Q141K homozygotes tend to have much earlier disease onset than others. (C) Gout and hyperuricemic patients had higher BMIs than controls. Homozygous patients were slightly leaner than others. A statistically significant interaction suggests different associations for p.Q141K among groups. This may have been influenced by the pediatric hyperuricemia subset.

Elevated BMI increases the probability of metabolic syndrome as well as the probability of hyperuricemia and gout. This is in line with our data: Patients with hyperuricemia or gout had a higher BMI than normouricemic patients ( $p < 0.0001$ ). In contrast, homozygotes for the p.Q141K variant tended to have lower BMIs ( $p = 0.056$ , Figure 1C). The homozygotes with lower BMIs were mostly very similar to those with young-age hyperuricemia onset.

Similarly, to age and BMI, CRP levels were higher in hyperuricemic and gouty patients than in normouricemic individuals ( $p < 0.0001$ ). But significantly lower levels of CRP were measured in p.Q141K homozygous hyperuricemic and gout patients ( $p = 0.007$ , Figure 2A).

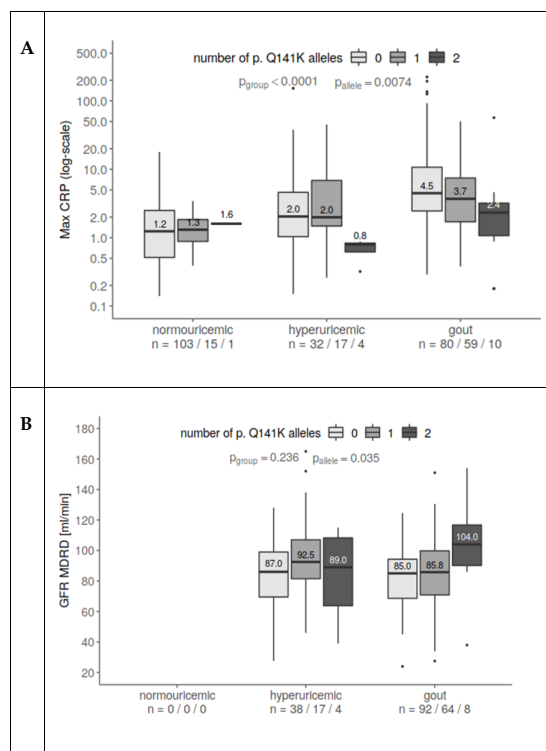


**Figure 2.** The connection between the presence of p.Q141K, maximum CRP, and eGFR-MDRD. (A) CRP increased with hyperuricemia and even more for gout patients compared to normouricemic subjects. At the same time, p.Q141K homozygotes had lower CRP than heterozygotes and wild type. The relationship prevailed after including age as a covariate (CRP slightly rises with subject age). (B) GFR increases with an increasing number of p.Q141K alleles, in a similar way for both hyperuricemic and gout patients. One extreme observation (426 mL/min) was excluded since it heavily influenced the fit. All values were log-transformed for a better fit.

Although GFR should be decreased in patients with hyperuricemia and gout because of worsened renal function, heterozygous and mainly homozygous carriers of the p.Q141K variant had significantly higher GFRs ( $p = 0.035$ , Figure 2B, data for normouricemic subjects were not available).

### 3.3. Analysis of the p.Q141K Variant in Association with Cytokine Plasma Levels

To determine the possible differences between normouricemic, hyperuricemic, gout, and acute gout patients on immunological levels, we determined the cytokine plasma profiles of our cohort. Then, we analyzed the possible influence of the p.Q141K variant on cytokine production between patient groups.

We found that levels of IL-1 $\beta$ , IL-1ra, IL-4, IL-6, IL-7, IL-8, IL-9, IL-13, IL-17, fibroblast growth factor-basic (FGF-basic), interferon gamma (IFN $\gamma$ ), and TNF $\alpha$  were significantly increased in patients with acute gouty arthritis compared to other groups (multiple correction  $p$ -values ranging from  $p < 0.05$  to  $p < 0.001$ , see Figure 3). On the other hand, eotaxin, monocyte chemoattractant protein-1 (MCP-1), and regulated on activation, normal T cell expressed and secreted (RANTES) were decreased in all patient groups compared to normouricemic individuals (multiple correction  $p$ -values ranging  $p < 0.001$ ,  $p = 0.014$ , and  $p < 0.001$ , respectively). IL-5, IL-10, and IL-12 levels gradually decreased from control, subsequently hypouricemia, and gout to gout attack group. Plasma levels of IL-2, IL-15, granulocyte-colony stimulating factor (G-CSF), granulocyte-macrophage colony stimulating factor (GM-CSF), interferon gamma-induced protein-10 (IP-10), macrophage inflammatory protein-1 beta (MIP-1 $\beta$ ), platelet derived growth factor (PDGF), and vascular endothelial growth factor (VEGF) were comparable among all groups (Figure 3, the  $p$ -values shown are after the Benjamini–Hochberg

correction). We did not find any impact of p.Q141K on the plasma cytokine levels of patients or normouricemic subjects.

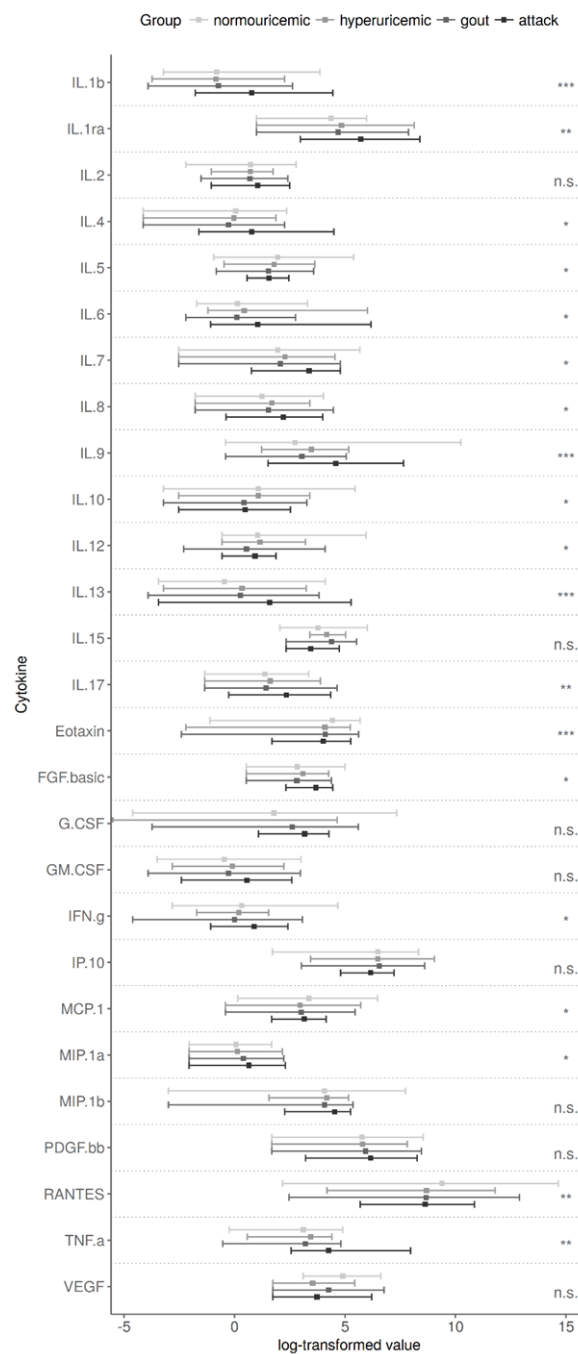


**Figure 3.** Individual cytokine measurements in the compared groups. Post-hoc pairwise comparisons revealed the main source of differences in the gout attack group were: interleukin (IL)-1b, IL-1ra, IL-4, IL-6, IL-7, IL-8, IL-9, IL-13, IL-17, fibroblast growth factor (FGF)-basic, interferon gamma (IFN $\gamma$ ), and tumor necrosis factor alpha (TNF $\alpha$ ). IL-5, IL-10, and IL-12 levels gradually decreased from control to gout attack group. Eotaxin, monocyte chemoattractant protein 1 (MCP-1), and regulated on activation, normal T cell expressed and secreted (RANTES) showed significantly higher values for controls. There were no associations between the p.Q141K allele and cytokine levels. *p*-values via an ANOVA model using log-transformed measurements (except eotaxin) are corrected for multiple comparisons (Benjamini–Hochberg method). n.s. *p* > 0.05, \* *p* ≤ 0.05, \*\* *p* < 0.01, \*\*\* *p* < 0.001.

#### 4. Discussion

The ABCG2 protein is a membrane-associated transporter with a wide range of functions including excretion of urate. The ABCG2 gene is expressed in the intestine, liver, kidney, and several other tissues that have a barrier function. The renal excretion of urate accounts for approximately two-thirds of total urate excretion while intestinal excretion accounts for the rest [27]. Dysfunction in this protein is particularly caused by the p.Q141K variant, which occurs at a high frequency in the Caucasian population. The variant leads to hyperuricemia and gout. Homozygotes for p.Q141K have 53% reduced excretion of urate compared to wild types [28]. Hypothetically, this allele also promotes progression from hyperuricemia to gout by stimulating the immune response to MSU crystals [1]. Therefore, we looked for a possible relationship between the number of p.Q141K alleles (i.e., wild type, heterozygous, and homozygous) and risk factors (age, BMI) or related determinants (CRP, GFR), and plasma levels of pro/anti-inflammatory cytokines.

Risk of gout increases with age, which is in line with our results where patients with hyperuricemia or gout were older than normouricemic individuals [13,29]. However, hyperuricemic and gout patients homozygous for p.Q141K were significantly younger than wild-types and heterozygotes. They also had an earlier disease onset. These findings are supported by the fact that non-functional ABCG2 transporters have a greater impact on disease progression (PAR% = 29.2%) than risk factors such as age (PAR% = 5.74%), obesity (PAR% = 18.7%), and alcohol consumption (PAR% = 15.4%) [29].

Another risk factor for hyperuricemia and gout as well as for metabolic syndrome is increased BMI [30]. This corresponds to our data showing that patients with hyperuricemia or gout had higher BMIs than normouricemic individuals. In contrast with previously mentioned data, homozygotes for the p.Q141K variant tended to have lower BMIs. These patients were very similar to those with young-age onset. This finding suggests that the beginning of the disease was mainly influenced by the presence of p.Q141K rather than risk factors such as BMI.

In addition to the fact that high CRP levels indicate infection- or non-infection-based inflammation, serum CRP levels positively correlate with serum urate levels and can be used as a gout determinant [31]. Moreover, CRP levels increase with age and the amount of adipose tissue [32,33]. In this study, we found higher CRP levels in hyperuricemic and gouty patients than in normouricemic controls. However, significantly lower levels of CRP were found in p.Q141K homozygotes. These results show a similar trend as BMI, which could be explained by the younger age of the homozygous p.Q141K allele carriers.

GFR defines kidneys function and deteriorates in patients with hyperuricemia and gout due to worsened renal function [34]. In our study, heterozygous and mainly homozygous carriers of the p.Q141K variant had significantly higher eGFR-MDRD than patients with the wild-type variant. This finding could be explained by the gradually decreasing age of disease onset between wild-type, heterozygous, and homozygous carriers of the p.Q141K variant, although, mainly in hyperuricemic patients. Although eGFR-MDRD was not measured in normouricemic controls, all patients reached eGFR-MDRD reference levels; thus, we did not observe deteriorated renal function in our patient cohort. Another explanation for the high eGRF-MDRD could be the low mean age (53.6 years) of our study cohort compared to the mean age (61.9 years) of the gout patients described in the literature [35]. Our patients were younger, and they did not have impaired kidney function. The higher eGFR-MDRD in homozygotes might not be representative because of the low number of patients (five with hyperuricemia and seven with gout). Further experiments on a larger cohort are necessary to confirm or disprove this particular finding.

Another aim of our study was to examine the differences in cytokine levels between normouricemic, hyperuricemic, gouty, and acute gouty arthritis patients in the presence of the p.Q141K variant of the ABCG2 gene. Expression of the ABCG2 gene is impacted by pro-inflammatory cytokines and signaling cascades. One of the major transcription factors of pro-inflammatory pathways, nuclear factor kappa B (NF- $\kappa$ B), is able to bind to the promoter of the ABCG2 gene and upregulate it, with or without the influence of an estrogen receptor [23,36]. On the other hand, the ABCG2 gene

alone is capable of inhibiting NF- $\kappa$ B activation, which leads to the downregulation of IL-8 [37]. Pro-inflammatory cytokines IL-1 $\beta$  and TNF $\alpha$  can have an impact on *ABCG2* expression at the mRNA as well as the protein level, depending on the kind of cell line. Further, the *ABCG2* protein is seen to be downregulated in colon biopsies from patients with active inflammatory bowel disease [38–40]. The presence of the p.Q141K variant in the *ABCG2* protein leads to misfolding and decreased cell surface expression [17]. These data led us to study the impact of p.Q141K on cytokine levels. Unfortunately, we did not find any influence of this variant on cytokine protein expression in the plasma of patients from different groups or in normouricemic individuals. The likely reason our hypothesis failed was the relatively small number of patients included in the study. Further investigations using larger cohorts are needed.

Nonetheless, we found higher plasma levels of IL-1 $\beta$ , IL-1ra, IL-4, IL-6, IL-8, IL-9, IL-13, IL-17, FGF-basic, IFN $\gamma$ , and TNF $\alpha$  in acute gouty arthritis patients. All these cytokines are involved in interconnected pro-/anti-inflammatory cascades, which suggest an active immune response in patients with acute gouty arthritis. On the other hand, IL-5, IL-10, and eotaxin were lower in patients with acute gout inflammation, which can be explained by their role in inhibiting inflammation (IL-10) or eosinophilic inflammation (IL-5, eotaxin) [41]. Our results regarding IL-10 levels are supported by similar findings of circulating IL-10 in a Netherlands gouty arthritis study cohort and in New Zealand patients with intercritical gout study [42]. Estevez-Garcia and colleagues measured serum levels of IL-5 among groups of normouricemic controls, hyperuricemic, and gouty patients [43] and found, in contrast to our results, IL-5 levels were the same among groups, which may be explained by IL-5 determination in serum vs. plasma. Plasma is a more sensitive matrix for detecting levels of low-abundance cytokines [44]. Eotaxin was described to be increased in obese patients with metabolic syndrome (mean BMI 38.9  $\pm$  6.3) compared to lean subjects (mean BMI 22.4  $\pm$  2.5) and decreased after their weight-loss [45]. This suggests that eotaxin should have been higher in our patients than in normouricemic individuals; however, our patients were not extremely obese. MCP-1 and RANTES were also lower in acute gouty arthritis patients compare to normouricemic controls in our study. However, increased serum levels of MCP-1 have been observed in hyperuricemic, gouty, and acute gouty arthritis patients, and MCP-1 has been positively correlated with elevated serum levels of uric acid [46]. The contradictory results could be explained by measurement of cytokines in plasma samples in our study. To date no association of RANTES plasma/serum levels with gout has been published; however, it is known that urate stimulates mRNA and protein expression of RANTES and MCP-1 in mice tubular epithelial cells [47]. On the other hand, synovial fluid levels of RANTES were found to be significantly lower in patients with acute gout than in patients with acute rheumatoid arthritis [48].

One of the limitations of our study was the relatively small number of p.Q141K homozygotes with hyperuricemia and gout and also a small cohort size of those with acute gouty arthritis. A larger group for p.Q141K homozygotes and acute gouty arthritic patients is necessary to confirm the lower age of onset, BMI, CRP, and higher eGFR-MDRD, and cytokine levels between groups. Our results reflect the fact that our study cohort was purposefully compiled from patients with primary hyperuricemia and gout who are younger (mean age = 53.6 years) than the common gouty population (mean age = 61.9 years) and have a positive family correlation [35]. This characteristic can be considered to be one of the strengths of the study because the cohort was well-defined and excluded those with secondary hyperuricemia and gout. Our study also used explicit definitions of medication and comorbidities for the study cohorts. Finally, according to available data, and for the first time, our study examined a possible link between the p.Q141K variant and plasma cytokine levels.

## 5. Conclusions

In conclusion, we found that the p.Q141K variant of the *ABCG2* gene impacts the age of hyperuricemia and gout onset, levels of BMI and CRP, and renal function. This variant has no effect on plasma cytokine levels of hyperuricemic and gouty patients. However, we did find higher cytokine levels, but mainly in patients with acute gouty arthritis.

**Author Contributions:** Conceptualization, B.S. and V.H.; methodology, B.S. and V.H.; validation, B.S. and M.P.; formal analysis and investigation, V.H., J.B., and K.P. (Kateřina Pavelcová); data curation, M.P.; writing—original draft preparation, V.H. and J.B.; writing—review and editing, B.S., L.Š., and K.P. (Karel Pavelka); visualization, M.P.; supervision, B.S. and L.Š.; project administration, B.S.; funding acquisition, B.S.

**Funding:** This research was funded by the Czech Ministry of Health: AZV 15-26693 A and projects for conceptual development of research organization 00023728 (Institute of Rheumatology), RVO VFN64165, SVV 260367, and SVV 260373.

**Conflicts of Interest:** The authors declare no conflict of interest.

## References

1. Major, T.J.; Dalbeth, N.; Stahl, E.A.; Merriman, T.R. An update on the genetics of hyperuricaemia and gout. *Nat. Rev. Rheumatol.* **2018**, *14*, 351–353. [[CrossRef](#)] [[PubMed](#)]
2. Cadzow, M.; Merriman, T.R.; Dalbeth, N. Performance of gout definitions for genetic epidemiological studies: Analysis of UK Biobank. *Arthritis Res. Ther.* **2017**, *19*, 181. [[CrossRef](#)] [[PubMed](#)]
3. So, A.K.; Martinon, F. Inflammation in gout: Mechanisms and therapeutic targets. *Nat. Rev. Rheumatol.* **2017**, *13*, 639–647. [[CrossRef](#)] [[PubMed](#)]
4. El Ridi, R.; Tallima, H. Physiological functions and pathogenic potential of uric acid: A review. *J. Adv. Res.* **2017**, *8*, 487–493. [[CrossRef](#)]
5. Deuteraiou, K.; Kitas, G.; Garyfallos, A.; Dimitroulas, T. Novel insights into the role of inflammasomes in autoimmune and metabolic rheumatic diseases. *Rheumatol. Int.* **2018**, *38*, 1345–1354. [[CrossRef](#)]
6. Martinon, F.; Pétrilli, V.; Mayor, A.; Tardivel, A.; Tschopp, J. Gout-associated uric acid crystals activate the NALP3 inflammasome. *Nature* **2006**, *440*, 237–241. [[CrossRef](#)]
7. Schlesinger, N.; Thiele, R.G. The pathogenesis of bone erosions in gouty arthritis. *Ann. Rheum. Dis.* **2010**, *69*, 1907–1912. [[CrossRef](#)]
8. Cavalcanti, N.G.; Marques, C.D.L.; Lins e Lins, T.U.; Pereira, M.C.; Rêgo, M.J.B.D.M.; Duarte, A.L.B.P.; Pitta, I.D.R.; Pitta, M.G.D.R. Cytokine profile in gout: Inflammation driven by IL-6 and IL-18? *Immunol. Investig.* **2016**, *45*, 383–395. [[CrossRef](#)]
9. Liu, Y.; Zhao, Q.; Yin, Y.; McNutt, M.A.; Zhang, T.; Cao, Y. Serum levels of IL-17 are elevated in patients with acute gouty arthritis. *Biochem. Biophys. Res. Commun.* **2018**, *497*, 897–902. [[CrossRef](#)]
10. Mills, K.H.G.; Dungan, L.S.; Jones, S.A.; Harris, J. The role of inflammasome-derived IL-1 in driving IL-17 responses. *J. Leukoc. Biol.* **2013**, *93*, 489–497. [[CrossRef](#)]
11. Matsuo, H.; Ichida, K.; Takada, T.; Nakayama, A.; Nakashima, H.; Nakamura, T.; Kawamura, Y.; Takada, Y.; Yamamoto, K.; Inoue, H.; et al. Common dysfunctional variants in *ABCG2* are a major cause of early-onset gout. *Sci. Rep.* **2013**, *3*, 8–11. [[CrossRef](#)] [[PubMed](#)]
12. Stiburkova, B.; Miyata, H.; Závada, J.; Tomčík, M.; Pavelka, K.; Storkanova, G.; Toyoda, Y.; Takada, T.; Suzuki, H. Novel dysfunctional variant in *ABCG2* as a cause of severe tophaceous gout: Biochemical, molecular genetics and functional analysis. *Rheumatology* **2016**, *55*, 191–194. [[CrossRef](#)] [[PubMed](#)]
13. Stiburkova, B.; Pavelcova, K.; Závada, J.; Petru, L.; Simek, P.; Cepek, P.; Pavlikova, M.; Matsuo, H.; Merriman, T.R.; Pavelka, K. Functional non-synonymous variants of *ABCG2* and gout risk. *Rheumatology* **2017**, *56*, 1982–1992. [[CrossRef](#)] [[PubMed](#)]
14. Higashino, T.; Takada, T.; Nakaoka, H.; Toyoda, Y.; Stiburkova, B.; Miyata, H.; Ikebuchi, Y.; Nakashima, H.; Shimizu, S.; Kawaguchi, M.; et al. Multiple common and rare variants of *ABCG2* cause gout. *RMD Open* **2017**, *3*, e000464. [[CrossRef](#)]
15. Woodward, O.M.; Tukaye, D.N.; Cui, J.; Greenwell, P.; Constantoulakis, L.M.; Parker, B.S.; Rao, A.; Kottgen, M.; Maloney, P.C.; Guggino, W.B. Gout-causing Q141K mutation in *ABCG2* leads to instability of the nucleotide-binding domain and can be corrected with small molecules. *Proc. Natl. Acad. Sci. USA* **2013**, *110*, 5223–5228. [[CrossRef](#)]
16. Mizuarai, S.; Aozasa, N.; Kotani, H. Single nucleotide polymorphisms result in impaired membrane localization and reduced atpase activity in multidrug transporter *ABCG2*. *Int. J. Cancer* **2004**, *109*, 238–246. [[CrossRef](#)]

17. Cleophas, M.C.; Joosten, L.A.; Stamp, L.K.; Dalbeth, N.; Woodward, O.M.; Merriman, T.R. *ABCG2* polymorphisms in gout: Insights into disease susceptibility and treatment approaches. *Pharmgenom. Pers. Med.* **2017**, *10*, 129–142. [[CrossRef](#)]
18. Dehghan, A.; Köttgen, A.; Yang, Q.; Hwang, S.J.; Kao, W.L.; Rivadeneira, F.; Boerwinkle, E.; Levy, D.; Hofman, A.; Astor, B.C.; et al. Association of three genetic loci with uric acid concentration and risk of gout: A genome-wide association study. *Lancet* **2008**, *372*, 1953–1961. [[CrossRef](#)]
19. Li, R.; Miao, L.; Qin, L.; Xiang, Y.; Zhang, X.; Peng, H.; Mailamuguli, Sun, Y.; Yao, H. A meta-analysis of the associations between the Q141K and Q126X *ABCG2* gene variants and gout risk. *Int. J. Clin. Exp. Pathol.* **2015**, *8*, 9812–9823.
20. Roberts, R.L.; Wallace, M.C.; Phipps-Green, A.J.; Topless, R.; Drake, J.M.; Tan, P.; Dalbeth, N.; Merriman, T.R.; Stamp, L.K. *ABCG2* loss-of-function polymorphism predicts poor response to allopurinol in patients with gout. *Pharm. J.* **2017**, *17*, 201–203. [[CrossRef](#)]
21. Mosaffa, F.; Lage, H.; Afshari, J.T.; Behravan, J. Interleukin-1 beta and tumor necrosis factor-alpha increase *ABCG2* expression in MCF-7 breast carcinoma cell line and its mitoxantrone-resistant derivative, MCF-7/MX. *Inflamm. Res.* **2009**, *58*, 669–676. [[CrossRef](#)] [[PubMed](#)]
22. Evseenko, D.A.; Paxton, J.W.; Keelan, J.A. Independent regulation of apical and basolateral drug transporter expression and function in placental trophoblasts by cytokines, steroids, and growth factors. *Drug Metab. Dispos.* **2007**, *35*, 595–601. [[CrossRef](#)] [[PubMed](#)]
23. Pradhan, M.; Bembinster, L.A.; Baumgarten, S.C.; Frasier, J. Proinflammatory cytokines enhance estrogen-dependent expression of the multidrug transporter gene *ABCG2* through estrogen receptor and NFκB cooperativity at adjacent response elements. *J. Biol. Chem.* **2010**, *285*, 31100–31106. [[CrossRef](#)] [[PubMed](#)]
24. Stiburkova, B.; Pavelcova, K.; Pavlikova, M.; Ješina, P.; Pavelka, K. The impact of dysfunctional variants of *ABCG2* on hyperuricemia and gout in pediatric-onset patients. *Arthritis Res. Ther.* **2019**, *21*, 77. [[CrossRef](#)] [[PubMed](#)]
25. Toyoda, Y.; Mančíková, A.; Krylov, V.; Morimoto, K.; Pavelcová, K.; Bohatá, J.; Pavelka, K.; Pavlíková, M.; Suzuki, H.; Matsuo, H.; et al. Functional characterization of clinically-relevant rare variants in *ABCG2* identified in a gout and hyperuricemia cohort. *Cells* **2019**, *8*, 363. [[CrossRef](#)] [[PubMed](#)]
26. Wallace, S.L.; Robinson, H.; Masi, A.T.; Decker, J.L.; McCarty, D.J.; Yü, T.F. Preliminary criteria for the classification of the acute arthritis of primary gout. *Arthritis Rheum.* **1977**, *20*, 895–900. [[CrossRef](#)]
27. Takada, T.; Ichida, K.; Matsuo, H.; Nakayama, A.; Murakami, K.; Yamanashi, Y.; Kasuga, H.; Shinomiya, N.; Suzuki, H. *ABCG2* dysfunction increases serum uric acid by decreased intestinal urate excretion. *Nucleosides Nucleotides Nucleic Acids* **2014**, *33*, 275–281. [[CrossRef](#)]
28. Woodward, O.M.; Köttgen, A.; Coresh, J.; Boerwinkle, E.; Guggino, W.B.; Köttgen, M. Identification of a urate transporter, *ABCG2*, with a common functional polymorphism causing gout. *Proc. Natl. Acad. Sci. USA* **2009**, *106*, 10338–10342. [[CrossRef](#)]
29. Nakayama, A.; Matsuo, H.; Nakaoka, H.; Nakamura, T.; Nakashima, H.; Takada, Y.; Oikawa, Y.; Takada, T.; Sakiyama, M.; Shimizu, S.; et al. Common dysfunctional variants of *ABCG2* have stronger impact on hyperuricemia progression than typical environmental risk factors. *Sci. Rep.* **2014**, *4*, 5227. [[CrossRef](#)]
30. Aune, D.; Norat, T.; Vatten, L.J. Body mass index and the risk of gout: A systematic review and dose–response meta-analysis of prospective studies. *Eur. J. Nutr.* **2014**, *53*, 1591–1601. [[CrossRef](#)]
31. Evrin, P.-E.; Nilsson, S.E.; Öberg, T.; Malmberg, B. Serum C-reactive protein in elderly men and women: Association with mortality, morbidity and various biochemical values. *Scand. J. Clin. Lab. Investig.* **2005**, *65*, 23–31. [[CrossRef](#)] [[PubMed](#)]
32. Michaud, M.; Balardy, L.; Moulis, G.; Gaudin, C.; Peyrot, C.; Vellas, B.; Cesari, M.; Nourhashemi, F. Proinflammatory cytokines, aging, and age-related diseases. *J. Am. Med. Dir. Assoc.* **2013**, *14*, 877–882. [[CrossRef](#)] [[PubMed](#)]
33. Wyczalkowska-Tomasik, A.; Czarkowska-Paczek, B.; Zielenkiewicz, M.; Paczek, L. Inflammatory markers change with age, but do not fall beyond reported normal ranges. *Arch. Immunol. Ther. Exp.* **2016**, *64*, 249–254. [[CrossRef](#)] [[PubMed](#)]
34. Krishnan, E. Reduced glomerular function and prevalence of gout: NHANES 2009–10. *PLoS ONE* **2012**, *7*, e50046. [[CrossRef](#)]



35. Rothenbacher, D.; Primatesta, P.; Ferreira, A.; Cea-Soriano, L.; Rodriguez, L.A.G. Frequency and risk factors of gout flares in a large population-based cohort of incident gout. *Rheumatology* **2011**, *50*, 973–981. [[CrossRef](#)]
36. Wang, X.; Wu, X.; Wang, C.; Zhang, W.; Ouyang, Y.; Yu, Y.; He, Z. Transcriptional suppression of breast cancer resistance protein (BCRP) by wild-type p53 through the NF- $\kappa$ B pathway in MCF-7 cells. *FEBS Lett.* **2010**, *584*, 3392–3397. [[CrossRef](#)]
37. Shen, S.; Callaghan, D.; Juzwik, C.; Xiong, H.; Huang, P.; Zhang, W. ABCG2 reduces ROS-mediated toxicity and inflammation: A potential role in Alzheimer's disease. *J. Neurochem.* **2010**, *114*, 1590–1604. [[CrossRef](#)]
38. Von Wedel-Parlow, M.; Wölte, P.; Galla, H.-J. Regulation of major efflux transporters under inflammatory conditions at the blood-brain barrier in vitro. *J. Neurochem.* **2009**, *111*, 111–118. [[CrossRef](#)]
39. Mosaffa, F.; Kalalinia, F.; Lage, H.; Afshari, J.T.; Behravan, J. Pro-inflammatory cytokines interleukin-1 beta, interleukin 6, and tumor necrosis factor-alpha alter the expression and function of ABCG2 in cervix and gastric cancer cells. *Mol. Cell. Biochem.* **2012**, *363*, 385–393. [[CrossRef](#)]
40. Deuring, J.J.; de Haar, C.; Koelewijn, C.L.; Kuipers, E.J.; Peppelenbosch, M.P.; van der Woude, C.J. Absence of ABCG2-mediated mucosal detoxification in patients with active inflammatory bowel disease is due to impeded protein folding. *Biochem. J.* **2012**, *441*, 87–93. [[CrossRef](#)]
41. Wen, T.; Rothenberg, M.E. The regulatory function of eosinophils. *Microbiol. Spectr.* **2016**, *4*. [[CrossRef](#)]
42. Kienhorst, L.B.E.; van Lochem, E.; Kievit, W.; Dalbeth, N.; Merriman, M.E.; Phipps-Green, A.; Loof, A.; van Heerde, W.; Vermeulen, S.; Stamp, L.K.; et al. Gout is a chronic inflammatory disease in which high levels of interleukin-8 (CXCL8), myeloid-related protein 8/myeloid-related protein 14 complex, and an altered proteome are associated with diabetes mellitus and cardiovascular disease. *Arthritis Rheumatol.* **2015**, *67*, 3303–3313. [[CrossRef](#)]
43. Estevez-Garcia, I.O.; Gallegos-Nava, S.; Vera-Pérez, E.; Silveira, L.H.; Ventura-Ríos, L.; Vancini, G.; Hernández-Díaz, C.; Sánchez-Muñoz, F.; Ballinas-Verdugo, M.A.; Gutierrez, M.; et al. Levels of cytokines and microRNAs in individuals with asymptomatic hyperuricemia and ultrasonographic findings of gout: A bench-to-bedside approach. *Arthritis Care Res.* **2018**, *70*, 1814–1821. [[CrossRef](#)] [[PubMed](#)]
44. Rosenberg-Hasson, Y.; Hansmann, L.; Liedtke, M.; Herschmann, I.; Maecker, H.T. Effects of serum and plasma matrices on multiplex immunoassays. *Immunol. Res.* **2014**, *58*, 224–233. [[CrossRef](#)] [[PubMed](#)]
45. Vasudevan, A.R.; Wu, H.; Xydakis, A.M.; Jones, P.H.; Smith, E.O.; Sweeney, J.F.; Corry, D.B.; Ballantyne, C.M. Eotaxin and obesity. *J. Clin. Endocrinol. Metab.* **2006**, *91*, 256–261. [[CrossRef](#)]
46. Grainger, R.; McLaughlin, R.J.; Harrison, A.A.; Harper, J.L. Hyperuricaemia elevates circulating CCL2 levels and primes monocyte trafficking in subjects with inter-critical gout. *Rheumatology* **2013**, *52*, 1018–1021. [[CrossRef](#)]
47. Zhou, Y.; Fang, L.; Jiang, L.; Wen, P.; Cao, H.; He, W.; Dai, C.; Yang, J. Uric acid induces renal inflammation via activating tubular NF- $\kappa$ B signaling pathway. *PLoS ONE* **2012**, *7*, e39738. [[CrossRef](#)]
48. Mcnearney, T.; Baethge, B.A.; Cao, S.; Alam, R.; Lisse, J.R.; Westlund, K.N. Excitatory amino acids, TNF-alpha, and chemokine levels in synovial fluids of patients with active arthropathies. *Clin. Exp. Immunol.* **2004**, *137*, 621–627. [[CrossRef](#)]



## RESEARCH ARTICLE

## Open Access

## Circulating microRNA alternations in primary hyperuricemia and gout

Jana Bohatá<sup>1,2</sup>, Veronika Horváthová<sup>1,3</sup>, Markéta Pavlíková<sup>4</sup> and Blanka Stibůrková<sup>1,5\*</sup>**Abstract**

**Objectives:** MicroRNAs (miRNAs) are short single-stranded RNAs that play a role in the post-transcriptional regulation of gene expression. Their deregulation can be associated with various diseases, such as cancer, neurodegenerative, and immune-related diseases. The aim of our study was to compare miRNA levels in plasma that could potentially influence the progression of hyperuricemia to gout, since the mechanism of progression is still unclear.

**Methods:** Total RNA, including miRNA, was isolated from the plasma of 45 patients with asymptomatic hyperuricemia, 131 patients with primary gout (including 16 patients having a gout attack), and 130 normouricemic controls. The expression of 18 selected miRNAs (cel-miR-39 and cel-miR-54 as spike-in controls, hsa-miR-16-5p and hsa-miR-25-3p as endogenous controls, hsa-miR-17-5p, hsa-miR-18a-5p, hsa-miR-30a-3p, hsa-miR-30c-5p, hsa-miR-126-3p, hsa-miR-133a-3p, hsa-miR-142-3p, hsa-miR-143-3p, hsa-miR-146a-5p, hsa-miR-155-5p, hsa-miR-222-3p, hsa-miR-223-3p, hsa-miR-488-3p and hsa-miR-920) was measured using qPCR.

**Results:** We found that hsa-miR-17-5p, hsa-miR-18a-5p, hsa-miR-30c-5p, hsa-miR-142-3p, and hsa-miR-223-3p were significantly upregulated ( $p < 0.001$ ) in the plasma of hyperuricemia and gout patients compared to normouricemic individuals. As part of the follow-up of our previous study, we found a negative correlation between hsa-miR-17-5p, hsa-miR-30c-5p, hsa-miR-126-3p, hsa-miR-142-3p, and hsa-miR-223-3p with plasma levels of chemokine MCP-1. Additionally, we found a positive correlation between CRP and plasma levels of hsa-miR-17-5p, hsa-miR-18a-5p, hsa-miR-30c-5p, hsa-miR-126-3p, hsa-miR-142-3p, hsa-miR-146a-5p, hsa-miR-155-5p, hsa-miR-222-3p, and hsa-miR-223-3p. Five of those miRNAs (hsa-miR-126-3p, hsa-miR-142-3p, hsa-miR-146a-5p, hsa-miR-155-5p, and hsa-miR-222-3p) also had a positive correlation with serum creatinine and therefore a negative correlation with eGFR.

**Conclusion:** Five miRNAs were significantly upregulated in the plasma of patients with hyperuricemia and gout (and those during a gout attack) compared to normouricemic controls. We also found a correlation between the plasma levels of several miRNA and plasma levels of MCP-1, CRP, serum creatinine, and eGFR.

**Keywords:** miRNA, Uric acid, Hyperuricemia, Gout, Acute gouty arthritis

\* Correspondence: [stiburkova@revma.cz](mailto:stiburkova@revma.cz)<sup>1</sup>Institute of Rheumatology, Prague, Czech Republic<sup>5</sup>Department of Pediatrics and Inherited Metabolic Disorders, First Faculty of Medicine, Charles University and General University Hospital, Prague, Czech Republic

Full list of author information is available at the end of the article



© The Author(s). 2021 **Open Access** This article is licensed under a Creative Commons Attribution 4.0 International License, which permits use, sharing, adaptation, distribution and reproduction in any medium or format, as long as you give appropriate credit to the original author(s) and the source, provide a link to the Creative Commons licence, and indicate if changes were made. The images or other third party material in this article are included in the article's Creative Commons licence, unless indicated otherwise in a credit line to the material. If material is not included in the article's Creative Commons licence and your intended use is not permitted by statutory regulation or exceeds the permitted use, you will need to obtain permission directly from the copyright holder. To view a copy of this licence, visit <http://creativecommons.org/licenses/by/4.0/>. The Creative Commons Public Domain Dedication waiver (<http://creativecommons.org/publicdomain/zero/1.0/>) applies to the data made available in this article, unless otherwise stated in a credit line to the data.

## Introduction

Uric acid is the end product of purine metabolism in the human body. Two-thirds of which is excreted by the kidneys and one-third is excreted by the gastrointestinal tract. Hyperuricemia is caused by excessive production of uric acid (10% of cases) and/or reduced excretion (the majority of cases); about 10% of hyperuricemia cases escalate to clinically definable gout. There are risk factors for hyperuricemia and gout, e.g., lifestyle, metabolic syndrome, age, sex, and genetic predispositions. Major genes affecting uric acid excretion and reabsorption are *ABCG2*, respectively *SLC2A9* and *SLC22A12*, which encode membrane transporters *ABCG2*, *GLUT9*, and *URAT1*. Variants in the *SLC22A12* gene can cause renal hypouricemia type 1 (OMIM 220150); similarly, variants in the *SLC2A9* gene can cause renal hypouricemia type 2 (OMIM 612076). *SLC2A9* is sometimes present in association with hyperuricemia and gout, but this has not been confirmed by functional analysis [1]. The most relevant gene that plays a role in hyperuricemia and gout is *ABCG2*. For example, variants Q126X (rs7252713) and Q141K (rs2231142) in the *ABCG2* gene can cause severe dysfunction in this transporter and account for 90% of early-onset gout patients [2]. In our previous studies, we published on the influence of nonsynonymous allelic variants, including functional characterizations, relative to the increased risk of gout progression [3, 4].

Gout is a common inflammatory arthritis. The condition is caused by an accumulation of monosodium urate (MSU) crystals in tissues, which can sometimes lead to gout flare-ups (flares). MSU crystals initiate a macrophage reaction, which activates NLRP3 inflammasomes leading to a release of interleukine-1 $\beta$  (IL-1 $\beta$ ). IL-1 $\beta$  is a crucial cytokine in gout flares. However, patients with hyperuricemia can also have MSU crystal deposits [5]. An acute gout flare is conditioned not only on activation of NLRP3 inflammasomes but also on upregulation of *IL1B* transcription. IL-1 $\beta$  and other interleukins (IL-6, IL-8) attract neutrophils to the site of inflammation resulting in an acute gout flare [6].

The mechanism of hyperuricemia to gout progression is still not fully understood. Gout has four stages of development: asymptomatic hyperuricemia, acute gouty arthritis, intercritical gout, and chronic tophaceous gout. There are probably many variables influencing the progress, and they can vary for each individual.

This study seeks to determine if miRNAs are variable factors that can stimulate the development of gout from asymptomatic hyperuricemia. According to the first GWAS study addressing aggravation of asymptomatic hyperuricemia to gout, there were three genetic loci associated with hyperuricemia to gout development. One

of them is rs9952962 near miR-302f [7]. Finding indicators of hyperuricemia to gout development is an important step in preventive gout therapy.

MicroRNAs (also miRNAs) are short single-stranded non-coding RNAs that play a role in the regulation of gene expression. These molecules were first described in 1993 in *Caenorhabditis elegans* [8]. MiRNAs are involved in the normal function of cells; however, their dysregulation is associated with various diseases. MiRNAs are present in cells as intracellular miRNAs, or they are released from cells into the extracellular environment (often within extracellular vesicles) and are called extracellular, circulating, or cell-free miRNAs, where they play a role in intercellular communication [9]. Cell-free miRNAs are potentially suitable as non-invasive or minimally invasive biomarkers [10]. There are many studies about the role of miRNA in cancer, cardiovascular diseases, immune-related diseases, and others, but only a few studies have dealt with miRNA in hyperuricemia and gout. More than 60% of human protein-coding genes are targets for various miRNA [11]. There are different ways miRNAs can influence serum uric acid and the mechanism of gout pathophysiology. MiRNAs can regulate the expression of urate transporters genes, for example, miR-34a targets mRNA of the *SLC22A12* gene and inhibits expression of *URAT1* in hyperuricemic animal models [12]. Further, miRNAs can influence the expression of essential enzymes such as xanthine oxidase, which can be regulated by miR-448 [13]. Another way of miRNA interference is regulating the expression of genes involved in gout immune response, e.g., miR-223 can suppress NLRP3 expression and reduce inflammasome activity [14]. We aimed to detect and confirm circulating miRNAs that are expressed differently in hyperuricemia and/or gout. Further, we wanted to apply data from our miRNA analysis to our previous research addressing plasma cytokine levels in the same cohort of patients. The association between miRNA levels and biochemical/clinical parameters was also studied.

## Methods

### Sample collection/cohort

The study cohort comprised 115 patients (147 samples; 83 patients with one measurement and 32 patients with two measurements) with primary gout (118 males, 13 females; median age 53 years), 16 patients having a gout attack (24 samples; 10 patients with one measurement, five patients with two measurements, and one patient with four measurements), 45 patients (54 samples; 36 patients with one measurement and nine patients with two measurements) with asymptomatic hyperuricemia (33 males, 12

females; median age 48 years), and 130 normouricemic controls (53 males, 77 females; median age 41 years). All plasma samples were stored at  $-80^{\circ}\text{C}$  in the biobank of the Institute of Rheumatology, Prague, the Czech Republic. Gout patients met the 1977 American Rheumatism Association preliminary classification criteria [15]. Primary hyperuricemic patients were classified as having serum uric acid (SUA)  $>420\ \mu\text{mol/L}$  for men and SUA  $>360\ \mu\text{mol/L}$  for women. Patients were compared to 130 normouricemic individuals from the general population, with no history of primary hyperuricemia, gout, or autoimmune disease. We used the same group of patients used in a previous study addressing plasma cytokines levels in these patients [16]. Written informed consent was obtained from each subject before enrollment in the study. All tests were performed in accordance with standards set by the institutional ethics committees, which was approved 30 June 2015, the project no. 6181/2015. All the procedures were performed in accordance with the Declaration of Helsinki. All demographic, biochemical, genetic, and

presence and type of medical treatment data of patients and normouricemic individuals are presented in Table 1.

#### miRNA analysis

We performed a screening of expressed miRNAs in 12 samples—3 representatives of each studied group (normouricemic controls, patients with hyperuricemia, patients with gout, patients during a gout attack). For screening, TLDA cards were used—TaqMan™ Array Human MicroRNA A+B Cards Set v3.0 (ThermoFisher). We got results for 754 miRNAs, and subsequently, we were able to choose miRNAs that showed potentially different expressions between the studied cohorts but not within them (hsa-miR-17-5p, hsa-miR-18a-5p, hsa-miR-30c-5p, hsa-miR-133a-3p, hsa-miR-142-3p, hsa-miR-143-3p, and hsa-miR-222-3p). Using TaqMan™ Advanced miRNA Human Endogenous Controls Card (ThermoFisher) and NormFinder software, we selected two stable endogenous control miRNAs (hsa-miR-16-5p and hsa-miR-25-3p). We also did a review of published studies and found potential target miRNAs. According

**Table 1** Main demographic, biochemical, and genetic characteristics of patients

	Normouricemic subjects (n = 130)		Hyperuricemic patients (n = 45)		Gout patients (n = 131)		Fisher test p-value
	n	%	n	%	n	%	
Sex M/F	53/77	40.8/59.2	33/12	73.3/26.7	118/13	90.1/9.9	< 0.0001
Familial occurrence			17	41.5	50	38.5	0.8546
No treatment	130	100	21	46.7	18	13.7	< 0.0001
Allopurinol	No treatment		24	53.3	98	74.8	< 0.0001
Febuxostat			0	0	15	11.5	< 0.0001
p.Q141K, GG	102	87.2	25	58.1	73	56.6	< 0.0001
GT	14	12.0	13	30.2	49	38.0	< 0.0001
TT	1	0.9	5	11.6	7	5.4	< 0.0001
no genetic data	13	10.0	2	4.4	2	1.5	< 0.0001
p.Q141K, MAF	16	6.8	23	26.7	63	24.4	< 0.0001
	Median (IQR)	Range	Median (IQR)	Range	Median (IQR)	Range	KW test p-value
Age of onset	Not applicable		34 (40.5)	6–76	41.0 (23.0)	12–84	0.197
Age at the time of taking samples	41 (25.0)	18–76	48.0 (49.0)	11–78	53.0 (20.5)	14–90	< 0.0001
BMI	25.3 (4.8)	17.9–38.5	28.7 (6.1)	17.7–41	28.6 (5.4)	20.6–50	< 0.0001
SUA off treatment, $\mu\text{mol/L}$	337.0 (118.8)	140–617	450.5 (105.0)	253–601	462.0 (124.0)	245–683	< 0.0001
SUA on treatment, $\mu\text{mol/L}$	Not applicable		424.0 (143.0)	250–608	378.0 (124.0)	167–725	0.2325
FE-UA	Not collected		3.9 (2.0)	1.8–20	3.6 (1.5)	0.8–14.3	0.1716
eGFR-MDRD, mL/min/1.73 m <sup>2</sup>	Not collected		88.0 (35.6)	27.6–165	86.0 (21.5)	27.5–151	0.5505
Serum creatinine, $\mu\text{mol/L}$	75.5 (21.8)	49–121	79.0 (19.0)	47–132	81.0 (16.5)	48–189	0.0075
Max CRP	1.3 (1.8)	0.1–17.9	1.9 (4.6)	0.2–45.3	4.1 (7.2)	0.2–224.4	< 0.0001

Reference range: SUA 120–416  $\mu\text{mol/L}$  for men, 120–360  $\mu\text{mol/L}$  for women; FE-UA  $7.3 \pm 1.3$  for men,  $10.3 \pm 4.2$  for women; eGFR-MDRD  $>90\ \text{mL/min/1.73 m}^2$  for healthy subjects (levels decline with age); serum creatinine 64–104  $\mu\text{mol/L}$  for men, 49–90  $\mu\text{mol/L}$  for women; CRP 0–5 mg/L

GG—wild-type variant; GT—heterozygotic; TT—homozygotic; MAF minor frequency allele, IQR interquartile range, BMI body mass index, SUA serum uric acid, FE-UA fractional excretion of uric acid, eGFR-MDRD estimated glomerular filtration rate calculated using the Modification of Diet in Renal Disease, CRP C-reactive protein, KW test Kruskal-Wallis test

to those published studies, we chose other miRNAs (hsa-miR-30a-3p, hsa-miR-126-3p, hsa-miR-146a-5p, hsa-miR-155-5p, hsa-miR-223-3p, hsa-miR-488-3p, and hsa-miR-920), and we also confirmed our TLDA selection (Table 2, Fig. 1). The names of all miRNAs are abbreviated in the following text as miR-x.

Cell-free RNA, including miRNA, was isolated from plasma using the miRNeasy Serum/Plasma kit (Qiagen). During isolation, we added the first spike-in control (0.1 nmol cel-miR-39) to check the isolation efficiency between samples. All plasma samples were prepared using standard protocols and stored at  $-80^{\circ}\text{C}$  until isolation. Next, we performed reverse transcription using TaqMan™ Advanced miRNA cDNA Synthesis Kits (ThermoFisher). The initial step in reverse transcription was the addition of a second spike-in control (0.1 nmol cel-miR-54), which was used to verify its efficiency. This process contains four steps: (1) 3' poly-A tailing, (2) 5' ligation of an adaptor sequence, (3) reverse transcription to cDNA, and (4) miRNA amplification. The last step of the analysis was qPCR using TaqMan™ Advanced miRNA Assays specific for each individual target miRNA (ThermoFisher). qPCR was done using a QuantStudio 7 Flex Real-Time PCR System. For data normalization, levels of endogenous miR-25-3p were used.

### Statistical analysis

Continuous variables were summarized as medians with interquartile range (IQR). Demographic and anamnestic variables in normouricemic, hyperuricemic, and gout cohorts were compared using the Kruskal-Wallis test for

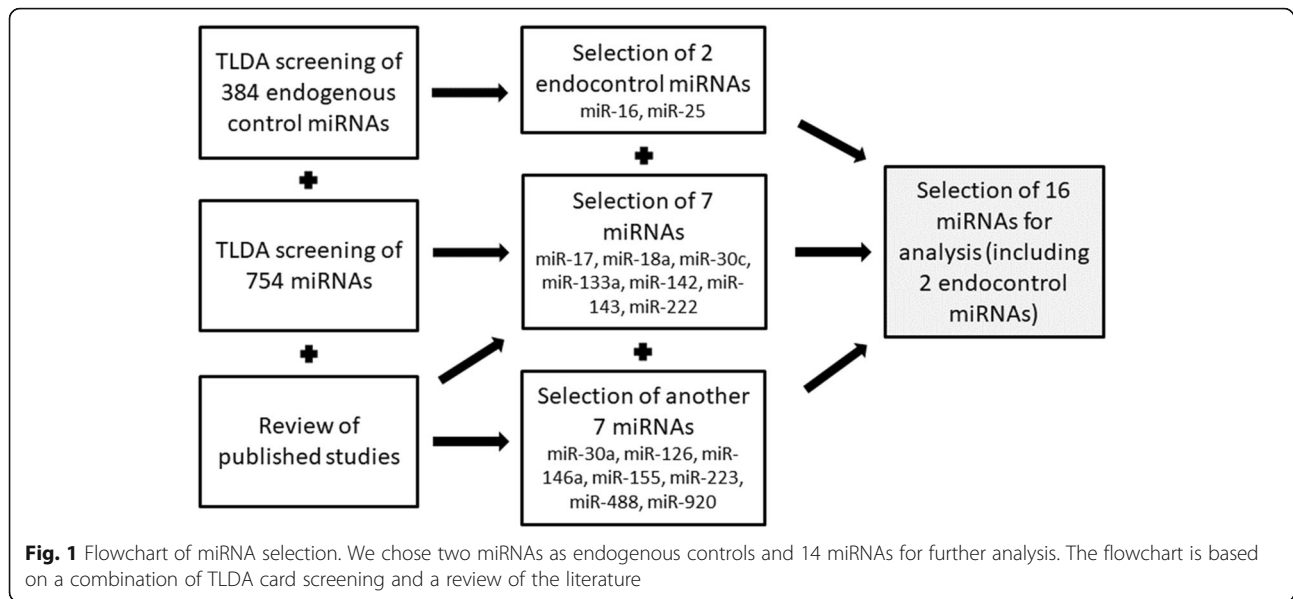
continuous and Fisher's exact test for categorical variables.

Missing data and discordance between replicates in miRNA data were treated using the method published by de Ronde et al. [30] for duplicates; the efficiency coefficient was set to 1.8. For each miRNA and each individual, the mean quantification cycle (Cq) value was computed as the mean of the two duplicates. Undetectable Cq values (over 35) were replaced by the maximal measured Cq+1 for each respective miRNA. We first considered replacing discordant duplicates (the difference between duplicates larger than 0.5) with multiple imputation MICE (Multivariate Imputation by Chained Equations) according to the patient's age, sex, and diagnosis. However, those imputed values varied even more than the original measurements: e.g., for miR-25, the most discordant replicates differed by 1.1 while some of the imputed values differed by more than three from the mean of the duplicates. We, therefore, opted for keeping the mean of the discordant duplicates for the reference miR-25 (18 duplicates in total, representing 5.1% of all measurements) and not using discordant replicates for the other targeted miRNA. Sensitivity analysis using original and imputed values for reference miRNA showed no substantial difference in *p*-value estimates. An overview of undetectable, valid, and invalid replicates is given in Supplementary Table S1. After several sets of measurements (62 samples), we failed to detect levels of miR-488 and miR-920 in our plasma samples. We decided to remove these miRNAs from further analysis of the set of tested miRNAs. Similarly, we excluded miR-30a and miR-133a, which

**Table 2** List of selected miRNAs

Selected miRNA	Function related to hyperuricemia/gout	Reference
miR-17-5p*	suppresses NLRP3 inflammasome activation, miR-17-92 cluster	[17, 18]
miR-18a-5p*	increased by IL-1 $\beta$ in OA, miR-17-92 cluster	[19]
miR-30a-3p	regulates the autoimmune responses occurring in RA	[20]
miR-30c-5p*	inhibits pyroptosis incurred by NLRP3	[21]
miR-126-3p	targets the CCL2 mRNA	[22]
miR-133a-3p*	suppresses NLRP3 inflammasome activation	[23]
miR-142-3p*	inhibits the expression of ABCG2	[24]
miR-143-3p*	targets the GLUT9 mRNA	[25]
miR-146a-5p	increased by MSU crystals, regulates the inflammatory response	[26]
miR-155-5p	increased by MSU crystals, promotes the production of proinflammatory cytokines	[27]
miR-222-3p*	targets the ABCG2 mRNA	[28]
miR-223-3p	reduces NLRP3 inflammasome activity	[14]
miR-488-3p	regulates the production of proinflammatory cytokines, targets the IL1B mRNA, decreased at patients with GA	[29]
miR-920	regulates the production of proinflammatory cytokines, targets the IL1B mRNA, decreased at patients with GA	[29]

OA osteoarthritis, RA rheumatoid arthritis, MSU monosodium urate, GA gouty arthritis  
miRNAs signed with a \* indicate significant differences in TLDA screening



showed a high percentage (48% and 57%, respectively) of undetectable or invalid data in our cohort.

Relative expression of all miRNAs was calculated using the delta cycle threshold (dCt) method. For normalization, we used endogenous control miRNA miR-25 that showed equal expression between samples since miR-16 could be influenced by hemolysis [31].

To compare dCt between normouricemic, hyperuricemic, gout, and gout attack groups, the non-parametric Kruskal-Wallis ANOVA test was used. *P*-values were adjusted for multiple comparisons using the Benjamini-Hochberg method. Possible associations with the *ABCG2* p.Q141K genotype and various cytokine levels were explored using mixed linear regression models; dCt log<sub>2</sub>-transformed was used for a better fit and an individual random intercept factor was used to accommodate for the occasional repeated measurements. Post hoc pairwise comparisons of log<sub>2</sub>-transformed dCt values between study groups were performed using the Tukey method.

When using the Kruskal-Wallis ANOVA, we assumed independence between individual measurements. However, 46 individuals had two and one individual had four samples. To explore the influence of a possible dependence structure, we estimated the differences between cohorts using General Estimating Equations with both independence variance structure and unstructured variance settings, with dCt log<sub>2</sub>-transformed as the response variable and the diagnostic group as an independent variable. Both variance models showed very little difference, justifying the use of the independence assumption.

All analyses were performed in statistical language and environment R, version 4.0.2. The level of statistical significance was set to 0.05.

## Results

### Comparison of miRNA levels between studied groups

We found five miRNAs (miR-17, miR-18a, miR-30c, miR-142, and miR-223) that showed significantly decreased expression in the normouricemic cohort compared to hyperuricemic, gout, and gout attack patients, in most cases.

Two miRNAs, belonging to the miR-17-92 cluster, miR-17 and miR-18a, were significantly more expressed in patients with hyperuricemia ( $p < 0.001$  and  $p < 0.028$ , respectively), gout ( $p < 0.001$ ), in for miR-17 also in gout attack patients ( $p = 0.002$ ). These clustered miRNAs often showed a very similar trend in their expression.

The remaining miRNAs (miR-30c and miR-223) also had significantly higher expression levels for each of the studied groups compared to normouricemic controls ( $p < 0.001$  and  $p < 0.01$ , respectively), and miR-142 showed the same trend as miR-18a ( $p < 0.01$ ). A deviation of miR-18a and miR-142 in the gout attack cohort could be explained by the small number of patients in this group. Relevant *p*-values are graphically represented in Fig. 2. The remaining miRNAs (miR-30a, miR-126, miR-133a, miR-143, miR-146a, miR-155, miR-222, miR-488, and miR-920) did not vary in our analyzed groups. All results are listed in Supplementary Table S2.

### Association of miRNA levels and cytokines

Our aim was to extend our previous study dealing with plasma cytokines in the same patients [16]. By using the same groups, we could take a closer look at the correlations between miRNA and cytokine levels. We found a correlation between low levels of MCP-1 and several miRNA levels. Levels of miR-17, miR-30c, miR-126,

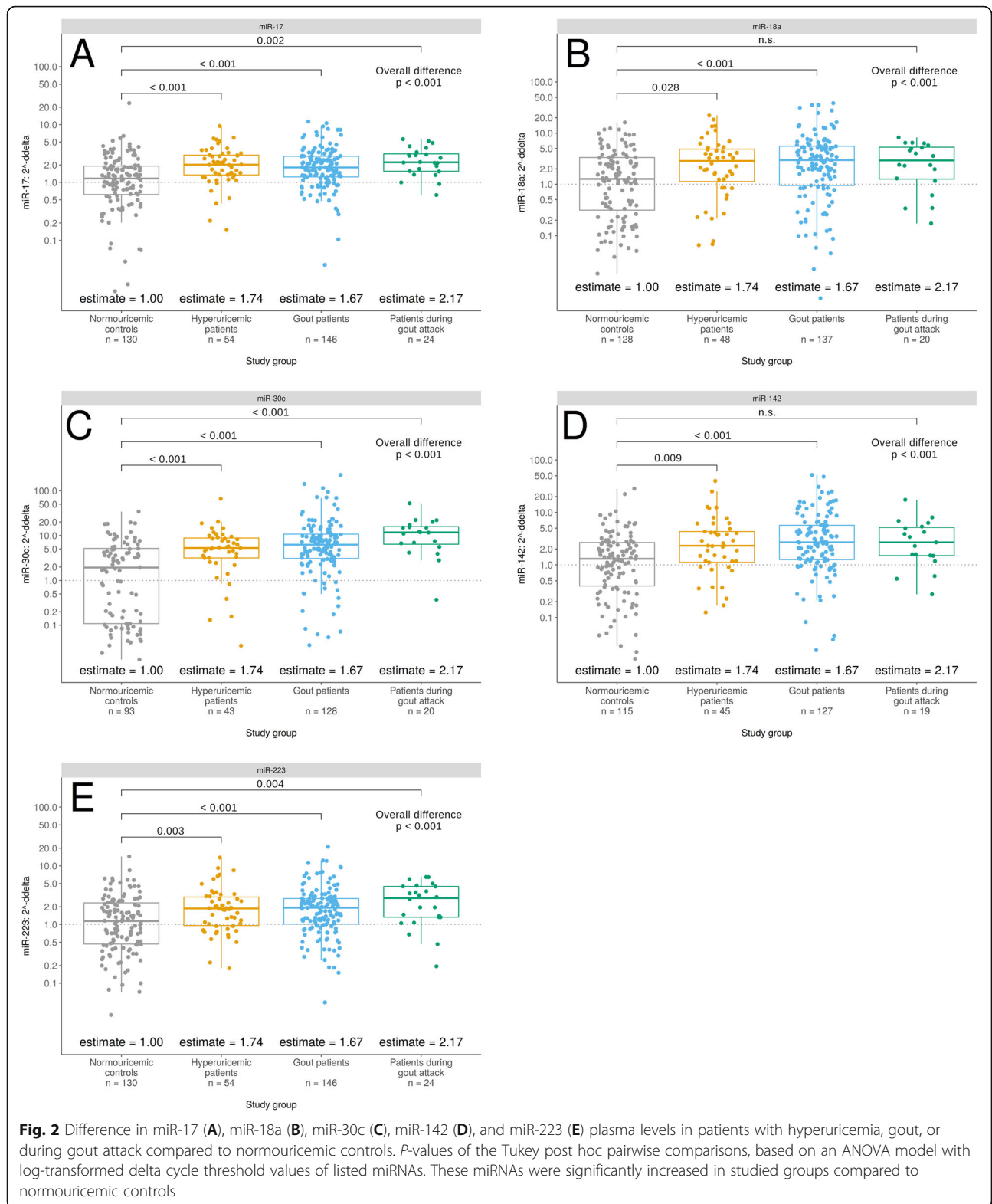


**Fig. 2** Difference in miR-17 (A), miR-18a (B), miR-30c (C), miR-142 (D), and miR-223 (E) plasma levels in patients with hyperuricemia, gout, or during gout attack compared to normouricemic controls. *P*-values of the Tukey post hoc pairwise comparisons, based on an ANOVA model with log-transformed delta cycle threshold values of listed miRNAs. These miRNAs were significantly increased in studied groups compared to normouricemic controls

miR-142, and miR-223 were negatively correlated with levels of MCP-1. Results are plotted in Fig. 3.

#### Correlation of miRNA levels and biochemical parameters

Several biochemical parameters were measured in our patient groups (Table 1). We found positive correlations ( $p < 0.05$ ) between CRP and all miRNA levels (except miR-143). Another positive correlation was between serum creatinine and levels of miR-126, miR-142, miR-146a, miR-155, and miR-222 ( $p < 0.01$ ); linked to these results, the same miRNAs were negatively correlated with eGFR. Other results are presented in Supplementary Table S3.

#### Association of miRNA levels and p.Q141K polymorphism in ABCG2

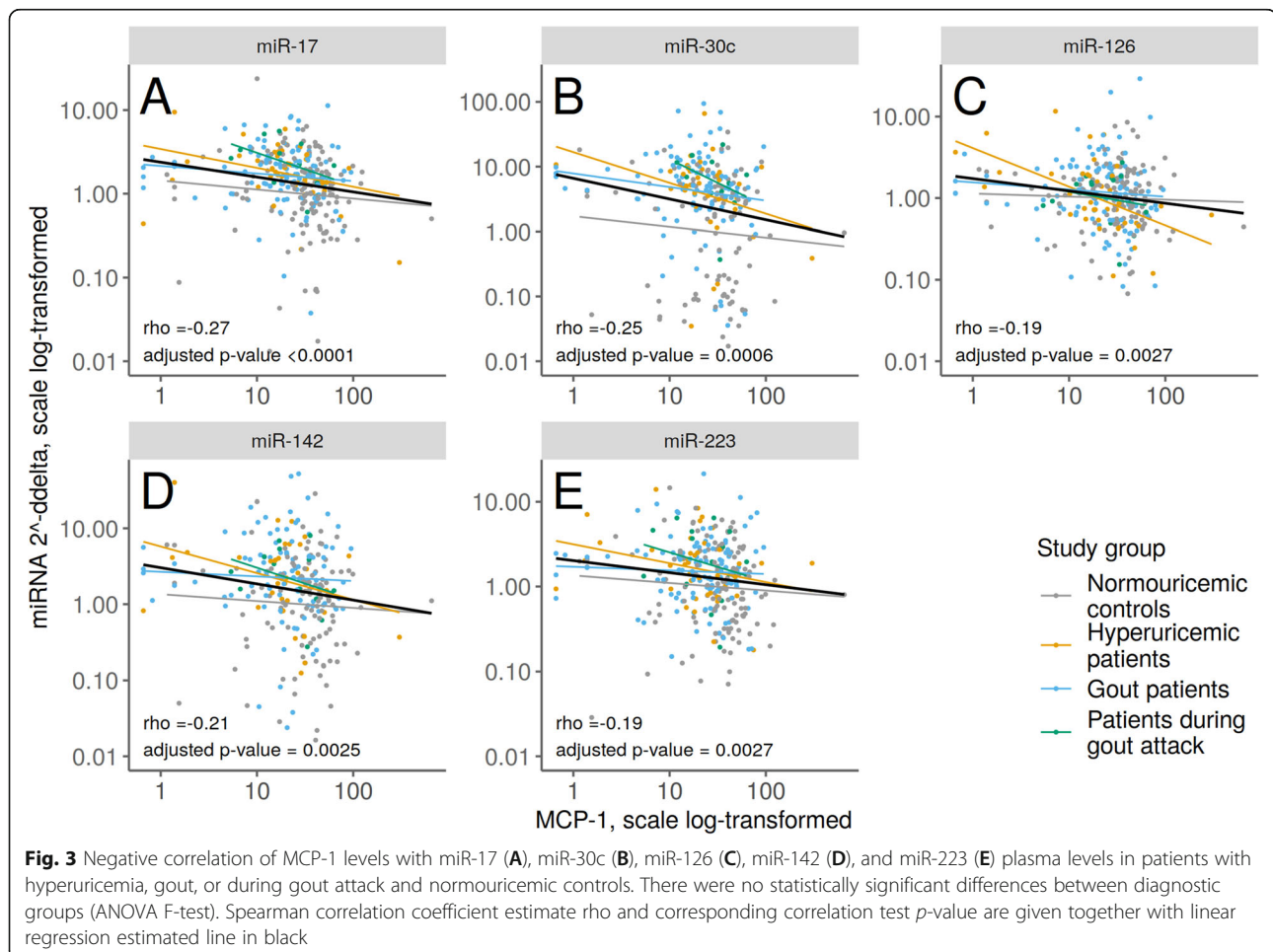
Based on the study that explained how the presence of the p.Q141K polymorphism changes the mRNA structure of the *ABCG2* gene and thus facilitates binding of miRNAs [32], we tried to examine if there was a difference in miRNA levels between carriers of the p.Q141K

variant and wild-types. However, the association between miRNA levels and p.Q141K genotype was weak.

#### Discussion

##### Comparison of miRNA levels between studied groups

MiRNAs have been extensively studied in recent years, revealing evidence that miRNAs play a role in the pathophysiology of many diseases, including gout [33]. The first study related to miRNAs and gout was published seven years ago and worked on the assumption that miR-155 plays a key role in the proinflammatory activation of human myeloid cells and antigen-driven inflammatory arthritis [34]. They examined the role of miR-155 in the acute phase of gout, which resulted in finding that miR-155 was upregulated in synovial fluid mononuclear cells in patients with acute gouty arthritis. This upregulation was negatively correlated with the expression of the SHIP-1 protein, which can increase the production of proinflammatory cytokines [27]. Thus the team of Yang et al. decided to verify these results in vivo using a mouse model; however, they did not find any significant differences in acute in vivo gout manifestation





between diverse models [35]. In our study, we also did not find any significant differences in miR-155 plasma levels between the studied groups; there was only a slightly increasing trend with diagnosis progression. A study of the role of miR-146a in the acute inflammatory response to MSU crystals was created on the basis that miR-146a has been repeatedly described in connection with rheumatoid arthritis [36]. MSU crystals induce miR-146a expression in monocytic THP-1 cells, which results in inhibition of MSU crystal-induced proinflammatory cytokine gene expression in those cells. The peripheral blood mononuclear cells (PBMCs) of patients in the intercritical phase of gout expressed higher levels of miR-146a compared to the acute gout group and control group [26]. Our results did not show any differences within groups of patients with hyperuricemia, gout, or a gout attack, not even compared to normouricemic controls.

Because the proinflammatory cytokine IL-1 $\beta$  is crucial for inflammation, as well as in acute gouty arthritis, there have been several studies addressing its regulation by miRNAs. Zhou et al. discovered five miRNAs (miR-30c-1-3p, miR-488-3p, miR-550a-3p, miR-663a, and miR-920) that possibly target IL-1 $\beta$ ; furthermore, they demonstrated significantly decreased levels of miR-488 and miR-920 in the peripheral white blood cells of patients with acute gouty arthritis. They showed that levels of IL-1 $\beta$  were significantly higher in these patients. They also described the effects of MSU crystals on the inhibited expression of miR-488 and miR-920 and induced mRNA expression of proinflammatory cytokines, such as IL-1 $\beta$ , IL-8, and TNF- $\alpha$  in monocytic THP-1 cells. In addition, they demonstrated direct targeting of IL-1 $\beta$  3' UTR by miR-488 and miR-920 [29]. After several sets of measurements (62 samples), we failed to detect altered levels of these miRNAs in our plasma samples. These miRNAs are probably not released into the extracellular environment. During further analysis, we decided to remove these miRNAs from the set of tested miRNAs. In a similar way, we excluded miR-30a and miR-133a since both showed a high percentage (48% and 57%, respectively) of undetectable or invalid data in our groups of patients. We discontinued the analysis of these miRNAs in the course of our research.

The expression of miR-18a is induced by IL-1 $\beta$  and accelerates the progression of osteoarthritis [19]. IL-1 $\beta$  is a pivotal cytokine in the inflammatory gout cascade; our results are consistent when we consider differences between groups where patients with hyperuricemia and gout had significantly higher levels of miR-18a; however, we did not find any difference for gout attack patients or a direct correlation between IL-1 $\beta$  and miR-18a levels.

The miR-17-92 cluster, including miR-17 and miR-18a, plays a role in oncogenesis [37] and proliferation

and activation of B-cells, T-cells, and macrophages [38]. We found a significantly higher expression of miR-17 and miR-18a in groups of patients with hyperuricemia and gout, and in the case of miR-17, we found higher expression in patients experiencing a gout flare in comparison with the normouricemic group. miR-17-5p can also deactivate NLRP3 inflammasomes through binding and decreasing the thioredoxin-interacting protein (TXNIP) mRNA [17, 18].

There many studies on NLRP3 inflammasome and its regulation by miRNAs; it is a key component not only in gout but also in other inflammatory diseases. In a recent summary review by Zamani et al., they present a list of 20 miRNAs associated with NLRP3 regulation, including miR-17-5p, miR-133a-1, miR-146a, miR-155, and miR-223 [39]. miR-223 was described earlier as a myeloid-specific miRNA capable of suppressing NLRP3 expression, which leads to reduced NLRP3 inflammasome activity [14]. Our data showed upregulation of miR-223 in the hyperuricemia, gout, and gout flare patients. miR-223 targets and negatively regulates NLRP3 expression and controls inflammasome activation in macrophages [14]. Upregulation of miR-223 in our plasma samples of patients with hyperuricemia, gout, and gout flare could indicate persistent inflammation even during hyperuricemia.

Experiments using human aortic endothelial cells (HAEC) revealed that miR-30c-5p could inhibit pyroptosis incurred by NLRP3 via FOXO3 targeting [21]. FOXO3 is a transcription factor associate with serum uric acid levels [40]. Our data show upregulation of this miRNA in patients with hyperuricemia, gout, and during a gout attack.

We also tried to analyze miR-302f in one set of measurements, but all samples in the set showed undetectable levels of this miRNA. Our results did not help clarify the role of miR-302f as a potential gout locus [7].

#### **Correlation of miRNA levels and biochemical parameters**

We found correlations between several miRNAs and clinical/biochemical parameters such as BML, serum uric acid, fractional uric acid excretion, glomerular filtration rate, serum creatinine, and CRP. Almost all miRNA levels were positively correlated with CRP levels. Higher levels of CRP are associated with the acute-phase of inflammation. In our previous study, we showed higher CRP levels in patients with hyperuricemia and gout; however, those patients who were not carriers of the p.Q141K variant of the *ABCG2* gene had significantly lower CRP levels [16]. This could be a possible explanation for the results of an earlier study where CRP levels were not connected with hyperuricemia [41]. There are few studies describing an association between circulating miRNA and CRP levels; for example, a positive

correlation between miR-155 and CRP was recently published [42]. Five miRNAs (miR-126, miR-142, miR-146a, miR-155, and miR-222) showed a positive correlation with serum creatinine and, therefore, a negative correlation with eGFR. Higher levels of serum creatinine and, therefore, lower values of eGFR are associated with abnormal renal function, which is also a risk factor for gout [43].

#### Association of miRNA levels and cytokines

We were interested in the association between levels of miRNA and cytokines. In our previous study, we examined the association between 27 cytokines with disease level. We found negative correlations between MCP-1 levels and miR-17, miR-30c, miR-126, miR-142, and miR-223 levels. Chemokine MCP-1 (monocyte chemoattractant protein-1) is a chemotactic factor for monocytes. Uric acid increases MCP-1 production, which is an essential part of the immune response to hyperuricemia and gout [44, 45]. We did not confirm this in our cohort of hyperuricemia and gout patients; in fact, the normouricemic control group showed significantly higher levels of MCP-1 in plasma samples [16]. On the other hand, we showed a negative correlation between this cytokine and several miRNAs that could possibly influence MCP-1 expression. According to the online miRNA target database (<http://www.mirdb.org/>), there are 46 target miRNAs for the *CCL2* gene (equal to MCP-1), but none of them are coincident with our miRNA selection. However, miR-126 can bind to 3'UTR of *CCL2*, according to the study investigating *CCL2* production in white adipose tissue inflammation. Furthermore, this study did not reveal any effect of miR-30c on adipocyte *CCL2* secretion [22]. Also, miR-223 overexpression decreased several cytokines, including MCP-1 in glioblastoma cell lines [46]. On the contrary, overexpression of miR-142 increased *CCL2* levels in monocyte-derived dendritic cells [47]. Other of the published miRNAs associated with MCP-1 are for example miR-124a [48], miR-122 [49], miR-421 [50], and miR-374a [51]. More studies are necessary in order to clarify all possible miRNAs targeting MCP-1.

#### Association of miRNA levels and p.Q141K polymorphism in *ABCG2*

One of the first studies in the field of oncology showed that RNA interference with the *ABCG2* gene could downregulate gene expression and modulate the functional phenotype of cells [52]. Importantly, a study connecting our previous and current research describes the impact of the p.Q141K polymorphism on miRNA-dependent *ABCG2* repression. The study concluded that the presence of the p.Q141K polymorphism alters the secondary structure of *ABCG2* mRNA and facilitates

translational repression by miRNAs [32]. However, we did not find any significant association between the studied miRNAs and the p.Q141K polymorphism in our groups. MiR-142-3p binds to 3'UTR and the coding sequence of *ABCG2* and inhibits its expression [24]. We reported upregulation of miR-142-3p in the plasma of hyperuricemic, gout, and gout flare patients. Moreover, a recent study reported that miR-143-3p could directly target GLUT9 (*SLC2A9* gene). MiR-143-3p was significantly reduced in kidney tissues from a hyperuricemia mice model. They also confirmed this result in humans, where miR-143-3p was significantly more expressed in the serum of healthy controls compared to hyperuricemic patients [25]. We did not find any significant differences in miR-143-3p levels between the studied groups.

#### Conclusions

In conclusion, plasma levels of several analyzed miRNAs (miR-17, miR-18a, miR-30c, miR-142, and miR-223) were upregulated in hyperuricemic, gout, and gout attack patients compared to normouricemic controls. Unfortunately, we did not find any differences in miRNA levels between particular stages of the disease, i.e., hyperuricemia, gout, and gout attack. On the other hand, we found negative correlations between several miRNAs (miR-17, miR-30c, miR-126, miR-142, and miR-223) and plasma chemokine MCP-1 levels. Furthermore, a positive correlation between CRP and all analyzed miRNAs (except miR-143) was noticed. Five of those miRNAs (miR-126, miR-142, miR-146a, miR-155, and miR-222) also showed a positive correlation with serum creatinine and, therefore, a negative correlation with eGFR.

#### Abbreviations

ABCG2: ATP-binding cassette super-family G member 2; BMI: Body mass index; CCL2: C-C Motif Chemokine Ligand 2; Cq: Quantification cycle; CRP: C-reactive protein; dCt: Delta cycle threshold; eGFR: Estimated glomerular filtration rate; FOXO3: Forkhead Box O3; GLUT9: Glucose Transporter Type 9; GWAS: Genome-wide association studies; HAEC: Human aortic endothelial cells; IL-1 $\beta$ : Interleukin-1 $\beta$ ; IL-6: Interleukin-6; IL-8: Interleukin-8; IQR: Interquartile range; MCP-1: Monocyte chemoattractant protein-1; MICE: Multivariate Imputation by Chained Equations; MSU: Monosodium urate; NLRP3: NLR Family Pyrin Domain Containing 3; OMIM: Online Mendelian Inheritance in Man; PBMCs: Peripheral blood mononuclear cells; qPCR: Quantitative PCR; SLC22A12: Solute Carrier Family 22 Member 12; SLC2A9: Solute Carrier Family 2 Member 9; SUA: Serum uric acid; THP-1 cells: Human acute monocytic leukemia cell line; TLDA: TaqMan Low Density Arrays; TNF- $\alpha$ : Tumor necrosis factor  $\alpha$ ; TXNIP: Thioredoxin-interacting protein; URAT1: Urate Transporter 1; UTR: Untranslated region

#### Supplementary Information

The online version contains supplementary material available at <https://doi.org/10.1186/s13075-021-02569-w>.

**Additional file 1: Supplementary Table S1.** List of all undetectable, valid, and invalid measurements. **Supplementary Table S2.** Comparison of delta cycle threshold (dCt) miRNA values between studied groups. **Supplementary Table S3.** P-values of miRNA levels and biochemical parameters correlations.

### Acknowledgements

We are grateful to all the patients who took part in this study as well as our colleagues at the Institute of Rheumatology for their help in recruiting patients for the study (namely Jakub Závada, Karel Pavelka, Lenka Hasíková, and Pavel Ješina).

### Authors' contributions

Study conception and design: BS and JB; acquisition of data: JB and VH; analysis and interpretation of data: BS, JB, and MP. All authors were involved in drafting the manuscript or revising it critically for content. All the authors approved the final version for publication.

### Funding

This work was supported by a grant from the Czech Republic Ministry of Health RVO 00023728 (Institute of Rheumatology), RVO VFN64165, BBMRI-CZ LM2018125, and by Charles University SVV 260367 UK.

### Availability of data and materials

The datasets used and/or analyzed during the current study are available from the corresponding author on reasonable request.

### Declarations

#### Consent for publication

Not applicable.

#### Competing interests

The authors declare that they have no competing interests.

#### Author details

<sup>1</sup>Institute of Rheumatology, Prague, Czech Republic. <sup>2</sup>Department of Rheumatology, First Faculty of Medicine, Charles University, Prague, Czech Republic. <sup>3</sup>Faculty of Science, Charles University, Prague, Czech Republic. <sup>4</sup>Department of Probability and Mathematical Statistics, Faculty of Mathematics and Physics, Charles University, Prague, Czech Republic. <sup>5</sup>Department of Pediatrics and Inherited Metabolic Disorders, First Faculty of Medicine, Charles University and General University Hospital, Prague, Czech Republic.

Received: 22 March 2021 Accepted: 28 June 2021

Published online: 10 July 2021

### References

- Hurba O, Mancikova A, Krylov V, Pavlikova M, Pavelka K, Stibůrková B. Complex analysis of urate Transporters SLC2A9, SLC22A12 and functional characterization of non-synonymous allelic variants of GLUT9 in the Czech population: no evidence of effect on hyperuricemia and gout. *PLoS One*. 2014;9. <https://doi.org/10.1371/journal.pone.0107902>.
- Matsuo H, Ichida K, Takada T, Nakayama A, Nakashima H, Nakamura T, et al. Common dysfunctional variants in ABCG2 are a major cause of early-onset gout. *Sci Rep*. 2013;3:8–11. <https://doi.org/10.1038/srep02014>.
- Stibůrková B, Pavelcová K, Závada J, Petru L, Simek P, Cepek P, et al. Functional non-synonymous variants of ABCG2 and gout risk. *Rheumatol (United Kingdom)*. 2017;56:1982–92. <https://doi.org/10.1093/rheumatology/kex295>.
- Toyoda Y, Pavelcová K, Klein M, Suzuki H, Takada T, Stibůrková B. Familial early-onset hyperuricemia and gout associated with a newly identified dysfunctional variant in urate transporter ABCG2. *Arthritis Res Ther*. 2019;21:219. <https://doi.org/10.1186/s13075-019-2007-7>.
- Perez-Ruiz F, Marimon E, Chinchilla SP. Hyperuricaemia with deposition: latest evidence and therapeutic approach. *Ther Adv Musculoskelet Dis*. 2015;7:225–33. <https://doi.org/10.1177/1759720X15599734>.
- Dalbeth N, Choi HK, Joosten LAB, Khanna PP, Matsuo H, Perez-Ruiz F, et al. Gout. *Nat Rev Dis Prim*. 2019;5:69. <https://doi.org/10.1038/s41572-019-0115-y>.
- Kawamura Y, Nakaoka H, Nakayama A, Okada Y, Yamamoto K, Higashino T, et al. Genome-wide association study revealed novel loci which aggravate asymptomatic hyperuricaemia into gout. *Ann Rheum Dis*. 2019;78:1430–7. <https://doi.org/10.1136/annrheumdis-2019-215521>.
- Lee RC, Feinbaum RL, Ambros V. The *C. elegans* heterochronic gene *lin-4* encodes small RNAs with antisense complementarity to *lin-14*. *Cell*. 1993;75:843–54. [https://doi.org/10.1016/0092-8674\(93\)90529-y](https://doi.org/10.1016/0092-8674(93)90529-y).
- Sohel MH. Extracellular/Circulating MicroRNAs: Release Mechanisms, Functions and Challenges. *Achiev Life Sci*. Elsevier BV. 2016;10:175–86. <https://doi.org/10.3390/ijms22020542>.
- Mi S, Zhang J, Zhang W, Huang RS. Circulating MicroRNAs as Biomarkers for Inflammatory Diseases. *MicroRNA*. 2013;2:64–72. <https://doi.org/10.2174/2211536611302010007>.
- Friedman RC, Farh KKH, Burge CB, Bartel DP. Most mammalian mRNAs are conserved targets of microRNAs. *Genome Res*. Cold Spring Harbor Laboratory Press. 2009;19:92–105. <https://doi.org/10.1101/gr.082701.108>.
- Sun WF, Zhu MM, Li J, Zhang XX, Liu YW, Wu XR, et al. Effects of Xie-Zhuo-Chu-Bi-Fang on miR-34a and URAT1 and their relationship in hyperuricemic mice. *J Ethnopharmacol*. Elsevier Ireland Ltd. 2015;161:163–9. <https://doi.org/10.1016/j.jep.2014.12.001>.
- Knake C, Stamp L, Bahn A. Molecular mechanism of an adverse drug-drug interaction of allopurinol and furosemide in gout treatment. *Biochem Biophys Res Commun*. Elsevier Inc. 2014;452:157–62. <https://doi.org/10.1016/j.bbrc.2014.08.068>.
- Bauernfeind F, Rieger A, Schildberg FA, Knolle PA, Schmid-Burgk JL, Hornung V. NLRP3 inflammasome activity is negatively controlled by miR-223. *J Immunol*. 2012;189:4175–81. <https://doi.org/10.4049/jimmunol.1201516>.
- Wallace SL, Robinson H, Masi AT, Decker JL, McCarty DJ, Yü TF. Preliminary criteria for the classification of the acute arthritis of primary gout. *Arthritis Rheum*. 1977;20:895–900. <https://doi.org/10.1002/art.1780200320>.
- Horváthová V, Bohatá J, Pavlíková M, Pavelcová K, Pavelka K, Šenolt L, et al. Interaction of the p.Q141K variant of the ABCG2 gene with clinical data and cytokine levels in primary hyperuricemia and gout. *J Clin Med*. 2019;8:1965. <https://doi.org/10.3390/jcm8111965>.
- Lerner AG, Upton JP, Praveen PVK, Ghosh R, Nakagawa Y, Igbaria A, et al. IRE1 $\alpha$  induces thioredoxin-interacting protein to activate the NLRP3 inflammasome and promote programmed cell death under irremediable ER stress. *Cell Metab*. 2012;16:250–64. <https://doi.org/10.1016/j.cmet.2012.07.007>.
- Chen D, Dixon BJ, Doycheva DM, Li B, Zhang Y, Hu Q, et al. IRE1 $\alpha$  inhibition decreased TXNIP/NLRP3 inflammasome activation through miR-17-5p after neonatal hypoxic-ischemic brain injury in rats. *J Neuroinflammation*. 2018; 15:32. <https://doi.org/10.1186/s12974-018-1077-9>.
- Lian C, Tao T, Su P, Liao Z, Wang X, Lei Y, et al. Targeting miR-18a sensitizes chondrocytes to anticytokine therapy to prevent osteoarthritis progression. *Cell Death Dis*. 2020;11:947. <https://doi.org/10.1038/s41419-020-03155-9>.
- Alsaleh G, François A, Philippe L, Gong YZ, Bahram S, Cetin S, et al. MiR-30a-3p negatively regulates BAFF synthesis in systemic sclerosis and rheumatoid arthritis fibroblasts. *PLoS One*. Public Library of Science. 2014;9. <https://doi.org/10.1371/journal.pone.0111266>.
- Li P, Zhong X, Li J, Liu H, Ma X, He R, et al. MicroRNA-30c-5p inhibits NLRP3 inflammasome-mediated endothelial cell pyroptosis through FOXO3 down-regulation in atherosclerosis. *Biochem Biophys Res Commun*. 2018;503:2833–40. <https://doi.org/10.1016/j.bbrc.2018.08.049>.
- Arner E, Mejhert N, Kulyté A, Balwierz PJ, Pachkram M, Cormont M, et al. Adipose tissue MicroRNAs as regulators of CCL2 production in human obesity. *Diabetes American Diabetes Association*. 2012;61:1986–93. <https://doi.org/10.2337/db11-1508>.
- Bandyopadhyay S, Lane T, Venugopal R, Parthasarathy PT, Cho Y, Galam L, et al. MicroRNA-133a-1 regulates inflammasome activation through uncoupling protein-2. *Biochem Biophys Res Commun*. NIH Public Access. 2013;439:407–12. <https://doi.org/10.1016/j.bbrc.2013.08.056>.
- Shen WW, Zeng Z, Zhu WX, Fu GH. MiR-142-3p functions as a tumor suppressor by targeting CD133, ABCG2, and Lgr5 in colon cancer cells. *J Mol Med*. 2013;91:989–1000. <https://doi.org/10.1007/s00109-013-1037-x>.
- Zhou Z, Dong Y, Zhou H, Liu J, Zhao W. MiR-143-3p directly targets GLUT9 to reduce uric acid reabsorption and inflammatory response of renal tubular epithelial cells. *Biochem Biophys Res Commun*. 2019;517:413–20. <https://doi.org/10.1016/j.bbrc.2019.07.114>.
- Dalbeth N, Pool B, Shaw OM, Harper JL, Tan P, Franklin C, et al. Role of miR-146a in regulation of the acute inflammatory response to monosodium urate crystals. *Ann Rheum Dis*. 2015;74:786–90. <https://doi.org/10.1136/annrheumdis-2014-205409>.
- Jin HM, Kim TJ, Choi JH, Kim MJ, Cho YN, Nam K. II, et al. MicroRNA-155 as a proinflammatory regulator via SHIP-1 down-regulation in acute gouty arthritis. *Arthritis Res Ther*. 2014;16:R88. <https://doi.org/10.1186/ar4531>.

28. Zhao L, Ren Y, Tang H, Wang W, He Q, Sun J, et al. Deregulation of the miR-222-ABC2 regulatory module in tongue squamous cell carcinoma contributes to chemoresistance and enhanced migratory/invasive potential. *Oncotarget*. Impact Journals LLC. 2015;6:44538–50. <https://doi.org/10.18632/oncotarget.6253>.
29. Zhou W, Wang Y, Wu R, He Y, Su Q, Shi G. MicroRNA-488 and -920 regulate the production of proinflammatory cytokines in acute gouty arthritis. *Arthritis Res Ther*. 2017;19:203. <https://doi.org/10.1186/s13075-017-1418-6>.
30. de Ronde MWJ, Ruijter JM, Lanfer D, Bayes-Genis A, Kok MGM, Creemers EE, et al. Practical data handling pipeline improves performance of qPCR-based circulating miRNA measurements. *RNA*. 2017;23:811–21. <https://doi.org/10.1261/ma.059063.116>.
31. Kirschner MB, Edelman JJB, Kao SCH, Vallyely MP, Van Zandwijk N, Reid G. The impact of hemolysis on cell-free microRNA biomarkers. *Front Genet*. 2013;4:94. <https://doi.org/10.3389/fgene.2013.00094>.
32. Ripperger A, Benndorf RA. The C421A (Q141K) polymorphism enhances the 3'-untranslated region (3'-UTR)-dependent regulation of ATP-binding cassette transporter ABCG2. *Biochem Pharmacol*. 2016;104:139–47. <https://doi.org/10.1016/j.bcp.2016.02.011>.
33. Wang Y, Xu D, Wang B, Hou X. Could microRNAs be regulators of gout pathogenesis? *Cell Physiol Biochem*. 2015;36:2085–92. <https://doi.org/10.1159/000430176>.
34. Kurowska-Stolarska M, Alivernini S, Ballantine LE, Asquith DL, Millar NL, Gilchrist DS, et al. MicroRNA-155 as a proinflammatory regulator in clinical and experimental arthritis. *Proc Natl Acad Sci U S A*. 2011;108:11193–8. <https://doi.org/10.1073/pnas.1019536108>.
35. Yang Q, Zhang Q, Qing Y, Zhou L, Mi Q, Zhou J. miR-155 is dispensable in monosodium urate-induced gouty inflammation in mice. *Arthritis Res Ther*. 2018;20:177. <https://doi.org/10.1186/s13075-018-1550-y>.
36. Bae SC, Lee YH. MiR-146a levels in rheumatoid arthritis and their correlation with disease activity: a meta-analysis. *Int J Rheum Dis*. 2018;21:1335–42. <https://doi.org/10.1111/1756-185X.13338>.
37. He L, Thomson JM, Hemann MT, Hernando-Monge E, Mu D, Goodson S, et al. A microRNA polycistron as a potential human oncogene. *Nature*. 2005;435:828–33. <https://doi.org/10.1038/nature03552>.
38. Kuo G, Wu CY, Yang HY. MiR-17-92 cluster and immunity. *J Formos Med Assoc*. 2019;118:2–6. <https://doi.org/10.1016/j.jfma.2018.04.013>.
39. Zamani P, Oskuee RK, Atkin SL, Navashenaq JG, Sahebkar A. MicroRNAs as important regulators of the NLRP3 inflammasome. *Prog Biophys Mol Biol*. 2020;150:50–61. <https://doi.org/10.1016/j.pbiomolbio.2019.05.004>.
40. Lang S, Hilsabeck TA, Wilson KA, Sharma A, Bose N, Brackman DJ, et al. A conserved role of the insulin-like signaling pathway in diet-dependent uric acid pathologies in *Drosophila melanogaster*. *PLoS Genet*. 2019;15:e1008318. <https://doi.org/10.1371/journal.pgen.1008318>.
41. Okuda C, Koyama H, Tsutsumi Z, Yamamoto A, Kurajoh M, Moriwaki Y, et al. Serum CRP in patients with gout and effects of benzbromarone. *Int J Clin Pharmacol Ther*. 2011;49:191–7. <https://doi.org/10.5414/cp201425>.
42. Su Q, Yang H, Li L. Circulating miRNA-155 as a potential biomarker for coronary slow flow. *Dis Markers*. 2018;2018:6345284. <https://doi.org/10.1155/2018/6345284>.
43. Krishnan E. Reduced Glomerular Function and Prevalence of Gout: NHANES 2009–10. *PLoS One*. 2012;7:e50046. <https://doi.org/10.1371/journal.pone.0050046>.
44. Kanellis J, Watanabe S, Li JH, Kang DH, Li P, Nakagawa T, et al. Uric acid stimulates monocyte chemoattractant protein-1 production in vascular smooth muscle cells via mitogen-activated protein kinase and cyclooxygenase-2. *Hypertension*. 2003;41:1287–93. <https://doi.org/10.1161/01.HYP.0000072820.07472.3B>.
45. Grainger R, McLaughlin RJ, Harrison AA, Harper JL. Hyperuricaemia elevates circulating CCL2 levels and primes monocyte trafficking in subjects with inter-critical gout. *Rheumatol (Oxford)*. 2013;52:1018–21. <https://doi.org/10.1093/rheumatology/kes326>.
46. Ding Q, Shen L, Nie X, Lu B, Pan X, Su Z, et al. MiR-223-3p overexpression inhibits cell proliferation and migration by regulating inflammation-associated cytokines in glioblastomas. *Pathol Res Pract*. Elsevier. 2018;214:1330–9. <https://doi.org/10.1016/j.prp.2018.05.012>.
47. Wang Y, Liang J, Qin H, Ge Y, Du J, Lin J, et al. Elevated expression of miR-142-3p is related to the pro-inflammatory function of monocyte-derived dendritic cells in SLE. *Arthritis Res Ther*. BioMed Central Ltd. 2016;18:1–11. <https://doi.org/10.1186/s13075-016-1158-z>.
48. Nakamachi Y, Kawano S, Takenokuchi M, Nishimura K, Sakai Y, Chin T, et al. MicroRNA-124a is a key regulator of proliferation and monocyte chemoattractant protein 1 secretion in fibroblast-like synoviocytes from patients with rheumatoid arthritis. *Arthritis Rheum*. 2009;60:1294–304. <https://doi.org/10.1002/art.24475>.
49. Liao M-F, Hsu J-L, Lu K-T, Chao P-K, Cheng M-Y, Hsu H-C, et al. Granulocyte Colony Stimulating Factor (G-CSF) Can Attenuate Neuropathic Pain by Suppressing Monocyte Chemoattractant Protein-1 (MCP-1) Expression, through Upregulating the Early MicroRNA-122 Expression in the Dorsal Root Ganglia. *Cells*. 2020;9:1669. <https://doi.org/10.3390/cells9071669>.
50. Zhu F, Yin J, Li J, Xue J. MicroRNA-421 affects the chemotaxis of monocytes via MCP-1, and regulates the local immune responses in injured cartilage site of elbow joint of upper limbs. *Biotechnol Biotechnol Equip*. 2020;34:294–302. <https://doi.org/10.1080/13102818.2020.1738955>.
51. Yang Z, Guo Z, Dong J, Sheng S, Wang Y, Yu L, et al. miR-374a regulates inflammatory response in diabetic nephropathy by targeting MCP-1 expression. *Front Pharmacol*. 2018;9:900. <https://doi.org/10.3389/fphar.2018.00900>.
52. Ee PLR, He X, Ross DD, Beck WT. Modulation of breast cancer resistance protein (BCRP/ABCG2) gene expression using RNA interference. *Mol Cancer Ther*. 2004;3:1577–83 PMID: 15634651.

## Publisher's Note

Springer Nature remains neutral with regard to jurisdictional claims in published maps and institutional affiliations.

**Ready to submit your research? Choose BMC and benefit from:**

- fast, convenient online submission
- thorough peer review by experienced researchers in your field
- rapid publication on acceptance
- support for research data, including large and complex data types
- gold Open Access which fosters wider collaboration and increased citations
- maximum visibility for your research: over 100M website views per year

**At BMC, research is always in progress.**

Learn more [biomedcentral.com/submissions](https://biomedcentral.com/submissions)



**Supplementary material:**

**Supplementary Table S1** List of all undetectable, valid, and invalid measurements.

<b>miRNA</b>	<b>undetectable</b>	<b>valid</b>	<b>invalid</b>	<b>all</b>
<b>miR-16</b>	1 (0.3%)	336 (94.6%)	18 (5.1%)	355 (100%)
<b>miR-25</b>	0	337 (94.9%)	18 (5.1%)	355 (100%)
<b>miR-17</b>	12 (3.4%)	342 (96.3%)	1 (0.3%)	355 (100%)
<b>miR-18a</b>	84 (23.7%)	249 (70.1%)	22 (6.2%)	355 (100%)
<b>miR-30a</b>	68 (46.9%)	75 (51.7%)	2 (1.4%)	145 (100%)
<b>miR-30c</b>	52 (14.6%)	232 (65.4%)	71 (20.0%)	355 (100%)
<b>miR-126</b>	1 (0.3%)	346 (97.5%)	8 (2.3%)	355 (100%)
<b>miR-133a</b>	76 (52.4%)	63 (43.4%)	6 (4.1%)	145 (100%)
<b>miR-142</b>	25 (7.0%)	281 (79.2%)	49 (13.8%)	355 (100%)
<b>miR-143</b>	45 (12.7%)	285 (80.3%)	25 (7.0%)	355 (100%)
<b>miR-146a</b>	1 (0.3%)	350 (98.6%)	4 (1.1%)	355 (100%)
<b>miR-155</b>	105 (29.6%)	250 (70.4%)	0	355 (100%)
<b>miR-222</b>	14 (3.9%)	337 (94.9%)	4 (1.1%)	355 (100%)
<b>miR-223</b>	2 (0.6%)	352 (99.2%)	1 (0.3%)	355 (100%)

**Supplementary Table S2** Comparison of delta cycle threshold (dCt) miRNA values between studied groups.

miRNA	NC N	NC median	NC IQR	HUA N	HUA median	HUA IQR	GA N	GA median	GA IQR	GF N	GF median	GF IQR	ALL N	ALL median	ALL IQR	KW-test p-value	adjusted p-value
miR_16	118	-0.11	1.05	53	-0.58	0.89	145	-0.42	0.94	21	-0.60	1.37	337	-0.34	1.06	<b>0.0208</b>	<b>0.0450</b>
miR_25	125	0.00	0.00	53	0.00	0.00	138	0.00	0.00	21	0.00	0.00	337	0.00	0.00	NA	NA
miR-17	130	1.17	1.30	54	2.03	1.62	146	1.81	1.59	24	2.23	1.56	354	1.65	1.77	<b>0.0000</b>	<b>0.0000</b>
miR-18a	128	1.27	3.02	48	2.89	3.72	137	2.97	4.59	20	2.99	4.06	333	2.19	4.28	<b>0.0001</b>	<b>0.0004</b>
miR-30a	59	0.71	2.28	23	0.72	1.46	54	0.76	1.99	7	1.18	1.94	143	0.73	1.91	0.7805	0.8045
miR-30c	93	1.94	5.01	43	5.26	5.64	128	6.22	7.64	20	11.72	9.38	284	4.76	7.88	<b>0.0000</b>	<b>0.0000</b>
miR-126	127	1.12	1.15	53	1.15	1.37	144	1.30	1.59	23	1.26	0.98	347	1.20	1.40	0.0627	0.1018
miR-133a	59	0.91	4.01	23	1.22	1.73	50	1.12	3.91	7	1.68	2.50	139	1.03	3.38	0.6660	0.7892
miR-142	115	1.30	2.27	45	2.31	3.20	127	2.69	4.42	19	2.68	3.68	306	2.03	3.33	<b>0.0000</b>	<b>0.0000</b>
miR-143	125	1.42	2.94	48	1.26	1.99	134	1.21	2.26	23	1.85	0.84	330	1.40	2.30	0.6678	0.7892
miR-146a	127	1.01	1.75	54	0.79	1.28	146	0.97	1.12	24	0.98	1.41	351	0.97	1.32	0.8045	0.8045
miR-155	130	1.13	2.07	54	1.41	2.59	147	1.66	3.48	24	1.55	2.59	355	1.43	2.91	<b>0.0247</b>	<b>0.0458</b>
miR-222	128	1.11	1.24	54	1.11	1.12	145	1.18	1.22	24	1.01	0.91	351	1.12	1.20	0.3483	0.5031
miR-223	130	1.14	1.87	54	1.87	1.98	146	1.92	1.76	24	2.82	3.12	354	1.58	1.99	<b>0.0000</b>	<b>0.0001</b>

NC, normouricemic controls; HUA, hyperuricemia patients; GA, gouty arthritis patients; GF, gout patients during gout flare (attack); IQR, interquartile range; KW-test, Kruskal–Wallis test. adjusted p-value, adjustment for multiple comparisons by Benjamini-Hochberg method.

**Supplementary Table S3** P-values of miRNA levels and biochemical parameters correlations.

<b>miRNA</b>	<b>BMI</b>	<b>SUA off</b>	<b>SUA on</b>	<b>FE-UA</b>	<b>eGFR-MDRD</b>	<b>CREA</b>	<b>logCRP</b>
<b>miR-17</b>	ns	ns	ns	ns	ns	ns	< 0.001
<b>miR-18a</b>	ns	ns	ns	ns	ns	ns	< 0.05
<b>miR-30c</b>	< 0.05	< 0.05	ns	ns	ns	ns	0.0001
<b>miR-126</b>	ns	ns	ns	ns	0	0.0001	0
<b>miR-142</b>	< 0.01	ns	< 0.05	ns	< 0.05	< 0.01	0
<b>miR-143</b>	ns	ns	ns	ns	ns	ns	ns
<b>miR-146a</b>	ns	ns	ns	ns	< 0.001	< 0.01	< 0.01
<b>miR-155</b>	ns	ns	ns	ns	< 0.001	< 0.001	< 0.001
<b>miR-222</b>	ns	ns	ns	< 0.01	0	< 0.001	0
<b>miR-223</b>	ns	ns	ns	ns	ns	ns	0

BMI – body mass index; SUA – serum uric acid (off treatment/on treatment); FE-UA –fractional uric acid excretion; eGFR-MDRD – estimated glomerular filtration rate calculated using the Modification of Diet in Renal Disease; CREA – serum creatinine; CRP – C-reactive protein.



## Article

# Evaluation of the Influence of Genetic Variants of *SLC2A9* (GLUT9) and *SLC22A12* (URAT1) on the Development of Hyperuricemia and Gout

Katerina Pavelcova <sup>1,2</sup> , Jana Bohata <sup>1,2</sup> , Marketa Pavlikova <sup>3</sup>, Eliska Bubenikova <sup>1,2</sup>, Karel Pavelka <sup>1</sup> and Blanka Stiburkova <sup>1,4,\*</sup>

<sup>1</sup> Department of Molecular Biology and Immunogenetics, Institute of Rheumatology, 128 50 Prague, Czech Republic; pavelcova@revma.cz (K.P.); bohata@revma.cz (J.B.); bubenikova@revma.cz (E.B.); pavelka@revma.cz (K.P.)

<sup>2</sup> Department of Rheumatology, First Faculty of Medicine, Charles University, 128 50 Prague, Czech Republic

<sup>3</sup> Department of Probability and Mathematical Statistics, Faculty of Mathematics and Physics, Charles University, 186 75 Prague, Czech Republic; marketa@ucw.cz

<sup>4</sup> Department of Pediatrics and Adolescent Medicine, First Faculty of Medicine, Charles University and General University Hospital in Prague, 120 00 Prague, Czech Republic

\* Correspondence: stiburkova@revma.cz; Tel.: +420-234-075-319

Received: 1 July 2020; Accepted: 1 August 2020; Published: 4 August 2020



**Abstract:** Urate transporters, which are located in the kidneys, significantly affect the level of uric acid in the body. We looked at genetic variants of genes encoding the major reabsorption proteins GLUT9 (*SLC2A9*) and URAT1 (*SLC22A12*) and their association with hyperuricemia and gout. In a cohort of 250 individuals with primary hyperuricemia and gout, we used direct sequencing to examine the *SLC22A12* and *SLC2A9* genes. Identified variants were evaluated in relation to clinical data, biochemical parameters, metabolic syndrome criteria, and our previous analysis of the major secretory urate transporter ABCG2. We detected seven nonsynonymous variants of *SLC2A9*. There were no nonsynonymous variants of *SLC22A12*. Eleven variants of *SLC2A9* and two variants of *SLC22A12* were significantly more common in our cohort than in the European population ( $p = 0$ ), while variants p.V282I and c.1002+78A>G had a low frequency in our cohort ( $p = 0$ ). Since the association between variants and the level of uric acid was not demonstrated, the influence of variants on the development of hyperuricemia and gout should be evaluated with caution. However, consistent with the findings of other studies, our data suggest that p.V282I and c.1002+78A>G (*SLC2A9*) reduce the risk of gout, while p.N82N (*SLC22A12*) increases the risk.

**Keywords:** gout; hyperuricemia; urate transporters; sequencing; *SLC2A9*; *SLC22A12*

## 1. Introduction

Uric acid is the final product of purine metabolism in humans. If the balance between uric acid production and excretion is impaired, hyperuricemia can occur [1]. Since uric acid is poorly soluble, at higher concentrations, in the blood, monosodium urate crystals can form [2]. In the early stages, hyperuricemia is asymptomatic; however, over time, monosodium urate crystals can lead to gout, a form of inflammatory arthritis. In addition to gout, hyperuricemia is also associated with kidney disease, hypertension, cardiovascular disease, and type 2 diabetes mellitus [3–5].

Uric acid levels are influenced by various factors, such as the intake of dietary purines, the formation of endogenous purines, the excretion of uric acid via the kidneys and intestines, genetic predisposition, medications, and health conditions [1,6]. Different studies indicate that genetic factors are involved in 25–73% of cases [7]. GWAS studies have shown an association between hyperuricemia and gout



and dysfunction of urate transporters [8,9]. These urate transport proteins are located primarily in the proximal tubules of the kidneys, and they are responsible for the excretion and reuptake of uric acid [1]. Variants of the genes that encode urate transporters are associated with both hyperuricemia and, in very rare cases, hypouricemia.

The major excretion urate transporter is ABCG2, while the GLUT9 and URAT1 proteins are important for reabsorption [6].

The *SLC2A9* gene (ENSG00000109667, solute carrier family 2 member 9, located on chromosome 4p16) encodes glucose transporter 9 (GLUT9). It occurs in two isoforms, GLUT9a, which is located on the basolateral membrane and GLUT9b, which is located on the apical membrane of the proximal tubules in the kidneys [2]. GLUT9 provides urate reuptake, and single-nucleotide polymorphisms (SNPs) of *SLC2A9* are associated not only with hyperuricemia and gout, but also with renal hypouricemia type 2 (OMIM(Online Mendelian Inheritance in Man) # 612076) [10].

The *SLC22A12* gene (ENSG00000197891, solute carrier family 22 member 12, located on chromosome 11q13) encodes urate transporter 1 (URAT1). Genetic variants of this gene lead, as in the case of *SLC2A9*, to hyperuricemia and gout and rare cases to hypouricemia type 1 (OMIM # 220150) [11].

The *ABCG2* gene (ENSG00000118777, located on chromosome 4q22) encodes the ATP-binding cassette sub-family G member 2 protein (ABCG2), which is the major secretor of uric acid. In addition to the kidneys, the ABCG2 protein is also located in the intestines, where it facilitates up to one-third of the excretion of uric acid [12]. In our previous work, we reported that genetic variants of the *ABCG2* gene (ENSG00000118777) increases the risk of developing gout, especially the common nonsynonymous variant p.Q141K (*rs2231142*) [13]. These variants are also associated with early disease onset, as confirmed by the findings of our study using a cohort of patients with pediatric-onset primary hyperuricemia and gout [14].

There are other urate transporters in the proximal tubules that are also responsible for uric acid transport, i.e., NPT1 (solute carrier family 17 member 1, *SLC17A1*), NPT4 (solute carrier family 17 member 3, *SLC17A3*), OAT4 (solute carrier family 22 member 11, *SLC22A11*), OAT10 (solute carrier family 22 member 13, *SLC22A13*), and MRP4 (ATP binding cassette subfamily C member 4, *ABCC4*) [2,15]. However, recent evidence suggests that these proteins have less impact on uric acid levels in the blood than GLUT9, URAT1, and ABCG2 [2,16].

The aims of our study were to identify which variants of the *SLC2A9* and *SLC22A12* genes existed in a cohort of 250 individuals with primary hyperuricemia and gout, and at what frequency they existed. We also intended to determine whether the variants were associated with uric acid levels and/or other important factors related to the development of hyperuricemia and gout. Polymorphisms of the *ABCG2* gene, biochemical parameters, and metabolic syndrome markers in this cohort were previously investigated in one of our other studies [13].

## 2. Experimental Section

The cohort consisted of 177 patients with primary gout and 73 patients with primary hyperuricemia under care from The Institute of Rheumatology. The gout diagnosis was determined using criteria developed by the American College of Rheumatology (ACR) Board of Directors and the European League Against Rheumatism (EULAR) Executive Committee [17]. The hyperuricemia group included individuals with elevated levels of uric acid (women > 360  $\mu\text{mol/L}$  and men > 420  $\mu\text{mol/L}$ ). Increased levels of uric acid had to be repeatedly detected over a period of at least four weeks.

In our previous study, we examined 234 individuals from our cohort in search of pathogenic variants of the *ABCG2* gene [13]. The advantage of using this cohort was that we had already excluded individuals suspected of secondary hyperuricemia and secondary gout from our study. Using questionnaires filled out by physicians, we noted the presence of chronic kidney disease, active malignancy, diabetes, hypertension, or severe psoriasis. Furthermore, the age of onset of the first signs of gout and the patient's family history of this disease were noted. In addition, an extensive

biochemical examination was performed from peripheral blood samples. These same data were also recorded for an additional 16 individuals who were added to the cohort used in this, our current study.

Prior to data collection, all 250 participants signed informed consent. Ethics approval for this study was obtained from the Ethics Committee of the Institute of Rheumatology (reference number 6181/2015).

In order to identify SNPs of the *SLC2A9* and *SLC22A12* genes, PCR amplification and sequencing were performed. Peripheral blood was collected into EDTA tubes, and total DNA was isolated by using QIAamp DNA Mini Kits (Qiagen, Hilden, Germany) and stored immediately at  $-20^{\circ}\text{C}$  until analysis.

Specific PCR primers for coding regions of the *SLC2A9* and *SLC22A12* genes were designed, and PCR reaction conditions were optimized. For analysis of *SLC22A12*, the longest transcript, ENST00000377574, coding 553 amino acids and containing 10 exons was chosen. Other transcripts of *SLC22A12* were shorter but did not differ in the amino acid sequence. As for the *SLC2A9* gene, it occurs in two transcripts that differ in exon 3. The longer transcript, ENST00000264784, contains 540 amino acids and PCR primers were designed for all twelve exons. In the shorter transcript, ENST00000506583, coding 511 amino acids, exons 1 and 2 were missing. In addition to the twelve exons in *SLC2A9*, PCR primers were also designed for exon 3 in which the amino acid sequence differs, in exon 3, from the longer transcript, ENST00000264784. The remaining exons of the two transcripts have the same sequence.

PCR products were first verified using electrophoretic analysis with 2% agarose gels.

Following electrophoresis, Presto 96 Well PCR Cleanup Kits (Geneaid, New Taipei City, Taiwan) were used to purify PCR products.

To determine nucleic acid sequences, purified PCR products were analyzed using an Applied Biosystems 3130 Genetic Analyzer (Thermo Fisher Scientific, Waltham, MA, USA), i.e., a 4-capillary electrophoretic instrument based on the Sanger sequencing method.

For evaluation of the data, reference sequences of the *SLC2A9* and *SLC22A12* transcripts listed in the Ensembl database were needed. We used Lasergene (DNASTAR) software (version 10.1.2, [www.dnastar.com](http://www.dnastar.com)) to search for SNPs having the sequences of the individuals in our cohort.

Data were summarized as medians with interquartile ranges (IQR) or as absolute and relative frequencies where appropriate. Continuous characteristics between patients with hyperuricemia and patients with gout were compared using the Wilcoxon two-sample test; categorical characteristics were compared using the Fisher exact test. The binomial test was used for comparisons of sample minor allele frequencies (MAF) with population MAFs; results with  $p$ -values  $< 0.0001$  were considered statistically significant. Differences in MAF between patients with hyperuricemia and with gout were explored using the Fisher exact test. Associations of the allelic variants with biochemical measurements (serum uric acid, creatinine, FEUA) and anamnestic data (age of onset of hyperuricemia or gout) were explored using the Kruskal-Wallis nonparametric ANOVA.

Associations between the allelic variants and hypertension were examined using the Fisher exact test. The level of statistical significance was set at 0.05; the Benjamini-Hochberg adjustment for multiple comparisons was used wherever appropriate. All analyses were performed using statistical language and environment R, version 3.6.3 ([www.r-project.org](http://www.r-project.org)).

### 3. Results

The characteristics of the cohort are summarized in Tables 1 and 2. Basic clinical data and biochemical data relevant for hyperuricemia are also included. The overview also indicates how many individuals have the p.Q141K variant of the *ABCG2* gene, which significantly increases the risk of gout since it reduces urate transport capacity.

**Table 1.** Main demographic and genetic characteristics of the hyperuricemic (*n* = 68) and gout patients (*n* = 182).

	All (Number)	All (%)	Hyperuricemic (Number)	Hyperuricemic (%)	Gout (Number)	Gout (%)	Fisher Test <i>p</i> -Value
sex (men/women)	214/36	85.6/14.4	48/20	70.6/29.4	166/16	91.2/8.8	0.0002
familial occurrence of gout	97	59.8	31	48.3	66	63.5	0.0480
no treatment	58	23.2	30	44.1	28	15.4	
treatment with allopurinol	175	70.0	38	55.9	137	75.3	<0.0001
treatment with febuxostat	17	6.8	0	0.0	17	9.3	
p.Q141K-wild type	147	58.8	44	64.7	103	56.6	
p.Q141K-heterozygous variant	87	34.8	19	27.9	68	37.4	0.3682
p.Q141K-homozygous variant	16	6.4	5	7.4	11	6.0	
hypertension	100	52.8	24	58.6	76	50.6	0.3551

Fisher exact test for comparisons between categorical variables in hyperuricemia and gout cohorts. p.Q141K, variant of the *ABCG2* gene.

**Table 2.** Main clinical and biochemical characteristics of the hyperuricemic (*n* = 68) and gout patients (*n* = 182).

	All Median (IQR)	All Range	Hyperuricemic Median (IQR)	Hyperuricemic Range	Gout Median (IQR)	Gout Range	Wilcoxon Test <i>p</i> -Value
age of onset [years]	40.0 (28.0)	1.2–84	27.0 (40.5)	1.2–76	42.0 (24.0)	11–84	0.0026
age [years]	51.5 (25.0)	3–90	36.0 (42.0)	3–78	54.0 (21.0)	11–90	<0.0001
BMI	28.4 (5.8)	16–50	28.1 (6.4)	16–41	28.4 (5.4)	19.5–50	0.0822
WHR	1.0 (0.1)	0.6–1.7	1.0 (0.1)	0.7–1.3	1.0 (0.1)	0.6–1.7	0.0038
SUA off treatment [ $\mu$ mol/L]	460.0 (123.8)	181–683	446.0 (111.0)	253–608	462.0 (124.5)	181–683	0.6298
SUA on treatment [ $\mu$ mol/L]	375.0 (134.0)	163–808	424.0 (140.0)	240–628	372.0 (128.0)	163–808	0.0515
FEUA [fraction]	3.6 (1.7)	0.8–20	3.8 (2.0)	1.6–20	3.6 (1.6)	0.8–14.3	0.6066
GFR.MDRD	86.0 (27.6)	24–426	88.0 (36.0)	28–426	86.0 (26.0)	24–154	0.2312
serum creatinine [ $\mu$ mol/L]	80.5 (19.8)	26–226	79.0 (19.2)	26–132	81.5 (20.5)	47–226	0.0240
CRP	3.5 (6.4)	0.2–224.4	1.9 (4.6)	0.2–153.1	4.0 (6.4)	0.2–224.4	0.0025

Wilcoxon two-sample test for comparisons between continuous variables in hyperuricemic and gout cohorts. IQR, interquartile ranges; WHR, waist-hip ratio; SUA, serum uric acid; FEUA, excretion fraction of uric acid; GFR.MDRD, estimation of glomerular filtration rate; CRP, C-reactive protein. Note: These are data from the initial examination at the Institute of Rheumatology. At this time, uric acid levels were in the reference range in five individuals diagnosed with hyperuricemia.

An overview of the variations found in our cohort of 250 individuals of the *SLC2A9* and *SLC22A12* genes is presented in Table 3. No nonsynonymous variants were found of the *SLC22A12* gene; however, five synonymous variants were detected: p.N82N, p.H86H, p.H142H, p.A416H, and p.L437L. We also identified three intronic variants.

In the *SLC2A9* gene, we detected seven nonsynonymous variants. Six of them were found in transcript ENST00000264784 (p.G25R, p.T275M, p.D281H, p.V282I, p.R294H, p.P350L) and the p.A17T variant was detected in exon 3 of transcript ENST00000506583. We also identified five synonymous variants in transcript ENST00000264784: p.L108L, p.T125T, p.I168I, p.L189L, and p.S515S. In transcript ENST00000264784 of the *SLC2A9* gene, we detected 16 intron variants and a novel variant, c.1002 + 68C > T, which is not yet listed in the Ensembl (Ensembl Genome Browser, [www.ensembl.org](http://www.ensembl.org)) and NCBI (National Center for Biotechnology Information, [www.ncbi.nlm.nih.gov](http://www.ncbi.nlm.nih.gov)) databases. We analyzed this variant using the Human Splicing Finder; the result was that this mutation probably has no impact on splicing. By examining the intron-exon boundaries of exon 3 of transcript ENST00000506583, we discovered three additional intronic variants.

Statistical analysis using the binomial test revealed genetic variants that were significantly more common in our cohort of 250 individuals with hyperuricemia and gout compared to their frequency in the European population (data from the Ensembl database). The variants of the *SLC2A9* gene were p.L108L, p.T125T, p.L18L, c.151-60T>C, c.249+35C>T, c.249+119G>A, c.250-40A>G, c.410+49A>G, c.1002+72G>A, c.63+18delT, and c.-40-45G>A ( $p = 0$ ). A higher allelic frequency was found in *SLC22A12* for variants c.662-7C>T and c.955-38G>A ( $p = 0$ ). On the other hand, some variants of the *SLC2A9* gene had higher MAFs in the European population, namely p.V282I, p.A17T, c.535+67A>G, c.1002+78A>G, c.1113+9A>C, c.1114-89G>C, and c.-40-13T>C ( $p = 0$ ).

Table 4 shows the results of the Fisher test comparing differences in the occurrence of genetic variants in individuals with hyperuricemia vs. patients with gout. Interestingly, variants p.A17T (OR (odds ratio) = 3.44,  $p = 0.0023$ ,  $p$ -value adjusted = 0.0432) and c.-40-13T>C (OR = 3.18,  $p = 0.0306$ ,  $p$ -value adjusted = 0.2510) of *SLC2A9* were observed to be more frequent in patients with gout. In contrast, variants c.249 + 119G > A (OR = 0.42,  $p = 0.0012$ ,  $p$ -value adjusted = 0.0432), c.151-60T>C (OR = 0.49,  $p = 0.0035$ ,  $p$ -value adjusted = 0.0432) and c.249+35C>T (OR = 0.49,  $p = 0.0042$ ,  $p$ -value adjusted = 0.0432) were more frequently found in the hyperuricemia subgroup. All associations except for c.-40-13T>C were statistically significant after adjustment for multiple comparisons.

**Table 3.** SNPs in *SLC2A9* and *SLC22A12* that were identified in a cohort of 250 patients with primary hyperuricemia and gout.

Variant	Gene	Region of the Gene	Reference SNP Number	Wild Type Homozygotes (Number)	Wild Type/Variant Heterozygotes (Number)	Variant Allele Homozygotes (Number)	Allelic Variant MAF	European Population MAF	Binomial Test <i>p</i> -Value
p.G25R, c.73G>A	<i>SLC2A9</i>	exon 1	rs2276961	44	109	97	0.606	0.528	0.0005
p.R294H, c.881G>A	<i>SLC2A9</i>	exon 7	rs3733591	161	78	11	0.200	0.191	0.6087
p.V282I, c.844G>A	<i>SLC2A9</i>	exon 7	rs16890979	195	51	4	0.118	0.214	0.0000
p.T275M, c.824C>T	<i>SLC2A9</i>	exon 7	rs112404957	244	6	0	0.012	0.009	0.4690
p.D281H, c.841G>C	<i>SLC2A9</i>	exon 7	rs73225891	238	12	0	0.024	0.029	0.5945
p.P350L, c.1049C>T	<i>SLC2A9</i>	exon 8	rs2280205	54	123	73	0.538	0.484	0.0176
p.A17T, c.49G>A	<i>SLC2A9</i>	exon 3	*rs6820230	222	0	28	0.112	0.297	0.0000
p.L108L, c.322T>C	<i>SLC2A9</i>	exon 3	rs13113918	7	48	195	0.876	0.800	0.0000
p.T125T, c.375G>A	<i>SLC2A9</i>	exon 3	rs10939650	10	58	182	0.844	0.752	0.0000
p.I168L, c.504C>T	<i>SLC2A9</i>	exon 4	rs3733589	237	13	0	0.026	0.045	0.0397
p.L189L, c.567T>C	<i>SLC2A9</i>	exon 6	rs13125646	7	47	196	0.878	0.801	0.0000
p.S515S, c.1545C>T	<i>SLC2A9</i>	exon 12	rs144428359	243	7	0	0.014	0.007	0.0944
c.150+24A>G	<i>SLC2A9</i>	intron 1–2	rs2276962	241	9	0	0.018	0.042	0.0050
c.150+65C>T	<i>SLC2A9</i>	intron 1–2	rs2276963	239	11	0	0.022	0.054	0.0007
c.151-60T>C	<i>SLC2A9</i>	intron 1–2	rs2240722	44	52	154	0.720	0.528	0.0000
c.249+35C>T	<i>SLC2A9</i>	intron 2–3	rs2240721	42	46	162	0.740	0.528	0.0000
c.249+119G>A	<i>SLC2A9</i>	intron 2–3	rs2240720	45	25	180	0.770	0.601	0.0000
c.250-40A>G	<i>SLC2A9</i>	intron 2–3	rs28592748	8	48	194	0.872	0.800	0.0000
c.410+29G>T	<i>SLC2A9</i>	intron 3–4	rs16891971	246	4	0	0.008	0.026	0.0069
c.410+49A>G	<i>SLC2A9</i>	intron 3–4	rs772544951	249	1	0	0.002	0.000	0.0000
c.535+67A>G	<i>SLC2A9</i>	intron 4–5	rs3733590	236	14	0	0.028	0.071	0.0000
c.681+25G>A	<i>SLC2A9</i>	intron 5–6	rs13115193	50	109	91	0.582	0.505	0.0006
c.681+13C>T	<i>SLC2A9</i>	intron 5–6	rs202000076	248	2	0	0.004	0.001	0.0901
c.682-31C>T	<i>SLC2A9</i>	intron 5–6	rs4292327	142	97	11	0.238	0.224	0.4528
c.1002+68C>T	<i>SLC2A9</i>	intron 7–8	NA	249	1	0	0.002	NA	NA
c.1002+72G>A	<i>SLC2A9</i>	intron 7–8	rs1050991059	249	1	0	0.002	0.000	0.0000
c.1002+78A>G	<i>SLC2A9</i>	intron 7–8	rs6823877	128	71	51	0.346	0.651	0.0000
c.1113+9A>C	<i>SLC2A9</i>	intron 8–9	rs2280204	196	48	6	0.120	0.200	0.0000
c.1114-89G>C	<i>SLC2A9</i>	intron 8–9	rs114361719	249	1	0	0.002	0.028	0.0000
c.63+18delT	<i>SLC2A9</i>	intron 3–4	*rs61256984	1	236	13	0.524	0.299	0.0000
c.-40-13T>C	<i>SLC2A9</i>	5' UTR	*rs6449237	232	0	18	0.072	0.293	0.0000
c.-40-45G>A	<i>SLC2A9</i>	5' UTR	*rs752032126	249	0	1	0.004	0.000	0.0000
p.N82N, c.246C>T	<i>SLC22A12</i>	exon 1	rs3825017	248	2	0	0.004	0.004	1.0000

Table 3. Cont.

Variant	Gene	Region of the Gene	Reference SNP Number	Wild Type Homozygotes (Number)	Wild Type/Variant Heterozygotes (Number)	Variant Allele Homozygotes (Number)	Allelic Variant MAF	European Population MAF	Binomial Test p-Value
p.H86H, c.258C>T	SLC22A12	exon 1	rs3825016	37	106	107	0.640	0.706	0.0014
p.H142H, c.426T>C	SLC22A12	exon 2	rs11231825	36	106	108	0.644	0.706	0.0027
p.A416A, c.1248A>G	SLC22A12	exon 7	rs1630320	0	0	250	1.000	1.000	1.0000
p.L437L, c.1309T>C	SLC22A12	exon 8	rs7932775	154	77	19	0.230	0.202	0.1191
c.662-7C>T	SLC22A12	intron 3–4	rs373881060	245	5	0	0.010	0.000	0.0000
c.1598+18C>T	SLC22A12	intron 9–10	rs11231837	152	79	19	0.234	0.199	0.0566
c.955-38G>A	SLC22A12	intron 5–6	rs368284669	248	2	0	0.004	0.000	0.0000

SNPs found in the *SCL2A9* gene in transcript ENST00000506583 are marked with an asterisk (\*) sign, others come from longer transcript ENST00000264784. Genetic variants of the *SLC22A12* gene originate from transcript ENST00000377574. The minor allele frequency (MAF) in our cohort was compared to the European MAF using the binomial test.

Table 4. Comparison of genetic variants in individuals with primary hyperuricemia and patients with primary gout.

Variant	Individuals with Hyperuricemia				Patients with Gout				OR	Fisher Test p-Value	Benjamini-Hochberg Method: p-Value Adjusted
	Wild Type Homozygotes (Number)	Wild Type/Variant Heterozygotes (Number)	Variant Allele Homozygotes (Number)	Variant Allele MAF	Wild Type Homozygotes (Number)	Wild Type/Variant Heterozygotes (Number)	Variant Allele Homozygotes (Number)	Variant Allele MAF			
p.G25R	7	33	28	0.654	37	76	69	0.588	0.75	0.1829	0.7374
p.R294H	42	22	4	0.221	119	56	7	0.192	0.84	0.5300	1.0000
p.V282I	53	14	1	0.118	142	37	3	0.118	1.00	1.0000	1.0000
p.T275M	68	0	0	0.000	176	6	0	0.016	–	0.1966	0.7374
p.N281H	65	3	0	0.022	173	9	0	0.025	1.12	1.0000	1.0000
p.P350L	15	35	18	0.522	39	88	55	0.544	1.9	0.6875	1.0000
p.A17T	65	0	3	0.044	157	0	25	0.137	3.44	0.0023	0.0432
p.L108L	0	17	51	0.875	7	31	144	0.876	1.1	1.0000	1.0000
p.T125T	0	20	48	0.853	10	38	134	0.841	0.91	0.7834	1.0000
p.I168I	66	2	0	0.015	171	11	0	0.030	2.9	0.5291	1.0000
p.L189L	0	15	53	0.890	7	32	143	0.874	0.86	0.7589	1.0000
p.S515S	68	0	0	0.000	175	7	0	0.019	–	0.1978	0.7374
c.150+24A>G	66	2	0	0.015	175	7	0	0.019	1.31	1.0000	1.0000
c.150+65C>T	66	2	0	0.015	173	9	0	0.025	1.70	0.7351	1.0000
c.151-60T>C	4	17	47	0.816	40	35	107	0.684	0.49	0.0035	0.0432
c.249+35C>T	4	15	49	0.831	38	31	113	0.706	0.49	0.0042	0.0432
c.249+119G>A	4	10	54	0.868	41	15	126	0.734	0.42	0.0012	0.0432
c.250-40A>G	0	17	51	0.875	8	31	143	0.871	0.96	1.0000	1.0000
c.410+29G>T	67	1	0	0.007	179	3	0	0.008	1.12	1.0000	1.0000

Table 4. Cont.

Variant	Individuals with Hyperuricemia				Patients with Gout				OR	Fisher Test <i>p</i> -Value	Benjamini -Hochberg Method: <i>p</i> -Value Adjusted
	Wild Type Homozygotes (Number)	Wild Type/Variant Heterozygotes (Number)	Variant Allele Homozygotes (Number)	Variant Allele MAF	Wild Type Homozygotes (Number)	Wild Type/Variant Heterozygotes (Number)	Variant Allele Homozygotes (Number)	Variant Allele MAF			
c.410+49A>G	68	0	0	0.000	181	1	0	0.003	–	1.0000	1.0000
c.535+67A>G	65	3	0	0.022	171	11	0	0.030	1.38	0.7676	1.0000
c.681+25G>A	8	34	26	0.632	42	75	65	0.563	0.75	0.1855	0.7374
c.681+13C>T	68	0	0	0.000	180	2	0	0.005	–	1.0000	1.0000
c.682-31C>T	43	23	2	0.199	99	74	9	0.253	1.36	0.2383	0.8141
c.1002+68C>T	68	0	0	0.000	181	1	0	0.003	–	1.0000	1.0000
c.1002+72G>A	68	0	0	0.000	181	1	0	0.003	–	1.0000	1.0000
c.1002+78A>G	37	17	14	0.331	91	54	37	0.352	1.10	0.7514	1.0000
c.1113+9A>C	53	15	0	0.110	143	33	6	0.124	1.14	0.7585	1.0000
c.1114-89G>C	68	0	0	0.000	181	1	0	0.003	–	1.0000	1.0000
c.63+18delT	0	66	2	0.515	1	170	11	0.527	1.5	0.8407	1.0000
c.-40-13T>C	66	0	2	0.029	166	0	16	0.088	3.18	0.0306	0.2510
c.-40-45G>A	68	0	0	0.000	181	0	1	0.005	–	1.0000	1.0000
p.N82N	67	1	0	0.007	181	1	0	0.003	0.37	0.4704	1.0000
p.H86H	8	24	36	0.706	29	82	71	0.615	0.67	0.0749	0.4385
p.H142H	7	25	36	0.713	29	81	72	0.618	0.65	0.0586	0.4006
p.A416A	0	0	68	1.000	0	0	182	1.000	0.00	1.0000	1.0000
p.L437L	45	16	7	0.221	109	61	12	0.234	1.8	0.8119	1.0000
c.662-7C>T	67	1	0	0.007	178	4	0	0.011	1.50	1.0000	1.0000
c.1598+18C>T	44	17	7	0.228	108	62	12	0.236	1.5	0.9058	1.0000
c.955-38G>A	67	1	0	0.007	181	1	0	0.003	0.37	0.4704	1.0000

OR, odds ratio. In cases without a variant allele among hyperuricemic patients, the OR could not be enumerated (shown as a ‘–’ sign in the cell).

The results of the statistical evaluation of the associations between variants of the genes and serum uric acid levels and fractional excretion of uric acid are shown in Table 5. After adjustment for multiple comparisons, there were no statistically significant associations. We also evaluated the relationship between genetic variants and creatinine, hypertension, age of onset of hyperuricemia or gout, but no associations were detected.

Since we already knew the *ABCG2* gene sequencing results for the investigated cohort, we also focused on comparing the mutual occurrence of variants in the *ABCG2*, *SLC2A9*, and *SLC22A12* genes. As for the *ABCG2* gene, we focused on dysfunctional variants p.Q141K (*rs2231142*), p.R147W (*rs372192400*), p.T153M (*rs753759474*), p.F373C (*rs752626614*), p.T434M (*rs769734146*), p.S476P, and p.S572R (*rs200894058*) [13]. Concerning the *SLC2A9* and *SLC22A12* genes, we were particularly interested in nonsynonymous variants (p.G25R, p.T275M, p.D281H, p.V282I, p.R294H, p.P350L) and other variants known from the literature to be associated with hyperuricemia and gout, or vice versa, i.e., to reduce the risk of gout, namely p.N82N, p.H86H, p.H142H, p.L108L, p.I168I, c.1002+78A>G, and c.535+67A>G [18–23]. We found that individuals with any of the above-mentioned dysfunctional variants of *ABCG2* (except p.Q141K) were more likely to have the p.D281H allele in *SLC2A9* ( $p = 0.0389$ ). An interesting finding was that individuals with any of the dysfunctional variants of *ABCG2* were less likely to have the homozygous variant p.P350L of *SLC2A9*. Furthermore, we found that individuals with the intronic variant c.1002+78A>G of *SLC2A9* were less likely to have dysfunctional variants of *ABCG2* ( $p = 0.014$ ). Comparisons of the mutual occurrence of other variants did not show any statistically significant results, so only results for variants p.D281H, p.P350L, and c.1002+78A>G are summarized in Tables 6–9.



**Table 5.** The relationship between the detected variants and serum uric acid levels and fractional excretion of uric acid.

Variant	Median of Serum Uric Acid Levels [µmol/L]			Kruskal-Wallis ANOVA	Benjamini-Hochberg Method: <i>p</i> -Value Adjusted	Median of FEUA [%]			Kruskal-Wallis ANOVA	Benjamini-Hochberg Method: <i>p</i> -Value Adjusted
	Wild Type Homozygotes	Wild Type/Variant Heterozygotes	Variant Allele Homozygotes			Wild Type Homozygotes	Wild Type/Variant Heterozygotes	Variant Allele Homozygotes		
p.G25R	470	446	448	0.2114	0.653	3.6	3.5	3.7	0.5943	0.933
p.R294H	461	442	430	0.9211	0.921	3.6	3.6	4.2	0.2394	0.933
p.V282I	451	464	395	0.6131	0.735	3.7	3.3	3.1	0.2560	0.933
p.T275M	461	408	NA	0.1623	0.622	3.6	3.4	NA	0.9092	0.937
p.N281H	458	463	NA	0.4241	0.728	3.6	3.7	NA	0.6986	0.933
p.P350L	467	458	440	0.7566	0.830	3.6	3.6	3.7	0.9675	0.968
p.A17T	454	NA	476	0.3181	0.728	3.7	NA	3.6	0.5109	0.933
p.L108L	464	468	451	0.5179	0.734	3.3	3.6	3.6	0.5890	0.933
p.T125T	485	462	452	0.8198	0.867	3.6	3.6	3.6	0.6707	0.933
p.I168I	460	333	NA	0.1300	0.622	3.6	3.9	NA	0.5167	0.933
p.L189L	464	472	455	0.5865	0.735	3.3	3.2	3.7	0.3902	0.933
p.S515S	456	464	NA	0.6484	0.735	3.6	4.4	NA	0.5417	0.933
c.150+24A>G	460	312	NA	0.0215	0.622	3.6	3.9	NA	0.7131	0.933
c.150+65C>T	460	333	NA	0.1300	0.622	3.6	3.9	NA	0.4553	0.933
c.151-60T>C	473	444	446	0.0732	0.622	3.6	4.0	3.6	0.0656	0.736
c.249+35C>T	478	458	444	0.1310	0.622	3.6	4.0	3.6	0.0803	0.736
c.249+119G>A	482	458	444	0.0829	0.622	3.6	4.5	3.5	0.0037	0.127
c.250-40A>G	464	468	451	0.5179	0.734	3.2	3.6	3.6	0.5163	0.933
c.410+29G>T	460	568	NA	0.1830	0.622	3.6	4.2	NA	0.2784	0.933
c.410+49A>G	460	NA	NA	NA	NA	3.6	14.3	NA	NA	NA
c.535+67A>G	460	401	NA	0.3475	0.728	3.6	4.2	NA	0.1387	0.893
c.681+25G>A	477	451	442	0.0679	0.622	3.4	3.7	3.7	0.8218	0.933
c.681+13C>T	460	482	NA	0.6450	0.735	3.6	2.8	NA	0.1577	0.893
c.682-31C>T	442	462	482	0.2579	0.728	3.7	3.5	3.7	0.8507	0.933
c.1002+68C>T	460	600	NA	NA	NA	3.6	5.5	NA	NA	NA
c.1002+72G>A	460	437	NA	NA	NA	3.6	3.1	NA	NA	NA
c.1002+78A>G	450	451	469	0.3498	0.728	3.6	3.4	3.9	0.0865	0.736
c.1113+9A>C	462	441	385	0.6242	0.735	3.7	3.6	3.8	0.8498	0.933
c.1114-89G>C	460	NA	NA	NA	NA	3.6	2.9	NA	NA	NA
c.63+18delT	462	455	495	0.4499	0.728	3.1	3.6	3.8	0.6716	0.933
c.-40-13T>C	454	NA	477	0.1799	0.622	3.6	NA	3.6	0.9065	0.937
c.-40-45G>A	460	NA	548	NA	NA	3.6	NA	4.3	NA	NA
p.N82N	460	430	NA	0.8417	0.867	3.6	4.4	NA	0.3696	0.933
p.H86H	415	470	451	0.3873	0.728	3.6	3.6	3.7	0.4343	0.933
p.H142H	418	470	450	0.4299	0.728	3.6	3.6	3.7	0.4044	0.933
p.A416A	NA	NA	460	NA	NA	NA	NA	3.6	NA	NA
p.L437L	460	464	406	0.4105	0.728	3.6	3.6	3.4	0.7912	0.933
c.662-7C>T	460	414	NA	0.5885	0.735	3.6	2.7	NA	0.7552	0.933
c.1598+18C>T	460	468	406	0.3664	0.728	3.6	3.6	3.4	0.7872	0.933
c.955-38G>A	460	492	NA	0.4847	0.734	3.6	4.2	NA	0.4767	0.933

**Table 6.** Comparison of mutual occurrence of dysfunctional variants of *ABCG2* (p.R147W, p.T153M, p.F373C, p.T434M, p.S476P, and p.S572R) and the variant p.D281H in a cohort of individuals with hyperuricemia and gout.

		Without <i>ABCG2</i> Variants (Number)	Without <i>ABCG2</i> Variants (%)	Occurrence of Variants of <i>ABCG2</i> (Number)	Occurrence of Variants of <i>ABCG2</i> (%)	Total Number (without Distinction of Alleles in <i>ABCG2</i> )	Portion of the Whole Cohort (%)
p.D281H	wild type	233	95.9	5	71.4	238	95.2
	heterozygotes + homozygotes	10	4.1	2	28.6	12	4.8
total in the given column		243	100.0	7	100.0	250	100.0

Fisher's Exact Test: *p*-value = 0.0389, odds ratio 9.11.

**Table 7.** Comparison of mutual occurrence of dysfunctional variants of *ABCG2* (p.R147W, p.T153M, p.F373C, p.T434M, p.S476P, and p.S572R) and the variant p.D281H in a cohort of individuals with gout.

		Without <i>ABCG2</i> Variants (Number)	Without <i>ABCG2</i> Variants (%)	Occurrence of Variants of <i>ABCG2</i> (Number)	Occurrence of Variants of <i>ABCG2</i> (%)	Total Number (without Distinction of Alleles of <i>ABCG2</i> )	Portion in the Whole Cohort (%)
p.D281H	wild type	169	96	4	66.7	173	95.1
	heterozygotes + homozygotes	7	4	2	33.3	9	4.9
total in the given column		176	100	6	100.0	182	100.0

Fisher's Exact Test: *p*-value = 0.0295, odds ratio 11.6.

**Table 8.** Comparison of mutual occurrence of dysfunctional variants of *ABCG2* (p.Q141K, p.R147W, p.T153M, p.F373C, p.T434M, p.S476P, and p.S572R) and the variant p.350L in a cohort of individuals with hyperuricemia and gout.

		Without <i>ABCG2</i> Variants (Number)	Without <i>ABCG2</i> Variants (%)	Occurrence of Variants of <i>ABCG2</i> (Number)	Occurrence of Variants of <i>ABCG2</i> (%)	Total Number (without Distinction of Alleles of <i>ABCG2</i> )	Portion in the Whole Cohort (%)
p.P350L	wild type + heterozygotes	175	72	2	28.6	177	70.8
	homozygotes	68	28	5	71.4	73	29.2
total in the given column		243	100	7	100.0	250	100.0

Fisher's Exact Test: *p*-value = 0.0239, odds ratio 6.38.

**Table 9.** Comparison of mutual occurrence of dysfunctional variants of *ABCG2* (p.Q141K, p.R147W, p.T153M, p.F373C, p.T434M, p.S476P, and p.S572R) and the variant c.1002+78A>G in a cohort of individuals with hyperuricemia and gout.

		Without <i>ABCG2</i> Variants (Number)	Without <i>ABCG2</i> Variants (%)	Occurrence of Heterozygous Variants of <i>ABCG2</i> (Number)	Occurrence of Heterozygous Variants of <i>ABCG2</i> (%)	Occurrence of Homozygous Variants of <i>ABCG2</i> (Number)	Occurrence of Homozygous Variants of <i>ABCG2</i> (%)	Total Number (without Distinction of Alleles of <i>ABCG2</i> )	Portion in the Whole Cohort (%)
c.1002+78A>G	wild type	68	47.6	48	54.5	12	63.2	128	51.2
	heterozygotes	52	36.4	17	19.3	2	10.5	71	28.4
	homozygotes	23	16.1	23	26.1	5	26.3	51	20.4
total in the given column		143	100.0	88	100.0	19	100.0	250	100.0

Fisher's Exact Test: *p*-value = 0.014.

#### 4. Discussion

The main aims of our single center study were to (1) identify variants of the *SLC2A9* and *SLC22A12* genes, (2) determine their frequency compared to the European population, and (3) to evaluate the variants in relation to clinical, biochemical, and genetic data of a cohort with primary hyperuricemia and gout.

No nonsynonymous variants were found of the *SLC22A12* gene, which was highly conserved. This leads to an important question about the effect of synonymous and intronic variants on the development of hyperuricemia and gout. From variants detected in our cohort, we found references in the literature to three synonymous variants. In one study comparing the effect of single nucleotide polymorphisms on uric acid levels, the p.N82N variant was found to be associated with hyperuricemia [18]. Another synonymous variant, p.H86H, was also associated with hyperuricemia and gout [19,24,25]. In contrast, variant p.H142H reduces the risk of gout, according to authors of the study carried out on the Vietnamese population [20]. However, variants p.H86H and p.H142H are common in the European population as well as in our cohort. In contrast, the p.N82N variant rarely occurs; the MAF for the European population is 0.004; in our cohort, this variant occurred in two individuals.

In the *SLC2A9* gene, the variant p.V282I was found to be significantly more frequent in the European population (0.214) than in our cohort (0.118) ( $p = 0$ ). According to a previously published study, this variant reduces the risk of gout [21]. Results regarding intronic variant c.1002+78A>G were also interesting. We found that this variant is significantly more common in the European population compared to our cohort. Our results also seem to be consistent with other research that found c.1002+78A>G reduces the risk of gout [23].

Functional studies have already been performed for all seven nonsynonymous variants that we found of the *SLC2A9* gene. Evaluation of urate uptake and expression was performed using *Xenopus laevis* oocytes. The results did not show significant differences (i.e., expression, location, and urate uptake) between native GLUT9 and proteins with nonsynonymous variants [26].

The association between genetic variants and serum uric acid levels and fractional excretion of uric acid cannot be interpreted with certainty. However, no association was found between creatinine, hypertension, age of onset of hyperuricemia or gout, and variants of the genes.

It is worth mentioning that in patients with primary gout, variants of the *ABCG2* gene occur more frequently than SNPs in *SLC2A9*, *SLC22A12*, and the other genes coding urate transporters. This matches our earlier observations, which showed that, in our cohort of 250 individuals with primary hyperuricemia and gout, the p.Q141K variant of *ABCG2* has a higher allele frequency relative to its allele frequency in the European population (0.24 vs. 0.09). Interestingly, the p.Q141K variant reduces urate transport capacity by up to 53% [16]. This variant also appears to be associated with a lower body mass index and C-reactive protein value [27].

Since different urate transporters are involved in the regulation of uric acid, it was interesting to compare the mutual occurrence of dysfunctional variants of the *ABCG2* gene with variants of the *SLC2A9* and *SLC22A12* genes. One study has already focused on the co-occurrence of selected variants of these genes, i.e., which variants p.H142H (*SLC22A12*), p.V282I (*SLC2A9*) or p.G141K (*ABCG2*) were associated with reduced uric acid excretion [28]. According to our results, variant p.D281H appears to occur more frequently along with the dysfunctional variants of the *ABCG2* gene, so this allele could contribute, together with other variants of *ABCG2*, to increased levels of uric acid. Results regarding two other variants, p.P350L and c.1002+78A>G, are also noteworthy, i.e., they occur more frequently in individuals who do not have dysfunctional variants of *ABCG2*. Taking into account that, according to the conclusion of another study, variant c.1002+78A>G reduces the risk of gout, our results suggest that c.1002+78A>G and p.P350L could reduce the risk of hyperuricemia and gout [23].

It is also important to mention that GLUT9 and URAT1 are referred to as proteins that are associated not only with hyperuricemia and gout, but also with hypouricemia since they are urate reuptake transporters. Figure 1 provides an overview of selected variants of the *SLC2A9* and *SLC22A12*

genes that are associated with hyperuricemia and gout, or vice versa, with hypouricemia. None of the variants found in our cohort were associated with hypouricemia, which is not surprising in light of the characteristics of our cohort and also because renal hypouricemia is a very rare disease [29,30].

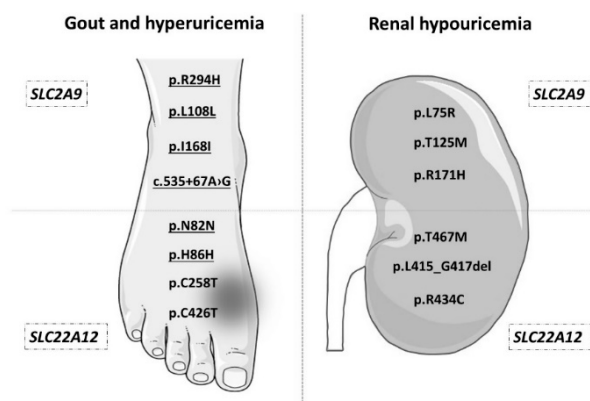


**Figure 1.** Genetic variants of *SLC2A9* and *SLC22A12* associated with hyperuricemia, gout, and renal hypouricemia. The picture shows some of the genetic variants that are, according to various studies, associated with elevated uric acid levels and increased risk of gout (on the left), or with rare renal hypouricemia (on the right). In the upper two quadrants, SNPs in the *SLC2A9* gene are shown, while in the lower quadrants, SNPs in *SLC22A12* are listed. The underlined genetic variants were found in our cohort. References to studies relating to genetic variants in this figure: p. R294H and p.I168I [22], p.L108L [31], c.535 + 67A > G [23], p.N82N [18], p.H86H [19], p.C258T and p.C426T [32], p.L75R [33], p.T125M [34], p.R171H [35], p.T467M and p.L415\_G417del [29], p.R434M [36]. Foot and kidney images were copied from Servier Medical Art, by Servier (<https://smart.servier.com>; kidney image: [https://smart.servier.com/smart\\_image/kidney-2/](https://smart.servier.com/smart_image/kidney-2/); foot image: [https://smart.servier.com/smart\\_image/pied/](https://smart.servier.com/smart_image/pied/)) and adapted for the purposes of this article. Servier Medical Art by Servier is licensed under a Creative Commons Attribution 3.0 Unported License.

The lack of nonsynonymous variants of *SLC22A12* in our cohort was not so surprising since it is likely that these variants act as gout suppressors based on the reabsorption function of the URAT1 protein. This possibility is supported by a study that focused on nonsynonymous variant p.G774A, which is known to lead to the development of idiopathic renal hypouricemia in the Japanese population. In a cohort of 185 individuals with gout, the authors did not find p.G774A in any patient, while in healthy control subjects, it was present with a frequency of 2.3% [37]. Another study, which focused on two nonsynonymous variants p.R90H and p.W258X of *SLC22A12*, had very similar findings. These variants were also associated with renal hyperuricemia and were not detected in a large cohort of 1993 gout patients. In the group of healthy controls, these variants occur and reduce the risk of hyperuricemia [38]. However, the authors of another study came to different conclusions; they found nonsynonymous variants of the *SLC22A12* gene in 16 patients from a cohort of 69 individuals with gout. The p.C850G variant was detected in 11 patients from the cohort, while no nonsynonymous variants were found in the healthy controls. The unexpected results of this study can be explained by the different frequencies of the variants in diverse populations, i.e., the research was done in the Mexican population. Insight into this issue could provide useful information on the functional impact of the variants detected in this study, which is a question for further research [39].

The main advantage of our study was primarily its detailed genetic analysis of urate transporters GLUT9, URAT1, and the previously analyzed ABCG2 in a clinically and biochemically characterized cohorts of Czech patients with primary hyperuricemia and gout. However, our study has some limitations. A larger cohort would provide a clearer view of the effects of the variants of the *SLC22A12* and *SLC2A9* genes on the development of hyperuricemia and gout. This would also facilitate a more accurate statistical evaluation of less frequent variants in terms of uric acid levels. We also do

not have data on the possible occurrence of asymptomatic urate crystal deposition in individuals with hyperuricemia, which could explain the association with genetic variants of the examined genes. It should also be noted that other urate transporters are involved in the transport of uric acid. Collectively these proteins act as a complex mechanism in the proximal kidney tubules, and it is very likely that the impaired function of one transporter could be compensated for by one or more of the other proteins.

However, more research on this topic needs to be done before the complexities of uric acid transport are fully understood, and other genes that encode urate transporters need to be examined.

**Author Contributions:** Conceptualization, B.S.; Formal analysis, K.P. (Katerina Pavelcova), J.B., M.P. and E.B.; Investigation, K.P. (Katerina Pavelcova) and J.B.; Writing—original draft, K.P. (Katerina Pavelcova); Writing—review & editing, J.B., M.P., E.B., K.P. (Karel Pavelka) and B.S. All authors have read and agreed to the published version of the manuscript.

**Funding:** This study was supported by the project for the conceptual development of research organization 00023728 (Institute of Rheumatology).

**Conflicts of Interest:** The authors declare no conflict of interest.

## References

1. Bobulescu, I.A.; Moe, O.W. Renal transport of uric acid: Evolving concepts and uncertainties. *Adv. Chronic Kidney Dis.* **2012**, *19*, 358–371. [[CrossRef](#)] [[PubMed](#)]
2. So, A.; Thorens, B. Uric acid transport and disease. *J. Clin. Investig.* **2010**, *120*, 1791–1799. [[CrossRef](#)] [[PubMed](#)]
3. Nath, S.D.; Voruganti, V.S.; Arar, N.H.; Thameem, F.; Lopez-Alvarenga, J.C.; Bauer, R.; Blangero, J.; MacCluer, J.W.; Comuzzie, A.G.; Abboud, H.E. Genome scan for determinants of serum uric acid variability. *J. Am. Soc. Nephrol.* **2007**. [[CrossRef](#)] [[PubMed](#)]
4. Sluijs, I.; Beulens, J.W.J.; van der A, D.L.; Spijkerman, A.M.W.; Schulze, M.B.; van der Schouw, Y.T. Plasma uric acid is associated with increased risk of type 2 diabetes independent of diet and metabolic risk factors. *J. Nutr.* **2013**. [[CrossRef](#)]
5. Feig, D.I. Hyperuricemia and hypertension. *Adv. Chronic Kidney Dis.* **2012**, *19*, 377–385. [[CrossRef](#)]
6. Reginato, A.M.; Mount, D.B.; Yang, I.; Choi, H.K. The genetics of hyperuricaemia and gout. *Nat. Rev. Rheumatol.* **2012**, *8*, 610–621. [[CrossRef](#)]
7. Yang, Q.; Guo, C.Y.; Cupples, L.A.; Levy, D.; Wilson, P.W.F.; Fox, C.S. Genome-wide search for genes affecting serum uric acid levels: The Framingham Heart Study. *Metabolism* **2005**, *54*, 1435–1441. [[CrossRef](#)]
8. Matsuo, H.; Yamamoto, K.; Nakaoka, H.; Nakayama, A.; Sakiyama, M.; Chiba, T.; Takahashi, A.; Nakamura, T.; Nakashima, H.; Takada, Y.; et al. Genome-wide association study of clinically defined Gout identifies multiple risk loci and its association with clinical subtypes. *Ann. Rheum. Dis.* **2016**, *75*, 652–659. [[CrossRef](#)]
9. Nakayama, A.; Nakaoka, H.; Yamamoto, K.; Sakiyama, M.; Shaikat, A.; Toyoda, Y.; Okada, Y.; Kamatani, Y.; Nakamura, T.; Takada, T.; et al. GWAS of clinically defined gout and subtypes identifies multiple susceptibility loci that include urate transporter genes. *Ann. Rheum. Dis.* **2017**, *76*, 869–877. [[CrossRef](#)]
10. Stiburkova, B.; Taylor, J.; Marinaki, A.M.; Sebesta, I. Acute kidney injury in two children caused by renal hypouricaemia type 2. *Pediatr. Nephrol.* **2012**, *27*, 1411–1415. [[CrossRef](#)]
11. Mancikova, A.; Krylov, V.; Hurba, O.; Sebesta, I.; Nakamura, M.; Ichida, K.; Stiburkova, B. Functional analysis of novel allelic variants in URAT1 and GLUT9 causing renal hypouricemia type 1 and 2. *Clin. Exp. Nephrol.* **2016**, *20*, 578–584. [[CrossRef](#)]
12. Hosomi, A.; Nakanishi, T.; Fujita, T.; Tamai, I. Extra-renal elimination of uric acid via intestinal efflux transporter BCRP/ABCG2. *PLoS ONE* **2012**, *7*, 2–9. [[CrossRef](#)] [[PubMed](#)]
13. Toyoda, Y.; Mančíková, A.; Krylov, V.; Morimoto, K.; Pavelcová, K.; Bohatá, J.; Pavelka, K.; Pavlíková, M.; Suzuki, H.; Matsuo, H.; et al. Functional characterization of clinically-relevant rare variants in abcg2 identified in a gout and hyperuricemia cohort. *Cells* **2019**, *8*, 363. [[CrossRef](#)] [[PubMed](#)]
14. Stiburkova, B.; Pavelcova, K.; Pavlikova, M.; Ješina, P.; Pavelka, K. The impact of dysfunctional variants of ABCG2 on hyperuricemia and gout in pediatric-onset patients. *Arthritis Res. Ther.* **2019**, *21*. [[CrossRef](#)] [[PubMed](#)]

15. Zhu, W.; Deng, Y.; Zhou, X. Multiple membrane transporters and some immune regulatory genes are major genetic factors to gout. *Open Rheumatol. J.* **2018**, *12*, 94–113. [[CrossRef](#)] [[PubMed](#)]
16. Stiburkova, B.; Pavelcova, K.; Zavada, J.; Petru, L.; Simek, P.; Cepek, P.; Pavlikova, M.; Matsuo, H.; Merriman, T.R.; Pavelka, K. Functional non-synonymous variants of ABCG2 and gout risk. *Rheumatology* **2017**, *56*, 1982–1992. [[CrossRef](#)] [[PubMed](#)]
17. Neogi, T.; Jansen, T.L.T.A.; Dalbeth, N.; Fransen, J.; Schumacher, H.R.; Berendsen, D.; Brown, M.; Choi, H.; Edwards, N.L.; Janssens, H.J.E.M.; et al. 2015 Gout classification criteria: An American College of Rheumatology/European League against Rheumatism Collaborative Initiative. *Arthritis Rheumatol.* **2015**, *67*, 2557–2568. [[CrossRef](#)]
18. Cho, S.K.; Kim, S.; Chung, J.Y.; Jee, S.H. Discovery of URAT1 SNPs and association between serum uric acid levels and URAT1. *BMJ Open* **2015**, *5*. [[CrossRef](#)]
19. Sun, H.; Qu, Q.; Qu, J.; Lou, X.Y.; Peng, Y.; Zeng, Y.; Wang, G. URAT1 gene polymorphisms influence uricosuric action of losartan in hypertensive patients with hyperuricemia. *Pharmacogenomics* **2015**, *16*, 855–863. [[CrossRef](#)]
20. Duong, N.T.; Ngoc, N.T.; Thang, N.T.M.; Phuong, B.T.H.; Nga, N.T.; Tinh, N.D.; Quynh, D.H.; Ton, N.D.; van Hai, N. Polymorphisms of ABCG2 and SLC22A12 genes associated with gout risk in Vietnamese population. *Medicina* **2019**, *55*, 8. [[CrossRef](#)]
21. Meng, Q.; Yue, J.; Shang, M.; Shan, Q.; Qi, J.; Mao, Z.; Li, J.; Zhang, F.; Wang, B.; Zhao, T.; et al. Correlation of GLUT9 polymorphisms with gout risk. *Medicine* **2015**, *94*, e1742. [[CrossRef](#)] [[PubMed](#)]
22. Tu, H.P.; Chen, C.J.; Tovosia, S.; Ko, A.M.S.; Lee, C.H.; Ou, T.T.; Lin, G.T.; Chang, S.J.; Chiang, S.L.; Chiang, H.C.; et al. Associations of a non-synonymous variant in SLC2A9 with gouty arthritis and uric acid levels in Han Chinese subjects and Solomon Islanders. *Ann. Rheum. Dis.* **2010**, *69*, 887–890. [[CrossRef](#)] [[PubMed](#)]
23. Zhang, D.; Yang, M.; Zhou, D.; Li, Z.; Cai, L.; Bao, Y.; Li, H.; Shan, Z.; Liu, J.; Lv, D.; et al. The polymorphism rs671 at ALDH2 associated with serum uric acid levels in Chinese Han males: A genome-wide association study. *Gene* **2018**, *651*, 62–69. [[CrossRef](#)] [[PubMed](#)]
24. Tu, H.P.; Ko, A.M.S.; Lee, S.S.; Lee, C.P.; Kuo, T.M.; Huang, C.M.; Ko, Y.C. Variants of ALPK1 with ABCG2, SLC2A9, and SLC22A12 increased the positive predictive value for gout. *J. Hum. Genet.* **2018**, *63*, 63–70. [[CrossRef](#)] [[PubMed](#)]
25. Zou, Y.; Du, J.; Zhu, Y.; Xie, X.; Chen, J.; Ling, G. Associations between the SLC22A12 gene and gout susceptibility: A meta-analysis. *Clin. Exp. Rheumatol.* **2018**, *36*, 0442–0447.
26. Hurba, O.; Mancikova, A.; Krylov, V.; Pavlikova, M.; Pavelka, K.; Stiburková, B. Complex analysis of urate transporters SLC2A9, SLC22A12 and functional characterization of non-synonymous allelic variants of GLUT9 in the Czech population: No evidence of effect on hyperuricemia and gout. *PLoS ONE* **2014**, *9*. [[CrossRef](#)]
27. Horváthová, V.; Bohatá, J.; Pavlíková, M.; Pavelcová, K.; Pavelka, K.; Šenolt, L.; Stibůrková, B. Interaction of the p.Q141K variant of the ABCG2 gene with clinical data and cytokine levels in primary hyperuricemia and gout. *J. Clin. Med.* **2019**, *8*, 1965. [[CrossRef](#)]
28. Torres, R.J.; De Miguel, E.; Bailén, R.; Banegas, J.R.; Puig, J.G. Tubular urate transporter gene polymorphisms differentiate patients with gout who have normal and decreased urinary uric acid excretion. *J. Rheumatol.* **2014**, *41*, 1863–1870. [[CrossRef](#)]
29. Stiburkova, B.; Gabrikova, D.; Čepek, P.; Šimek, P.; Kristian, P.; Cordoba-Lanus, E.; Claverie-Martin, F. Prevalence of URAT1 allelic variants in the Roma population. *Nucleosides Nucleotides Nucleic Acids* **2016**. [[CrossRef](#)]
30. Matsuo, H.; Chiba, T.; Nagamori, S.; Nakayama, A.; Domoto, H.; Phetdee, K.; Wiriyaermkul, P.; Kikuchi, Y.; Oda, T.; Nishiyama, J.; et al. Mutations in glucose transporter 9 gene SLC2A9 cause renal hypouricemia. *Am. J. Hum. Genet.* **2008**, *83*, 744–751. [[CrossRef](#)]
31. Sarzynski, M.A.; Jacobson, P.; Rankinen, T.; Carlsson, B.; Sjöström, L.; Bouchard, C.; Carlsson, L.M.S. Changes in uric acid levels following bariatric surgery are not associated with SLC2A9 Variants in the swedish obese subjects study. *PLoS ONE* **2012**, *7*. [[CrossRef](#)] [[PubMed](#)]
32. Graessler, J.; Graessler, A.; Unger, S.; Kopprasch, S.; Tausche, A.K.; Kuhlisch, E.; Schroeder, H.E. Association of the human urate transporter 1 with reduced renal uric acid. Excretion and hyperuricemia in a German caucasian population. *Arthritis Rheum.* **2006**, *54*, 292–300. [[CrossRef](#)] [[PubMed](#)]

33. Dinour, D.; Gray, N.K.; Campbell, S.; Shu, X.; Sawyer, L.; Richardson, W.; Rechavi, G.; Amariglio, N.; Ganon, L.; Sela, B.A.; et al. Homozygous SLC2A9 mutations cause severe renal hypouricemia. *J. Am. Soc. Nephrol.* **2010**. [[CrossRef](#)] [[PubMed](#)]
34. Claverie-Martin, F.; Trujillo-Suarez, J.; Gonzalez-Acosta, H.; Aparicio, C.; Justa Roldan, M.L.; Stiburkova, B.; Ichida, K.; Martín-Gomez, M.A.; Herrero Goñi, M.; Carrasco Hidalgo-Barquero, M.; et al. URAT1 and GLUT9 mutations in Spanish patients with renal hypouricemia. *Clin. Chim. Acta* **2018**, *481*, 83–89. [[CrossRef](#)]
35. Windpessl, M.; Ritelli, M.; Wallner, M.; Colombi, M. A novel homozygous SLC2A9 mutation associated with renal-induced hypouricemia. *Am. J. Nephrol.* **2016**. [[CrossRef](#)]
36. Tasic, V.; Hynes, A.M.; Kitamura, K.; Cheong, H., II; Lozanovski, V.J.; Gucev, Z.; Jutabha, P.; Anzai, N.; Sayer, J.A. Clinical and functional characterization of URAT1 variants. *PLoS ONE* **2011**. [[CrossRef](#)]
37. Taniguchi, A.; Urano, W.; Yamanaka, M.; Yamanaka, H.; Hosoyamada, M.; Endou, H.; Kamatani, N. A common mutation in an organic anion transporter gene, SLC22A12, is a suppressing factor for the development of gout. *Arthritis Rheum.* **2005**, *52*, 2576–2577. [[CrossRef](#)]
38. Sakiyama, M.; Matsuo, H.; Shimizu, S.; Nakashima, H.; Nakamura, T.; Nakayama, A.; Higashino, T.; Naito, M.; Suma, S.; Hishida, A.; et al. The effects of URAT1/SLC22A12 nonfunctional variants, R90H and W258X, on serum uric acid levels and gout/hyperuricemia progression. *Sci. Rep.* **2016**, *6*, 1–6. [[CrossRef](#)]
39. Vázquez-Mellado, J.; Jiménez-Vaca, A.L.; Cuevas-Covarrubias, S.; Alvarado-Romano, V.; Pozo-Molina, G.; Burgos-Vargas, R. Molecular analysis of the SLC22A12 (URAT1) gene in patients with primary gout. *Rheumatology* **2007**, *46*, 215–219. [[CrossRef](#)]



© 2020 by the authors. Licensee MDPI, Basel, Switzerland. This article is an open access article distributed under the terms and conditions of the Creative Commons Attribution (CC BY) license (<http://creativecommons.org/licenses/by/4.0/>).





## Article

# Renal Hypouricemia 1: Rare Disorder as Common Disease in Eastern Slovakia Roma Population

Blanka Stiburkova <sup>1,2,\*</sup> , Jana Bohatá <sup>1,3</sup> , Kateřina Pavelcová <sup>1</sup> , Velibor Tasic <sup>4</sup> ,  
Dijana Plaseska-Karanfilska <sup>5</sup> , Sung-Kweon Cho <sup>6</sup>, Ludmila Potočňaková <sup>7</sup> and Jana Šaligová <sup>7</sup>

- <sup>1</sup> Institute of Rheumatology, 128 00 Prague, Czech Republic; bohata@revma.cz (J.B.); pavelcova@revma.cz (K.P.)  
<sup>2</sup> Department of Pediatrics and Inherited Metabolic Disorders, First Faculty of Medicine, Charles University, General University Hospital, 121 00 Prague, Czech Republic  
<sup>3</sup> Department of Rheumatology, First Faculty of Medicine, Charles University, 121 08 Prague, Czech Republic  
<sup>4</sup> Faculty of Medicine, University Ss. Cyril and Methodius, 1000 Skopje, North Macedonia; vtasic2003@gmail.com  
<sup>5</sup> Research Centre for Genetic Engineering and Biotechnology “Georgi D. Efremov”, Macedonian Academy of Sciences and Arts, 1000 Skopje, North Macedonia; dijana@manu.edu.mk  
<sup>6</sup> Department of Pharmacology, Ajou University School of Medicine, 164, Worldcup-ro, Yeongtong-gu, Suwon 16499, Korea; wontan@ajou.ac.kr  
<sup>7</sup> Metabolic Ambulance of Department of Paediatrics and Adolescent Medicine, Children’s Faculty Hospital, 040 11 Košice, Slovakia; lpotocnakova@gmail.com (L.P.); jana.saligova@gmail.com (J.Š.)  
\* Correspondence: stiburkova@revma.cz; Tel.: +420-234-075-319



**Citation:** Stiburkova, B.; Bohatá, J.; Pavelcová, K.; Tasic, V.; Plaseska-Karanfilska, D.; Cho, S.-K.; Potočňaková, L.; Šaligová, J. Renal Hypouricemia 1: Rare Disorder as Common Disease in Eastern Slovakia Roma Population. *Biomedicines* **2021**, *9*, 1607. <https://doi.org/10.3390/biomedicines9111607>

Academic Editors: Shinji Takai and Paola Pontrelli

Received: 15 September 2021  
Accepted: 30 October 2021  
Published: 3 November 2021

**Publisher’s Note:** MDPI stays neutral with regard to jurisdictional claims in published maps and institutional affiliations.



**Copyright:** © 2021 by the authors. Licensee MDPI, Basel, Switzerland. This article is an open access article distributed under the terms and conditions of the Creative Commons Attribution (CC BY) license (<https://creativecommons.org/licenses/by/4.0/>).

**Abstract:** Renal hypouricemia (RHUC) is caused by an inherited defect in the main reabsorption system of uric acid, *SLC22A12* (URAT1) and *SLC2A9* (GLUT9). RHUC is characterized by a decreased serum uric acid concentration and an increase in its excreted fraction. Patients suffer from hypouricemia, hyperuricosuria, urolithiasis, and even acute kidney injury. We report clinical, biochemical, and genetic findings in a cohort recruited from the Košice region of Slovakia consisting of 27 subjects with hypouricemia and relatives from 11 families, 10 of whom were of Roma ethnicity. We amplified, directly sequenced, and analyzed all coding regions and exon–intron boundaries of the *SLC22A12* and *SLC2A9* genes. Sequence analysis identified dysfunctional variants c.1245\_1253del and c.1400C>T in the *SLC22A12* gene, but no other causal allelic variants were found. One heterozygote and one homozygote for c.1245\_1253del, nine heterozygotes and one homozygote for c.1400C>T, and two compound heterozygotes for c.1400C>T and c.1245\_1253del were found in a total of 14 subjects. Our result confirms the prevalence of dysfunctional URAT1 variants in Roma subjects based on analyses in Slovak, Czech, and Spanish cohorts, and for the first time in a Macedonian Roma cohort. Although RHUC1 is a rare inherited disease, the frequency of URAT1-associated variants indicates that this disease is underdiagnosed. Our findings illustrate that there are common dysfunctional URAT1 allelic variants in the general Roma population that should be routinely considered in clinical practice as part of the diagnosis of Roma patients with hypouricemia and hyperuricosuria exhibiting clinical signs such as urolithiasis, nephrolithiasis, and acute kidney injury.

**Keywords:** renal hypouricemia; *SLC22A12*; URAT1; ethnic specificity; Roma

## 1. Introduction

Hypouricemia, defined as a serum uric acid (UA) concentration < 120 µmol/L, is a rare laboratory finding with a prevalence of 0.21–0.53% that varies with age [1,2]. Secondary hypouricemia may be caused by Fanconi syndrome, cystinosis, diabetes mellitus, and/or inappropriate antidiuretic hormone secretion syndrome. Primary hypouricemia can result from decreased UA production by a blockade of the last step of purine degradation, e.g., hereditary xanthinuria, but is more commonly due to decreased renal tubular UA reabsorption, e.g., renal hypouricemia.

Renal hypouricemia (RHUC) is a rare heterogeneous inherited disease caused by a dysfunction of the primary renal urate transporters: URAT1 (gene *SLC22A12*, OMIM #220150) and GLUT9 (gene *SLC2A9*, OMIM #612076), resulting in impaired tubular transport of UA, insufficient reabsorption, and/or increased secretion by a mechanism of endothelial dysfunction [3–7]. The biochemical markers are characterized by hypouricemia and an increased fractional excretion of UA (FE-UA). Clinically, the disease presents with urolithiasis, nephrolithiasis, and, in some patients, acute kidney injury that often occurs after physical exertion [8]. No treatment is available; however, allopurinol has been used to prevent the recurrence of acute kidney injury episodes [9].

RHUC patients have been described in different ethnic groups and geographically noncontiguous countries; over 200 cases with URAT1 variants and ~20 cases with GLUT9 defects have been reported to date worldwide. The loss-of-function *SLC22A12* variants (in compound heterozygous and/or homozygous state) are the primary cause of renal hypouricemia (> 90%), with significant population specificity: the high incidence of RHUC1 in Japanese and Korean patients reflects the 2.3% allelic frequency of the prevalent dysfunctional variant rs121907892 (p.W258X) [10], with null allele frequency in African/American, Ashkenazi Jewish, South Asia, and European populations (130,978 subjects, ExAc database). However, the world's highest frequency of predominant dysfunctional RHUC1 variants was identified in the European Roma population (1016 individuals from regions of the Czech Republic, Slovakia, and Spain): the rs200104135 (p.T467M) variant has a frequency of 5.6%, and the deletion variant p.L415\_G417 has a frequency of 1.9% [11].

In the present study, we collected a cohort of pediatric subjects with repeated findings of serum uric acid below 120  $\mu\text{mol/L}$ . A cohort of 27 subjects was recruited as part of a single-center study by the Metabolic Ambulance of the Department of Paediatrics and Adolescent Medicine, Children's Faculty Hospital, Košice, Slovakia, between 2018 and 2020 and consisted of probands and relatives from 11 families. The aims of the study were (a) to determine whether renal hypouricemia type 1 and 2 occurs in the cohort, (b) to determine which type of renal hypouricemia predominates, and (c) to identify causal variants for this rare Mendelian disease of urate transport associated with hypouricemia.

## 2. Materials and Methods

### 2.1. Clinical Subjects

The studied probands and their family members were Slovaks of Roma ethnicity, except for family I, who did not report their ethnicity. Participants were repeatedly diagnosed with serum uric acid below 120  $\mu\text{mol/L}$  in children and below 150  $\mu\text{mol/L}$  in adults during a two-year study period. The families under investigation did not indicate a family relationship. All participants were fully informed of the study's goals and written informed consent was obtained from each participant before enrollment in the study. All tests were performed following standards set by institutional ethics committees. The study was approved on 24 July 2018 as part of project no. 7131/2018. All the procedures were performed per the Declaration of Helsinki. A cohort of genomic DNA of 109 unrelated subjects of Roma ethnicity (chosen irrespective of their state of health) from Macedonia and a previously reported cohort of 1016 Roma individuals from five European regions (Slovakia, Czech Republic, Spain) was used as a control group [11,12].

### 2.2. Clinical Investigations and Sequence Analyses

Urate and creatinine levels were measured using specific enzymatic methods, and the Jaffé reaction, which was adapted for use with an auto-analyzer (Hitachi Automatic Analyzer 902; Roche, Basel, Switzerland). Whole blood was collected and stored in the biobank of the Institute of Rheumatology, Prague, Czech Republic. Subsequently, genomic DNA was extracted using QIAamp DNA Mini Kits (Qiagen GmbH, Hilden, Germany). All coding exons and intron–exon boundaries of *SLC22A12* and *SLC2A9* were amplified from genomic DNA using polymerase chain reaction and subsequently purified using PCR DNA Fragments Extraction Kits (Geneaid, New Taipei City, Taiwan). DNA sequencing

was performed on an automated 3130 Genetic Analyzer (Applied Biosystems Inc., Foster City, CA, USA). Primer sequences and PCR conditions used for amplification were previously described [12–14].

The reference sequences for GLUT9/*SLC2A9* (NM\_020041.2; NP\_064425.2; SNP source dbSNP 132) and URAT1/*SLC22A12* (NM\_144585.3) were defined as version NC\_000004.12 (Chromosome 4: 9,771,153–10,054,936) and NC\_000011.8 (Chromosome 11:64,114,688–64,126,396), respectively.

In the control group of 109 unrelated subjects of Roma ethnicity from Macedonia, we only analyzed exon 7 and exon 9 of *SLC22A12* for identifying prevalent variants c.1245\_1253del (p.L415\_G417del) and c.1400C>T (rs200104135, p.T467M).

### 3. Results

#### 3.1. Clinical Subjects

The cohort consisted of nine hypouricemia probands and 18 family relatives. The probands had repeated hypouricemia and/or increased FE-UA. Hypouricemia was the determining factor for inclusion in the study, not ethnicity; however, all subjects were of Roma origin, except family I, who did not report their ethnicity. No clinical or laboratory symptoms of renal disease were present in the probands. However, other hereditary disorders were present in the cohort: five subjects were diagnosed with phenylketonuria (PKU, OMIM #261600), four subjects with short-chain acyl-CoA dehydrogenase deficiency (SCADD, OMIM #201470), one subject with Gilbert syndrome (OMIM #143500), one subject with congenital hypothyroidism (OMIM #275200), and one subject with mild hyperhomocysteinemia due to a methylenetetrahydrofolate reductase deficiency (OMIM #607093.0004). The clinical and biochemical data from this study are summarized in Table 1. Family pedigrees could not be prepared due to the disinterest of family members.

**Table 1.** The clinical and biochemical data of the analyzed cohort.

Family	Patient	Sex	Year of Birth	Year of Onset	sUA μmol/L	FE-UA %	Associated Diseases
A	1	F	1962	N/A	263	7.6	PKU heterozygote PKU
	2	F	1991	N/A	137	9.7	
B	3	M	2014	4	101 (2018), 102 (2021)	13.1 (2018), 16.2 (2021)	autism, ADHD
	4	M	1985	N/A	326	7.3	
	5	F	1981	20	167	8.6	
C	6	M	2006	12	94 (2018)	23.4 (2018)	PKU PKU PKU
	7	M	2012	6	122 (2017), 150 (2018)	15.8 (2018)	
	8	F	2011	7	118 (2018)	12.4 (2018)	
D	9	F	2008	10	194 (2018)	7.3 (2018)	MTHFR homozygote, PAI heterozygote SCADD heterozygote
	10	F	1999	20	141 (2019)	16.2 (2019)	
E	11	F	2018	10 mth	95 (2018), 146 (2019), 151 (2021)	17.1 (2018), 12.0 (2021)	SCADD SCADD heterozygote
	12	F	1994	24	N/A	N/A	
F	13	F	1991	N/A	309 (2018)	5.1 (2018)	xanthinuria heterozygote PKU SCADD
	14	M	2017	18 mth	72 (2018), 136 (2019), 141 (2021)	10.3 (2021)	
	15	M	2016	3	135 (2016), 140 (2019)	11.3 (2019)	
G	16	M	2018	6 mth	140 (2018), 114 (2019), 235 (2020)	16.5 (2018)	transitory hypertyrosinemia
	17	F	1981	38	247 (2018)	8.4 (2018)	
	18	M	1988	31	415 (2018)	5.9 (2018)	
H	19	M	2008	11	55 (2019), 77 (2020)	28.8 (2020)	hypogonadotropic hypogonadism, Gilbert syndrome, hepatopathy, cholesterolithiasis, obesity
	20	F	1986	34	125	11.6	
	21	M	1983	37	44	43	

Table 1. Cont.

Family	Patient	Sex	Year of Birth	Year of Onset	sUA $\mu\text{mol/L}$	FE-UA %	Associated Diseases
I	22	F	2016	27 mth	118 (2017), 131 (2019), 152 (2021)	10.6 (2019)	central hypocorticism, epilepsy, familial hypercholesterolemia neurofibromatosis type 1 familial hypercholesterolemia
	23	F	1982	37	161	8.2	
	24	M	1984	35	366	6.1	
J	25	M	2019	23 mth	61 (2019), 43 (2020)	51 (2019)	SCADD SCADD heterozygote
	26	F	2002	18	N/A	N/A	
K	27	M	2010	10	108 (2012), 88 (2013), 84 (2018), 71 (2019), 49 (2021)	56 (2012), 30 (2013), 40 (2018), 40 (2019), 50 (2021)	SCADD, prematurity, perinatal hypoxia, psychom. retardation, cardiomyopathy

Reference ranges are as follows. SUA: 120–360  $\mu\text{mol/L}$  (2.02–6.05 mg/dL) (< 15 years and female), 120–420  $\mu\text{mol/L}$  (2.02–7.06 mg/dL; male); FE-UA: reference range 5–20% (< 13 years), 5–12% (male) and 5–15% (female). PKU, phenylketonuria; SCADD, short-chain acyl-CoA dehydrogenase deficiency; MTHFR, methylenetetrahydrofolate; PAI-1, plasminogen activator inhibitor-1; ADHD, attention deficit hyperactivity disorder; mth, months; N/A, not available.

### 3.2. Clinical Investigations and Sequence Analyses

Sequencing analysis of *SLC2A9* revealed 12 intron variants (rs2276962, rs2276963, rs2240722, rs2240721, rs2240720, rs28592748, rs16891971, rs3733590, rs13115193, rs4292327, rs6823877, and rs61256984), three synonymous variants (rs13113918, rs10939650, and rs13125646), and four common nonsynonymous allelic variants (rs2276961, p.G25R; rs16890979, p.V282I; rs3733591, p.R294H, and rs2280205, p.P350L). Sequencing analysis of *SLC22A12* revealed three intron variants (rs373881060, rs368284669, and rs11231837), four synonymous (rs3825016, rs11231825, rs1630320, and rs7932775), and two previously identified rare nonsynonymous allelic variants c.1245\_1253del (p.L415\_G417del) and c.1400C>T (rs200104135, p.T467M), Figure 1. In 14 subjects, we identified one heterozygote and one homozygote for c.1245\_1253del, nine heterozygotes and one homozygote for c.1400C>TT, and two compound heterozygotes for c.1400C>T and c.1245\_1253del. The genetics data are summarized in Table 2.

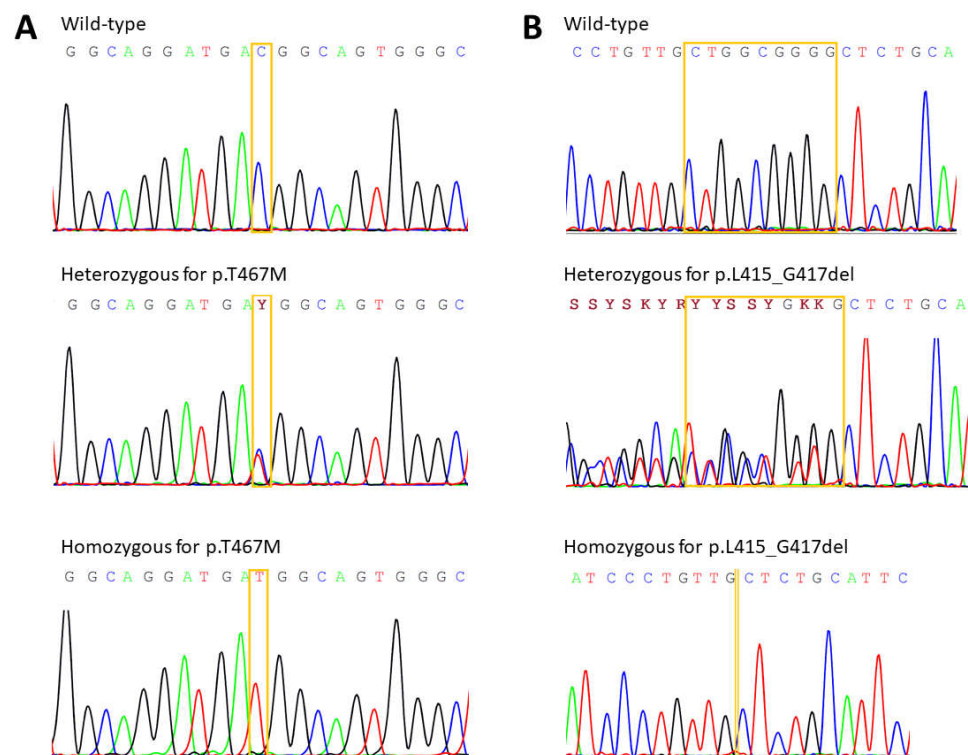
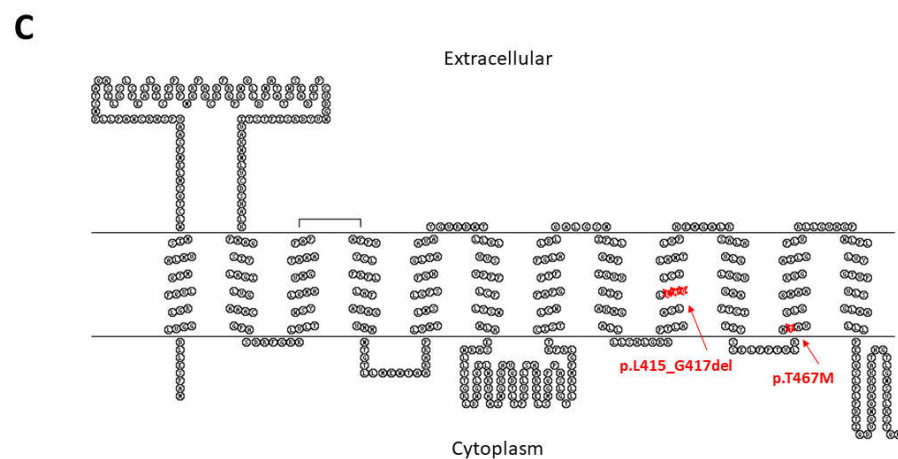


Figure 1. Cont.



**Figure 1.** Illustration of allelic variant p.L415\_G417del and p.T467M in genetic and protein context. (A) Electropherograms of partial sequences of exon 7 showing the wild-type, heterozygous, and homozygous c.1245\_1253del variant. (B) Electropherograms of partial sequences of exon 9 showing wild-type, heterozygous, and homozygous c.1400C>T variant. (C) Position of identified allelic variant p.T467M and p.L415\_G417del in a URAT1 membrane topology model created via Johns S.J., TOPO2, Transmembrane protein display software, <http://www.sacs.ucsf.edu/TOPO2/> [23 July 2021].

**Table 2.** The genetic data of the analyzed cohort identified nonsynonymous allelic variants in URAT1 and GLUT9 transporter; homozygous variants are shown in bold font; causal variants for RHUC1 are in *SLC22A12* gene.

Family	Patient	Gene <i>SLC22A12</i> , URAT1	Gene <i>SLC2A9</i> , GLUT9
A	1	reference	N/A
	2	reference	p.G25R, <b>p.V282I</b> , p.P350L
B	3	reference	p.G25R, p.V282I
	4	reference	p.G25R, p.V282I, p.R294H
	5	p.T467M	N/A
C	6	p.T467M	p.G25R, p.V282I, p.R294H
	7	p.T467M	p.G25R, p.V282I, p.R294H
	8	p.T467M	<b>p.G25R</b> , p.R294H
D	9	reference	<b>p.G25R</b> , p.R294H, p.P350L
	10	p.T467M	<b>p.G25R</b> , p.R294H, p.P350L
E	11	p.T467M	p.G25R, p.V282I
	12	reference	p.G25R
F	13	reference	p.G25R, p.V282I, <b>p.P350L</b>
	14	p.T467M	p.G25R, p.V282I, p.P350L
	15	p.L415_G417del	p.G25R, p.P350L
G	16	reference	N/A
	17	reference	p.P350L
	18	reference	<b>p.G25R</b> , p.R294H, p.P350L
H	19	p.L415_G417del, p.T467M	<b>p.R294H</b> , <b>p.P350L</b>
	20	p.T467M	N/A
	21	<b>p.L415_G417del</b>	N/A
I	22	reference	<b>p.G25R</b> , p.V282I, p.P350L
	23	reference	p.G25R, p.V282I, p.P350L
	24	reference	<b>p.G25R</b> , p.R294H, p.V282I, p.P350L
J	25	p.L415_G417del, p.T467M	<b>p.G25R</b> , p.R294H, p.P350L
	26	p.T467M	N/A
K	27	<b>p.T467M</b>	N/A

In the control group of 109 unrelated subjects of Roma ethnicity from Macedonia, we identified none subject for c.1245\_1253del, 10 heterozygotes, and two homozygotes for c.1400C>T.

#### 4. Discussion

Renal hypouricemia 1 is a rare inherited disorder, and like other genetic traits and conditions, shows genetic allelic and locus heterogeneity. However, population-specific common variants have been observed in hypouricemia in Japanese, Korean, and Roma patients. In the Japanese [10] and Korean populations [15], the prevalent RHUC1 variants are c.774G>A (p.W258X, frequency 2.30–2.37%) and c.269G>A (p.R90H, frequency 0.40%); in the European Roma population, the prevalent variants are c.1245\_1253del (p.L415\_G417del, frequency 1.92%) and c.1400C>T (p.T467M, frequency 5.56%). The number of published cases of patients with RHUC1 is about 200, and they are very unlikely to match the frequencies of prevalent variants mentioned above. The key to an early diagnosis is greater awareness of URAT1 deficiency among primary care physicians, nephrologists, and urologists; the recently published clinical practice guidelines for renal hypouricemia will certainly contribute to this [16].

The cohort analyzed in this study was of Roma ethnicity. The Roma represent a transnational ethnic population of 8–10 million, originating in India; currently, they are the largest and most widespread ethnic minority in Europe. In the Slovak Republic, the Roma population is the second-largest minority, with most of the Roma living in the eastern and southern parts of Slovakia. The founder effect and subsequent genetic isolation of the Roma have led to a population specificity, i.e., variants associated with rare diseases in the Roma population tend to be at extremely low frequencies in other European populations and vice versa. Multiple homozygosity for ethnically prevalent mutations is typical in closely related populations with high levels of endogamy, and many rare-disease-causing mutations present in other European populations are found at very low frequencies in the Roma population. Several mutations that cause rare diseases unique to the Roma and have been discovered, e.g., Charcot Marie Tooth disease type 4D and 4G (OMIM #601455 and #605285), congenital cataract facial dysmorphism neuropathy (OMIM #604166), Gitelman syndrome (OMIM #263800), and Galactokinase deficiency (OMIM # 230200) [11,12]. Roma population specificity was confirmed by the findings of comorbidities in our hypouricemic cohort. Of the 27 participants, 5 were diagnosed with phenylketonuria (PKU, OMIM #261600), 4 with short-chain acyl-CoA dehydrogenase deficiency (SCADD, OMIM #201470), 1 with Gilbert syndrome (OMIM #143500), 1 with congenital hypothyroidism (OMIM #275200), and 1 with mild hyperhomocysteinemia due to a methylenetetrahydrofolate reductase deficiency (OMIM #607093.0004). The unusually high prevalence of SCADD deficiency among Roma was confirmed by data from the Slovak newborn screening program in 2016, in which the prevalence of SCADD in Caucasian newborns is 1:9745, while in Roma newborns, it was roughly 1:100 [17].

The first findings indicating population specificity of RHUC1 in the Roma population occurred in 2013, in the context of diagnosing the first RHUC patients in the Czech Republic [18] when two of the three nonconsanguineous probands (compound heterozygotes c.[1245\_1253del] + [1400C>T] and homozygotes c.1245\_1253del) were from the minority Roma population. Functional studies found significantly reduced urate uptake and a mislocalized URAT1 signal in both variants [14], which were subsequently identified in other patients with hypouricemia of Roma ethnicity in the Czech Republic [19,20]. We subsequently collected a control set of 218 alleles from the Roma population in the Czech Republic and found two heterozygous control subjects with the variant p.L415\_G417del. Serum UA and FE-UA in the 9 year old girl was 256  $\mu\text{mol/L}$  and 18%; in the 34 year old man, it was 232  $\mu\text{mol/L}$  and 8%. Further analysis of a cohort of 881 randomly chosen ethnic Roma from two regions in Eastern Slovakia (Prešov and Košice) and two regions in the Czech Republic, identified 25 heterozygous and 3 homozygous subjects for the c.1245\_1253del and 92 subjects were heterozygous, 2 were homozygous for the c.1400C>T,

and 2 participants were compound heterozygotes. Frequencies of the c.1245\_1253del and c.1400C>T variants were determined as 1.87% and 5.56%, respectively [12]. In a subsequent study, we expanded this cohort to include other regions: a total of 1016 Roma from five regions were included: 471 from the Prešov region (Slovakia), 331 from the Košice region (Slovakia), 90 from the Central Bohemia region (Czech Republic), 64 from the Hradec Kralove region (Czech Republic), and 60 from the Iberian Peninsula (Spain). Frequencies of the c.1245\_1253del and c.1400C>T variants were determined to be 1.92% and 5.56%, respectively. Genotypes were in Hardy–Weinberg equilibrium (HWE) at the c.1400C>T locus in all five cohorts, but, due to a large number of homozygotes, they were grossly deviated at the c.1245\_1253del locus ( $p < 0.001$  and  $p = 0.004$ ) in the one Czech and Spanish cohorts. On the other hand, in the control group of 109 nonrelated Macedonia Roma subjects, we did not identify deletion variant c.1245\_1253del, while variant c.1400C>T was represented in high frequency of 6.4%. The frequencies of both c.1245\_1253del and c.1400C>T variants differ significantly between cohorts. These differences were likely caused by genetic drift, which is a typical phenomenon among Roma subisolates. These findings were subsequently supported by a study of renal hypouricemia in Spanish patients, where eight RHUC1 probands from eight families, all of Roma ethnicity, were identified carrying these prevalent variants (one heterozygote c.1245\_1253del, two heterozygotes, four homozygotes c.1400C>T, and one compound heterozygote) [21].

Historic, linguistic, and genetic studies identify India as the original homeland of the Roma. Analysis of paternal and maternal lineages as well as autosomal whole-genome studies date the time of the Roma departure from India to approximately 1000 years ago. The data suggest that the group of Roma who left India had a limited size of around 1000 individuals and came from one specific caste or group [22]. Our findings of the presence of the c.1400C>T variant in all analyzed Roma subcohort, together with data from ExAC database when p.T467M was identified in only one heterozygote subject [12] and three homozygotes in a South Asia cohort of 15,296 subjects but in none of the subjects from all other populations (total 105,759 subjects), suggest the origin of the c.1400C>T variant in Asia. At present, in Genome Aggregation Database (gnomAD), which is the largest and most widely used publicly available collection of population variation, indicates c.1400C>T is present with a global frequency of 0.11% (275 c.1400C>T alleles out of a total of 273,462 sequenced). Worldwide, the highest frequency is present in South Asia (0.70%), while in Europe, it is more common in the southern parts, with the highest frequency among Bulgarians (0.26%). The NGS data from a total of 270 Macedonian patients with different rare diseases, referred for clinical exome analysis at RCGEB-MASA, revealed 5 c.1400C>T heterozygotes (personal communication). All c.1400C>T carriers were of Macedonian ethnic origin. This frequency of 0.93% among Macedonians is the highest reported among the non-Roma populations. The study of the chromosomal background of the c.1400C>T allele could help trace the age/region of origin and the spread of this variant. Taken together, our findings show that the founder effect played a key role in forming the current gene pool of the Roma population — a very small group of migrants from India gave rise to the current population numbering in the low millions. In addition to the primary effect that resulted in the specific gene pool of the Roma ethnic group in general, secondary and even tertiary founder effects played an important role in forming the gene pools of individual Roma subpopulations together with a high degree of consanguinity [22].

The absence of deletion variant c.1245\_1253del in two of the Roma subgroups studied may be due to the limitations of the small sample size. However, deletion variant c.1245\_1253del has yet to be identified in any of the publicly available databases. These findings suggest the possible origin of the c.1400C>T variants as a founder effect after the departure from India. Taken together, and due to the putative founder effect and genetic drift, the prevalence of this otherwise rare inherited disease is significantly increased in selected populations such as the Roma. In our cohort, most RHUC1 patients also carry the p.G25R variant of GLUT9. However, this allelic variant p.G25R in the GLUT9 transporter, as other identified variants p.V282I, p.R294H, and p.P350L in our clinical cohort,

was previously functionally characterized with no influence on expression, subcellular localization, or urate uptake of GLUT9 [23]. Further gene–gene interaction studies are needed to address the possible interaction of URAT1 and GLUT9 variants.

In addition, we can emphasize the clinical importance of documentation regarding RHUC1 in Slovak Roma, which was our focus in this study, given that detailed studies on serum UA and FE-UA levels in Roma are rare. Hypouricemia in children is relatively rare in clinical practice and is often associated with rare conditions. As we showed previously [24], serum UA and FE-UA levels are quite dynamic in the first year of life. Briefly, serum UA levels are low in infancy (131–149  $\mu\text{mol/L}$  at 2–3 months of age) due to high FE-UA levels (>10%); FE-UA levels decrease to approximately 8% by one year of age, where they remains throughout childhood; this is associated with mean serum UA levels of 208–268  $\mu\text{mol/L}$  in children. After age 12, FE-UA levels decrease significantly in boys but not in girls, resulting in a further significant increase in serum UA levels in young men but not in young women. Our data suggest that the high prevalence of URAT1 allelic variants causing impaired urate transport may affect serum UA concentrations in the general Roma population. This hypothesis is supported by clinical studies suggesting that Roma have a 2.85-fold higher risk of end-stage renal disease compared to non-Roma [25] and that Roma women have half-higher odds for nephropathy (OR 1.56; 95% CI 1.01–2.42;  $p < 0.05$ ) than non-Roma women [26]. Moreover, a recent study of Eastern Slovak Roma and non-Roma populations showed that serum UA is ethnicity-specific: the mean UA level  $\pm$  standard deviation was significantly lower in Roma than in non-Roma ( $226.54 \pm 79.8 \mu\text{mol/L}$  vs.  $259.11 \pm 84.53 \mu\text{mol/L}$ ;  $p < 0.0001$ ) [27].

Most patients with RHUC are asymptomatic. However, the prevalence of renal stones due to excesses of UA excretion is 6–7 times higher in patients with RHUC than in individuals with normal uric acid levels [28]. The incidence of urolithiasis, nephrolithiasis, and acute kidney injury among the Roma may be explainable in relation to the population's risk of RHUC1. To prevent patients from developing complications, physicians often advise patients to drink water before exercise and/or limit the intensity of exercise. Early diagnosis of RHUC has great clinical relevance for correct disease control, thus is important to prevent serious clinical manifestations.

## 5. Conclusions

Generally, the Roma ethnic group represents a cluster of genetically isolated founder populations with a spectrum of frequent Mendelian disorders due to a high rate of consanguinity associated with the occurrence of founder mutations. Therefore, it is necessary to study individual Roma groups to reveal differences in the number of carriers and prevalence of rare diseases in Roma subpopulations. Our data show a high incidence of genetic variants leading to renal hypouricemia 1 among the Roma, and this genetic background should be kept in mind during initial diagnosis.

**Author Contributions:** Conceptualization, B.S.; methodology, B.S., J.Š., and J.B.; validation, B.S.; investigation, L.P., J.Š., J.B., K.P., V.T., D.P.-K., and S.-K.C.; writing—original draft preparation, B.S.; writing—review and editing, J.Š., J.B., and K.P.; visualization, J.B.; supervision, B.S.; project administration, B.S.; funding acquisition, B.S. All authors have read and agreed to the published version of the manuscript.

**Funding:** This research was funded by grants from the Czech Republic Ministry of Health RVO 00023728 (Institute of Rheumatology), RVO VFN64165, and by Biobanks and Biomolecular Resources Research Infrastructure Consortium BBMRICZ LM2018125 of Ministry of Education, Youth and Sports of the Czech Republic.

**Institutional Review Board Statement:** The study was conducted according to the guidelines of the Declaration of Helsinki and approved by the Institutional Ethics Committee of the Institute of Rheumatology, Prague, Czech Republic (project no. 7131/2018).

**Informed Consent Statement:** Informed consent was obtained from all study participants.



**Data Availability Statement:** The data presented in this study are available on request from the corresponding author.

**Acknowledgments:** We are grateful to all the patients who took part in this study.

**Conflicts of Interest:** The authors declare no conflict of interest.

## References

1. Bugdayci, G.; Balaban, Y.; Sahin, O. Causes of Hypouricemia among Outpatients. *Lab. Med.* **2008**, *39*, 550–552. [[CrossRef](#)]
2. Koo, B.S.; Jeong, H.J.; Son, C.N.; Kim, S.H.; Kim, H.J.; Kim, G.H. Distribution of serum uric acid levels and prevalence of hyper- and hypouricemia in a Korean general population of 172,970. *Korean J. Intern. Med.* **2021**, *36* (Suppl. S1), S264–S272. [[CrossRef](#)] [[PubMed](#)]
3. Enomoto, A.; Kimura, H.; Chairoungdua, A.; Shigeta, Y.; Jutabha, P.; Cha, S.H.; Endou, H. Molecular identification of a renal urate anion exchanger that regulates blood urate levels. *Nature* **2002**, *417*, 447–452. [[CrossRef](#)]
4. Matsuo, H.; Chiba, T.; Nagamori, S.; Nakayama, A.; Domoto, H.; Phetdee, K.; Shinomiya, N. Mutations in glucose transporter 9 gene SLC2A9 cause renal hypouricemia. *Am. J. Hum. Genet.* **2008**, *83*, 744–751. [[CrossRef](#)] [[PubMed](#)]
5. Sugihara, S.; Hisatome, I.; Kuwabara, M.; Niwa, K.; Maharani, N.; Kato, M.; Yamamoto, K. Depletion of Uric Acid Due to SLC22A12 (URAT1) Loss-of-Function Mutation Causes Endothelial Dysfunction in Hypouricemia. *Circ. J.* **2015**, *79*, 1125–1132. [[CrossRef](#)] [[PubMed](#)]
6. Mancikova, A.; Krylov, V.; Hurba, O.; Sebesta, I.; Nakamura, M.; Ichida, K.; Stiburkova, B. Functional analysis of novel allelic variants in URAT1 and GLUT9 causing renal hypouricemia type 1 and 2. *Clin. Exp. Nephrol.* **2016**, *20*, 578–584. [[CrossRef](#)] [[PubMed](#)]
7. Dinour, D.; Gray, N.K.; Campbell, S.; Shu, X.; Sawyer, L.; Richardson, W.; Holtzman, E.J. Homozygous SLC2A9 mutations cause severe renal hypouricemia. *J. Am. Soc. Nephrol.* **2010**, *21*, 64–72. [[CrossRef](#)] [[PubMed](#)]
8. Stiburkova, B.; Taylor, J.; Marinaki, A.M.; Sebesta, I. Acute kidney injury in two children caused by renal hypouricaemia type 2. *Pediatric Nephrol.* **2012**, *27*, 1411–1415. [[CrossRef](#)]
9. Bhasin, B.; Stiburkova, B.; De Castro-Pretelt, M.; Beck, N.; Bodurtha, J.N.; Atta, M.G. Hereditary renal hypouricemia: A new role for allopurinol? *Am. J. Med.* **2014**, *127*, e3–e4. [[CrossRef](#)] [[PubMed](#)]
10. Ichida, K.; Hosoyamada, M.; Kamatani, N.; Kamitsuji, S.; Hisatome, I.; Shibasaki, T.; Hosoya, T. Age and origin of the G774A mutation in SLC22A12 causing renal hypouricemia in Japanese. *Clin. Genet.* **2008**, *74*, 243–251. [[CrossRef](#)]
11. Stiburkova, B.; Gabrikova, D.; Cepek, P.; Simek, P.; Kristian, P.; Cordoba-Lanus, E.; Claverie-Martin, F. Prevalence of URAT1 allelic variants in the Roma population. *Nucleosides Nucleotides Nucleic Acids* **2016**, *35*, 529–535. [[CrossRef](#)] [[PubMed](#)]
12. Gabrikova, D.; Bernasovska, J.; Sokolova, J.; Stiburkova, B. High frequency of SLC22A12 variants causing renal hypouricemia 1 in the Czech and Slovak Roma population; simple and rapid detection method by allele-specific polymerase chain reaction. *Urolithiasis* **2015**, *43*, 441–445. [[CrossRef](#)] [[PubMed](#)]
13. Stiburkova, B.; Ichida, K.; Sebesta, I. Novel homozygous insertion in SLC2A9 gene caused renal hypouricemia. *Mol. Genet. Metab.* **2011**, *102*, 430–435. [[CrossRef](#)]
14. Stiburkova, B.; Sebesta, I.; Ichida, K.; Nakamura, M.; Hulkova, H.; Krylov, V.; Jahnova, H. Novel allelic variants and evidence for a prevalent mutation in URAT1 causing renal hypouricemia: Biochemical, genetics and functional analysis. *Eur. J. Hum. Genet.* **2013**, *21*, 1067–1073. [[CrossRef](#)]
15. Cha, D.H.; Gee, H.Y.; Cachau, R.; Choi, J.M.; Park, D.; Jee, S.H.; Ryu, S.; Cho, S.K. Contribution of SLC22A12 on hypouricemia and its clinical significance for screening purposes. *Sci. Rep.* **2019**, *9*, 14360. [[CrossRef](#)] [[PubMed](#)]
16. Nakayama, A.; Matsuo, H.; Abhishek, A.; Ichida, K.; Shinomiya, N.; Guideline Development Committee of Clinical Practice Guideline for Renal Hypouricaemia. First clinical practice guideline for renal hypouricemia: A rare disorder that aided the development of urate-lowering drugs for gout. *Rheumatology* **2021**, *60*, 3961–3963. [[CrossRef](#)] [[PubMed](#)]
17. Lisyova, J.; Chandoga, J.; Jungova, P.; Repisky, M.; Knapkova, M.; Machkova, M.; Bohmer, D. An unusually high frequency of SCAD deficiency caused by two pathogenic variants in the ACADS gene and its relationship to the ethnic structure in Slovakia. *BMC Med. Genet.* **2018**, *19*, 64. [[CrossRef](#)] [[PubMed](#)]
18. Sebesta, I.; Stiburkova, B.; Bartl, J.; Ichida, K.; Hosoyamada, M.; Taylor, J.; Marinaki, A. Diagnostic tests for primary renal hypouricemia. *Nucleosides Nucleotides Nucleic Acids* **2011**, *30*, 1112–1116. [[CrossRef](#)]
19. Stiburkova, B.; Sebesta, I. Hypouricemia and hyperuricosuria in a pubescent girl: Answers. *Pediatric Nephrol.* **2018**, *33*, 2277–2279. [[CrossRef](#)]
20. Stiburkova, B.; Sebesta, I. Hypouricemia and hyperuricosuria in a pubescent girl: Questions. *Pediatric Nephrol.* **2018**, *33*, 2275. [[CrossRef](#)]
21. Claverie-Martin, F.; Trujillo-Suarez, J.; Gonzalez-Acosta, H.; Aparicio, C.; Roldan, M.L.J.; Stiburkova, B.; Garcia-Nieto, V.M. URAT1 and GLUT9 mutations in Spanish patients with renal hypouricemia. *Clin. Chim. Acta* **2018**, *481*, 83–89. [[CrossRef](#)] [[PubMed](#)]
22. Morar, B.; Gresham, D.; Angelicheva, D.; Tournev, I.; Gooding, R.; Guerguelcheva, V.; Kalaydjieva, L. Mutation history of the roma/gypsies. *Am. J. Hum. Genet.* **2004**, *75*, 596–609. [[CrossRef](#)] [[PubMed](#)]

23. Hurba, O.; Mancikova, A.; Krylov, V.; Pavlikova, M.; Pavelka, K.; Stiburkova, B. Complex analysis of urate transporters SLC2A9, SLC22A12 and functional characterization of non-synonymous allelic variants of GLUT9 in the Czech population: No evidence of effect on hyperuricemia and gout. *PLoS ONE* **2014**, *9*, e107902. [[CrossRef](#)] [[PubMed](#)]
24. Stiburkova, B.; Bleyer, A.J. Changes in serum urate and urate excretion with age. *Adv. Chronic Kidney Disease* **2012**, *19*, 372–376. [[CrossRef](#)] [[PubMed](#)]
25. Kolvek, G.; Rosicova, K.; Rosenberger, J.; Podracka, L.; Stewart, R.E.; Nagyova, I.; van Dijk, J.P. End-stage renal disease among Roma and non-Roma: Roma are at risk. *Int. J. Public Health* **2012**, *57*, 751–754. [[CrossRef](#)] [[PubMed](#)]
26. Rosenberger, J.; Majernikova, M.; Jarcuska, P.; Pella, D.; Marekova, M.; Geckova, A.M. Higher prevalence of nephropathy in young Roma females compared with non-Roma females. *Cent. Eur. J. Public Health* **2014**, *22*, S28–S31. [[CrossRef](#)] [[PubMed](#)]
27. Pallayova, M.; Brenisin, M.; Putrya, A.; Vrsko, M.; Drazilova, S.; Janicko, M.; Team, H. Roma Ethnicity and Sex-Specific Associations of Serum Uric Acid with Cardiometabolic and Hepatorenal Health Factors in Eastern Slovakian Population: The HepaMeta Study. *Int. J. Environ. Res. Public Health* **2020**, *17*, 7673. [[CrossRef](#)]
28. Ichida, K.; Hosoyamada, M.; Hisatome, I.; Enomoto, A.; Hikita, M.; Endou, H.; Hosoya, T. Clinical and molecular analysis of patients with renal hypouricemia in Japan—influence of URAT1 gene on urinary urate excretion. *J. Am. Soc. Nephrol.* **2004**, *15*, 164–173. [[CrossRef](#)] [[PubMed](#)]

Article

# Clinical and Functional Characterization of a Novel URAT1 Dysfunctional Variant in a Pediatric Patient with Renal Hypouricemia

Blanka Stiburkova <sup>1,2,\*</sup> , Jana Bohata <sup>1,3</sup> , Iveta Minarikova <sup>1</sup>, Andrea Mancikova <sup>4</sup>, Jiri Vavra <sup>4</sup>, Vladimír Krylov <sup>4</sup>  and Zdenek Doležel <sup>5</sup>

<sup>1</sup> Institute of Rheumatology, Na Slupi 4, 128 50 Prague, Czech Republic

<sup>2</sup> Department of Pediatrics and Adolescent Medicine, First Faculty of Medicine, Charles University and General University Hospital in Prague, Ke Karlovu 2, 120 00 Prague, Czech Republic

<sup>3</sup> Department of Rheumatology, First Faculty of Medicine, Charles University, Na Slupi 4, 128 50 Prague, Czech Republic

<sup>4</sup> Department of Cell Biology, Faculty of Science, Charles University, Vinicna 7, 128 00 Prague, Czech Republic

<sup>5</sup> Department of Pediatrics, University Hospital Brno, Medical Faculty of Masaryk University, Jihlavská 20, 625 00 Brno, Czech Republic

\* Correspondence: stiburkova@revma.cz; Tel.: (+420)-234-075-319; Fax: (+420)-224-914-451

Received: 22 July 2019; Accepted: 20 August 2019; Published: 23 August 2019



**Abstract:** Renal hypouricemia (RHUC) is caused by an inherited defect in the main (reabsorptive) renal urate transporters, URAT1 and GLUT9. RHUC is characterized by decreased concentrations of serum uric acid and an increase in its excretion fraction. Patients suffer from hypouricemia, hyperuricosuria, urolithiasis, and even acute kidney injury. We report the clinical, biochemical, and genetic findings of a pediatric patient with hypouricemia. Sequencing analysis of the coding region of *SLC22A12* and *SLC2A9* and a functional study of a novel RHUC1 variant in the *Xenopus* expression system were performed. The proband showed persistent hypouricemia (67–70  $\mu\text{mol/L}$ ; ref. range 120–360  $\mu\text{mol/L}$ ) and hyperuricosuria (24–34%; ref. range  $7.3 \pm 1.3\%$ ). The sequencing analysis identified common non-synonymous allelic variants c.73G > A, c.844G > A, c.1049C > T in the *SLC2A9* gene and rare variants c.973C > T, c.1300C > T in the *SLC22A12* gene. Functional characterization of the novel RHUC associated c.973C > T (p. R325W) variant showed significantly decreased urate uptake, an irregular URAT1 signal on the plasma membrane, and reduced cytoplasmic staining. RHUC is an underdiagnosed disorder and unexplained hypouricemia warrants detailed metabolic and genetic investigations. A greater awareness of URAT1 and GLUT9 deficiency by primary care physicians, nephrologists, and urologists is crucial for identifying the disorder.

**Keywords:** *SLC22A12*; URAT1; hypouricemia; uric acid transporters; excretion fraction of uric acid

## 1. Introduction

Hypouricemia is defined as serum uric acid concentrations below 119  $\mu\text{mol/L}$  (2 mg/dL). It is characterized by increased uric acid clearance or decreased uric acid production. Hypouricemia is a relatively rare condition, occurring in about 0.15–3.3% of the general population and 1.2–4% in hospitalized patients [1,2]. Malignancy is ranked first as a possible etiology of secondary hypouricemia, followed by diabetes mellitus, renal tubulopathies such as Fanconi syndrome, and medication. Excretion fraction of uric acid (EF-UA) is a key biochemical marker for a differential diagnosis of primary hypouricemia. Markedly elevated EF-UA suggests renal hypouricemia while lower or normal EF-UA suggests hereditary xanthinuria [3].

Renal hypouricemia (RHUC) is a heterogeneous hereditary disorder caused by a dysfunction of the main renal urate transporters, URAT1 and GLUT9. Characteristic biochemical markers include markedly decreased serum uric acid concentrations (S-UA) and elevated EF-UA. Clinical markers include exercise-induced acute renal failure, urolithiasis, and hematuria along with fatigue, nausea, vomiting, and diffuse abdominal discomfort. However, RHUC is also characterized by clinical variability, and only about 10% of all patients with a URAT1 defect have nephrolithiasis and/or acute kidney injury due to spasms of the renal artery. Currently there is no treatment for RHUC; however, allopurinol has been used to prevent recurrence of acute kidney injury episodes, and oral supplementation with antioxidants is recommended [4].

The role of URAT1 and the association of genetic variants of the *SLC22A12* gene with renal hypouricemia (RHUC type 1, OMIM no. 220150) were identified in 2002 [5], and to date, about 200 patients have been identified. The relationship between the GLUT9 transporter (gene *SLC2A9*) and renal hypouricemia (RHUC type 2, OMIM no. 612076) was reported in 2008 [6], and to date, about 15 patients have been identified. Homozygous or compound heterozygous loss-of-function mutations in the *SLC22A12* gene lead to a partial defect in absorption of uric acid, while variants in the *SLC2A9* are responsible for severe hypouricemia and hyperuricosuria (SUA < 10  $\mu\text{mol/L}$ , EF-UA > 90%), which is often complicated by nephrolithiasis and acute kidney injury, such as that seen in RHUC1. Genetic variants in the *SLC22A12* gene are the primary cause of renal hypouricemia (>90%) with major variants reported in Asia region (Japanese and Korea, variant p.W258X with frequencies 2.3%) and in the Roma population (p.L415\_G417del and p.T467M with frequencies of 1.9% and 5.6%, respectively) [7–10].

This case study expands our understanding of the molecular mechanisms of renal hypouricemia and confirms the distribution of dysfunctional URAT1 variants in non-Asian patients.

## 2. Materials and Methods

### 2.1. Patient

A three-year-old Caucasian girl was referred for an endocrine examination due to her small stature. The child's mother had been under long-term treatment for a psycho-affective disorder, which also included the pregnancy with her daughter; the father was healthy. The child was born during the 31st week of pregnancy, by C-section, due to premature discharge of amniotic fluid. Birth weight was 1330 g, and length was 37 cm. Oxygen therapy was necessary for 5 days but without the need for artificial pulmonary ventilation. During development, the child showed symptoms of psychomotor retardation. Therefore, developmental rehabilitation was initiated. Rehabilitation was carried out, however, family compliance was poor. The mother abandoned the family, and the girl was in alternating custody of her father and grandmother. On initial examination by an endocrinologist, the girl was 94.5 cm tall (−3.4 SD), had a body weight of 13.4 kg (−1.8 SD), and had only grown about 2.7 cm in the previous year. The father's body height was 163.5 cm, but the mother's height was unknown. The child's physical examination was without irregularities except for orbital hypertelorism. Her level psychomotor development corresponded approximately to that of a two-year-old child. Because hypouricemia (67–70  $\mu\text{mol/L}$ ) was repeatedly found during endocrine re-examinations, further analyses were carried out, mainly focused on purine metabolism disorders. High-performance liquid chromatography determination of hypoxanthine and xanthine in urine was performed on Waters Alliance 2695 [3].

### 2.2. Genetic Analysis

Genomic DNA was extracted from a blood sample using a QIAmp DNA Mini Kit (Qiagen GmbH, Hilden, Germany). All coding exons and intron-exon boundaries of *SLC22A12* and *SLC2A9* were amplified from genomic DNA using polymerase chain reaction and subsequent purified using a PCR DNA Fragments Extraction Kit (Geneaid, New Taipei City, Taiwan). DNA sequencing was performed on an automated 3130 Genetic Analyzer (Applied Biosystems Inc., Foster City, CA, USA). Primer

sequences and PCR conditions used for amplification were described previously [11,12]. The reference genomic sequence was defined as version NC\_000011.8, region 64,114,688..64126396, NM\_144585.3 for *SLC22A12*; NM\_020041.2, NP-064425.2, SNP source dbSNP 132 for *SLC2A9*.

### 2.3. Functional Analysis

A missense variant of URAT1, p.R325W, was tested for urate transport activity using in vitro expression analysis in *Xenopus* oocytes as previously described [11,13]. Subcellular localization was determined using immunocytochemical analysis. Immunodetection of URAT1 was performed on 3.5 µm paraffin sections using rabbit anti-*SLC22A12* polyclonal antibody (Sigma, St. Louis, MO, USA). The paraffin sections were stained after heat-induced antigen retrieval (10 mM citrate buffer, pH 6.1, for 20 min at 97.0 °C in a water base) using standard blocking procedures. The primary antibody against URAT1 was diluted 1:25 in PBS and applied overnight at 4 °C. Detection of bound primary antibodies was achieved using Alexa Fluor 488-conjugated with anti-rabbit IgG (diluted 1:500; Abcam, Cambridge, Britain). For image acquisition, we used an Olympus BX53 fluorescent microscope (Olympus, Hamburg, Germany).

## 3. Results

### 3.1. Patient

The proband had persistent hyperuricemia (67–70 µmol/L; ref. range 120–360 µmol/L) and an increased EF-UA (24.3–34.2%; ref. range  $7.3 \pm 1.3\%$ ) with normal urinary excretion of hypoxanthine and xanthine, Table 1. No clinical or laboratory symptoms of renal disease were present in the patient. During follow-up, the patient was without episodes of acute kidney injury; her ultrasound exam showed no nephrolithiasis, and her creatinine clearance (estimated as eGF) was within the normal range. Supporting examinations to determine the cause of her small stature found normal serum levels of Thyroid Stimulating Hormone (TSH) and fT4, however, IGFBP-3 was low, and IGF-1 was well below the reference level. A growth hormone deficit was demonstrated with stimulation tests (clonidine test, hypoglycemia test). Brain magnetic resonance imaging found a markedly small hypophysis; the pituitary stalk was evaluated as normal. Cytogenetic analysis demonstrated a normal 46, XX karyotype. Growth hormone replacement therapy was initiated.

**Table 1.** Biochemical and genetic parameters of the proband and her father. <sup>a</sup> reference range for women and children; <sup>b</sup> reference range for men.

Table Cont.	Serum UA (µmol/L)	EF-UA (%)	Serum Creatinine (µmol/L)	Identified Variants in <i>SLC22A12</i>
Proband	67–70	24.3–34.2	32	c.973C > T (C/T); c.1300C > T (C/T)
Father of proband	205	N/A	62	c.1300C > T (C/T)
Reference range	120–360 <sup>a</sup> 120–420 <sup>b</sup>	$7.3 \pm 1.3$ <sup>a</sup> $10.3 \pm 4.2$ <sup>b</sup>	50–110	-

### 3.2. Genetic Analysis

Sequencing analysis of *SLC2A9* revealed six intron variants (rs2240722, rs2240721, rs2240720, rs28592748, rs13115193 and rs61256984), three synonymous variants (rs13113918, rs10939650 and rs13125646) and three common non-synonymous allelic variants (rs2276961, p.G25R; rs16890979, p.V282I and rs2280205, p.P350L). A sequencing analysis of *SLC22A12* revealed one intron variant (rs11231837), four synonymous (rs3825016, rs11231825, rs1630320, and rs7932775), and two heterozygous rare non-synonymous allelic c.973C > T variants (p.R325W, rs150255373, Figure 1A,B), and a previously identified c.1300C > T variant (p.R434C, rs145200251) [14]. Segregation analysis was not fully performed because the child's family was not interested.

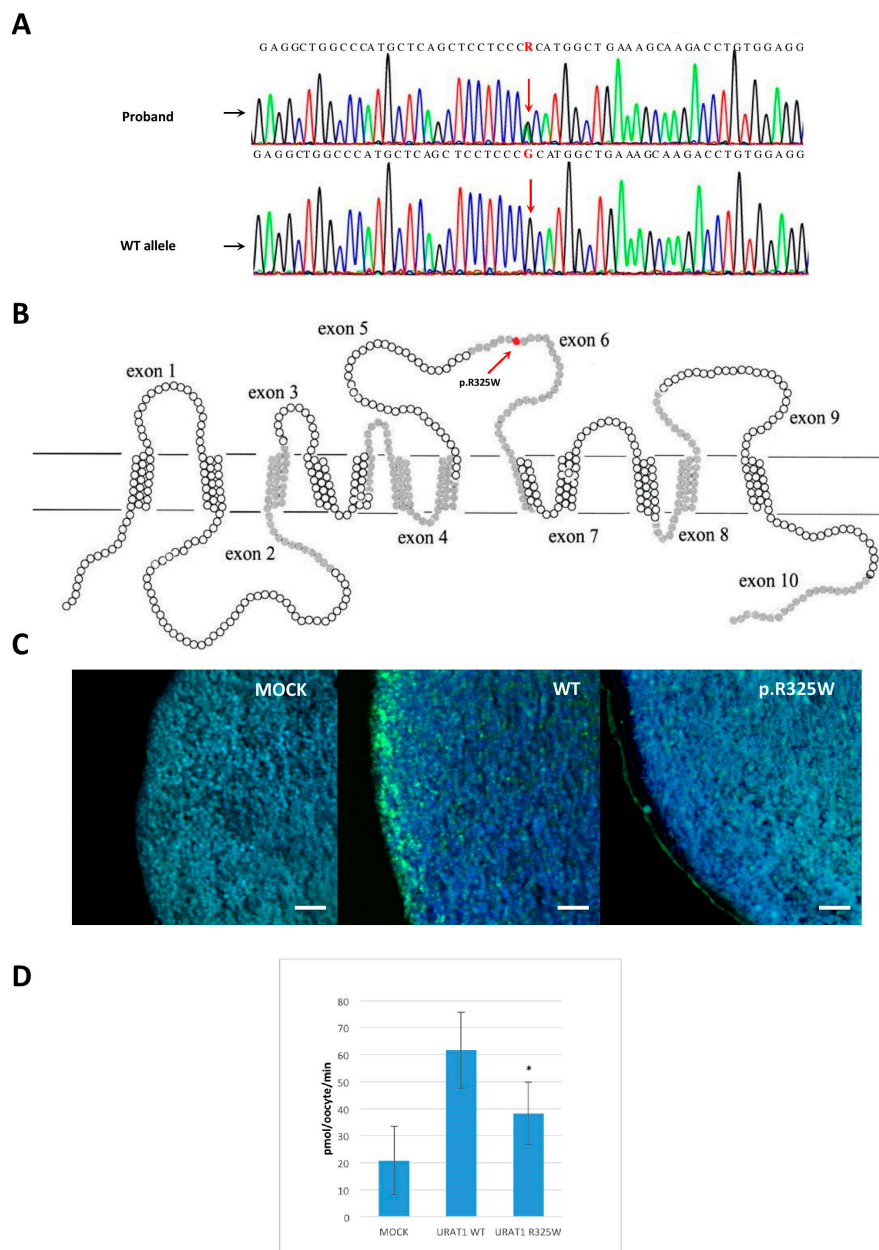


**Figure 1.** Illustration of allelic variant p.R325W in genetic, protein and functional context. **(A)** Electropherograms of partial sequences of exon 6 showing a heterozygous c.973C > T variant in the *SLC22A12* gene. **(B)** Position of identified allelic variant p.R325W in a URAT1 membrane topology model. **(C)** Immunohistochemical analysis of *Xenopus* oocytes injected with 50 ng of cRNA encoding the wt or p.R325W using anti-URAT1 polyclonal antibodies. The URAT1 signal is green, autofluorescent granules in the cytoplasm of oocytes are blue. Water-injected oocyte without any detectable URAT1 signal. Oocyte injected with wt cRNA exhibited a strong linear signal on the plasma membrane and a finely granular intracytoplasmic signal. The variant p.R325W was characterized by a weak discontinuous URAT1 signal on the plasma membrane, and reduced intracytoplasmic staining compared to the wt. Scale bar represents 50  $\mu$ m. **(D)** Uric acid accumulation in *Xenopus* oocytes transfected with wt URAT1 and p.R325W URAT1 allelic variant after 30 min of incubation in [8- $^{14}$ C] 600  $\mu$ M uric acid/ND - 96 solution. The data was tested by One-way Analysis of variance (ANOVA). In comparison to wt URAT1, significantly lower UA accumulation (\*  $p < 0.05$ ) was detected in p.R325W URAT1 injected oocytes (n = 5; means  $\pm$  SD). H<sub>2</sub>O injected (mock) oocytes were used as a negative control.

### 3.3. Functional Analysis

Urate transport via the p.R325W variant was significantly decreased in comparison to the wild type (wt) (\*  $p < 0.05$ ), Figure 1C. This finding indicated that the above-mentioned URAT1 variant leads to reduced urate reabsorption at the apical membrane of proximal renal tubules leading to decreased serum urate levels. Oocytes expressing the wt exhibited strong continuous URAT1 immunostaining on the plasma membrane and dispersed finely granular staining in the cytoplasm. Oocytes expressing p.R325W showed a weak discontinuous URAT1 signal on the plasma membrane and intracytoplasmic staining was lower than in the wt, Figure 1D.

## 4. Discussion and Conclusions

Urate transport in the kidney is a complex process involving several transmembrane proteins that provide reabsorption (URAT1, GLUT9) and secretion (ABCG2). In genome-wide association studies, the *SLC2A9* gene is a well-established locus that is significantly associated with hyperuricemia while the *ABCG2* locus had the most significant association with gout susceptibility [15–17]. The dysfunctional variants in URAT1 and GLUT9 cause hereditary renal hypouricemia, and genetic analysis is needed to confirm the diagnosis and/or to identify the specific type of renal hypouricemia.

The *SLC22A12* gene is located on chromosome 11q13. Ten exons encode two transcript variants of the URAT1 transporter (332 and 553 amino acids), which are specifically expressed on the epithelial cells of the proximal tubules in the renal cortex [4]. At present, 52 variations in the *SLC22A12* coding region (40 missense/nonsense, two splicing, three regulatory, three small deletions, two small insertions, one gross deletion, and one complex rearrangement) have been described (HGMD Professional 2018.4, <http://www.hgmd.cf.ac.uk>). Thirty-six URAT1 variants are currently associated with the hypouricemia phenotype. Functional analysis confirmed in part of these variants impact on urate uptake ability and/or cytoplasmic expression and localization [7,11,13,14]. However, not all URAT1 allelic variants have effect on decreasing of protein expression and/or function (p.R228E, R477H) [7,11].

The analysis of *SLC2A9* coding regions in our proband revealed three common non-synonymous variants: heterozygous rs2276961 (p.G25R, Caucasian MAF = 0.53), rs16890979 (p.V282I, Caucasian MAF = 0.21), and homozygous rs2280205 (p.P350L, Caucasian MAF = 0.48). These variants have not been previously reported in association with hypouricemia. Variant p.V282I was previously described relative to the hyperuricemia and gout phenotype [18]. Moreover, in our previous study, which used association analysis together with functional and immunohistochemical characterization of these variants identified in the adult population, we did not find any influence of these allelic variants on expression, subcellular localization, or urate uptake of GLUT9 transporters [19].

Our analysis of *SLC22A12* coding regions revealed two rare heterozygous non-synonymous variants: rs150255373 (p.R325W, Caucasian MAF = 0.001) and rs145200251 (p.R434C, Caucasian MAF unknown). Variant p.R434C was previously associated with renal hypouricemia 1 in a five-year-old Macedonian girl suffering from distal renal tubular acidosis and renal hypouricemia [14]. The patient had symptoms of dehydration, polyuria, and vomiting. The patient also had rickets and slow growth. There was evidence of hyperchloremic metabolic acidosis (pH 7.23, HCO<sub>3</sub> 13.6 mmol/L, BE = 12.6 mmol/L), hypokalemia (3.0 mmol/L), hypophosphatemia (0.84 mmol/L), hypouricemia (73 μmol/L), and hyperuricosuria (EF-UA 24–31%). Bilateral nephrocalcinosis and a solitary cyst in the left kidney were discovered during an ultrasound examination. The patient was given alkali therapy; metabolic compensation was achieved, serum electrolytes normalized, and low molecular proteinuria resolved. Only the hypouricemia parameter persisted during the two-year observational period. The mother of this patient was a heterozygote for the same missense variant (S-UA 136 μmol/L, EF-UA 19%) and a history of renal colic and the passage of a single renal calculus. Functional studies of p.R434Cs were previously performed using transiently transfected HEK293 cells [14]. Plasma membrane expression levels of the p.R434C variant were low, intracellular localization was not strongly observed, and urate uptake showed a significant reduction of urate transport function ( $P < 0.001$ ).

The structural model for URAT1 is mainly focused on the organization and alignment of residues within 12 transmembrane spanning domains. Variant p.R325W was localized within the putative extracellular loop. This variant has not yet been identified in the patients of those with renal hypouricemia, but the nature of this mutation strongly suggests that it is pathogenic; PolyPhen software (<http://genetics.bwh.harvard.edu/pph/>) suggested that the variant is possibly damaging (score 0.72). Moreover, another predictive software, SIFT (<http://sift.jcvi.org/>), suggests that this variant is deleterious (score 0). On the other hand, CADD (<https://cadd.gs.washington.edu/>), REVEL, and MetaLR predictive software indicate that the impact of the variant is likely to be tolerated or benign. In the middle stands Mutation Assessor (<http://mutationassessor.org/r3/>) which predicts a moderate functional impact. Evolutionary analysis of URAT1 paralogs, including six mammalian species, revealed conservation of p.R325W only between human and chimpanzee (Figure 2). Human and Simian monkeys possess high affinity and low capacity URAT1 transporter which diverged from the original low affinity, high capacity paralog (mouse, rat, horse and dog) 43 MYA [20]. Authors described four key amino acid substitutions in human URAT1 positions 25, 27, 365 and 414 as a crucial for the high to low affinity and low to high capacity shift. Similarly, as a variant p.R325W, all four amino acid residues are conserved between human and baboon, but not among other mammalian species. The functional characterization of p.R325W showed significantly decreased urate uptake and a weak, discontinuous URAT1 signal on the plasma membrane and reduced intracytoplasmic staining. The results suggested that p.R325W variant may not affect URAT1 function qualitatively (via alteration of its intrinsic transporter activity), but rather do so quantitatively (via decreasing its cellular protein level). Taken together, the data confirm the causality of the p.R325W variant relative to renal hypouricemia 1.

	p.R325W	p.R434C
<b>Human</b>	VLLSAMREELSMG...HEM <u>G</u> ALRSALAVL	
<b>Chimpanzee</b>	VLLSAM <u>R</u> EELSMG...HEM <u>G</u> AL <u>R</u> SALAVL	
<b>Horse</b>	VLLSAMQEELSAS...E <u>W</u> L <u>W</u> D <u>L</u> RSALAA <u>L</u>	
<b>Dog</b>	VLLSAMQEELSAG...Y <u>E</u> M <u>G</u> ALRSALAVL	
<b>Rat</b>	V <u>L</u> RSAMQE <u>E</u> PN <u>G</u> N...R <u>E</u> M <u>G</u> I <u>L</u> RS <u>S</u> LAVL	
<b>Mouse</b>	V <u>L</u> RSAM <u>E</u> EE <u>P</u> SRD...H <u>G</u> M <u>G</u> V <u>L</u> RSALAVL	

**Figure 2.** Alignment of the p.R325W URAT1 amino acids in the studied allelic variants with chimpanzee, horse, dog, rat and mouse paralogs.

Detailed investigations of serum uric acid concentrations and excretion fractions of uric acid in patients with unexplained hypouricemia are needed. Many patients with RHUC may be asymptomatic; however, pediatric nephrologists know that RHUC can cause acute renal failure, especially after strenuous physical activity. Another risk of RHUC is the development of nephrolithiasis. Although renal hypouricemia is a rare hereditary disorder, the frequency of novel URAT1 associated variants shows that this condition is underdiagnosed. RHUC should be considered not only in patients from Japan or Asia. The phenotypic severity of RHUC1 is not correlated with results from functional characterizations of URAT1 variants. Functional studies regarding the impact of novel associated variants are necessary to determine their correlation with scores from prediction algorithms and to confirm causality.

**Author Contributions:** Conceptualization, B.S.; validation, B.S.; J.B. conducted sequencing analyses; I.M., A.M., J.V. and V.K. worked on experiments using *Xenopus* oocytes, and analyzed the data; Z.D. was responsible for clinical observations; data curation, B.S.; writing, B.S.; project administration, B.S.; funding acquisition, B.S.

**Funding:** Supported by the Ministry of Health of the Czech Republic: AZV 15-26693A, the project for conceptual development of research organization 00023728 (Institute of Rheumatology) and RVO VFN64165.

**Conflicts of Interest:** The authors declare no conflict of interest.



## References

1. Son, C.N.; Kim, J.M.; Kim, S.H.; Cho, S.K.; Choi, C.B.; Sung, Y.K.; Kim, T.H.; Bae, S.C.; Yoo, D.H.; Jun, J.B. Prevalence and possible causes of hypouricemia at a tertiary care hospital. *Korean J. Intern. Med.* **2016**, *5*, 971–976. [[CrossRef](#)] [[PubMed](#)]
2. Bairaktari, E.T.; Kakafika, A.I.; Pritsivelis, N.; Hatzidimou, K.G.; Tsianos, E.V.; Seferiadis, K.I.; Elisaf, M.S. Hypouricemia in individuals admitted to an inpatient hospital-based facility. *Am. J. Kidney Dis.* **2003**, *41*, 1232–1255. [[CrossRef](#)]
3. Mraz, M.; Hurba, O.; Bartl, J.; Dolezel, Z.; Marinaki, A.; Fairbanks, L.; Stiburkova, B. Modern diagnostic approach to hereditary xanthinuria. *Urolithiasis* **2015**, *43*, 61–67. [[CrossRef](#)] [[PubMed](#)]
4. Bhasin, B.; Stiburkova, B.; De Castro-Pretelt, M.; Beck, N.; Bodurtha, J.N.; Atta, M.G. Hereditary renal hypouricemia: A new role for allopurinol? *Am. J. Med.* **2014**, *127*, e3–e4. [[CrossRef](#)] [[PubMed](#)]
5. Enomoto, A.; Kimura, H.; Chairoungdua, A.; Shigeta, Y.; Jutabha, P.; Cha, S.H.; Hosoyamada, M.; Takeda, T.; Sekine, T.; Igarashi, T.; et al. Molecular identification of a renal urate anion exchanger that regulates blood urate levels. *Nature* **2002**, *417*, 447–452. [[CrossRef](#)] [[PubMed](#)]
6. Matsuo, H.; Chiba, T.; Nagamori, S.; Nakayama, A.; Domoto, H.; Phetdee, K.; Wiriyasermkul, P.; Kikuchi, Y.; Oda, T.; Nishiyama, J.; et al. Mutations in glucose transporter 9 gene SLC2A9 cause renal hypouricemia. *Am. J. Hum. Genet.* **2008**, *83*, 744–751. [[CrossRef](#)] [[PubMed](#)]
7. Iwai, N.; Mino, Y.; Hosoyamada, M.; Tago, N.; Kokubo, Y.; Endou, H. A high prevalence of renal hypouricemia caused by inactive SLC22A12 in Japanese. *Kidney Int.* **2004**, *66*, 935–944. [[CrossRef](#)] [[PubMed](#)]
8. Lee, J.H.; Choi, H.J.; Lee, B.H.; Kang, H.K.; Chin, H.J.; Yoon, H.J.; Ha, I.S.; Kim, S.; Choi, Y.; Cheong, H.I. Prevalence of hypouricaemia and SLC22A12 mutations in healthy Korean subjects. *Nephrology* **2008**, *13*, 661–666. [[CrossRef](#)] [[PubMed](#)]
9. Gabrikova, D.; Bernasovska, J.; Sokolova, J.; Stiburkova, B. High frequency of SLC22A12 variants causing renal hypouricemia 1 in the Czech and Slovak Roma population; simple and rapid detection method by allele-specific polymerase chain reaction. *Urolithiasis* **2015**, *43*, 441–445. [[CrossRef](#)] [[PubMed](#)]
10. Stiburkova, B.; Gabrikova, D.; Čepek, P.; Šimek, P.; Kristian, P.; Cordoba-Lanus, E.; Claverie-Martin, F. Prevalence of URAT1 allelic variants in the Roma population. *Nucleosides Nucleotides Nucleic Acids* **2016**, *35*, 529–535. [[CrossRef](#)] [[PubMed](#)]
11. Stiburkova, B.; Sebesta, I.; Ichida, K.; Nakamura, M.; Hulkova, H.; Krylov, V.; Kryspinova, L.; Jahnova, H. Novel allelic variants and evidence for a prevalent mutation in URAT1 causing renal hypouricemia: Biochemical, genetics and functional analysis. *Eur. J. Hum. Genet.* **2013**, *21*, 1067–1073. [[CrossRef](#)] [[PubMed](#)]
12. Stiburkova, B.; Ichida, K.; Sebesta, I. Novel homozygous insertion in SLC2A9 gene caused renal hypouricemia. *Mol. Genet. Metab.* **2011**, *102*, 430–435. [[CrossRef](#)] [[PubMed](#)]
13. Mancikova, A.; Krylov, V.; Hurba, O.; Sebesta, I.; Nakamura, M.; Ichida, K.; Stiburkova, B. Functional analysis of novel allelic variants in URAT1 and GLUT9 causing renal hypouricemia type 1 and 2. *Clin. Exp. Nephrol.* **2016**, *20*, 578–584. [[CrossRef](#)] [[PubMed](#)]
14. Tasic, V.; Hynes, A.M.; Kitamura, K.; Cheong, H.I.; Lozanovski, V.J.; Gucev, Z.; Jutabha, P.; Anzai, N.; Sayer, J.A. Clinical and functional characterization of URAT1 variants. *PLoS ONE* **2011**, *6*, e28641. [[CrossRef](#)] [[PubMed](#)]
15. Köttgen, A.; Albrecht, E.; Teumer, A.; Vitart, V.; Krumsiek, J.; Hundertmark, C.; Pistis, G.; Ruggiero, D.; Seaghdha, M.C.O.; Haller, T.; et al. Genome-wide association analyses identify 18 new loci associated with serum urate concentrations. *Nat. Genet.* **2013**, *45*, 145–154. [[CrossRef](#)] [[PubMed](#)]
16. Nakayama, A.; Nakaoka, H.; Yamamoto, K.; Sakiyama, M.; Shaukat, A.; Toyoda, Y.; Okada, Y.; Kamatani, Y.; Nakamura, T.; Takada, T.; et al. GWAS of clinically defined gout and subtypes identifies multiple susceptibility loci that include urate transporter genes. *Ann. Rheum. Dis.* **2017**, *76*, 869–877. [[CrossRef](#)] [[PubMed](#)]
17. Stiburkova, B.; Pavelcova, K.; Zavada, J.; Petru, L.; Simek, P.; Cepek, P.; Pavlikova, M.; Matsuo, H.; Merriman, T.R.; Pavelka, K. Functional non-synonymous variants of ABCG2 and gout risk. *Rheumatology* **2017**, *56*, 1982–1992. [[CrossRef](#)] [[PubMed](#)]
18. Dehghan, A.; Köttgen, A.; Yang, Q.; Hwang, S.J.; Kao, W.H.L.; Rivadeneira, F.; Boerwinkle, E.; Levy, D.; Hofman, A.; Castor, B.; et al. Association of three genetic loci with uric acid concentration and risk of gout: A genome-wide association study. *Lancet* **2008**, *372*, 1953–1961. [[CrossRef](#)]

19. Hurba, O.; Mancikova, A.; Krylov, V.; Pavlikova, M.; Pavelka, K.; Stiburkova, B. Complex analysis of urate transporters SLC2A9, SLC22A12 and functional characterization of non-synonymous allelic variants of GLUT9 in the Czech population: No evidence of effect on hyperuricemia and gout. *PLoS ONE* **2014**, *9*, e107902. [[CrossRef](#)] [[PubMed](#)]
20. Tan, P.K.; Farrar, J.E.; Gaucher, E.A.; Miner, J.N. Coevolution of URAT1 and Uricase during Primate Evolution: Implications for Serum Urate Homeostasis and Gout. *Mol. Biol. Evol.* **2016**, *33*, 2193–2200. [[CrossRef](#)] [[PubMed](#)]



© 2019 by the authors. Licensee MDPI, Basel, Switzerland. This article is an open access article distributed under the terms and conditions of the Creative Commons Attribution (CC BY) license (<http://creativecommons.org/licenses/by/4.0/>).